MOLECULAR AND BIOCHEMICAL CHARACTERIZATION OF
TYPE 1 CYSTATIN STEFIN-2 OF THE LIVER FLUKE
FASCIOLA GIGANTICA

BY

MISS SINEE SIRICOON

A DISSERTATION SUBMITTED IN PARTIAL FULFILLMENT OF
THE REQUIREMENTS FOR THE DEGREE OF THE
DOCTOR OF PHILOSOPHY
(BIOMEDICAL SCIENCES)

GRADUATE PROGRAM IN BIOMEDICAL SCIENCES
FACULTY OF ALLIED HEALTH SCIENCES
THAMMASAT UNIVERSITY
ACADEMIC YEAR 2015

MOLECULAR AND BIOCHEMICAL CHARACTERIZATION OF

TYPE 1 CYSTATIN STEFIN-2 OF THE LIVER FLUKE

FASCIOLA GIGANTICA

BY

MISS SINEE SIRICOON

A DISSERTATION SUBMITTED IN PARTIAL FULFILLMENT OF

THE REQUIREMENTS FOR THE DEGREE OF THE

DOCTOR OF PHILOSOPHY

(BIOMEDICAL SCIENCES)

GRADUATE PROGRAM IN BIOMEDICAL SCIENCES

FACULTY OF ALLIED HEALTH SCIENCES

THAMMASAT UNIVERSITY

ACADEMIC YEAR 2015

THAMMASAT UNIVERSITY

FACULTY OF ALLIED HEALTH SCIENCES

DISSERTATION

BY

MISS SINEE SIRICOON

ENTITLED

MOLECULAR AND BIOCHEMICAL CHARACTERIZATION OF TYPE 1 CYSTATIN STEFIN-2

OF THE LIVER FLUKE *FASCIOLA GIGANTICA*

was approved as partial fulfillment of the requirements for the degree of the

Doctor of Philosophy (Biomedical Sciences)

on February 19, 2016

Chairman _____

(Assoc. Prof. Smarn Tesana, Ph.D.)

Member and Advisor _____

(Assoc. Prof. Hans Rudi Grams, Dr. rer. nat.)

Member and Co-Advisor _____

(Professor Peter Smooker, Ph.D.)

Member and Co-Advisor _____

(Assist. Prof. Suksiri Vichasri Grams, Dr. rer. nat.)

Member and Co-Advisor _____

(Assist. Prof. Amornrat Geadkaew, Ph.D.)

Dean _____

(Assoc. Prof. Kampol Ruchiwit, Ph.D.)

Dissertation Title	Molecular and biochemical characterization of type 1 cystatin stefin-2 of the liver fluke *Fasciola gigantica*
Author	Miss Sinee Siricoon
Degree	Doctor of Philosophy (Biomedical Sciences)
Department/Faculty/University	Graduate Program in Biomedical Sciences Faculty of Allied Health Sciences Thammasat University
Dissertation Advisor	Associate Professor Hans Rudi Grams, Dr. rer. nat.
Dissertation Co-Advisor	Professor Vithoon Viyanant, Ph.D.
Dissertation Co-Advisor	Professor Peter Smooker, Ph.D.
Dissertation Co-Advisor	Assistant Professor Suksiri Vichasri Grams, Dr. rer. nat.
Dissertation Co-Advisor	Assistant Professor Amornrat Geadkaew, Ph.D.
Academic Years	2015

ABSTRACT

Cysteine proteases including cathepsin B and cathepsin L are involved in physiological and biological processes in all living organisms and imbalanced activity of these proteases may cause several diseases. They are also important antigens in the trematode genus *Fasciola* and have vital roles in parasite survival including protection, infection and nutrition of the liver fluke. The biological roles and application of parasite cathepsins, e.g. in chemotherapy and as vaccines have been studied but data concerning their regulation is still incomplete. Especially, the cysteine protease inhibitors of the cystatin superfamily have not been investigated in depth in trematodes. This research was conducted to characterize the molecular

and biochemical properties of a type 1 cystatin (Stefin-2) in the liver fluke *Fasciola gigantica.*

In the present study, a cDNA encoding type 1 cystatin of the parasite, FgStefin-2, was isolated from total RNA of adult *F. gigantica* by RT-PCR. A FgStefin-2-specific probe detected gene and transcript in Southern and Northern analyses of genomic DNA and total RNA of the fluke. FgStefin-2, which unusually for type 1 cystatins carries a signal peptide, was expressed as active recombinant protein in *Escherichia coli* (rFgStefin-2). Purified rFgStefin-2 was used for cysteine protease inhibition assays, functional analysis and polyclonal antibody production. The polyclonal antibody was used to study the distribution of native FgStefin-2 in 2- and 4-week-old juveniles and adult *F. gigantica* and to detect rFgStefin-2 and native FgStefin-2 in crude worm (CW) extract and excretory/secretory (ES) products of adult *F. gigantica* in immunoblots. Immunohistochemical analysis showed that FgStefin-2 is located in several tissues of the parasite including the prostate gland in adults and gut epithelium in all stages. Immunoblots demonstrated that the polyclonal antibody reacted with rFgStefin-2, CW extract and ES product of the adult parasite, but did not cross-react with rFgMDCd10, rFgStefin-1 and CW extracts of other trematodes. The inhibitory properties of rFgStefin-2 against bovine cathepsin B, bovine cathepsin L and the proteolytic activity of ES products, CW extracts from metacercariae and adult parasite were characterized by using fluorogenic substrates and by zymography using gelatin as substrate. The recombinant protein exhibited inhibitory activity against cysteine proteases (cathepsins B and L) and the proteolytic activity of ES products, CW extracts from metacercariae and adult parasites. This protein was found to be active over a wide pH range and heat stable. Preliminary study on immunomodulatory properties of the protein showed that it may interfere with an immune response mechanism that is involved in polyclonal T-cell proliferation. Furthermore, the novel cathepsin B5 of *F. gigantica*, FgCB5, was expressed and purified in a yeast-based eukaryotic expression system. Immunoblots showed that procathepsin B5 was detected in CW extract and in minor amounts in ES product. Analyses of recombinant cathepsin B5 revealed that it was active at acidic pH, able to effectively digest several of the host substrates and also exhibited

substantial exopeptidase activity. Inhibitory activities of rFgStefin-1, rFgStefin-2 and human cystatin C against rFgCB5 demonstrated nanomolar inhibition constants. This experiment was used to confirm that rFgStefin-2 has been evolutionary adapted to block cathepsin B. In summary, FgStefin-2 may play important roles, for example in the protection of the minute newly excysted juvenile from autoproteolysis and in the regulation of cysteine protease activity in the reproductive system. This knowledge may help to evaluate application of the protein as diagnosis tool, drug target and vaccine candidate against fascioliasis.

Keywords: cystatin, cysteine protease, protease inhibitor, *Fasciola gigantica*

ACKNOWLEDGEMENTS

Sciences, Thammasat University for unconditional support, their friendship and helpfulness.

Finally, I would like to express my deepest thankfulness to my beloved family, my father, my mother and all of my best friends for their strong encouragement, understanding, never-ending support and who stayed with me at all times. I would not have achieved my goal without them.

Sinee Siricoon

TABLE OF CONTENTS

TABLE OF CONTENTS (Cont.)

TABLE OF CONTENTS (Cont.)

TABLE OF CONTENTS (Cont.)

TABLE OF CONTENTS (Cont.)

TABLE OF CONTENTS (Cont.)

TABLE OF CONTENTS (Cont.)

TABLE OF CONTENTS (Cont.)

TABLE OF CONTENTS (Cont.)

TABLE OF CONTENTS (Cont.)

TABLE OF CONTENTS (Cont.)

LIST OF TABLES

LIST OF FIGURES

LIST OF FIGURES (Cont.)

LIST OF FIGURES (Cont.)

LIST OF FIGURES (Cont.)

LIST OF FIGURES (Cont.)

LIST OF FIGURES (Cont.)

LIST OF ABBREVIATIONS

Symbols/Abbreviations	Terms
%	Percent
µg	Microgram
µl	Microliter
µm	Micrometer
µg/ml	Microgram per milliliter
µM	Micromolar
[S]	Substrate concentration
×g	Gravitational acceleration
Ad	Adults
AEC	3-amino-9-ethylcarbazole
AEP	Asparaginyl endopeptidase
AFU	Arbitrary fluorescence units
AMC	7-amino-4-methylcoumarin
AP	Alkaline phosphatase
APCs	Antigen presenting cells
A. viteae	*Acanthocheilonema viteae*
bcc	Bovine colostrum cystatin
BCIP	5-bromo-4-chloro-3-indolyl phosphate
bkl, bk2 and bk3	Three bovine kininogen segments
Bm-CPI-1, Bm-CPI-2 and Bm-CPI-3	Three cystatins of *B. malayi*
BMGY	Buffered Glycerol complex Medium
BMMY	Buffered Methanol complex Medium
bp	Base pairs
BSA	Bovine serum albumin

LIST OF ABBREVIATIONS (Cont.)

Symbols/Abbreviations	Terms
ca	Cecum
cat	Cathepsin
cc	Chicken cystatin
CD	Cluster of differentiation
cDNA	Complementary deoxyribonucleic acid
cli-1, 2	Cysteine protease inhibitor like
CLIP	Class II-associated invariant chain peptide
Con A	Concanavalin A
conc.	Concentration
cont.	Continuous
CT	Computed tomography
CW	Crude worm
DCs	Dendritic cells
DEPC	Diethylpyrocarbonate
DIG	Digoxigenin
DMSO	Dimethyl sulfoxide
DNA	Deoxyribonucleic acid
DNase	Deoxyribonuclease
dNTP	Deoxynucleotide triphosphate
drc	*Drosophila* cystatin
DTT	Dithiothreitol
dUTP	Deoxyuridine triphosphate
DW	Distilled water
ed	Ejaculatory Duct

LIST OF ABBREVIATIONS (Cont.)

Symbols/Abbreviations	Terms
E^0	Initial protease concentration
E-64	L-3-carboxy-2,3-trans -epoxypropionyl-leucylamido(4-guanidino)butane
E. coli	*Escherichia coli*
EC number	Enzyme Commission number
EDTA	Ethylenediamine tetraacetic acid
ELISA	Enzyme-linked immunosorbent assay
ER	Endoplasmic reticulum
ERCP	Endoscopic retrograde cholangiopancreatography
ES	Excretory-secretory
EST	Expressed sequence tags
et al.	et alii
FABP	Fatty acid-binding protein
F. gigantica	*Fasciola gigantica*
F. hepatica	*Fasciola hepatica*
g	Gram
gDNA	Genomic DNA
GER	Granular endoplasmic reticulum
GST	Glutathione S-transferase
h	Hour
Hb	Hemoglobin
hcc	Human cystatin C
HCl	Hydrochloric acid
hcs	Human cystatin S

LIST OF ABBREVIATIONS (Cont.)

Symbols/Abbreviations	Terms
hkl, hk2 and hk3	Three human kininogen segments
HLA	Human leukocyte antigen
hsa	Human cystatin SA
hsb	Human stefin B
hsn	Human cystatin SN
IAA	Iodoacetamide
IC_{50}	The half maximal inhibitory concentration
i.e.	*id est*
I^0	Initial inhibitor concentration
IFN-**γ**	Interferon-gamma
Ig	Immunoglobulin
Ii	Invariant chain
IL	Interleukin
IPG	Immobilized pH gradient
IPTG	Isopropyl-1-thio-**β**-D-galactopyranoside
I. scapularis	*Ixodes scapularis*
kb	Kilobase
kDa	Kilodalton
kg	Kilogram
K_i	Equilibrium inhibition constant
K_m	Michaelis Menten constant
LAM	Lipoarabinomannan
LAP	Leucine aminopeptidase

LIST OF ABBREVIATIONS (Cont.)

Symbols/Abbreviations	Terms
LB	Luria Bertani (broth)
leg	Legumain
L. palustris	*Lymnaea palustris*
LPS	Lipopolysaccharide
L. stagnalis	*Lymnaea stagnalis*
L. truncatula	*Lymnaea truncatula*
M	Molar
mA	Milliampere
MCA	7-amino-4-methylcoumarinamide
MDH	Minimal Dextrose Histidine
MES	2(N-morpholino)ethanesulphonic acid
mg	Milligram
mg/kg	Milligram/ Kilogram
mg/l	Milligram/ Liter
MHC	Major histocompatibility complex
min	Minute
ml	Milliliter
mm	Millimeter
mM	Millimolar
MMH	Minimal Methanol Histidine
MOPS	3-(N-morpholino)propanesulfonic acid
mRNA	Messenger ribonucleic acid
MRI	Magnetic Resonance Imaging
Mt	Metacercariae

LIST OF ABBREVIATIONS (Cont.)

Symbols/Abbreviations	Terms
MTT	3-(4,5-dimethylthiazol-2-yl)-2,5-diphenyltetrazolium bromide
mu	Muscle layers
N	Normal
NBT	Nitrobluetetrazolium
N. brasiliensis	*Nippostrongylus brasiliensis*
NEJ	Newly excysted juvenile
N. fowleri	*Naegleria fowleri*
ng	Nanogram
Ni-NTA	Nickel-nitrilotriacetic acid
nm	Nanometer
NO	Nitric oxide
NOS	NO-synthase
°C	Degree Celsius
O. volvulus	*Onchocerca volvulus*
OD	Optical density(-ies)
OPD	O-Phenylenediamine Dihydrochloride
orcl	Oryzacystatin I
orcll	Oryzacystatin II
os	Oral sucker
OVA	Ovalbumin
pa	Parenchyma
pac	African puff adder venom cystatin
pg	Prostate gland
ph	Pharynx

LIST OF ABBREVIATIONS (Cont.)

Symbols/Abbreviations	Terms
PBMCs	Peripheral blood mononuclear cells
PBS	Phosphate buffered saline
PCR	Polymerase chain reaction
pfu	Plaque-forming unit
pg	Picogram
pH	Negative logarithm of hydrogen ion activity
pI	Isoelectric point
PMSF	Phenylmethyl sulfonyl fluoride
PRX	Peroxiredoxin
R. auricularia	*Radix auricularia*
RBC	Red Blood Cell
rcc	Rat cystatin C
rcs	Rat Cystatin S
rkl, rk2 and rk3	Three rat kininogen segments
RNA	Ribonucleic acid
RNase A	Ribonuclease A
RNAi	RNA interference
R. natalensis	*Radix natalensis*
rpm	Revolutions per minute
RPMI	Roswell Park Memorial Institute medium
rsa	Rat cystatin α
rsb	Rat cystatin β
RST	Rapid Sedimentation Technique

LIST OF ABBREVIATIONS (Cont.)

Symbols/Abbreviations	Terms
rtll, rkl2, rkl3	Three rat T-kininogen 1 segment
rt21, rt22, rt23	Three rat T-kininogen 2 segments
RT-PCR	Reverse transcriptase polymerase chain reaction
s	Second
sac	Sarcocystatin A
SAP	Saposin
SDS	Sodium dodecyl sulfate
SDS-PAGE	Sodium dodecyl sulfate polyacrylamide gel electrophoresis
S. japonicum	Schistosoma japonicum
S. mansoni	Schistosoma mansoni
spp	Species
SSC	Saline-sodium citrate
sv	Seminal vesicle
TBE	Tris/Borate/EDTA
TBS	Tris buffered saline
TCBZ	Triclabendazole
TEMED	N,N,N',N'- tetramethylethylenediamine
tg	Tegument
Th2 cells	T helper 2 cells
TMB	3,3',5,5' tetramethylbenzidine
TNF-α	Tumor necrosis factor-alpha
Tris	Tris (hydroxymethyl) aminomethane
Triton X-100	Iso-octylphenoxypolyethoxyethanol

LIST OF ABBREVIATIONS (Cont.)

Symbols/Abbreviations	Terms
Tween 20	Polyoxyethylene-sorbitan monolaurate
U	Unit
ut	Uterus
UV	Ultraviolet
V	Volt
v_0	Initial velocities
V_{max}	Maximal velocity
vol	Volume
vs	Ventral sucker
v/v	Volume per volume
w/v	Weight per volume
YNB	Yeast Nitrogen Base
YPD	Yeast Extract-Peptone-Dextrose
Z	Benzyloxycarbonyl

LIST OF ABBREVIATIONS (Cont.)

Amino acid codes and abbreviations

Nonpolar and uncharged

A	Ala	Alanine
F	Phe	Phenylalanine
G	Gly	Glycine
I	Ile	Isoleucine
L	Leu	Leucine
M	Met	Methionine
P	Pro	Proline
V	Val	Valine
W	Trp	Tryptophan

Polar and uncharged

C	Cys	Cysteine
N	Asn	Asparagine
Q	Gln	Glutamine
S	Ser	Serine
T	Thr	Threonine
Y	Tyr	Tyrosine

Positively charged (basic)

H	His	Histidine
K	Lys	Lysine
R	Arg	Arginine

Negatively charged (acidic)

D	Asp	Aspartic Acid
E	Glu	Glutamic Acid

CHAPTER I

INTRODUCTION

Fascioliasis is an important helminth disease caused by flat worms of the genus *Fasciola* (*Fasciola hepatica* and *Fasciola gigantica*). *F. hepatica* is present mostly in temperate regions, particularly in Europe, South and Central America, Oceania, Asia and Africa while *F. gigantica* is distributed in tropical and subtropical regions, especially in Africa, Middle East and Asia including Thailand. These parasites cause a zoonotic infection affecting ruminants such as cattle, buffaloes, sheep, goats and swine. Humans are accidental hosts of these parasites if they ingest vegetation contaminated with metacercariae or drink contaminated water and recently a number of cases have been reported in Thailand. Fascioliasis is a major veterinary problem causing weight loss, diarrhea, loss of milk, meat, wool production, increased mortality in livestock which lead to an economic loss estimated at 3.2 billion US dollars per year.[1] The number of reported clinical cases of human fascioliasis is increasing significantly with an estimated 2.4 million people infected in many countries of Latin America, Europe, Africa and Asia and more than 180 million are estimated at risk.[2] The treatment of choice is triclabendazole (TCBZ) which is effective against all stages of the parasites. TCBZ is used in control of fascioliasis of livestock in many countries but now resistance to this drug has been reported. Resistance of TCBZ has been first reported in Australia in the 1990s and now resistance to this drug has also been found in a number of countries throughout Europe.[3,4] To solve this problem several sustainable strategies such as novel drugs and vaccines have been investigated for application. Nowadays, the major research is focused on the host-parasite interactions since parasites resistant to chemical treatments have emerged in several countries.

Cathepsins B and L cysteine proteases are the major lysosomal cathepsins that are involved in host-parasite interactions including tissue penetration, feeding, digestion of host tissue for nutrition and evasion of immune system.[5] In trematodes, the number of reports about the roles of cysteine protease inhibitors in

the cystatin superfamily (MEROPS inhibitor family I25, clan IH) is still small. Cystatins can be divided into three groups based on distinct structural details and their distribution in the body. Type I cystatins contain no disulfide bonds or carbohydrate groups and are mainly intracellular including stefin A and B. Type II cystatins contain one or two conserved disulfide bonds, a signal peptide for secretion and are found in most body fluids such as cystatins C, D, E/M, F, S, SA and SN. Type III cystatins are extracellular multi-domain cystatins, for example kininogens that are intravascular proteins of blood plasma. Cystatins are found in viruses, bacteria, parasites, microorganisms, plants and animals. Maintenance of the balance of cysteine proteases and cystatins is essential for proper functioning of all living organisms. Cystatins play an important role in the balance of the host–parasite interaction, protection of cells from inappropriate endogenous or external proteolysis, the control mechanisms responsible for intracellular or extracellular protein breakdown and regulation of normal proteolytic processes involving cysteine protease activity. Imbalance between cysteine proteases and inhibitors lead to metabolic error of the affected cells and results in various diseases such as renal failure[6], osteoporosis[7] and rheumatoid arthritis[8]. The mechanism of cystatin is to block the protease active site, obstruct the approach of substrate, but do not directly interact with the enzyme catalytic center. Several studies concerning trematode and nematode cystatins have been published. For example, the inhibitory activities of a type 1 cystatin from *Schistosoma mansoni* and *F. gigantica*[9,10], a multi-domain cystatin from *F. hepatica* and *F. gigantica*[11,12], onchocystatin of the human pathogenic filarial nematode *Onchocerca volvulus*[13], rAv17 of *Acanthocheilonema viteae*[14], Bm-CPI-1, Bm-CPI-2 and Bm-CPI-3 of *Brugia malayi*[15], cystatin of the rodent filaria *Litomosoides sigmodontis*[16] and nippocystatin of *Nippostrongylus brasiliensis* [17,18] have been reported. In the last few years, immunomodulatory effects of cystatins from parasitic nematodes have been demonstrated. These cystatins were found to be involved in the reduction of T cell responses by inhibition of proteases participating in MHC class II antigen processing and presentation, furthermore they stimulated the upregulation of interleukin 10 (IL-10) and nitric oxide (NO) production while downregulation of IL-12.[19-23]

To understand the biological function of type 1 cystatin in *F. gigantica*, several experiments were performed in this parasite including molecular cloning and characterization of a cystatin encoding cDNA from *F. gigantica*, expression and purification of recombinant cystatin in prokaryotic expression systems, tissue-specific distribution, the inhibition properties against mammalian and endogenous cysteine proteases, pH dependency, temperature stability and preliminary study on immunomodulatory properties of the protein. Moreover, recombinant *F. gigantica* cathepsin B5 was expressed in a eukaryotic expression system, purified and characterized for its biochemical functions. The recombinant cathepsin B5 was used to confirm the results of inhibitory activity of type 1 cystatins which were analyzed in this study. The results of this work might be helpful for the application of type 1 cystatin in diagnosis and vaccine development against fascioliasis.

CHAPTER II

OBJECTIVES

The aims of the research study are:

1. Molecular cloning of a complete cDNA encoding *Fasciola gigantica* Stefin-2 (FgStefin-2).

2. Characterization of the nucleic acids encoding FgStefin-2 at genomic DNA and RNA levels by Southern, Northern, and developmental stage-specific RT-PCR analyses.

3. Expression and purification of recombinant FgStefin-2 in a prokaryotic expression system.

4. Production of mouse polyclonal antibodies against rFgStefin-2.

5. Identification of native FgStefin-2 in immunoblots of parasite antigen preparations and analysis of cross reactivity with antigen preparations from other trematodes and recombinant cystatins.

6. Determination of the tissue-specific distribution of native FgStefin-2 by immunohistochemistry.

7. Functional characterization of rFgStefin-2.

8. Characterization of the immunomodulatory properties of rFgStefin-2.

9. Expression and purification of recombinant FgCB5 in a eukaryotic expression system.

10. Functional characterization of rFgCB5

CHAPTER III

REVIEW OF LITERATURE

3.1 Fascioliasis

3.1.1 Definition and classification of *Fasciola* species

Fascioliasis is an infectious parasitic disease common in livestock, especially cattle, sheep, goats, swine but occasionally found in humans. Economic losses such as reduction of both productivity (milk and meat yields) and life of ruminants are particularly incurred with infected cattle and sheep. This disease is caused by infection with *Fasciola* species[24], endoparasites classified in the kingdom of Animalia, phylum Platyhelminthes, class Trematoda, subclass Digenea, family Fasciolidae and genus *Fasciola*. The two species *Fasciola hepatica* (the common liver fluke) and *F. gigantica* (tropical liver fluke) are the main causative agents of fascioliasis. Most of the parasites in the family Fasciolidae are hermaphroditic and able of self-fertilization. In general, the life cycles of trematode parasites are complex and require one or more intermediate hosts for development, a lack of the intermediate host will terminate the life cycle.

3.1.2 Geographic distribution and epidemiology of *Fasciola* spp.

Fascioliasis has been found widespread in many geographical areas and affects more than 51 countries of the five continents. *F. hepatica* is present mainly in temperate regions, particularly in Europe, South and Central America, Oceania, Asia and Africa while *F. gigantica* is found in tropical and subtropical regions, especially in many areas of Africa and Asia.[25,26] The geographical spread routes and distribution of the two parasites are shown in **Figures 3.1 and 3.2**.

Epidemiology is the study of factors affecting disease in populations. The study of the epidemiology and transmission revealed that the worldwide geographical distribution of fascioliasis is related to the distribution of lymnaeid snail host populations, climatic conditions and general physical geography. Globally, there are many people infected with *Fasciola* spp. (up to 2.4 million

humans) and more than 180 million are estimated at risk.[2] Worldwide, *F. hepatica* and *F. gigantica* infect more than 300 million cattle and 250 million sheep that causes the economic losses estimated at more than US$3.2 billion per year.[1] An analysis of geographical distribution of human and animal fascioliasis shows that a correlation exists only at a basic level. Several factors that have an effect for the association between human and livestock infection are sanitation and hygiene conditions, education of people, culture in each country and human eating behavior. Therefore, areas with high prevalence of animal fascioliasis do not seem to be associated with areas that have a lot of human fascioliasis cases. For example, in Australia, many cases of animal fascioliasis have been reported, whereas human cases have only been sporadically observed.[27]

During 2003-2006, The National Institute of Animal Health, Thailand listed the prevalence of animal fascioliasis (**Figure 3.3**) and the results showed the high prevalence of the infection in Northeastern and Southern parts of Thailand. The number of infections that was reported in 2006 was impressively increased and the highest infection rate was observed during the rainy season. The average prevalence of *F. gigantica* in cattle and buffalo in Thailand has been reported at 11.8%.[28]

A
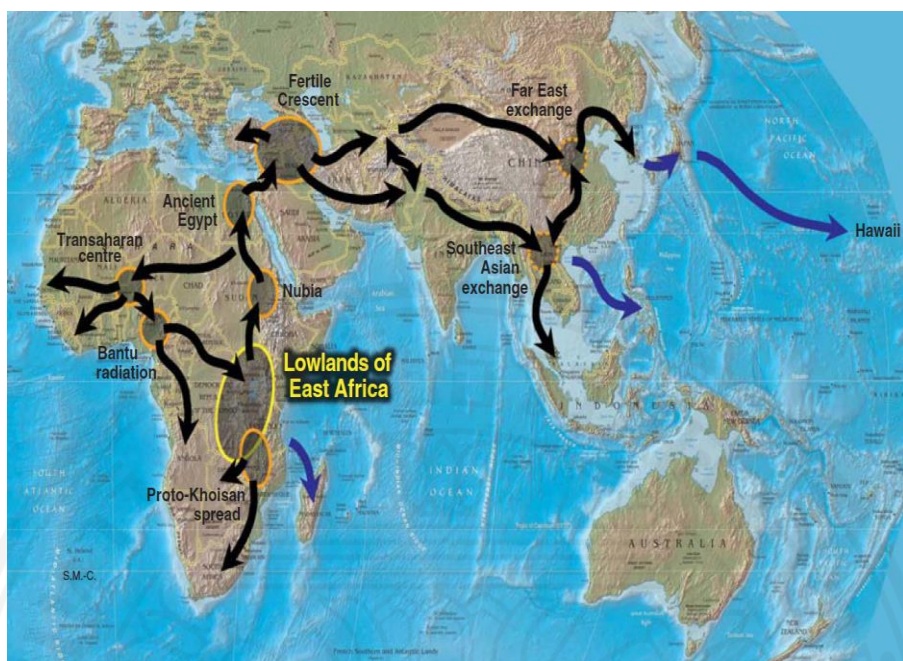
(A)

B
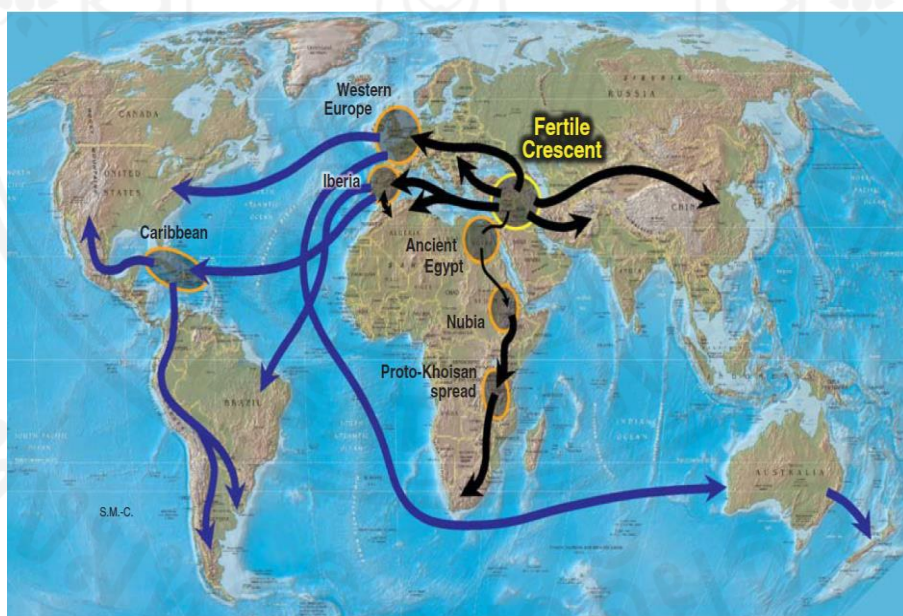
(B)

Figure 3.1 Geographical spread routes of *F. gigantica* (Panel A) and *F. hepatica* (Panel B) in the post-domestication period.[29]
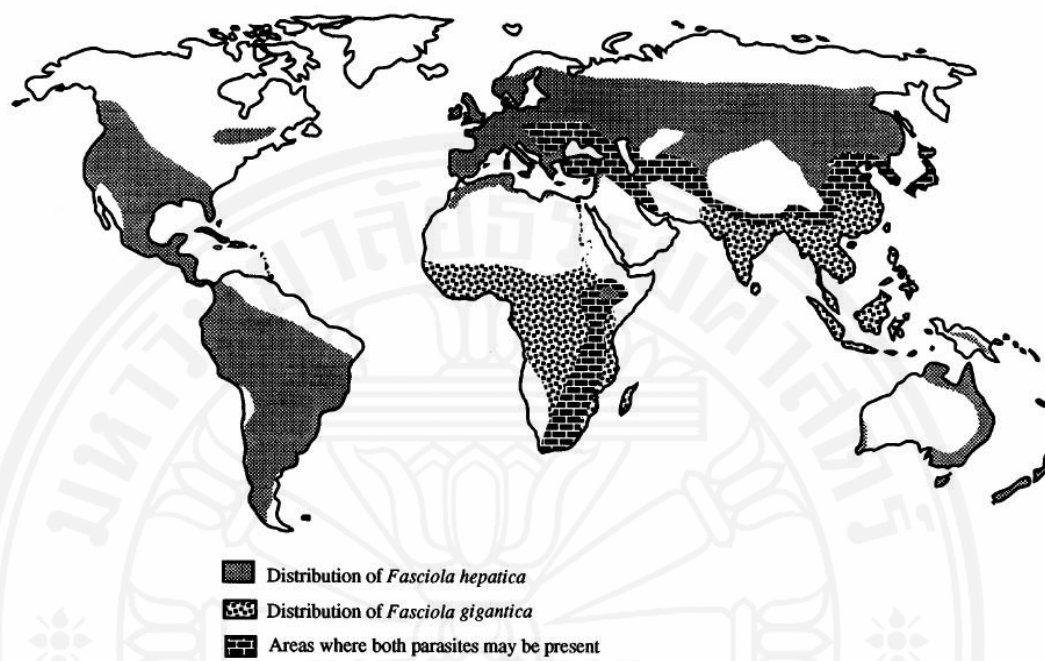
Figure 3.2 Global distribution of *F. hepatica* and *F. gigantica*.[29]
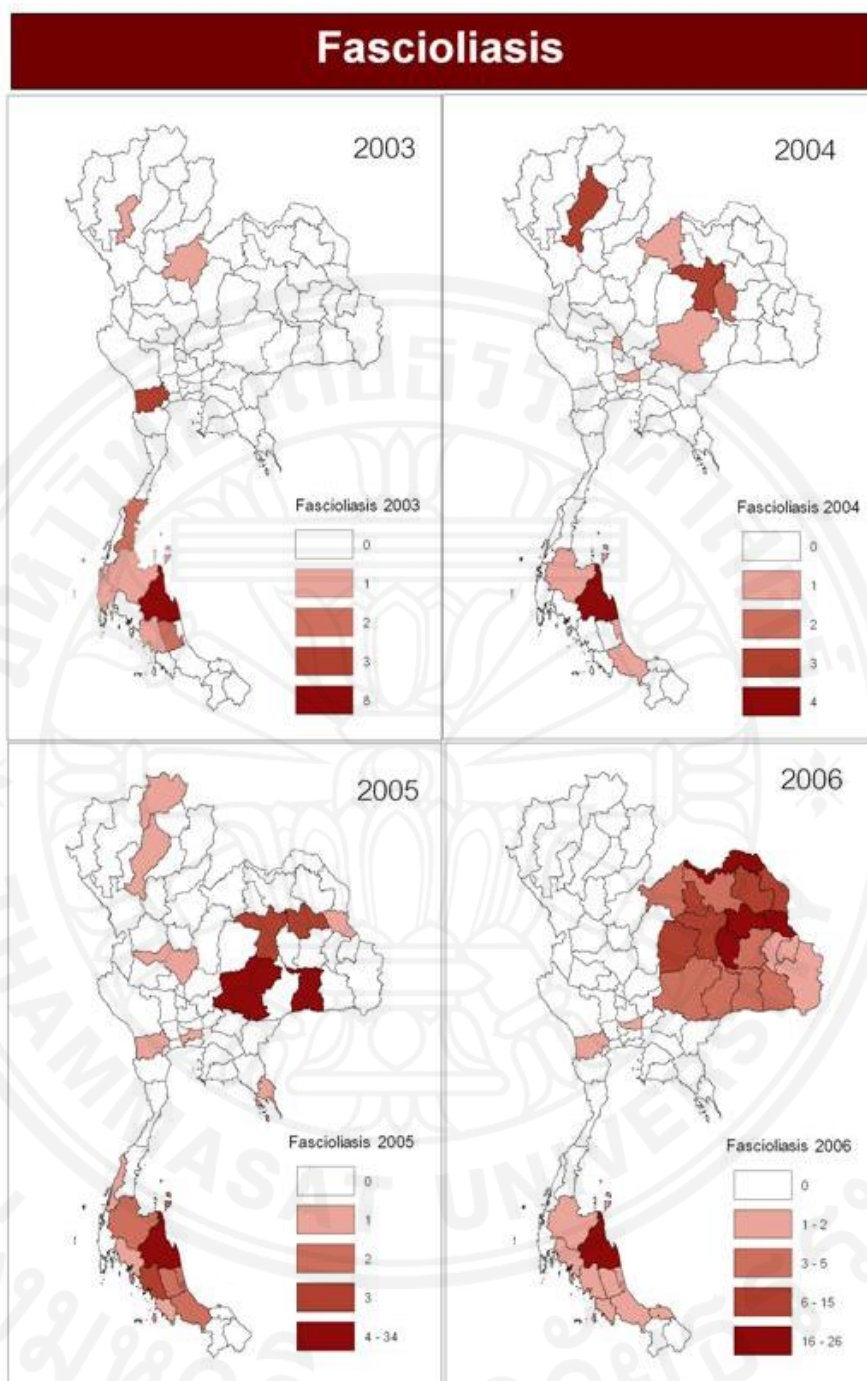
Figure 3.3 Distribution of animal fascioliasis in Thailand during 2003–2006.[30]

3.1.3 The Morphology and life cycle of *Fasciola* spp.

Both *Fasciola hepatica* and *Fasciola gigantica* have a leaf-like shape but are quite different in the size of their body. The size of adult *F. hepatica* is approximately 20-30 mm in length and 8-13 mm in width while *F. gigantica* which is approximately 20–70 mm in length and 8–15 mm in width.[31] The adult worm has a cephalic cone which consist of an oral sucker at the anterior end and a ventral sucker is located at the base. The digestive tract of the adult parasite extends from the anterior to the posterior end of the worm and the structure of the intestine looks like a branched tree. The two highly branched testes are found in the posterior half of the worm. The ovary, located above the testes, opens to a genital pore via a link to a short convoluted uterus. The genital pore is located anterior to the ventral sucker. In the lateral and posterior regions of the body, the vitellaria are highly diffused and branched to produce the shell material. The general surface of the worm is covered by spines that can help the parasite to preserve its position in the host tissue and serve to destroy the epithelium and penetrate the blood vessels for feeding. The external morphologies and internal structures of *F. hepatica* and *F. gigantica* are shown in **Figures 3.4A and 3.5**. The first larva stage that hatches from the egg is the miracidium and the size of this larva is approximately 130 μm in length. The structure of miracidium is large at the anterior end, tapering posteriorly to a blunt end and its body is covered with cilia. In the anterior region, papilliform protrusion and two darkly stained eye spots are found (**Figure 3.4B**). A sporocyst is elongated bag-like and contains a small ball of tightly packed germinal cells and eye spots can be found (**Figure 3.4C**). The redia, produced by the sporocyst contains an incomplete digestive system with an anterior mouth, a muscular pharynx, and a simple unbranched intestine. Several germinal cells contained in the redia are further differentiated into second generation daughter rediae or the next larva stage, the cercaria (**Figure 3.4D**). The cercaria has a structure like a tadpole which consists of a circular body measuring approximately 0.25-0.35 mm in length and a long thin unbranched tail measuring around 0.5 mm in length. An oral sucker is situated at the anterior end of the body and a ventral sucker is located at a similar position as in the adult. Leading from the oral sucker there is a pharynx which contains very

remarkable of cystogenous glands that secrete substrates to form a cyst wall, an esophagus, foregut and paired ceca. The cercaria has a parenchyma containing numerous germinal cells that support the formation of the male and female reproductive systems in adult stage and flame cells which act as excretory system (**Figure 3.4E**). The metacercaria (encysted cercaria) has a round shape measuring around 0.2 mm in diameter and its shell is composed of an outer cyst and an inner cyst. The outer cyst wall is also important for attachment to aquatic plants and vigorous adhesion for long times is essential for survival of metacercarial cyst and the infection of the definitive host. If the outer wall is eliminated, the inner wall must play a key role in the survival of the metacercaria.[32] Many cercaria components, including certain glands and sensory structures, disappear (**Figure 3.4F**). The eggs of *Fasciola* spp. are broadly ellipsoidal, operculated and sized in average around 0.13–0.15 mm in length and 0.06–0.09 mm in width which dirty gray to yellowish brown color. The eggs which are excreted through host feces on to pasture are unfertilized and several factors influence embryonation particularly, temperature, oxygen tension, pH and moisture (**Figure 3.4G**).[33]

(A) (B) (C)

(D) (E) (F) (G)
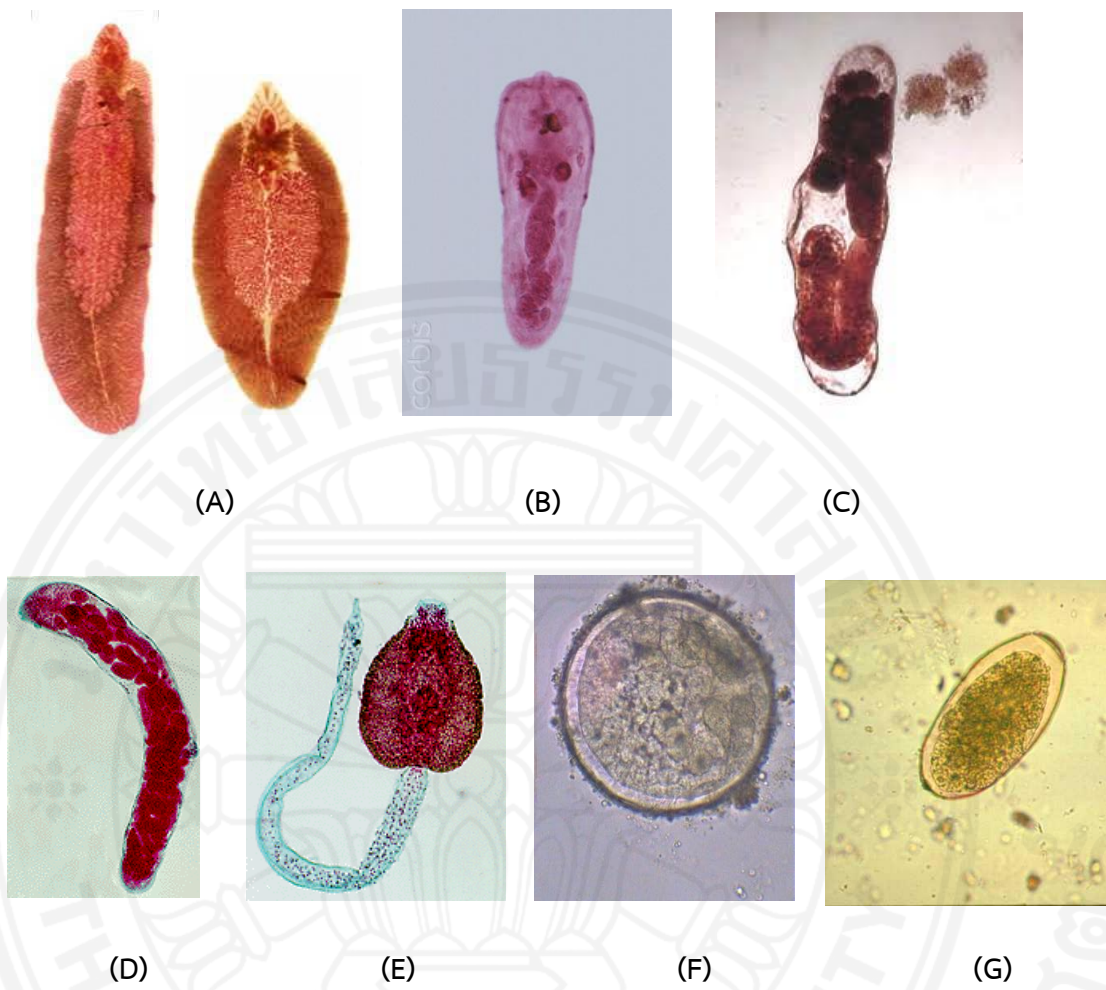
Figure 3.4 The developmental stages of *Fasciola* spp.[34-39]

(A) Adult *Fasciola* spp., left: *F. gigantica*, right: *F. hepatica*,

(B) Miracidium, (C) Sporocyst, (D) Redia, (E) Cercaria,

(F) Metacercaria and (G) Egg
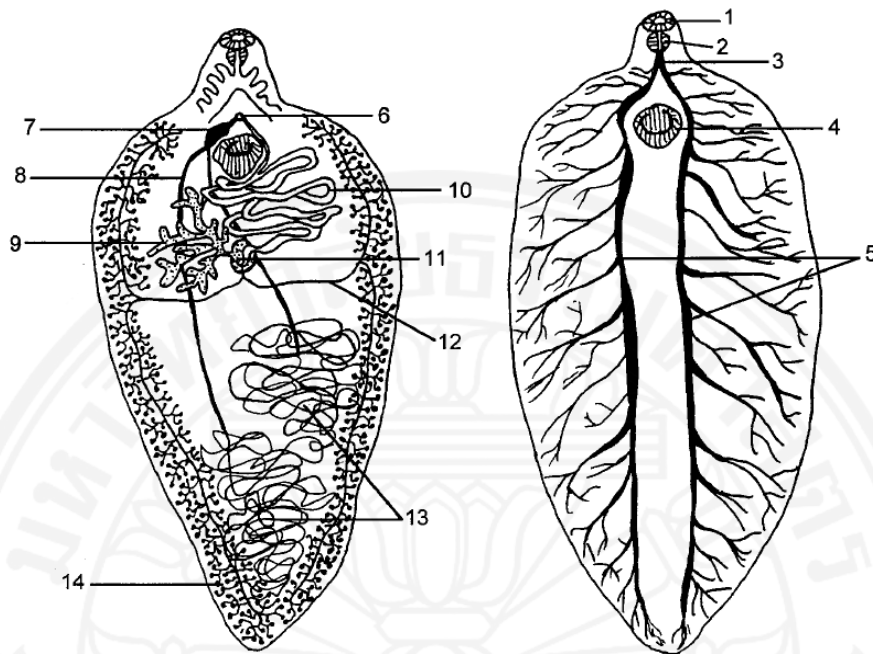
Figure 3.5 Diagram of an adult *Fasciola* spp. showing major internal structures: (1) Oral sucker; (2) Pharynx; (3) Esophagus; (4) Ventral sucker; (5) Ceca; (6) Genital pore; (7) Cirrus sac; (8) Vas deferens; (9) Ovary; (10) Uterus; (11) Ootype; (12) Vitelline duct; (13) Testes; (14) Vitelline gland.[33]

The general life cycle of *Fasciola* spp. is quite complex (**Figure 3.6**). *F. hepatica* and *F. gigantica* have a similar life cycle that consists of several stages including egg, miracidium, sporocyst, redia, cercaria, metacercaria, juvenile and adult. The life cycle of these parasites begins with unembryonated eggs which are released from the bile duct into the intestine and passed out in the feces of herbivorous animals such as ruminants (definitive hosts) or human (accidental host). Development of the embryo commences if the egg is flushed into freshwater at favorable environmental conditions. The miracidium excysts from the egg and invades the tissues of the intermediate molluscan host (first intermediate host): a snail in family Lymnaeidae such as *L. truncatula, L. stagnalis, and L. palustris* for *F. hepatica* and *Radix rubiginosa, R. auricularia, R. natalensis* and *Biomphalaria alexandrina* for *F. gigantica* (**Figure 3.7**).[25,40-42] Within the snail, the parasites undergo developmental changes from miracidia to sporocysts, rediae, cercariae, respectively in the digestive gland. The motile cercariae emerge from the snail and attach to aquatic plants and then encyst as metacercariae (infective stage of the worm). The infection occurs when ruminant or human consume the vegetation containing metacercariae. After ingestion of the contaminated vegetation, the cyst wall of the metacercariae is eliminated by digestive enzymes in the gastrointestinal tract of the host and the newly excysted juvenile (NEJ) emerges in the small intestine. The NEJs penetrate and pass through the gut epithelium into the peritoneal cavity and finally the liver. After 6–12 weeks, the parasites migrate into the bile ducts where they develop to adult stage.[1,43] The total period from ingestion of aquatic plants containing metacercariae to adult stage of the fluke is approximately 75-90 days.[43] The adult parasites remain for several years inside the bile ducts (more than 1-2 years in cattle or 20 years in sheep) and produce tens to hundreds of thousands of unembryonated eggs per day.[33,44]
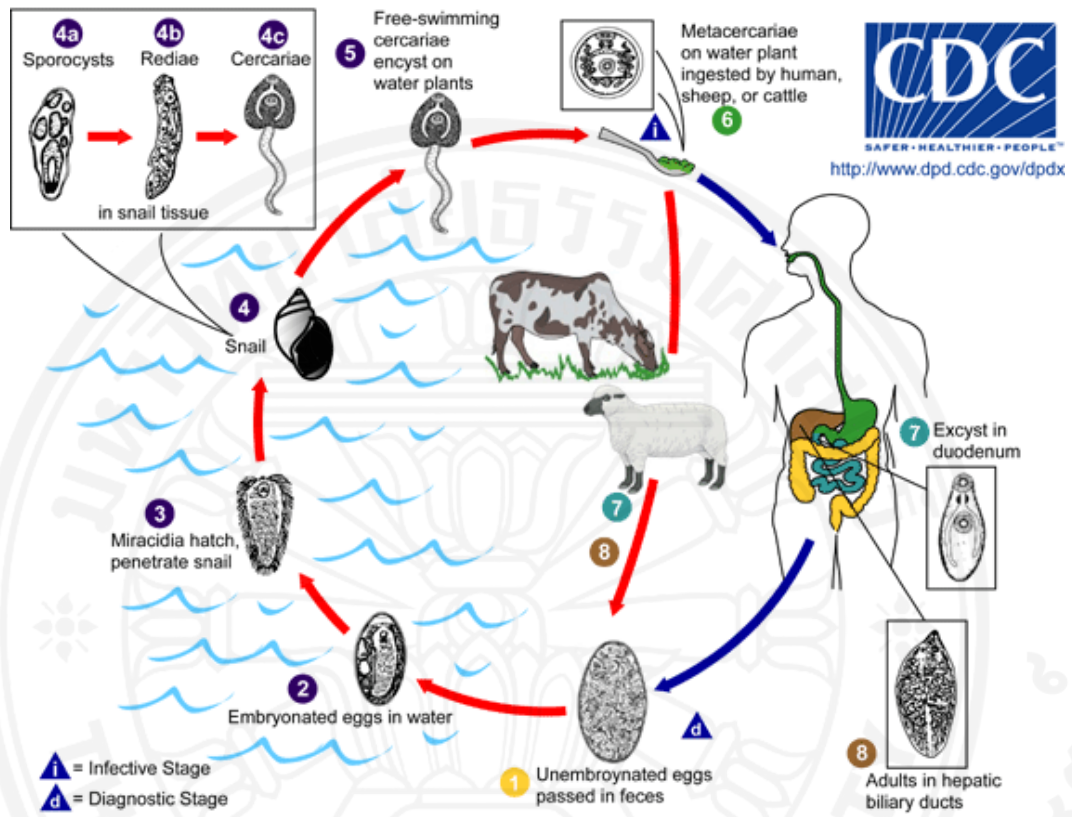
Figure 3.6 Life cycle of *Fasciola* spp.[45]
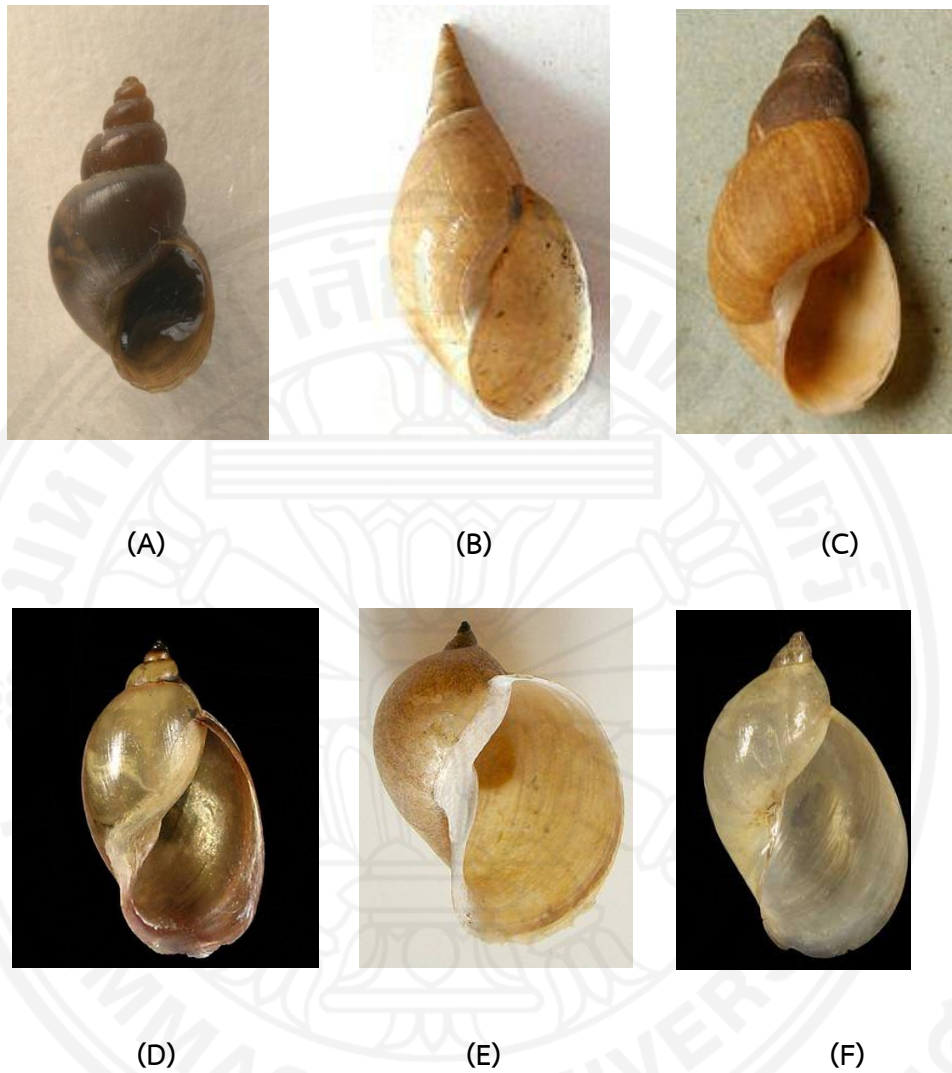
Figure 3.7 Snail intermediate hosts of *F. hepatica* and *F. gigantica.*[46-50]

(A) *L. truncatula*, (B) *L. stagnalis*, (C) *L. palustris*,

(D) *R. rubiginosa,* (F) *R. auricularia* and (G) *R. natalensis*

3.1.4 Parasite physiology in the mammalian host

3.1.4.1 Gut

The digestive tract is essential for survival of the parasite because it uses this system to consume food and clear waste out. The gut of the parasite can be divided into two parts, the foregut consists of mouth, pharynx and esophagus and the second part is formed by the paired intestinal ceca which are blind-ended and highly branched in the adult fluke. The epithelial lining of the ceca is composed of a single layer of cells that continually cycle between secretory and absorptive phases. In the secretory phase, cells that contain a lot of dense secretory vesicles crowded near the surface lamellae are abundant in active Golgi complexes, have an extensive network of granular endoplasmic reticulum (GER) cisternae and mitochondria (**Figure 3.8**). Proteins destined for secretion are synthesized in the GER at the base of the cell and transported to the Golgi where they are constructed into secretory granules. The secretory granules are transported to the apical surface where they are released into the lumen of the gut. The complete process of synthesis, transport and release of secretory proteins takes less than 60 minutes.[51] In the absorptive phase, cells show much longer and more numerous apical lamellae, possess few and largely inactive Golgi complexes, have a lack of a secretory vesicles, but contain membranous inclusions which supposedly indicate endocytosis and autophagy.[52]

The digestion in the parasite is generally an extracellular process, taking place in the cecal lumen and is then completed inside the cell. Many potential digestive enzymes have been reported that are effective in degrading various protein substrates, such as collagen, hemoglobin and immunoglobulins and cleaving trypsin and chymotrypsin substrates at alkaline pH. The substrate specificity of the enzymes is required for functions in nutrition and in immune evasion. The expression patterns of enzymes in the gut epithelial cells vary during development of the fluke.
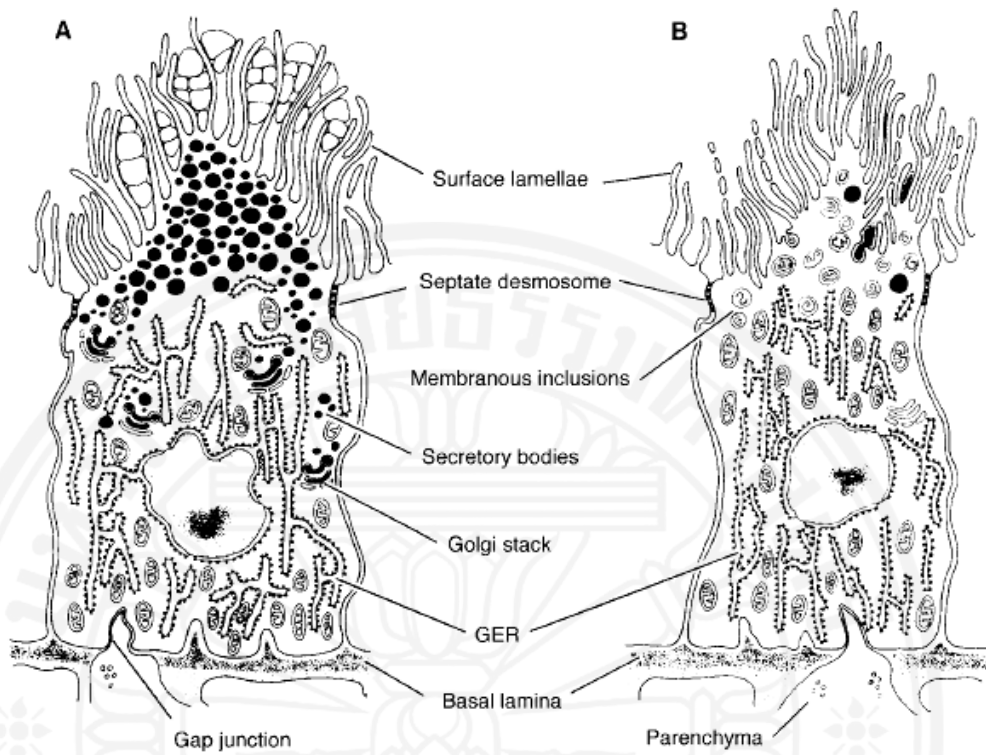
Figure 3.8 Cells of the gut epithelia. Panel A: The secretory phase and Panel B: The absorptive phase of cells lining the epithelium of the gut of adult *F. hepatica*.[53]

3.1.4.2 Reproductive System

The reproductive system of *Fasciola* spp. is hermaphrodite. The male reproductive system comprises testes, vas deferens, seminal vesicle, ejaculatory duct, cirrus sac, genital atrium and prostate glands (**Figure 3.9**). Two multi-branched testes with one located anterior to the other. The testes are connected to the seminal vesicle which is located within the cirrus sac via the vas deferens. The seminal vesicle, filled with mature spermatozoa, passes into a very narrow and coiled duct called ejaculatory duct and then towards the cirrus sac. The protrusible cirrus opens independently to the outside via the genital aperture in a common genital atrium that is located anterior to the ventral sucker. The ejaculatory duct is neighbored by numerous unicellular prostate glands. The prostate gland cells are pear-shaped and the individual cells of this gland present a high level of secretory activity. The ducts of the gland cells are long and lead through the parenchyma towards the ejaculatory duct. Junctional complexes between the prostate gland cells and the parenchyma cells have not been observed.

The female reproductive organs are composed of ovary, oviduct, vitelline glands, Mehlis' gland, uterus and Laurer's canal (**Figure 3.9**). The ovary is highly branched and situated at the right side of the proximal part of the uterus and the Mehlis' gland-ootype complex. The outer wall of the ovary consists of the muscle layers and it is lined by a layer of nurse cells. The nurse cells are composed of mitochondria and endoplasmic reticulum cisternae and in contact with oogonia. The oogonia are located at the periphery of the ovary and the latter differentiate into primary oocytes which move towards the center of the ovary. The short and narrow tube that connects the ovary to the uterus is called oviduct. Vitelline glands consist of several follicles and the vitelline cells in the follicle produce albumin, yolk, nutrients to support the development of embryo and shell material involved in egg formation. The newly formed egg passes from the ootype into the proximal part of the uterus, where the fertilization takes place. The ootype is the organ where the formation of eggs occurs and surrounded by the Mehlis' gland. The Mehlis' gland is composed of two types of secretory cells: one group

secretes a membranous body, and the other secretes a dense body. Several functions of this gland has been demonstrated such as the lubrication of the eggs in the uterus, activation of sperm and release of shell material from the vitelline cells.[52,54]
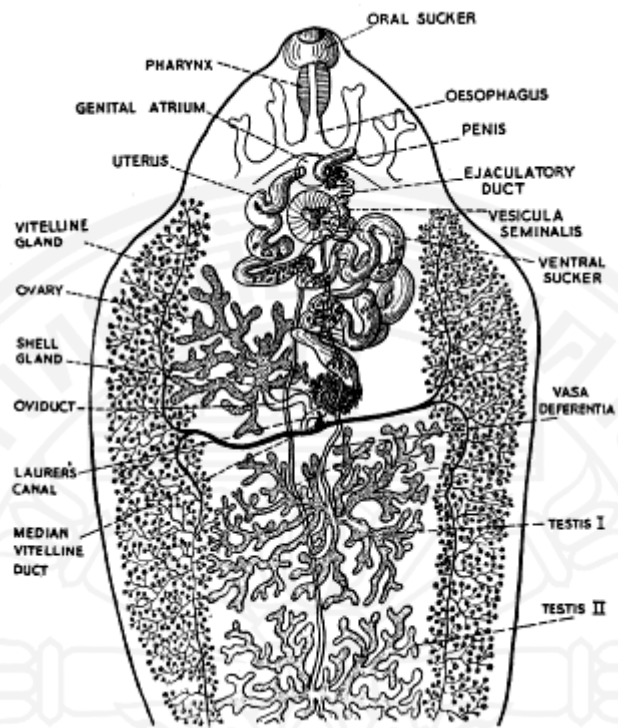
Figure 3.9 Diagram of an adult *Fasciola hepatica* showing major structures.[55]

3.1.5 Pathogenesis

Fascioliasis is a highly pathogenic disease in human and animal and pathogenesis of this disease depends on the number of infecting worms, the nutritional status and the resistance of the host.[28,56,57] The pathology of fascioliasis is divided into two phases; 1.) The parenchymal phase: in this phase, the pathology occurs during the migration of excysted juvenile flukes from intestine to the liver causing tissue damage, extensive hemorrhage, fibrosis, and severe liver damage.[58] The flukes occasionally migrate to ectopic sites (Ectopic fascioliasis) for example, diaphragm, kidneys, heart, brain, muscle, genitourinary tract, skin, lungs, eyes and subcutaneous tissue.[57,59] 2.) The biliary phase arises from mature parasites that are located in the bile ducts. The pathology of this phase results from feeding on host blood and hypertrophy of bile ducts which causes obstruction of the lumen and tissue damage.[60] The number of ingested metacercariae affects signs and symptoms of fascioliasis. Acute fascioliasis (more than 1,000 ingested metacercariae) may cause sudden death of livestock, particularly in sheep, goat and cattle. The clinical signs of this stage are acute hemorrhagic anemia, hypoalbuminemia, abdominal pain, eosinophilia and ascites. Subacute fascioliasis (800-1,000 ingested metacercariae) usually occurs 6-10 weeks after infection. This stage may cause sluggishness, anemia, weight loss and eventually death. Chronic fascioliasis (200-800 ingested metacercariae) is commonly seen in six months, when the flukes mature in the bile ducts. This stage is usually asymptomatic or shows anemia, hypoalbuminemia, ventral edema, pallor of mucous membranes, weight loss and wool break emaciation. Therefore, fascioliasis of livestock affects the economic system in countries where this disease has a high prevalence rate.

Human is an accidental host for *Fasciola* and the pathogenesis begins when young flukes migrate from the intestine to the liver parenchyma and become mature in the bile ducts as described above. The forms of human infection include the incubation phase, acute phase, chronic phase, ectopic fascioliasis, and halzoun. The period between ingestion of metacercariae to the presence of the first symptoms is called incubation period. This period usually occurs in a few days to 90 days after ingestion of metacercariae depending on immune system of the host and

the number of ingested metacercariae. Acute phase usually begins within 6 to 8 weeks after infection or until the excysted juvenile worms migrate through bile ducts and develop to mature parasites. The symptoms of this phase are fever, ascites, vomiting, diarrhea, abdominal pain, nausea, anemia, hepatomegaly, urticaria, anorexia, jaundice, mild eosinophilia (early infection), hypereosinophilia (mid or late acute infection) and some respiratory symptoms such as chest pain, cough may occur.[61,62] Chronic phase is usually seen six months after ingestion of metacercariae and may last several years (more than 10 years)[62]. Half of the infected cases are asymptomatic and others have some symptoms such as epigastric and right upper quadrant pain, hepatomegaly, biliary colic, extrahepatic cholestasis, diarrhea, nausea, fatty food intolerance, vomiting, wasting, jaundice, pancreatitis and cholangitis can occur.[63-66] Eosinophilia may or may not be present in the chronic phase. There are several publications that reported the percentage of eosinophilia in chronic infection cases such as only 11% of 18 cases with chronic fascioliasis in Turkey had eosinophilia at presentation, whereas 47% of 277 patients in Costa Rica had eosinophilia.[67,68] In Peru and other Latin American countries, 43.5% of subjects had eosinophilia.[69] Ectopic fascioliasis is similar to animals as described above. The pathology of this phase occurs during the migration of the flukes causing tissue damage with inflammation and fibrosis. Halzoun or pharyngeal fascioliasis begins when human consumes raw liver of an infected animal especially, sheep, goat and cattle. The living flukes move from the liver to upper respiratory tract (pharyngeal mucosa). The symptoms of this phase are pain, dysphagia, facial and neck edema, dyspnea, bleeding, pharyngitis and airway obstruction. Cases of halzoun have been reported in the Middle East including Lebanon.[70,71]

3.1.6 Diagnosis of fascioliasis

The most widely used method to diagnose fascioliasis is the finding of parasite eggs for example, the thick smear Kato-Katz method in which the parasite eggs in in the feces are examined to measure the intensity of infection. Other coprological examinations are the Rapid Sedimentation Technique (RST) and ether-formol concentration method. There are a lot of publications which used RST to identify this disease.[61,63,72-74] The coprological examinations are not completely

reliable because the fluke eggs cannot be detected in the acute phase and prepatent period of the disease. Furthermore, there are many situations that can cause trouble to detect the eggs in the stool sample such as sporadic release of eggs and weak infection.

Serodiagnostic techniques including ELISA and Western blots were developed to overcome the problems of the coproparasitological tests. These methods are used for diagnosis during the acute phase and based on the detection of antibodies against parasite antigens such as excretory/secretory (E/S) antigens, recombinant *F. hepatica* cathepsin L1, saposin-like protein-2 and *F. hepatica* antigen termed FAS 2.[1,61] In a study from Peru Fas2-ELISA (cathepsin L1-based antibody) was used for diagnosis of fascioliasis in 634 children. This study showed 92% sensitivity and 84% specificity, with a negative predictive value of 97.2% and the result demonstrates that Fas2-ELISA is a high sensitivity technique for the detection of *F. hepatica* infection.[75] An ELISA antigen capture technique has been developed using chicken egg cystatin to capture the recombinant cathepsin L1 in bacterial lysates containing the recombinant protein before analysis by the standard ELISA procedures. Analysis of the sera of *F. gigantica* infected patients, other parasitic infections patients and healthy controls demonstrated 100% sensitivity, 98.92% specificity, 98.97% accuracy and 100% negative predictive value. This result also demonstrates that this method is highly sensitive in the diagnosis of human fascioliasis.[76] The ELISA technique has high sensitivity and specificity but cross-reactivity with other parasitic infections such as *Schistosoma bovis, Paramphistomum microbothrium and Dicrocoelium hospes* has been reported.[77] Dot-ELISA, an easy and rapid test, is another method that is used for diagnosis of fascioliasis. The efficacy of sandwich ELISA and Dot-ELISA has been investigated and the study demonstrated that the ELISA technique had 94.8% sensitivity and 95% specificity, whereas Dot-ELISA showed 98.9% sensitivity and 98.3% specificity. This study indicates that the efficacy of Dot-ELISA is better than sandwich ELISA.[78] Furthermore, dipstick ELISA and lateral flow have been developed for easier diagnosis. These methods were reported to possess high sensitivity, specificity and accuracy, and to allow easy and rapid diagnosis of fascioliasis.[79-81]

Imaging, too has been applied for diagnosis of fascioliasis such as cholangiography, endoscopic retrograde cholangiopancreatography (ERCP) but the most common is ultrasonography, computed tomography (CT) and Magnetic Resonance Imaging (MRI).[82] CT scan and MRI were used to detect attenuation, structural change and location of multiple lesions in liver, track-like hypodense nodules with subcapsular position due to migration of the fluke through the liver, subcapsular hematoma, necrotic granuloma in the liver parenchyma and cystic calcifications.[62,83] Ultrasonography, cholangiography and ERCP can be used in the chronic infection phase to visualize the adult flukes in the gall bladder and bile ducts. Furthermore, these methods were used to detect hepatomegaly, multiple nodular, splenomegaly, thickened gall bladder and bile duct wall and cholelithiasis (gallstones).[62,83-85] A disadvantage of imaging techniques is potential misdiagnosis as cancer.

3.1.7 Treatment of fascioliasis

Several drugs are used to treat fascioliasis. Dehydroemetine, phenoxyalkanes (diamphenethide), salicylanilides (closantel), halogenated phenols (bithionol), sulfonamides (clorsulon) and benzimidazoles (triclabendazole) are drugs of choice for the treatment of fascioliasis. Many years ago, bithionol at doses of 30 to 50 mg/kg in three divided doses on alternate days with a total of 10 to 15 doses was recommended to control *Fasciola* infection. A cure rate of this drug in the treatment of fascioliasis varying from 50–90% has been reported.[1,86] The problems of this drug are high dose, costs and a lot of side effects such as abdominal pain, diarrhea, urticaria, nausea and anorexia. Currently, triclabendazole (Fasinex, TCBZ) a benzimidazole compound [6-chloro-5-(2, 3-dichlorophenoxy)-2-methyl is the most common drug that has high efficacy in acute and chronic fascioliasis in human and livestock. TCBZ is relatively well tolerated and the cure rate of this drug in fascioliasis is more than 90%, side effects have not been reported.[61,62] The recommended dose of this drug is 10 mg/kg body weight orally 1 or 2 days. TCBZ is quickly removed by the liver and oxidized to sulfoxide and sulfone metabolites.[87] However, resistance of the liver fluke to triclabendazole in animals has been reported in several countries including Australia (first country)[4], Scotland[88],

Netherlands[89], Argentina[90] and Peru[91]. To solve the problem of triclabendazole resistance, new drugs are developed to replace TCBZ. Compound alpha [5-chloro-2-methylthio-6-(1-naphthyloxy)-1H-benzimidazole] is a triclabendazole derivative and causes disruption of the circular muscle bundles, tubulin immunoreactivity within the tegumental syncytium and swelling of the tegument, blebbing, mitochondria and basal infolds of liver flukes from a TCBZ-resistant isolate.[87,92] This new drug has been shown to be 100% effective against different ages of flukes in sheep.[93] Other compounds that have been tested as replacement of triclabendazole are artemether and OZ78 that has shown 100% reduction of worm burden.[94] All new drugs are an alternative for treatment of fascioliasis in areas where triclabendazole resistance is common.

3.1.8 Control and prevention of fascioliasis

The infection with *Fasciola* depends on several factors such as the presence of fresh water reservoirs and the intermediate host (fresh water snails), lack of knowledge about the fluke and drug to treatment parasitic infection, the consumption of aquatic plants containing metacercariae or raw liver infected with immature flukes, etc. Therefore, the control and prevention of fascioliasis may be accomplished by giving education to all people in both endemic and non-endemic areas, using molluscicides and chemotherapy. People should be careful about dietary habits including the consumption of many aquatic plant species containing metacercariae, e.g. watercress, *Taraxacum dens leonis* (dandelion leaves), *Valerianella olitoria* (lamb's lettuce), *Mentha viridis* (spearmint)[27], *Nasturtium* spp. and *Mentha* spp.[95], *Juncus andicola* (Juncaceae), *Juncus ebracteatus* (Juncaceae), *Mimulus glabratus* (Scrophulariaceae), *Nostoc* sp. (Cianofitas).[96-98] Also, raw liver, possibly infected with *Fasciola* spp. should be avoided, kitchen utensils should not be cleaned with water from contaminated reservoirs. Educational and practical programs could help to decrease infection rates or prevent fascioliasis such as teaching about washing raw vegetables with potassium permanganate or 6% vinegar for 5-10 min to eliminate the encysted metacercariae or teaching children to avoid risky behavior that could lead to parasite infection, to drink only bottled or boiled water and to clean hands before and after the meal.[60] Molluscicides can be used to

control fascioliasis by reducing the population of snail intermediate hosts of *Fasciola* spp. However, control of the disease by using chemical treatment to block transmission and destroy the snail population exhibits problems such as toxicity to other organisms in the aquatic ecosystem. Snails have high reproductive capacity and a wide distribution within the aquatic system so, any survivors could rapidly re-populate the environment. The chemicals that can be used as molluscicides: metal salt (iron III phosphate and aluminium sulfate), metaldehyde, acetylcholinesterase inhibitors and methiocarb. Moreover, chemotherapy (drug-treatment) as described in 3.1.7 is another procedure to regulate this disease. Several factors that are involved in the control of *Fasciola* infection by interrupting the life cycle of the fluke are shown in **Figure 3.10**.
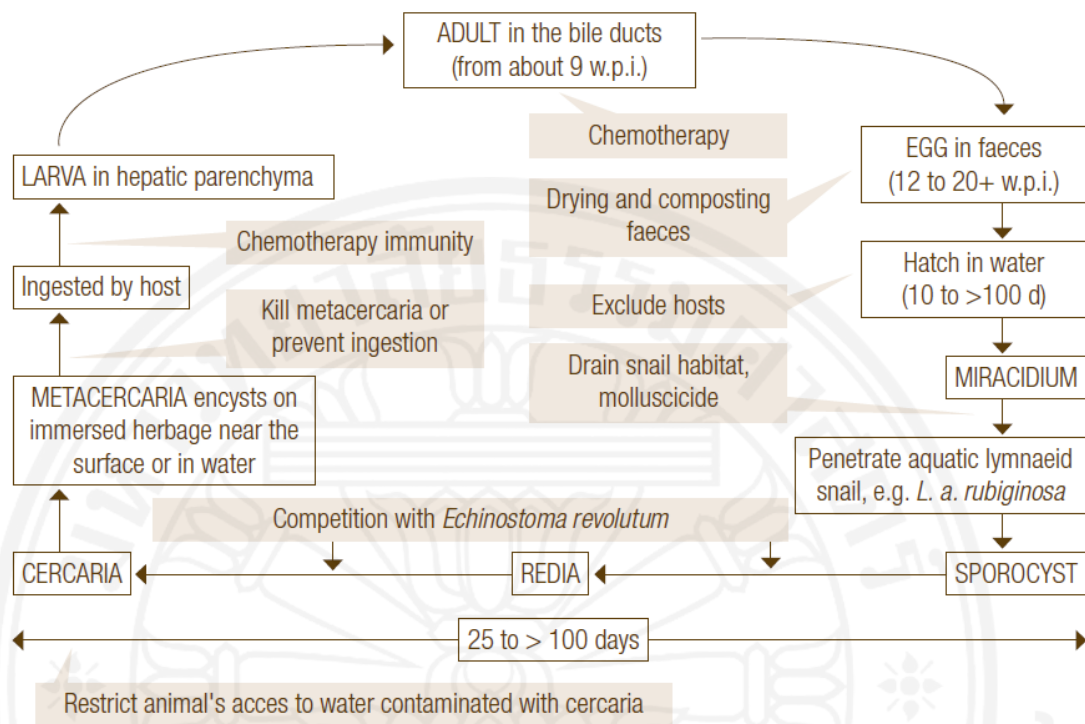
Figure 3.10 Diagram of control options (in shaded boxes) which show in the life cycle of *Fasciola* spp. (w.p.i. = weeks post infection)[99]

3.19 Vaccine against animal fascioliasis

Immunization with candidate vaccines did not only result in reduced fluke burdens, but also smaller flukes, fewer eggs, less liver pathology, all leading to better well-being of the livestock.[100] Several studies demonstrated that vaccines based on specific *Fasciola* antigens can protect animals from infection. Irradiated metacercariae and a number of specific proteins, including fatty acid-binding protein (FABP), glutathione S-transferase (GST), paramyosin, leucine aminopeptidase (LAP), hemoglobin (Hb), saposin (SAP), peroxiredoxin (PRX), phosphoglycerate kinase (PGK) and cysteine (cathepsin) protease have shown immunoprophylactic potential against fascioliasis.

3.2 Proteases

3.2.1 Definition and Classification of proteases

Proteases (also termed peptidases or proteases or proteolytic enzymes) comprise a large number of enzymes that bring about the breakdown of proteins into peptides or amino acids by hydrolysis of the peptide bonds that link amino acids together in the polypeptide chain forming the protein (**Figure 3.11**). They can be categorized as exopeptidases and endopeptidases depending on their site of action (**Table 3.1**). Exopeptidases catalyze the hydrolysis of the terminal amino acid of a peptide chain such as aminopeptidases and carboxypeptidase depending on whether they cleave at the N- or C-terminus respectively.[101] Endopeptidases catalyze the cleavage of internal peptide bonds in a polypeptide or protein for example, serine endopeptidases, cysteine endopeptidases, aspartic endopeptidases, metalloendopeptidases, and other endopeptidases.[102] Proteases are involved in a large number of biological regulatory processes and systems such as simple food digestion, inflammation, fertilization, protein activation, protein synthesis, protein turnover, cell growth, cell differentiation, apoptosis, tumor growth, allergy and bone remodeling. As genome-sequencing projects are completed it has become clear that approximately 2% of all expressed genes are peptidases, while 18% of SwissProt database are annotated as undergoing proteolytic cleavage.[103] The

proteases are divided into six major groups according to their basis of the catalytic mechanism, based on important chemical groups in their active site, similarity of amino acid sequence, the appropriate of pH range of activity and resemblance to inhibitors. The main catalytic types are the aspartyl (carboxyl), cysteine (thiol), glutamic, metallo-, serine and threonine proteases.[104] Examples of protease groups are shown in **Table 3.2**.

The MEROPS database has launched a new service aimed at providing comprehensive information and uniform classification of proteases and their protein inhibitors that provides a briefly detail review of the classification system by using a hierarchical structure. Proteases are classified into homologous families based on the basis of similarity of amino acid sequence. Families are grouped in a clan that can also be further subdivided such as, cathepsin B and cathepsin- L like proteases from trematodes. They are member of clan CA and belong to the C1 family, more specifically subfamily C1A. Cysteine proteases are involved in various biological processes in all living organisms (trematodes, nematodes, arthropods, plants, mammals etc.). In parasites, cysteine proteases have several important functions in excystment, hatching and molting of parasites, enzyme activation, evasion of host immune system, virulence and tissue invasion.[105]
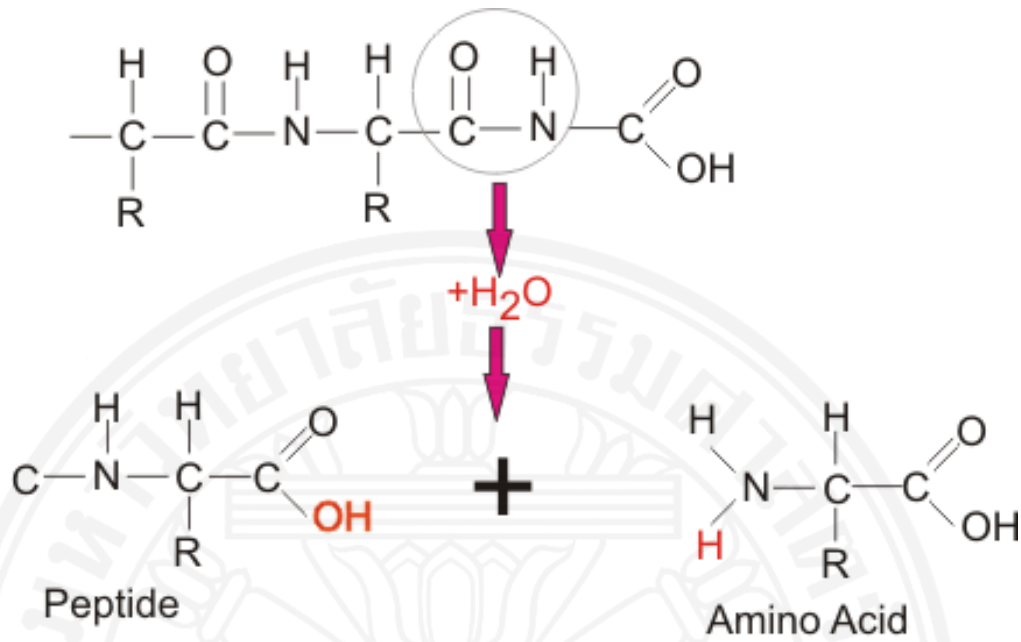
Figure 3.11 Hydrolysis of peptide bond.[106]

Table 3.1 Classification of exopeptidases and endopeptidases.

Protease	Mode of action[α]	EC no.
Exopeptidases		3.4.11
Aminopeptidases	●↓○-○-○-○---	3.4.14
Dipeptidyl peptidase	●-●↓○-○-○---	3.1.14
Tripeptidyl peptidase	●-●-●↓○-○---	3.4.16-3.4.18
Carboxypeptidase	---○-○-○-○-○↓●	3.4.16
Serine type protease		3.4.17
Metalloprotease		3.4.18
Cysteine type protease		3.4.15
Peptidyl dipeptidase	---○-○-○-○↓●-●	3.4.13
Omega peptidases	●↓● *-●↓○-○---	3.4.19
	---○-○-○↓●-*	3.4.19
Endopeptidases	----○-○-○↓○-○-○---	3.4.21-3.4.34
Serine protease		3.4.21
Cysteine protease		3.4.22
Aspartic protease		3.4.23
Metallopeptidase		3.4.24
Endopeptidase of unknown catalytic mechanism		3.4.99
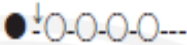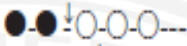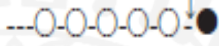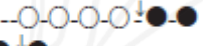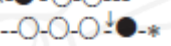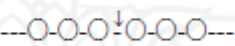
[α] Open circles represent the amino acid residues in the peptide chain. Solid circles indicate the terminal amino acids and the stars signify the blocked termini. Arrows show the sites of action of the enzyme.[102]

Table 3.2 Group of protease.[107]

Proteases	Amino acid in active site	pH optimum (range)	Proteins
Serine protease	Ser, His	7-9	Trypsin, Chymotrypsin, Elastase, Cathepsin (+) G
Cysteine protease	Cys	4-7	Papain, Ficin, Bromelain, Ananain, Cathepsin (+) B, C, H, K, L, O, S and W
Aspartic protease	(2) Asp, Try	below 5	Cathepsin (+) D and E, Renin, Pepsin
Metalloprotease	Metal ion	7-9	Carboxypeptidase A and B, aminopeptidases

3.2.2 Cysteine proteases and substrate specificity

Cysteine proteases are involved in physiological and biological processes in all living organisms and unbalanced activity of these proteases may cause several diseases such as neurological disorders, rheumatoid arthritis, osteoporosis, obesity, cancer metastasis, inflammatory diseases, muscular dystrophy, cardiovascular diseases and Alzheimer's disease.[5,108-115] The molecular mass of these proteases is approximately between 21–30 kDa and they possess highest hydrolytic activity at pH 4.0–6.5.[116] Cysteine proteases exist in viruses, bacteria, animals, and plants and have important roles in invertebrates and vertebrates, e.g. in the digestive system in nematodes, arthropods or in lysosomal protein degradation systems in vertebrates. In mammals, cysteine proteases are divided into 2 groups: (1) cytosolic calpains such as type I and type II calpain, (2) lysosomal cathepsins such as cathepsins B, C, L, S, K, V, W, X, H, F and O.[117] Trematode parasites secrete two types of cysteine proteases: (1) Clan CA (the papain-like cysteine proteases including cathepsin B and cathepsin L-like family C1) and (2) Clan CD (the legumain-like cysteine proteases).[118] In 1879, papain which is a member of the best characterized cysteine proteases family was the first isolated cysteine protease from papaya fruit (*Carica papaya*) and it was the first cysteine protease that with a resolved tertiary structure.[104] Papain has a two-domain structure, which permits a V-shaped active site (catalytic pocket) cleft to accommodate the active site residues Cys^{25}, His^{159} and Asn^{175} (papain numbering) (**Figure 3.12**).[119] The catalytic mechanism of cysteine protease is involved in formation of reactive thiolate/imidazolium ion pair ($Cys\text{-}S^-/His\text{-}Im^+$) at the pH interval 3.5–8.0 **Figure 3.13**.[110]
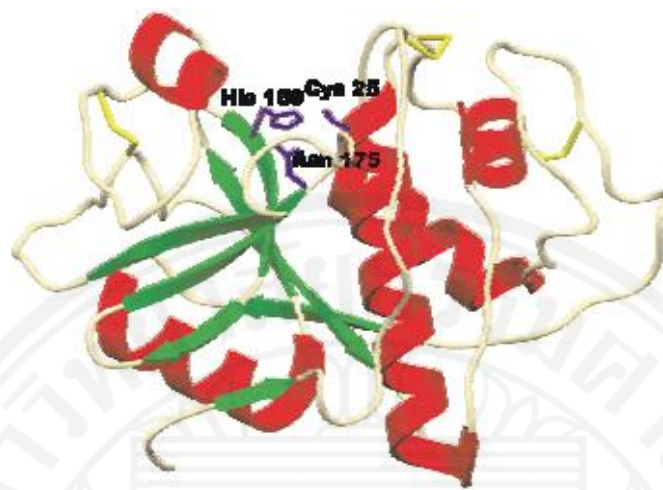
Figure 3.12 Structure of papain. Transparent molecular surface mapped onto the ribbon structure of papain, showing the secondary structure elements. Papain possesses comparable domains on each side of the active site cleft.[119]
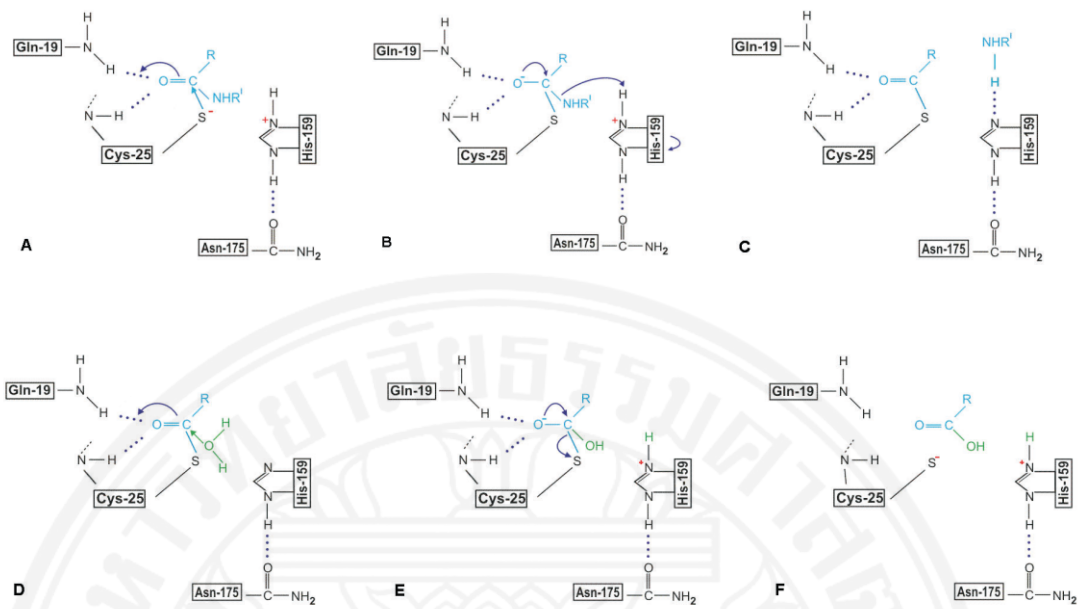
Figure 3.13 Catalytic mechanisms of cysteine proteases as exemplified by papain.[110]

Papain-like cysteine proteases consists of three regions, a prepeptide signal sequence, a propeptide, and a mature enzyme (**Figure 3.14**). The prepeptide (or signal sequence) is cleaved off following the translocation into the endoplasmic reticulum (ER). The N-terminal propeptide is involved in various roles such as intracellular targeting, intra-molecular chaperone, accommodation of correct folding of the mature enzyme and protection of uncontrolled proteolysis. The proregion can be removed by autoprocessing (self-processing or autocatalytic processing), or alternatively by other proteases. The mature protease comprises two parts: (1) the N-terminal portion consisting of two α- helices (2) the C-terminal portion containing β-strand and the helix runs through the center of the molecule starting at the catalytic cysteine.[120] The structures of human procathepsin L1 and mature human cathepsin L are shown in **Figure 3.15**.

Substrate peptides are bound by the proteases along the active site cleft before hydrolysis of peptide bonds. The binding efficiency is a function of both the respective chemical environments that the protease subsites create and the chemical nature of the peptide that interacts directly with the active site groove. Proteases have varying substrate sequence specificity based on the size, shape, polarity, charge, hydrophobicity and position of these subsite pockets. Although a single peptide bond is cleaved during catalysis, a number of amino acids on either side of the site of cleavage are critical to fix the register and specificity of an enzyme. A diagrammatic representation of peptide substrate interaction with the active site pockets of a cysteine protease is shown in **Figure 3.16**. The naming scheme of substrate residues and subsites is based on their nearness to the scissile bond. The subsites that interact with substrate residue side chains from the scissile bond towards the N-terminal are named S_1, S_2, S_3 and S_4 while the subsites which away from the scissile bond towards the C-terminal are referred to as S_1', S_2', S_3' and S_4'. The amino acid residues of the substrate from the scissile bond towards the N-terminal are referred to as P_1, P_2, P_3, and P_4 while the C-terminal residues that away from the scissile bond are names P_1', P_2', P_3', and P_4'.[121] The active site of papain-like cysteine proteases comprises four amino acid residue (P_2–P_1–P_1'–P_2') that interact with appropriate subsites from S_2–S_1–S_1'–S_2', the scissile bond being between P_1– P_1'.

The effective binding of substrate and enzyme is predominantly administered by the residues that form a deep S_2 subsite pocket capable of holding the side chain at P_2 and positioning the scissile bond P_1–P_1' into the S_1 subsite for cleavage, so only the S_2 subsite is a real pocket and the most studied subsite. Moreover, research on structural and kinetic data has shown that five subsites are essential for substrate residue side chain binding to papain-like cysteine proteases: S_2, S_1, and S_1' pockets are crucial for both backbone and side-chain binding while S_3 and S_2' are important only for amino acid side-chain binding.[116,122,123]

| NH2- | Pre | Pro | Mature | -COOH |
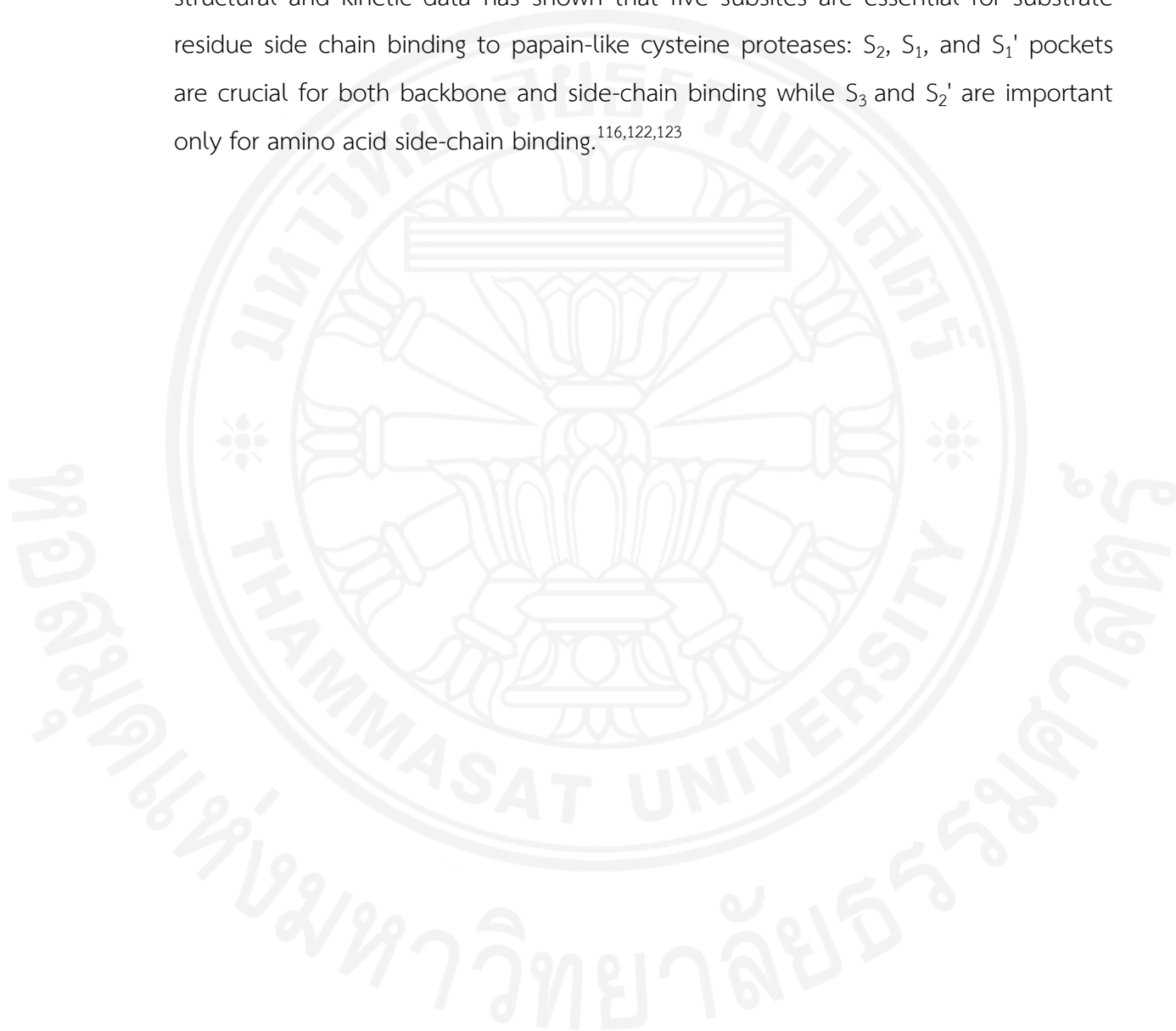
Figure 3.14 General structure of papain-like cysteine proteases. A schematic representation of a polypeptide with the pre- and pro-N-terminal extensions. The arrows indicate putative cleavage sites.[122]

(A)
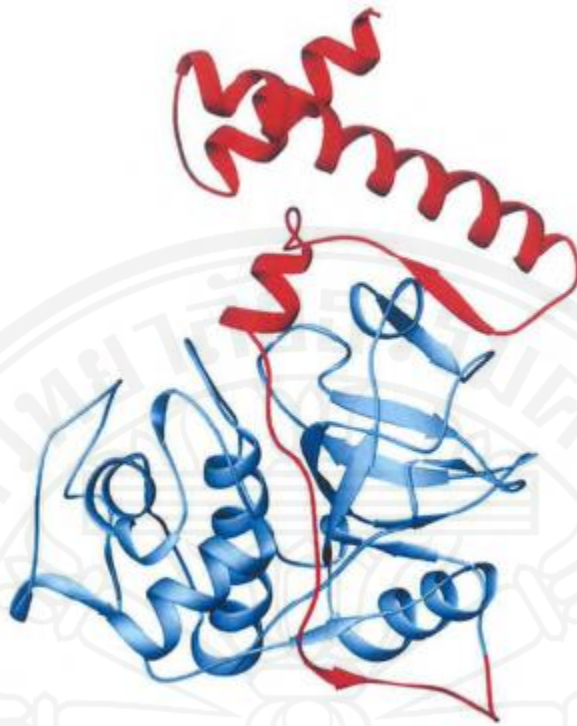
(B)
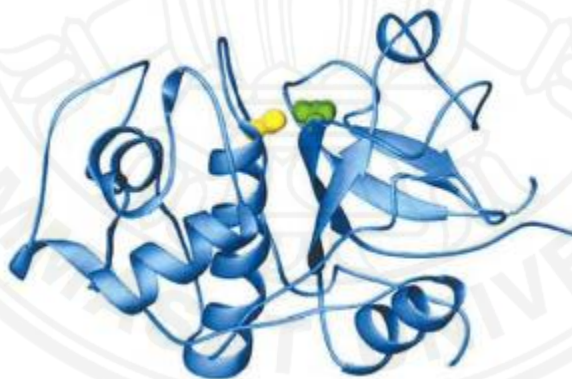
Figure 3.15 Typical structure of papain-like cysteine proteases. Panel A: structure of human procathepsin L1 with the propeptide shown in red and the mature region shown in blue and panel B: structure of mature human cathepsin L with the side chains of Cys25 and His159 (human cathepsin L numbering) indicated in yellow and green, respectively.[122]
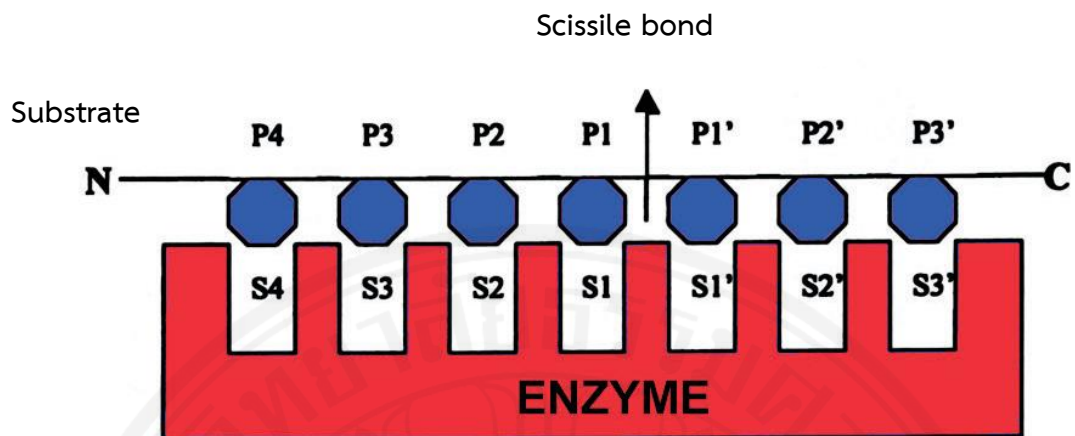
Figure 3.16 The Schechter and Berger nomenclature for protease specificity. Amino acid residues from the peptide are denoted by 'P' and the sub-sites that the peptide interact with is given the letter 'S'. The arrow indicates the scissile bond.[121]

3.2.3 Physiological roles of cysteine proteases

Cysteine proteases, cathepsins (Greek kathepsin = to digest), are a class of globular lysosomal proteases most of them contain an active-site cysteine residue and play an essential role in maintaining life in all organisms. In lysosomes, the environment is acidic appropriate for optimal activity of cathepsins except cathepsin S which is stable at faintly alkaline pH or a neutral. They are synthesized at ER-bound ribosomes and secreted from the trans-Golgi, and then translocated either into lysosomes or secretion vesicles for extracellular release. Cathepsins have various functions, they participate in protein turnover, immune system, physiological and biological processes, such as antigen or major histocompatibility complex (MHC) II invariant chain processing[124], bone remodeling[125], regulation of cell-cycle progression[126], keratinocyte differentiation[109], the processing of cytokines, hormones and inflammatory peptides, proteolytic processing of the N-terminus of the histone H3 tail[127,128], degradation of extracellular matrix (ECM) components[129], prohormone activation, and also the processing of various precursor (pro)proteins[130]. Hyper- or hypo-function of certain cathepsins leads to several pathological conditions as described above.

3.2.4 Mammalian cathepsins

The human genome is known to contain at least eleven different functional papain-like cysteine proteases (cathepsins B, F, O, S, V H, K, L, X, W, D) and lymphopain that share a high degree of sequence conservation and substrate specificity[131]. Cathepsins B and L are the major mammalian lysosomal cathepsins, they show pervasive tissue expression and are involved in protein turnover, protein degradation, cell death of regular cells and essential for embryo development[132]. Other cathepsins, e.g. cathepsins S, W and K show tissue or cell specificity and perform specific functions. For example, cathepsin K is involved in osteoporosis, rheumatoid arthritis and the only enzyme that is important in bone resorption.[133] The mammalian cathepsins have several functions and their imbalance has been implicated in the development and progression of many metabolic disorders that involve abnormal protein turnover as described in **Sections 3.2.2** and **3.2.3**.

3.2.4.1 Cathepsin L

Cathepsin L is the most active of all lysosomal endoproteases and belongs to the papain-like cysteine proteases. This cathepsin has several biological functions such as a major role in antigen processing, lysosomal proteolysis, tumor invasion and metastasis, spermatogenesis and bone resorption.[134-136] Although commonly recognized as a lysosomal protease, cathepsin L is also secreted. This broad-spectrum protease is potent in degrading several extracellular proteins, serum proteins, cytoplasmic and nuclear proteins (laminins, fibronectin, collagens I, II and IV, IL-8 precursor, neurotransmitter precursor, pro-enkephalin, immunoglobulin light chain-associated (AL) amyloid deposits elastin, and other structural proteins of basement membranes).[137] Cathepsin L has also been implicated in a number of disease processes, such as colorectal cancers and melanoma, degenerative cartilage and bone disorders, tumor metastases and rheumatoid arthritis.[138,139]

3.2.4.2 Cathepsin B

Cathepsin B is an intracellular lysosomal cysteine protease of the papain family with both endopeptidase, cleaving internal peptide bonds, and exopeptidase (dipeptidyl carboxypeptidase) activity that removes dipeptides from the C-terminus of proteins and peptides. The structure of cathepsin B (EC 3.4.22.1; 1HUC from PDB) is shown in **Figure 3.17**. This protease includes six disulfide bridges but in bovine it contains seven, one linking the light and heavy chains and it is associated with protein degradation and turnover.[140,141] The structure of cathepsin B is close to the other cysteine proteases of the papain superfamily but the occluding loop which partially occludes the active site is the unique structural element that differentiates cathepsin B from the other cysteine proteases. The occluding loop is also responsible for inhibition by cathepsin B-selective inhibitor CA074 [nPrHN-(2S,3S)-tEps-Ile-Pro-OH] and CA030 [EtO-(2S,3S)-tEps-Ile-Pro-OH].[142] Synthesis and processing of cathepsin B are shown in **Figure 3.18**. Preprocathepsin B, containing a 17-residue prepeptide, a 62-residue proregion, a 253–254-residue mature protease, and a C-terminal extension of 3 amino acids for bovine and 6 amino acids for rat, mouse and human cathepsin B, is synthesized on RER (rough endoplasmic reticulum). The signal

peptide is cleaved co-translationally in this part. Subsequently, the proprotein is transported to the Golgi apparatus, glycosylated at Asn 113 or probably at Asn-42 in the proregion and the mannose-6-phosphate receptor is accumulated (procathepsin B). Procathepsin B is transported to the lysosome and activated by cleavage of the propeptide, removal of the C-terminal extension (mammals) and endoproteolytic at residues 48-49. Moreover, increased levels and activity of cathepsin B might be involved in various pathophysiological states including inflammatory airways diseases[143], cancer[144,145], bone and joint disorders (osteoporosis, Paget's disease, rheumatoid arthritis)[143,146,147], acute pancreatitis[148], Alzheimer's disease[149,150], multiple sclerosis[140], muscular dystrophy[151] and gingivitis[152].
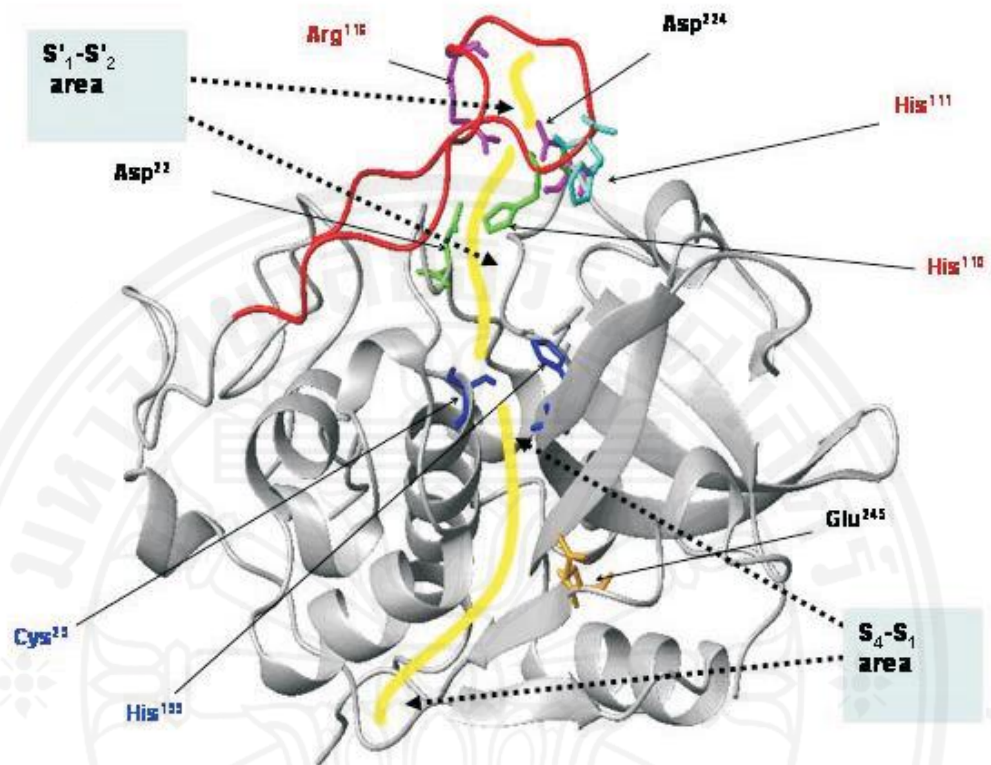
Figure 3.17 The three-dimensional structure of cathepsin B.[143]

- Red: the region of main chain of the occluding loop (Ile^{105}–Pro^{126}).

- Green: the side chains forming salt bridges (Asp^{22} – His^{110}).

- Pink: the side chains forming salt bridges (Arg^{116}–Asp^{224}).

- Yellow: the catalytic cleft.

- Blue: the catalytic center.
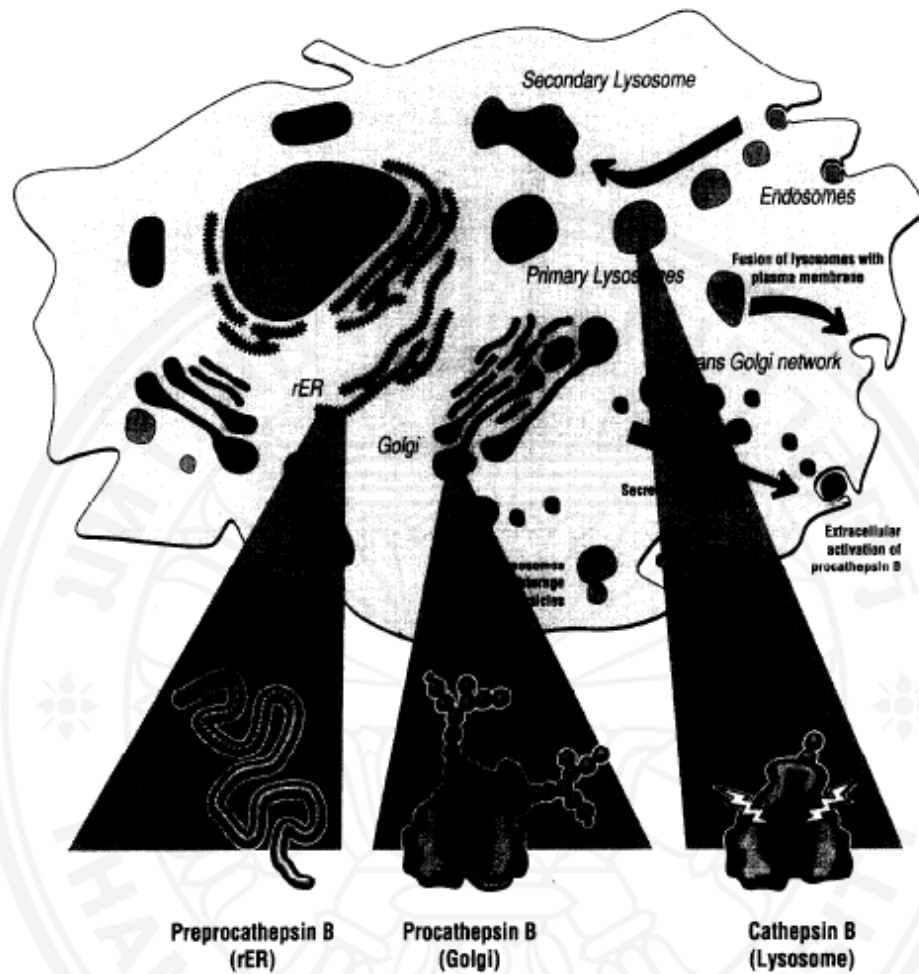
Figure 3.18 Schematic representation of the location of lysosomal cathepsin B in the cell. The unfolded preprocathepsin B, the procathepsin B and active cathepsin B are shown diagrammatically. Arrows indicate the direction of movement of several organelles.[143]

3.2.5 *Fasciola* **papain-like cysteine proteases**

The papain-like cysteine proteases of trematode parasites are involved in host-parasite interactions such as tissue penetration, feeding, digestion of host tissue for nutrition and evasion of the immune system. Proteolytic enzymes were detected from *F. hepatica* about 40 years ago and several researches have shown that theses enzymes can degrade numerous substrates including gelatin, collagen, laminin, fibronectin, albumin, hemoglobin and immunoglobulins.[153,154] Cathepsin B-like and cathepsin L-like enzymes have been isolated from metacercariae, NEJ and adult stage of *Fasciola* spp. In the adult stage of *F. hepatica*, cathepsin L was approximately encoded by 15% of all transcripts.[155] The enzymes are candidates for the development of new chemotherapeutic interventions to terminate the parasite infection in animals and humans, with attempt to produce specific inhibitors to prevent their activity and destroy a major part of the parasite metabolism.[156,157] The regulation of *F. hepatica* cathepsin proteases from NEJ penetrating the host intestinal wall to mature stage in the bile duct is shown in **Figure 3.19**.
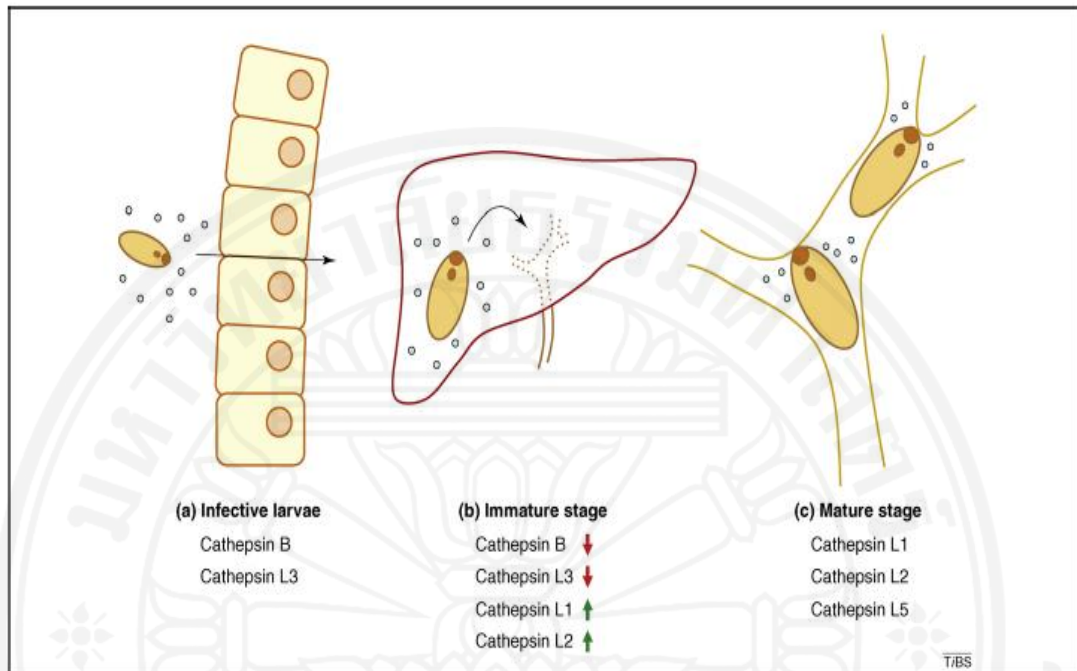
Figure 3.19 Developmental regulation *F. hepatica* cathepsin proteases from NEJ penetrating the host intestinal wall to mature stage in the bile duct.[5]

3.2.5.1 Cathepsin L-like proteases of *Fasciola*

Cathepsin L-like proteases have been shown as the most predominant molecules isolated from trematodes, other parasites but also non-parasitic helminths for example, *Fasciola* spp., *Schistosoma mansoni*, *Strongylus vulgaris*, *Caenorhabditis elegans*.[118,158,159] It has been reported that the cathepsin L-like cysteine proteases are important secretory products of *F. hepatica* and play pivotal roles in the pathogenicity, host adaptation and survival of the parasites.[160] Several cathepsin L-like proteases are secreted by *Fasciola* spp. that differ in enzymatic properties and timing of expression in the parasite's life cycle. There are numerous cathepsin L genes in the genome of *F. hepatica* but only 13 *Fasciola* cathepsin L cDNAs deposited in the public databases[161]. A study of proteomics and phylogenetic analysis of the cathepsin L protease family of *F. hepatica* has been performed and the result is shown in **Figure 3.20**.[162] It was demonstrated that the cathepsin L family can be classified into 5 distinct phylogenetic clades: three clades were associated with mature adult flukes taken from bile ducts (Clades FhCL1, FhCL2 and FhCL5) and two clades specific to early infective larvae stages that could be help juvenile worms penetrate through the intestinal wall of host (Clades FhCL3 and FhCL4).[162] The two clades FhCL1 and FhCL2 represented the major secreted proteases with approximately 67.39% and 27.63% of total secreted cathepsin L, respectively.[161] This finding might indicate that these two cathepsins are the most essential for survival and adaptation of the parasite. *Fasciola* cathepsin L proteases are produced within the gut epithelial cells of the fluke and kept in specialized secretory vesicles as inactive zymogens and the zymogen structure of these proteases are similar to the structure of vertebrate cathepsin Ls that are composed of a hydrophobic signal peptide (12-20 residues), proregion (100 residues) that binds the substrate cleft and prevents inappropriate proteolysis during trafficking and storage and mature enzyme (200 residues) (**Figure 3.21**). Mature FhCL1 and FhCL2 do not possess potential N-glycosylation sites and are not glycosylated in the parasite.[163-165] A sub-clade of FhCL1, FgCL1C was not detected in the secretory products of *F. hepatica* but only in *F. gigantica* which might indicate gene duplication after evolutionary separation of *F. hepatica* and *F. gigantica*. The auto-

activation from inactive proFhCL1 zymogen to mature active enzyme takes place over a wide pH range (3.0–8.0) but an acidic pH is the most appropriate (the gut lumen of the parasite has a slightly acidic pH). A stability study of FhCL1 revealed that it retained 100% activity when incubated at 37°C for 24 h. A pH value of 4 is suitable for human cathepsin L and the enzyme is irreversibly inactivated above pH 7.0. This property of the proteases might protect the cell from uncontrolled proteolysis if they are leaked from lysosomes.[166] The substrate specificity of cathepsin was verified by using synthetic fluorogenic peptide substrates: characterization of mammalian cathepsin L, S, K (Z-Phe-Arg-NHMec), cathepsin B (Z-Arg-Arg-NHMec) and cathepsin H (Z-Arg-NHMec). All enzymes showed high levels of catalytic efficiency (k_{cat}/K_m) for Z-Phe-Arg-NHMec.[167,168]

The expression of cysteine proteases is highly regulated and linked to migration and maturation of the fluke in the host. The newly excysted juvenile (NEJ) penetrates the host intestinal wall by facilitation of cathepsin B and L3. The immature fluke uses *Fasciola* cathepsin L1 and L2 to degrade the host protein and pass through the host liver tissue while the amount of cathepsin B and L3 is decreasing. The adult parasite uses cathepsins L clade 1, 2 and 5 to facilitate catabolizing host proteins and penetrate the bile ducts where it requires nutrients from the host such as hemoglobin and serum proteins.[162] Six different cathepsin L encoding cDNAs (cathepsin L-A to L-F) were isolated from *F. gigantica* which have high DNA sequence identities (87-99%) with the homologous genes from *F. hepatica*. The identities of their deduced amino acid sequences range from 75.3 to 99.1%. Alignment of the amino acid sequences of cathepsin L proteins of *F. gigantica* and *F. hepatica* also revealed that the proteins of the two species are highly conserved.[169]

Fasciola cathepsin-L like proteases can migrate through the host intestine and liver by digestion of a range of host compounds such as fibronectin, laminin, and native collagen.[153] These proteases can cleave immunoglobulins, protect the parasite surface from the antibody-mediated attachment of eosinophil, have potential to suppress T-lymphocyte proliferation in sheep and decrease the expression of CD4+ in sheep and human T-cells and help the fluke from immune attack of host.[170-172] Furthermore, cathepsin L is associated

with immunomodulation and immunosuppression of Th1 responses and induction of non-protective host Th2 responses. In addition to the other functions mentioned, cathepsin L2 is able to cleave fibrinogen to produce a fibrin clot. This may prevent excessive bleeding at feeding points in the bile ducts, or alternatively the clot may prevent access of immune effector cells to the parasites surface.[168] Due to *Fasciola* cathepsin L-like proteases suspected roles in vital parasite functions, they are considered important targets for vaccines or chemotherapies.[173,174]
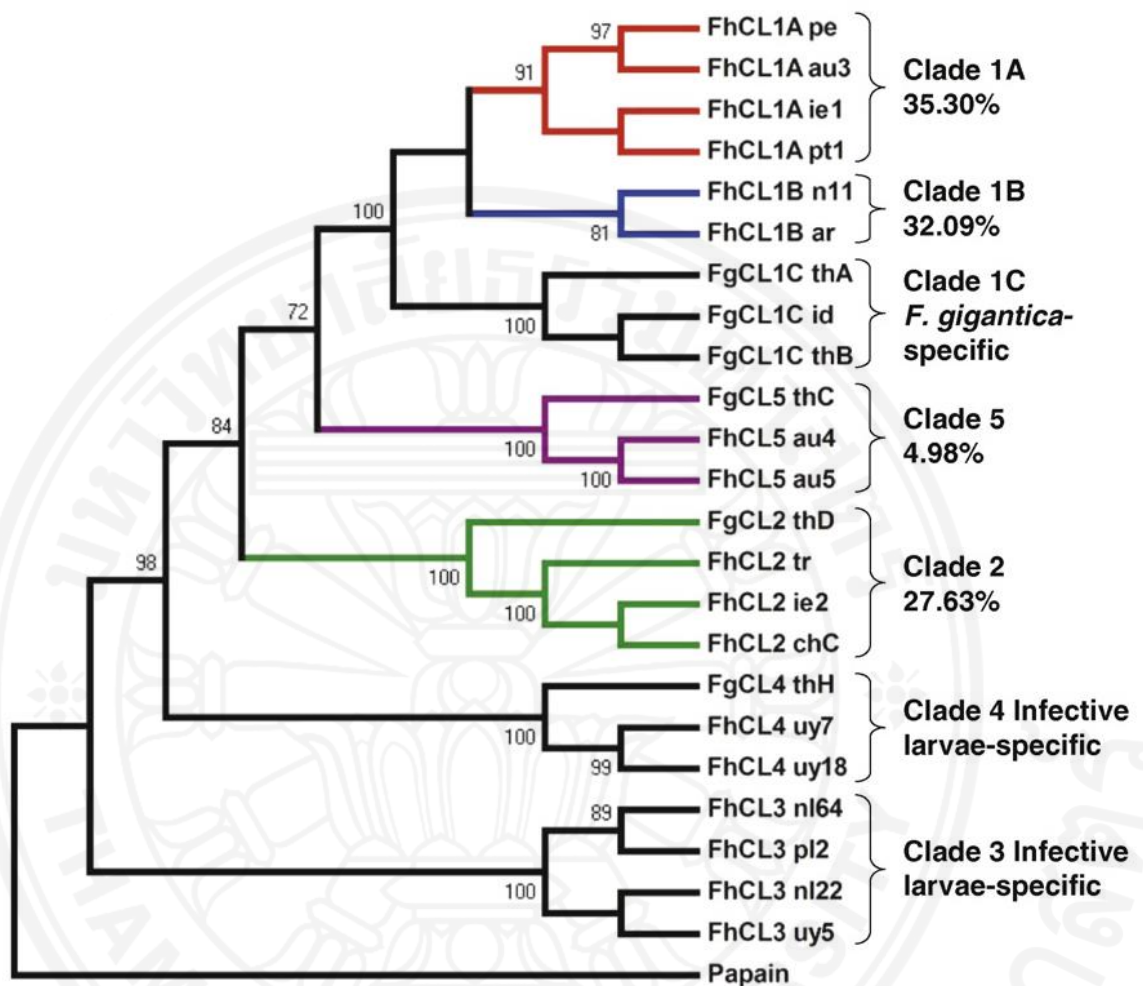
Figure 3.20 A study of proteomics and phylogenetic analysis of the *Fasciola* cathepsin L gene family.[162]
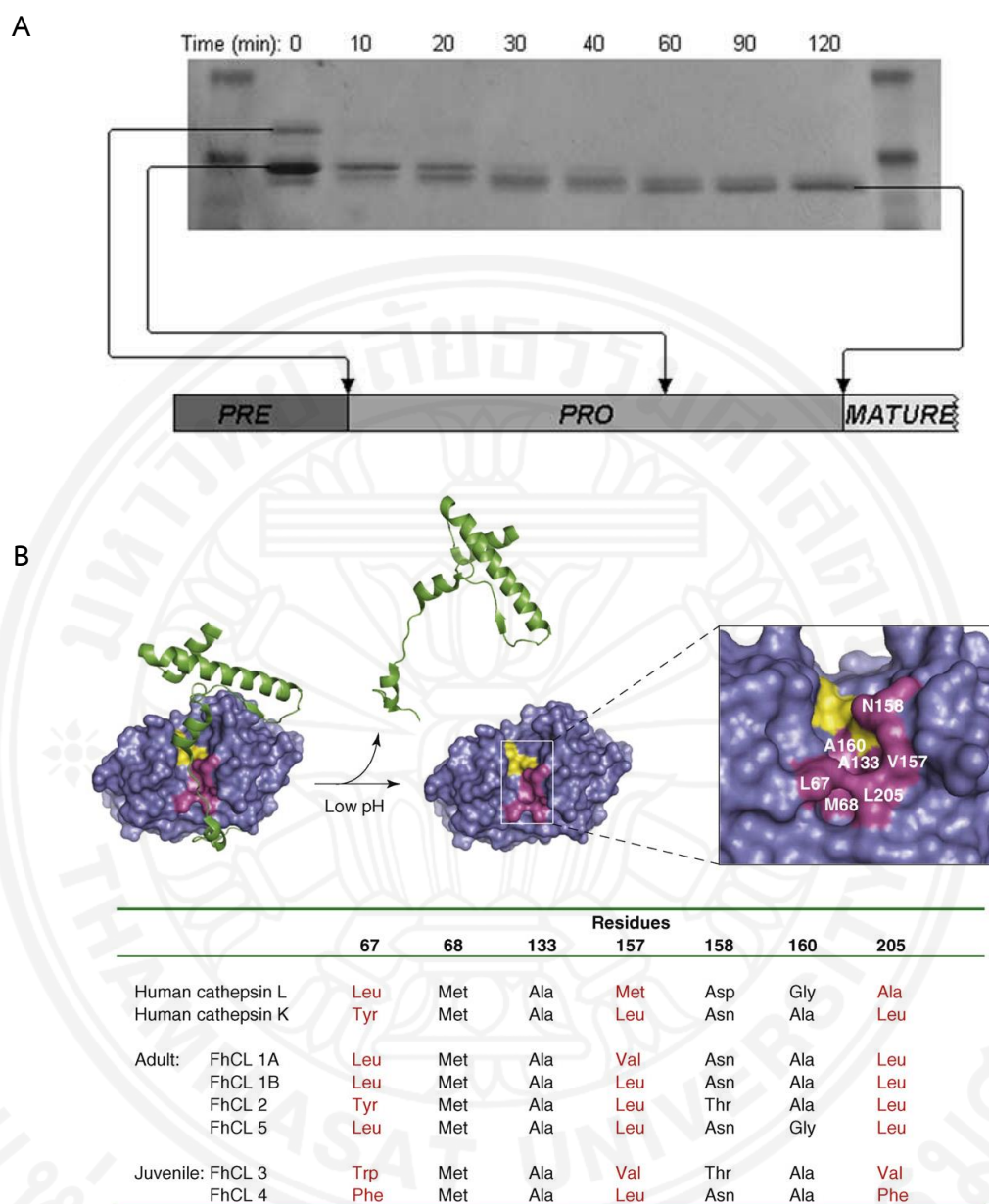
Figure 3.21 The structure of *F. hepatica* cathepsin L proteases. Panel A: purified recombinant FhCL1 represents the full pre, pre and mature enzyme and panel B: surface representation of FhCL1, the prosegment is shown as a green ribbon and the catalytic machinery is shown in yellow (P1 residues) and magenta (P2 residues). Moreover, the table illustrates difference of substrate-binding (residues from the S2 active site) in *F. hepatica* cathepsin L proteases and human cathepsins L and K.[5,161]

3.2.5.2 Cathepsin B-like proteases of *Fasciola*

Cathepsin B-like cysteine proteases are present in trematodes and other parasitic species such as *Schistosoma mansoni*, *Schistosoma japonicum*, *Trichobilharzia regent*, *Ancylostoma caninum*, *Clonorchis sinensis*, *Fasciola hepatica* and *Fasciola gigantica*. The percentage sequence identity between cathepsin B-like cysteine proteases of each species is shown in **Figure 3.22**. These proteases are the most abundant proteases secreted in metacercarial and NEJ stages of *Fasciola* spp. with progressively less abundance during maturation, eventually being expressed the least in the adult stage. Three abundant cathepsin B-like proteases have been identified in metacercariae, newly excysted juveniles or immature parasites of *F. hepatica* (termed FhCB1, FhCB2 and FhCB3) with sequence identities ranging from 64 to 66%.[175] In *F. gigantica*, two cathepsin B-like proteins were identified in metacercariae and newly excysted juveniles (termed FgCB2 and FgCB3) and a third isoform was detected in all stages of the parasite (metacercariae, NEJ flukes and adult parasites) and was termed FgCB1. These three cathepsin B-like proteases from *F. gigantica* have identities ranging from 64 to 79% and contain the highly conserved region of the cathepsin B family.[176] Cathepsin B acts as both endopeptidase and exopeptidase (dipeptidyl carboxypeptidase) but this protease is a less effective endopeptidase than other members of the papain family. A specific structure of cathepsin B-like proteases is the occluding loop (structural element unique 20-residue). The occluding loop contains two histidine residues His^{110} and His^{111} which are responsible for exopeptidase activity that removes C-terminal dipeptides of proteins and peptides. At an acidic pH, the anchoring of the loop by His^{110} and the action of His^{111} occurs but the function of His residues is destroyed at above pH 5.5 so, the exopeptidase activity of cathepsin B decreases and the enzyme acts only as an endopeptidase. The sequence alignment around the predicted occluding loop between cathepsin B-like proteases of vertebrates and parasites is shown in **Figure 3.23**. Localization and temporal expression of *Fasciola* cathepsin B-like proteases may help to study the functions of these proteases but the real functions are unknown. Cathepsin B-like proteases of NEJ and adult *Fasciola* have been localized to the secretory vesicles of the gut, gut lumen and tegumental cells

therefore, they may act as general digestive enzymes.[176,177]   These proteases were also detected in tissues of the reproductive system in the adult stage of *Fasciola* which might suggest that cathepsin B is associated with vitellogenic degradation, processing of eggshell precursor proteins, eggshell remodeling, hatching and molting.[176-179]   Moreover, the capacity of digesting immunoglobulin, albumin, collagen, fibronectin and hemoglobin and the location in the tegumental cells suggest functions in immune evasion, tissue invasion, excystment and migration.[178,180] A recent study on down-regulation of cathepsin B expression using RNA interference (RNAi) in *F. hepatica* NEJ revealed a significant reduction in intestinal wall penetration by this fluke stage.[181]   Vaccination studies with juvenile cathepsin B protease of *F. hepatica* (FhCatB1) have shown reduction in worm burdens, parasite mass and liver damage in rats.[182]

	SmCB1	SmCB2	SjCB	FhCB1	FhCB2	FhCB3	FhCB6	FgCB1	FgCB2	FgCB3	CsCB1	CsCB2	CsCB3	CsCB4	CsCB5	OvCB2	Human
SmCB1	100																
SmCB2	55	100															
SjCB	57	89	100														
FhCB1	58	55	56	100													
FhCB2	55	53	53	66	100												
FhCB3	55	55	55	66	64	100											
FhCB6	61	55	55	56	52	54	100										
FgCB1	54	54	55	68	62	79	54	100									
FgCB2	55	53	53	66	100	64	52	62	100								
FgCB3	55	55	55	66	64	99	54	79	64	100							
CsCB1	51	69	67	54	52	53	54	53	52	53	100						
CsCB2	61	57	56	58	57	60	60	58	57	59	52	100					
CsCB3	60	56	56	57	57	57	59	54	57	57	52	72	100				
CsCB4	58	53	52	57	51	51	61	52	51	51	51	56	56	100			
CsCB5	59	56	57	54	55	55	60	57	55	55	53	75	69	56	100		
OvCB2	59	57	55	59	58	57	58	55	58	57	52	73	85	59	69	100	
Human	57	59	58	55	53	54	56	54	53	54	58	55	56	51	54	57	100

Figure 3.22 The percentage sequence identity between full-length mature cathepsin B-like cysteine proteases of parasites.[175]

```
                                        ⇓⇓
 1 human-B                 -CRPY-SIPPCEHHV----------NG-SRPPCTGEG---DTPKCSKIC     X
 2 bovine-B                -CRPY-SIPPCEHHV----------NG-SRPPCTGEG---DTPKCNKTC     X
 3 mouse-B                 -CLPY-TIPPCEHHV----------NG-SRPPCTGEG---DTPRCNKSC     X
 4 rat-B                   -CLPY-TIPPCEHHV----------NG-SRPPCTGEG---DTPKCNKMC     X
 5 chick-B                 -CRAY-TIPPCEHHV----------NG-SRPPCTGEGG--ETPRCSRHC     X
 6 Sarcophaga(fleshfly)-B  -CRPY-EIAPCEHHV----------NG-TRPPCDGEHG--KTPSCRHEC     X
 7 S.mansoni-B2            -CQPY-EFPPCEHHV----------IG-PLPSCDGDV---ETPSCKTNC
 8 Toxoplasma-B            -CWPY-EVPFCAHHA----------KA-PFPDCDATLVPRKTPKCRKDC
 9 L.mexicana-B            -CQPY-PFGPCSHHG----------NSSKYPPCPNTIY--NTPKCNTTC     X
10 L.major-B               -CPQY-PFDPCSHHG----------NSEKYPPCPSTIY--DTPKCNTTC
11 T.cruzi-B               -CQPY-PFPSCAHHV----------NSSDLSPCSG-EY--DTPTCNSTC     X
12 F.hepatica-B            -CQPW-MFTKCDHVG----------DSRKYSRCPHYTY--PTPPCARAC
13 S.mansoni-B1            -CEPY-PFPKCEHHT----------KG-KYPPCGSKIY--NTPRCKQTC
14 S.japonicum-B1          -CQPY-PFPKCEHHT----------KG-KYPACGTKIY--KTPQCKQTC
15 C.elegans-B6            -CKPY-PFPPCEHHS----------KKTHFDPCPHDLY--PTPKCEKKC
16 Ascaris-B               -CKPY-PFPPCEHHS----------NKTHYQPCKHDLY--PTPKCEKKC     X
17 H.contortus-B7          -CKPY-VFPQCGAHK----------G-KAFNNCPSHPY--ATPACKPYC
18 C.elegans-B3            -CMPY-SFAPC--TK------------NCPES----TTPSCKTTC
19 C.elegans-B4            -CKPY-SLAPCGETV----------GNVTWPSCPDDGY--DTPACVNKC     X
20 C.elegans-B5            -CKPY-SIAPCGETV----------NGVKWPACPEDTE--PTPKCVDSC
21 Aedes-B                 -CHPY-PIDVCD-------------ASGEEA---DTPKCSKRC
22 Ancylostoma-B1          -CKPY-AFYPCGHHQ----------NDPYYGPCPGGLW--PTPKCRKTC
23 Ancylostoma-B2          -CKPY-AFYPCGNHT----------NERYYGPCPRGLW--PTPKCRKAC     X
24 Necator-B               -CKPY-AFHPCGNHE----------NQVYYGVCPKGSW--PTPRCEKFC
25 O.ostertagi-B3          -CRPY-EFPPCGRHG----------KEPYYGECYD-TA--KTPKCQKTC
26 H.contortus-B1          -CRPY-PIHPCGHHG----------NDTYYGECRG-TA--PTPPCKRKC     X
27 H.contortus-B2          -CRPY-PIHPCGHHG----------NDTYYGECRG-TA--PTPPCKRKC     X
28 H.contortus-B3          -CRPY-PIHPCGHHG----------NDTYYGECPE-EA--STPSCKKKC     X
29 H.contortus-B4          -CRPY-PIHPCGHHG----------NDTYYGECPR-EA--ATPPCKKKC     X
30 H.contortus-B5          -CSPY-PLHPCGRHG----------NDTFYGNCVG-MA--PTPPCKRKC     X
31 O.ostertagi-B           -CRPY-EIHPCGHHG----------NETYYGECVG-MA--DTPRCKRRC     X
32 Trichuris-B             -CKPYKPTGPIGRHLKRNDYAPCPNDTYYGECVG-MA--DTPRCKRRC     X
33 G.lamblia-B2            -CVPY-------------------KSGSTT-----LRGTCPTKC
34 G.lamblia-B3            -CVPY-------------------QSGSTG-----ARGTCPTKC
35 G.muris-B               -CLKY-------------------FSGMTG-----DRESCITHC
36 G.lamblia-B1            -CVKY-------------------VDYGHT-----VASPCPAVC
```

Figure 3.23 Sequence comparison around the predicted occluding loop between vertebrate and parasite cathepsin B-like proteases.[118]

        - Black box: the region loop

        - Arrow: the essential His^{110} and His^{111}

        - X and underline: sequences with predicted *N*-glycosylation site (N-X-S/T) within the loop

3.3 Cystatin and the mechanism of their interaction with cysteine proteases

Cystatins are reversible, competitive and tight-binding inhibitors of cysteine proteases in the papain superfamily that are ubiquitously present in plants, animals, parasites and microorganisms.[183] They have several important physiological functions in the immune system including immune evasion from their host, modulation of cathepsin activities and antigen presentation, balance of the host–parasite interaction, protection of cells from inappropriate endogenous or external proteolysis and regulation of normal proteolytic processes involving cysteine protease activity.[184,185] Imbalance between these protease inhibitors and cysteine proteases resulted in various diseases for example renal failure[6], osteoporosis[7], periodontitis[186], rheumatoid arthritis[8], metastasizing cancer[187], purulent bronchiectasis[188] and septic shock.[189]

The cystatin superfamily can be assigned to three major families based on molecular masses, primary sequence similarities, number of disulfide bonds, number of amino acid residues, physiological roles and subcellular localization.[184,185,190] Alignment of amino acid sequences of stefins, cystatins and kininogens is shown in **Figure 3.24**. Family 1 includes cystatins (stefins) A, B composed of 100 amino acid residues (11-12 kDa) and family members lack disulfide bridges, signal sequence and carbohydrate side chains.[190] They are unglycosylated inhibitors that are mainly intracellular, but can also found in extracellular fluids at significant concentrations. Human stefin A, pI values in the range 4.5–5.0, is encoded on chromosome 3 and present in epithelium, skin and polymorphonuclear leucocytes.[191] The high level of stefin A in skin suggests that it might be important in the control of normal keratinocyte proliferation and differentiation. It is a reversible and competitive inhibitor of cysteine proteases, particularly cathepsin L and cathepsin S whereas cathepsin B inhibition is weaker.[192] Human stefin B, pI values in the range 5.9–6.5, is an intracellular protein that is present in many different cell and tissue types and the gene encoding this stefin has been located on chromosome 21.[116,191] According to its property as a tight-binding reversible inhibitor of cathepsins B, H, L and S, it is regarded as a general cytosolic inhibitor protecting the cell against leakage of

lysosomal enzymes. Family 2 cystatins are single domain cystatins containing a signal sequence and two C-terminal disulfide bonds but also lack carbohydrates. They are composed of about 120–122 amino acid residues with molecular weight approximately 13–14 kDa. Members of this cystatin family are cystatins C, D, E/M, F, S, SA and SN and all of them are located in the cystatin multigene locus on human chromosome 20 (except cystatin E/M located on chromosome 11).[193] Family 2 inhibitors are mainly secreted and found in the cell and most biological fluids such as human cystatin C at high concentrations in seminal plasma (51 mg/l) and cerebro-spinal fluid (5.8 mg/l) and at much lower concentrations in amniotic fluid, milk, blood plasma, saliva, tears and urine.[191] Mature human cystatin C, after removal of a 26–residue signal peptide, consists of 120 amino acid residues with molecular mass 13.4 kDa and pI 9.3. Abnormalities caused by cystatin C deficiency have been demonstrated. Inflammatory diseases such as arteriosclerosis and abdominal aortic aneurysm that involve extensive extracellular matrix degradation and vascular wall remodeling were observed when the levels of cystatin C were decreased.[194] Other human cystatins, cystatins D, S, SA and SN have been demonstrated as specialized glandular inhibitors. Cystatin D (fully active), after removal of the 20-residue signal peptide, is composed of 122 amino acid residues with molecular mass approximately 13.8 kDa and found in saliva and in small amounts in tears.[195] Cystatins S, SA and SN consist of 121 amino acid residues with molecular mass approximately 14.2–14.4 kDa, share high sequence identity (90%) and are present in saliva, tears, urine and seminal plasma.[196] Cystatin E/M is composed of 122 amino acid residues and mostly expressed in epithelial cells.[197] Cystatin F consists of 126 amino acid residues and is predominantly expressed in hematopoietic cells and leukocytes.[198] Family 3 of the cystatin or Kininogen family which consisting of about 335 amino acid residues are glycosylated molecules, containing three type 2 cystatin-like domain with disulfide bonds and carbohydrate groups and not all cystatin domains might be functional. They have molecular masses of approximately 60–120 kDa. Kininogens are produced in the liver, secreted into the blood and play a crucial role in blood coagulation cascade. Furthermore, it is suggested that they are related with the regulation of vascular biology including vascularization, endothelial cell apoptosis.[199,200] There are

three distinct types of kininogens: high molecular weight (HK), low molecular weight (LK) and T-kininogens with molecular masses of about 120 kDa, 68 kDa and 68 kDa, respectively. Human kininogen is located on chromosome 3 and the pI is in the pH range 4.0–5.2.[191] They have been found in blood plasma, synovial fluid and in small amounts in other secretory fluids. The schematic picture of the protein structure in the cystatin superfamily is shown in **Figure 3.25.**

The mechanism of cysteine proteases and cystatins was explained by numerous kinetic and crystallographic studies. Cystatins are composed mainly of five-stranded antiparallel **β**-strand pleated sheets wrapped around a central long **α**-helix with an additional carboxyl-terminal strand that runs along the convex side of the sheet. The three-dimensional structure of the complex formed between human stefin B and papain is shown in **Figure 3.26**. Three highly conserved reactive domains (the N-terminal region and two hairpin loops) of the cystatins are principally involved in the interaction between protease and inhibitor (**Table 3.3**). The N-terminal domain containing a conserved Gly residue such as Gly9 of human stefin B and chicken cystatin and Gly11 of human cystatin C directly interacts with the substrate-binding-pockets S3, S2 and S1 of the protease.[201,202] The first hairpin loop is composed of the peptide segment between Gln53 and Gly57 (highly conserved motif QVVAG region) and the second hairpin loop that consists of the conserved Pro-Trp residues (Pro103 and Trp104).[14,203] The N-terminal segment and two **β**-hairpin loops form the edge of the wedge shaped surface which is highly complementary to the active site cleft of cysteine proteases.[204]

```
                 1         2         3         4         5         6         7          8         9        10        11
         12345678901abcd234567890123456789012345678901234567890123456789ab234567890123456789abcdef901234567890a1234567a89012a345a6789012345a6abcdefghij
Stefin family
hsa              MIPGGL····SEAKPATPEIQEIVDKVKPQLEEKTNETY··GKLEAVQYKTQVVAGTNYY··IKVRAGD································NKYHHL·KVFKSLPGQNEDLVLTGYQVDKNKDDELTGF
rsa      acMDPQ·TTGIVGGV····SEAKPATPEIQEVADKVKRQLEEKTNEKY··EKFKVVEFKSQVVAGQILF··HKVDVGN································GRFLHM·KVLRGLSGDD·DLKLLDYQTNKTKNDELTDF
hsb      acHMCGAP····SATQPATAETQHIADQVRSQLEEKYNKKF··PVFKAVSFKSQVVAGTNYF··IKVHVGD································EDFVHL·RVFQSLPHENKPLTLSHYQTNKAKHDELTYF
rsb      acHMCGAP····SATHPATTETQEIADKVKSQLEEKANQKF··DVFKAISFRRQVVAGTNFF··IKVDVGE································EKCVHL·RVFEPLPHENKPLTLSSYQTDKEKHDELTYF
orcI     HSSDGGPVLGGV····EPVGNENDLHLVQLARFAVTEHNKKANSLL··EFEKLVSVKQQVVAGTLYYFTIEVKEGD································AKKLYEAKVVEK·PWHDFKELQEFKPVDASANA
orcII    HAEEAQSHAREGGRHPRQPAGRENDLTTVELARFAVAEHNSKAWAHL··ELERVVKVRQQVVGQFNHYLTVEVKEPGG································ANKLYEAKVWER·AWENFKQLDDFKPLDATA
Cystatin family
drc      IATQAADEQVVGGV····SQLEGDSRKEALELLDATLAQLATGDGPSY··KAINVTSVTGQVVAGSLNT··YEVEL·DNGSD································KK·QCTV·KIVTQ·PULKENGTNIKIKCSGDDGELDRTW
sac      QCVGCP····SEVKGDKLKQSEETLNKSLSKLAAGDGPTY·KLVKIHSATTQVVSGSKDV··INADL·KDEND································KTKTCDI·TIVSQ·PULENGIEVT·FNCPGEPKVVKKHSA
cc       SEDRSRLLGAP····VPVDENDEGLQRALQFAMAEYNRASNDKYSSRVVRVI SAKRQLVSGIKYI··LQVEIGRTTCPKSSGDL······QSCEFHDEPEHA·KYTTCTF·VVYSI·PVL·NQIKLLESKC·Q
hcc      SSPGKPPRLVGGP····HDASVEEEGVRRALDFAVGEYNKASNDHYHSRALQVVRARKQIVAGVNYF··LDVELGRTTCTKTQPNL······DNC FHDQPHLK·RKAFCSF·QIYAV·PWQ·GTHTLSKSTC·QDA
hcs      SSSKEENRIIPGGI····YDADLNDEUVQORALHFAISEYNKATEDEYYRRPLQVLRAREQTFGGVNYF··FDVEVGRTICTKSQPNL·······DTCAFHEQPELQ·KKQLCSF·EVYEV·PWE·DRMSLVDSRC·QEA
hsn      IIPGGI····YNADLNDEUVQORALHFAISEYNKATKDDYYRRPLRVLRARQQTVGGVNYF··FDVEVGRTICTKSQPNL·······DTCAFHEQPELQ·KKQLCSF·EIYEV·PWE·NRRSLVKSRC·QES
hsa      EEDRIIEGGI····YDADLNDERVQORALHFVISEYNKATEDEYYRRLLRVLRAREQIVGGVNYF··FDIEVGRTICTKSQPNL······DTCAFHEQPELQ·KKQLCSF·QIYEV·PWE·DRMSLVDSRC·QEA
bcc      RLLGGL····HEADVNEEQVQEALSFAVSEFNKRSNDAYQSRVVRVVRARKQVVSGMNYF··LDVELGRTTCTKSQANL······DSCPFHNQPHLK·REKLCSF·QVYVV·PWH·MI    VKFSC·QD
rcc      GTSRPPPRLLGAP····QEADASEEGVQORALDFAVSEYNKGSNDAYHSRAIQVVRARKQLVAGINYY··LDVEHGRTTCTKSQTNL······TNCPFHDQPHLH·RKALCSF·QIYSV·PWK·GTHTLTKSSC·KNA
rcs      LSCLGHFLGGI····EKSSHEEEGASEALNYAVNEYNEKNSDLYLSRVVEVKDVQKQVVAGTKFF··FDVILGKTICLKTQGDL·······INCPLNEEADQQ·EHEFCSF·VVHDI·PWE·NYIVLLSSSC·HSI
pac      IPGGL····SPRDVTDPDVQEAAAFAVEKYNAGSKNDYYFKERRVVEAQSQVVSGVKYY··LMHELLKTTCKKTVGRPKGYQEIQNCN··LPPENQQEEITCRF·EVVWSR·PVL·PSTSLTK
Kininogen family (segment 1)
hk1            QESQS····EEIDCNDXDLFKAVDAALKKYHSQNQSNHQFVLYRITEATKTVGSDTFYS··FKYEIKEGDCPVQSGKT·····WQDCEYKDAAKAAT··GECTA·TVGKR·SST·KFSVATQT·C·QITP
bk1            QES·S····QEIDCNDQDVFKAVDAALTKYHSENKSGNQFVLYRITEVARMDNPDTFYS··LKYQIKEGDCPFQSNKT·····WQDCDYKDSAQAAT··GECTA·TVAKR·GNH·KFSVAIQT·C·LITP
rk1            QEEGA····QELMCNDETVFQAVDTALKKYHAELESGNQFVLYRVTEGTKKDQAETLYS··FKYQIKEGNCSVQSGLT·····WQDCDFKDAEEAAT··GECTT·TLGKK·EN··KFSVATQI·C·NITP
rt11           QEEGA····QELMCNDETVFQAVDTALKKYHAELESGNQFVLYRVTEGTKKDQAETLYS··FKYQIKEGNYSVQSGLT·····WQDCDFKDAEEAAT··GECTT·TLGKK·EN··KFSVATQI·C·NITP
rt21           QEEGA····QELMCNDETVFQAVDTALKKYHAELESGNQFVLYRVTEGTKKDQAETLYS··FKYQIKEGNYSVQSGLT·····WQDCDFKDAEEAAT··GECTT·TLEKR·RNN·KFSVATQI·C·NITP
(segment 2)
hk2      AEGPVVTAQYDCLGCV····HPISTQSPDLEPILRHGIQYFNHNTCHSSLFMLNEVKRAQRQVVAGLNFR··ITYSIVOTNCSKENFLF····LTPDCK·SLWNGDT··GECTD·NAYID··IQL·RIASFSQN·C·DIYP
bk2      AEGPVVTAQYECLGCV····HPISTKSPDLEPVLRYAIQYFNHNTSHSHLFDLKEVKRAQRQVVSGMNYE··VNYSIAQTNCSKEEFSF····LTPDCK·SLSSGDT··GECTD·KAHVD·VKL·RISSFSQK·C·DLYP
rk2      GKGPKKTEEDLCVGCF····QPIPHDSSDLKPVLKHAVEHSNNNTKHTHLFALREVKSAHSQVVAGMNYK··IIYSIVOTNCSKEDFPS····LREDCV··PLPYGDH··GECTG·HTHVD·IHN·TIAGFSQS·C·DLYP
rt12     GKGPKKTEEDLCVGCF····QPIPHDSSDLKPVLKHAVEHSNNNTKHTHLFALREVKSAHSQVVAGMNYK··IIYSIVOTNCSKEDFPS····LREDCV··PLPYGDH··GECTG·HTHVD·IHN·TIAGFSQS·C·DLYP
rt22     GKGPIVTNEYHCVGCH····HPISVDSSPELGPVLKHAVEHFNHNTKHTHLFALGEVKSADRQVVAGMNYQ··IIYSIVOTNCSKEDFPS····LHEDCV··PLPSGDD··GECKG·NAFVD·IHK·TIAGFSDS·C·EFYP
(segment 3)
hk3      GKDFVQPPTKICVGCP····RDIPTNSPELEETLTHTITKLNAEHNATFYFKIDNVKKARVQVVAGKKYF··IDFVARETTCSKESNEE····LTESCE·TKKLGQS··LDCNA·EVYVV·PWE·KKIYPTVN·C·QPLGM
bk3      VKDFVQPPTRLCAGCP····KPIPVQSPDLEEPLSHSIAKLNAEHDGAFYFKIDTVKKATVQVVAGLKYS··IVFIARETTCSKGSNEE····LTKSCE··INIHQQI·LHCDA·NVYVV·PWE·EKVVPTVN·C·QPLGQ
rk3      GDDLFELLPKKCFGCP····LNIPVDSPELKEALGHSIARLNAQHNHLFYFKIDTVKKATSQVVAGTKYV··IEFIARETNCSKTNTTE····LTADCE··TKHLGQS··LNCNA·NVYMR·PWE·NKVVPTVR·C·QALDM
rt13     GDDLFELLPKNCRGCP····REIPVDSPELKEALGHSIARLNAQHNHIFYFKIDTVKKATSQVVAGVIYV··IEFIARETNCSKQSKTE····LTADCE··TKHLGQS··LNCNA·NVYMR·PWE·NKVVPTVR·C·QALDM
rt23     GDDLFELLPEDCPGCP····RNIPVDSPELKEALGHSIARLNAENNHTFYFKIDTVKKATSQVVAGTKYV··IEFIARETNCSKESNAE····LTADCE··TKRLGQS··LNCNA·NVYMR·PWE·NKVVPTVK·C·KVLDM
```

Figure 3.24 Alignment of amino acid sequences of stefins, cystatins and kininogens.[191]

- hsa: human stefin A
- rsa: rat cystatin α
- hsb: human stefin B
- rsb: rat cystatin β
- orcl: oryzacystatin I
- orcll: oryzacystatin II
- drc: *Drosophila* cystatin
- sac: sarcocystatin A
- hcc: human cystatin C
- cc: chicken cystatin
- rcc: rat cystatin C
- rcs: rat Cystatin S
- hcs: human cystatin S
- hsn: human cystatin SN
- hsa: human cystatin SA
- bcc: bovine colostrum cystatin
- pac: African puff adder venom cystatin
- hkl, hk2 and hk3: three human kininogen segments
- bkl, bk2 and bk3: three bovine kininogen segments
- rkl, rk2 and rk3: three rat kininogen segments
- rtll, rkl2, rkl3: three rat T-kininogen 1 segments
- rt21, rt22, rt23: three rat T-kininogen 2 segments

The cystatin families

Figure 3.25 A schematic picture of protein structure of the three families in the cystatin superfamily. Human cystatin A and B are the examples of cystatin family 1. The nematode cystatins such as Onchocystatin from *Onchocerca volvulus*, Nippocystatin from *Nippostrongylus brasiliensis* and Bm-CPI-1 from *Brugia malayi* are involved into the cystatin family 2. The novel multi-domain *F. hepatica* cystatin is structurally related to the cystatin family 3 (kininogen family).[161]
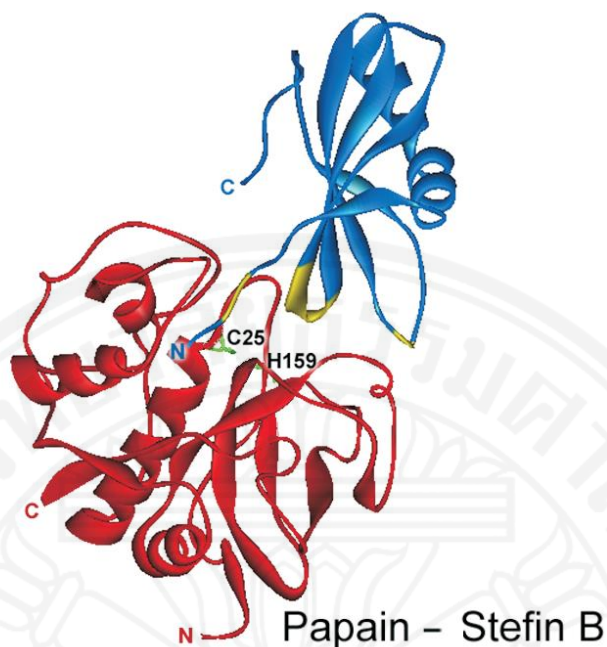
Figure 3.26 Ribbon drawing of inhibitory complexes formed between papain and stefin. The N- and C-terminal segment of stefin and papain are given together with the location of the 1st and 2nd hairpin loop. Figure made with WebLabProViewer.[110]

- Red: papain
- Blue: stefin
- Green: the location of the catalytic Cys and His residues
- Yellow: regions of inhibitor that are most important for interaction with enzyme

Table 3.3 Conserved amino-acid residues of three human cystatins regions [a].[116]

Cystatin		N terminus	I-loop	II-loop
A		MIP**G**G	**Q**V**VA**G	
B		AcMMC**GA**	**Q**V**VA**G	
C		RLV**G**G	**QI**V**A**G	**VPW**Q
D		TLA**G**G	**QI**V**A**G	**VPW**E
E		RMV**G**E	**Q**L**VA**G	**VPW**Q
F		VKP**G**F	**QI**V**K**G	**VPW**L
S		IIP**G**G	**Q**TF**G**G	**VPW**E
SA		IIE**G**G	**QI**V**G**G	**VPW**E
SN		IIP**G**G	**Q**TV**G**G	**VPW**E
H-kininogen	1-domain	*(QESQS)*	*(TVGSD)*	(RSST)
	2-domain	DCL**G**C	**Q**V**VA**G	(DIQL)
	3-domain	ICV**G**C	Q**V**VAG	VPWE
L-kininogen	1-domain	*QESQS)*	*(TVGSD)*	*(RSST)*
	2-domain	DCL**G**C	QV**VA**G	*(DIQL)*
	3-domain	ICV**G**C	QV**VA**G	**VPW**E

[a] Sequences in parenthesis correspond to the appropriate binding sequences of cystatins.

3.3.1 Cysteine protease inhibitors of mammalian and pathogenic organisms

Cystatins are the most effective natural inhibitors of cysteine proteases and have been characterized in a wide range of organisms.[205] They have also been found in viruses, bacteria, plants, animals and several different species of parasites. The following section provides examples of cysteine protease inhibitors belonging to the cystatin superfamily that have been described in detail. The result of a databank search for cystatins is shown in **Table 3.4**.

3.3.1.1 *Ixodes scapularis* (blood feeding tick)

The ticks *Ixodes scapularis* and *Haemaphysalis longicornis* are important vectors of various diseases such as Lyme disease, bovine theileriosis, bovine babesiosis, canine babesiosis and human rickettsiosis.[206-208] The distribution of *I. scapularis* is mainly in the United States but *H. longicornis* is in East Asia and Australia.[208,209] The active family 2 cystatin, sialostatin L, was found in the tick salivary glands of *I. scapularis* and showed an inhibitory activity specific to cathepsin L. The amino acid sequence of sialostatin L exhibited all of the characteristics of the family 2 cystatins, the secretion signal, the conserved QxVxG module and two disulfide bonds at the carboxyl terminus. Sialostatin L decreased the proliferation of cytotoxic T lymphocytes and showed an anti-inflammatory action. These properties encourage the transmission of tick-borne pathogens. Furthermore, understanding the vector immunity is predominant in defining the host-pathogen interactions which accelerate or restrict disease transmission.

3.3.1.2 *Schistosoma* spp.

Schistosoma mansoni and *Schistosoma japonicum* cause intestinal schistosomiasis which leads to chronic pathology affecting humans and animals. A cystatin (SmCys and Sjcystatin) expressed by adult *S. mansoni* and *S. japonicum* were characterized. SmCys and Sjcystatin sequence with a predicted molecular mass approximately 11 and 11.3 kDa respectively, was confirmed as a type 1 (stefin) cystatin. They contained the inhibition domain Gln-X-Val-X-Gly motif (Q^{49}VVAG^{53}), glycine residues at the N-terminal portion of cystatins and an LP pair at the C-terminus. SmCys and Sjcystatin also lacked a signal peptide, disulfide bonds

and the PW residues that are commonly present in all helminth species and in human cystatins C and D. SjCystatin presented the inhibitory activity against the cysteine protease papain (~60%).[185] Furthermore, The inhibitory activity of the full-length SmCys and two constructs having deletions corresponding to −10 and −20 amino acids from the N-terminus of the protein was analyzed *in vitro* and *in vivo*. Deletions of the N-terminal end were prepared because this region was essential for inhibitory activity of cystatins from other species. The results of *in vitro* experiments indicated that full-length SmCys was able to effectively inhibit papain hydrolysis while the inhibitory activity of SmCys-10 and SmCys-20 were decreased, respectively. The *in vivo* experiments demonstrated that full length SmCys and SmCys-10 were able to inhibit the formation of hemozoin (a dark pigment formed from hemoglobin) by live schistosomula.[9] Therefore, the *in vitro* and *in vivo* results confirmed that the N-terminal portion is important for the inhibitory activity of cystatins similar to previous reports of cystatin from other species.

3.3.1.3 *Fasciola hepatica*

Fasciola spp. express both cathepsin B and L cysteine proteases. Two cathepsin L-like proteases are predominantly expressed in adult stage of *F. hepatica* (FhCL1 and FhCL2) while two distinct cathepsins L (FhCL3 and FhCL4) and three cathepsins B (FhCB1, FhCB2 and FhCB3) are produced in NEJ flukes.[210,211] Recently, a novel multi-domain cystatin has been illustrated as a new member of the cystatin superfamily from the invasive stage of the parasite (NEJ).[11] *F. hepatica* multi-domain cystatin is the first multi-domain cystatin that has been found in an invertebrate species. This multi-domain cystatin is composed of six cystatin-like domains (two domains are significantly conserved, whereas four of which are degenerated cystatin signatures) and shows comparable structural features of the kininogens with functional and degenerated domains. Alignment of six putative cystatin domains presented low sequence similarities to each other (approximately 15.5–29%). *In vitro* experiment, two cystatin domains of a multi-domain cystatin showed the ability to inhibit the major cysteine protease of *F. hepatica* (cathepsin L1). Therefore, this multi-domain cystatin might be related with controlling of cysteine protease activity in the infective NEJ stage of the parasite.

3.3.1.4 Parasitic nematodes

Several cystatins have been identified from nematodes and the obtained data points to a variety of functions from cysteine protease regulation within the parasite itself to the modulation of the host immune response. The first described cystatin of parasite origin was 'onchocystatin' of the human pathogenic filarial nematode *Onchocerca volvulus*. *O. volvulus* is a subcutaneous parasitic filaria that is the causative agent of onchocerciasis or river blindness. This disease affects up to 20 million people in Africa and Latin America.[13] This protein was initially thought to regulate parasite proteases during the molting of the nematode. *O. volvulus* cystatin was shown to inhibit the human cysteine proteases cathepsin B, L and S that are involved in the proteolytic processing of polypeptides.[21] Determination of inhibition constants (K_i) revealed that recombinant *O. volvulus* cystatin effectively inhibited human cathepsin L (K_i = 0.038 nM) and cathepsin S activity (K_i = 0.033 nM) while the inhibitory activity towards human cathepsin B was less efficient (K_i = 494 nM). Onchocystatin affects the polyclonally stimulated and the Ag-driven proliferation of human peripheral blood mononuclear cells (PBMCs). Stimulated or unstimulated PBMC in the presence of onchocystatin induced an up-regulation of IL-10 and the proinflammatory cytokine TNF-**α** production, whereas IL-12p40 production and expression of HLA-DR and CD86 are decreased approximately 66% and 40%, respectively. Neutralization of anti-IL-10 antibodies restored the expression of HLA-DR and CD86. Furthermore, the reduction of monocytes from the PBMC thoroughly reversed the inhibitory effects on T-cell proliferation induced by onchocystatin, indicating that monocytes might be the target cells of immunomodulation. In conclusion, the experiments demonstrated that onchocystatin is a pathogenicity factor that is important for the persistence of *O. volvulus* in the host.

A cystatin of the rodent filaria *Acanthocheilonema viteae* has been isolated and characterized. This cystatin C-like protein has a molecular mass of approximately 17 kDa. Recombinant Av17 (rAv17) was expressed in *E. coli* and showed activity as a cysteine protease inhibitor. It was shown to down-regulate T cells response by nonspecific and antigen-specific stimuli while the production of

IL-10 and TNF-α by human PBMC and murine spleen cells were increased.[14] Moreover, rAV17 was able to enhance the NO production of IFN-γ activated murine macrophages.[212] Hence, this filarial cystatin is a likely effector molecule of immunomodulation.

Brugia malayi is an arthropod-borne nematode which causes lymphatic filariasis in humans (elephantiasis). This parasite is transmitted by mosquito vectors such as *Anopheles* and *Aedes* and affects people in South and South East Asia. Three cystatins of *B. malayi* (Bm-CPI-1, Bm-CPI-2 and Bm-CPI-3) have recently been identified.[15] Studies on one of the *B. malayi* cystatins provided the first evidence that a helminth parasite can directly interfere with the host's antigen processing and presentation pathway.[213] Bm-CPI-2 has the conserved Gly-x-Val-x-Gly, an N-terminal signal peptide, two internal disulfide bonds and PW motifs that are exhibited in type 2 cystatins and also has a conserved SND motif that was recently displayed to institute a distinct inhibitory site which is specific for asparaginyl endopeptidase (AEP), or legumain.[132] It inhibited the hydrolysis of synthetic fluorogenic substrates by cathepsin S, cathepsins B, cathepsin L, and asparaginyl endopeptidase (AEP). This inhibitor is able to block the *in vitro* antigen processing of the tetanus toxin by purified lysosome fractions. Furthermore, Bm-CPI-2 interferes with the invariant chain (Ii) and antigen processing that related with compartments of class II MHC system.[213]

A cystatin of the rodent filaria *Litomosoides sigmodontis* has also been identified and was shown to act as an immunomodulator that diminishes the antigen-specific cellular reactivity of mouse spleen cells to *L. sigmodontis* antigen.[16] *L. sigmodontis* cystatin (Ls-Cystatin) has a molecular mass of approximately 14 kDa. Alignment of the amino acid sequences revealed that the amino acid sequence similarities and identities of Ls-Cystatin and *O. volvulus, A. viteae* and *B. malayi* cystatins are around 71, 80 and 83% and 57, 64 and 66%, respectively.[214] Recombinant *L. sigmodontis* cystatin was administered into the peritoneal cavity of C57BL/6 mice via osmotic pumps and the results demonstrated that TNF-α mRNA production was up-regulated while the production of nitric oxide

and antigen-specific proliferative response of spleen cells to circulating microfilariae were significantly decreased.

Apart from the filarial cystatins, recent studies characterized cystatins of gastrointestinal nematodes. *Nippostrongylus brasiliensis* (reddish Nematoda) is a small natural parasite of wild rats. A cysteine protease inhibitor, nippocystatin, has been isolated from the excretory and secretory products (ES-product) of *N. brasiliensis* and is expressed in infective L3 and adult stages.[17] Nippocystatin is a type 2 cystatin and composed of 144 amino acids with a molecular mass of 14 kDa in mature form. The inhibitory activity of recombinant nippocystatin (rNbCys) to cathepsin L is higher than for cathepsin B. Ovalbumin (OVA)-immunized mice treated with rNbCys showed that the OVA-specific proliferation of spleen cells was inhibited but not non-antigen specific proliferation of splenocytes. Furthermore, the serum levels both OVA-specific IgG1 and IgG2a in rNbCys-treated mice were not significantly different while the levels of OVA-specific IgE was remarkably downregulated in rNbCys-treated mice. Functional studies indicated that *Nippostrongylus brasiliensis* cystatin (Nippocystatin) might have features of an immunomodulator, which inhibited antigen processing in APC of the host and related with the escape mechanism of this parasite in the host immune system.[18]

3.3.1.5 *Homo sapiens*

The cystatins of *Homo sapiens* are described in **Section 3.3**.

Table 3.4 Results of the database searches for cystatins.[11]

Protein name	Species	Acc. no	Tree name
Cysteine protease inhibitor	*Zea mays*	Q41897	Cyst1ZeaM
Cystatin II	*Zea mays*	Q41825	Cyst2ZeaM
Cysteine protease inhibitor	*Zea mays*	P93627	Cyst3ZeaM
Cystatin I precursor	*Zea mays*	P31726	Cyst4 ZeaM
Cystatin A	*Helianthus annuus*	Q10992	Cyst-HelA
Multicystatin precursor	*Solanum tuberosum*	P37842	Cyst1to Cyst8 SolT
Putative cysteine protease inhibitor B	*Arabidopsis thaliana*	O22202	Cyst1-AraT
Cysteine protease inhibitor	*Arabidopsis thaliana*	Q41906	Cyst2-AraT
Cysteine protease inhibitor like	*Arabidopsis thaliana*	O23494	Cyst3-AraT
Cysteine protease inhibitor	*Arabidopsis thaliana*	Q41916	Cyst4-AraT
Cysteine protease inhibitor	*Sorghum vulgare*	Q41294	Cyst-SorV
Cysteine protease inhibitor	*Pyrus communis*	O24462	Cyst-PyrC
Cysteine protease inhibitor	*Brassica campestris*	Q39268	Cyst1-BraC
Cysteine protease inhibitor	*Brassica campestris*	Q39270	Cyst2-BraC
Cysteine protease inhibitor	*Brassica campestris*	Q42380	Cyst3-BraC
Cysteine protease inhibitor	*Glycine max*	O04720	Cyst1-GlyM
Cysteine protease inhibitor	*Glycine max*	Q39840	Cyst2-GlyM
Cysteine protease inhibitor	*Glycine max*	Q39841	Cyst3-GlyM
Cysteine protease inhibitor	*Glycine max*	Q39842	Cyst4-GlyM

Table 3.4 Results of the database searches for cystatins (cont.).

Protein name	Species	Acc. no	Tree name
Cysteine protease inhibitor	*Ambrosia artemisiifolia*	Q38678	Cyst1-AmbA
Cysteine protease inhibitor	*Ricinus communis*	Q43635	Cyst-RicC
Cysteine protease inhibitor	*Carica papaya*	Q39561	Cyst-CarP
Oryzacystatin-I	*Oryza sativa*	P09229	Cyst1-Ory-S
Oryzacystatin-II	*Oryza sativa*	P20907	Cyst2-Ory-S
Cysteine protease inhibitor	*Vigna unguiculata*	Q06445	Cyst-VigU
Cystatin precursor	*Ornithodoros moubata*	AAS01021	Cyst-OrnM
Putative secreted cystatin	*Ixodes scapularis*	Q8MVB6	Cyst-IxoS
Putative cystatin	*Ixodes ricinus*	CAD68002	Cyst-IxoR
Cystatin	*Lepydoglyphus destructor*	Q8WQ46	Cyst-LepD
Cystatin	*Theromyson tessulatum*	Q8IT43	CystB-TheT
Cystatin-like protein	*Drosophila melanogaster*	P23779	CystL-DroM
Cystatin	*Drosophila melanogaster*	1702209A	Cyst-DroM
Sarcocystatin A precursor	*Sarcophaga peregrina*	P31727	CystA-SarP
Sarcocystatin B	*Sarcophaga crassipalpis*	Q8TYOY1	Cyst-B-SarC
Sarcocystatin A	*Sarcophaga crassipalpis*	BAB88880	Cyst-A-SarC
Cystatin precursor	*Tachypleus tridentatus*	JC4536	Cyst-TacT

Table 3.4 Results of the database searches for cystatins (cont.).

Protein name	Species	Acc. no	Tree name
Cysteine protease inhibitor like (cli-1)	*Caenorhabditis elegans*	O61973	Cyst-CaeE-cli1
Cysteine protease inhibitor like (cli-2)	*Caenorhabditis elegans*	Q9TYY2	Cyst-CaeE-cli2
Cystatin-1	*Haemonchus contortus*	O44396	Cyst-HaeC
Nippocystatin	*Nippostrongylus brasiliensis*	Q966W0	Cyst-NipB
Ls-cystatin precursor	*Litomosoides sigmodontis*	Q9NH95	Cyst-LitS
CPI-1	*Brugia malayi*	P90698	Cyst1-BruM
CPI-2	*Brugia malayi*	O16159	Cyst2-BruM
Cystatin	*Acanthocheilonema vitae*	Q17108	Cyst-AcaV
CPI-1	*Onchocerca volvulus*	Q9UA1	CPI1-OncV
Cystatin	*Onchocerca volvulus*	Q25620	Cyst-OncV
Onchocystatin precursor	*Onchocerca volvulus*	P22085	CystX-OncV
Cysteine protease inhibitor	*Schistosoma mansoni*	AAQ16180	Cyst1-SchM
Cystatin homologue	*Schistosoma mansoni*	A48570	Cyst2-SchM
Dopamine receptor	*Fugu rubripes*	Q90517	Cyst-FugR
Cystatin	*Acipenser sinensis*	AAK16731	Cyst-AciS
Cystatin precursor	*Cyprinus carpio*	P35481	Cyst-CypC

Table 3.4 Results of the database searches for cystatins (cont.).

Protein name	Species	Acc. no	Tree name
Cystatin	*Bitis ariensis*	P08935	Cyst-BitA
Cystatin	*Bitis gabonica*	AAR24527	Cyst-BitG
Family-2 cystatin precursor	*Onchorhynchus keta*	Q98967	Cyst-OncK
Cystatin precursor	*Onchorhynchus mykiss*	Q91195	Cyst-OncM
Cystatin	*Gallus gallus*	P01038	Cyst-GalG
Cystatin 8	*Mus musculus*	AAH49753	CRES-MusM
Hypothetical cysteine proteases inhibitor containing protein	*Mus musculus*	Q9DAP1	CRES-1-MusM
Stefin 1	*Mus musculus*	P35173	Cyst1-MusM
Stefin 2	*Mus musculus*	P35174	Cyst2-MusM
Stefin 3	*Mus musculus*	P35175	Cyst3-MusM
Stefin B	*Mus musculus*	Q62426	CystB-MusM
Cystatin C	*Mus musculus*	P21460	CystC-MusM
Leukocystatin	*Mus musculus*	O89098	CystF-MusM
Kininogen domain 2	*Mus musculus*	O08677	KNG2-MusM
Kininogen domain 3	*Mus musculus*	O08677	KNG3-MusM
Cystatin A	*Rattus norvegicus*	P01039	CystA-RatN
Stefin B	*Rattus norvegicus*	P01041	CystB-RatN
Cystatin C	*Rattus norvegicus*	P14841	CystC-RatN
Cystatin S	*Rattus norvegicus*	P19313	CystS-RatN
Kininogen domain 2	*Rattus norvegicus*	P08934	KNG2-RatN
Kininogen domain 3	*Rattus norvegicus*	P08934	KNG3-RatN
Rat T-kininogen	*Rattus norvegicus*	P01048	T-KNG2-RatN T-KNG3-RatN

Table 3.4 Results of the database searches for cystatins (cont.).

Protein name	Species	Acc. no	Tree name
Major acute phase alpha-1 protein	*Rattus norvegicus*	P70517	MAAP1-RatN MAAP2-RatN
Cystatin C	*Oryctolagus cuniculus*	O97862	Cyst-OryC
Stefin A1	*Sus scrofa*	Q28988	Cyst1-SusS
Stefin A5	*Sus scrofa*	Q28986	Cyst5-SusS
Stefin A8	*Sus scrofa*	Q28987	Cyst8-SusS
Stefin B	*Sus scrofa*	Q29290	CystB-SusS
Stefin D1	*Sus scrofa*	P35479	Cysti-SusS
Stefin B	*Ovis aries*	O10994	CystB-OviA
Stefin A	*Bos taurus*	P80416	CystA-Bos
Stefin B	*Bos taurus*	P25417	CystB1-Bos
Cystatin C	*Bos taurus*	P01035	CystB2-Bos
Stefin C	*Bos taurus*	P35478	CystO-BosT
Kininogen	*Bos taurus* *Bos taurus*	P01044	KNG2-BosT KNG3-BosT
Cystatin C	*Saimiri sciureus*	O19093	CytC-SaiS
Cystatin C	*Macaca mulatta*	O19092	CytC-MacM
Stefin A	*Homo sapiens*	P01040	CystA-HomS
Stefin B	*Homo sapiens*	P04080	CystB-HomS
Cystatin C	*Homo sapiens*	P01034	CystC-HomS
Cystatin D	*Homo sapiens*	P28325	CystD-HomS
Cystatin SN precursor	*Homo sapiens*	P01037	CystN-HomS
Cystatin E	*Homo sapiens*	Q15828	CystM-HomS
Cystatin S precursor	*Homo sapiens*	P01036	CystS-HomS

Table 3.4 Results of the database searches for cystatins (cont.).

Protein name	Species	Acc. no	Tree name
Cystatin SA precursor	*Homo sapiens*	P09228	CystT-HomS
Leukocystatin	*Homo sapiens*	O76096	Cyst7-HomS
Cystatin 8	*Homo sapiens*	O60676	Cyst8-HomS
CS13	*Homo sapiens*	Q8WXU6	Cyst11-HomS
Kininogen	*Homo sapiens*	P01042	KNG2-HomS
			KNG3-HomS

3.4 Immunomodulation by nematode cystatins

The immunomodulatory properties of nematode cystatins interfere with the antigen-processing pathway in MHC class II antigen presentation, cellular hyporeactivity of T cells, production of cytokines and production of NO and result in the modification of the host immune response.

3.4.1 Interference with antigen presentation and T cell responses

The first step of the immune response to exogenous antigens requires the formation of peptide–MHC class II complexes in antigen presenting cells (APCs) such as macrophages and dendritic cells (DCs) that capture and process antigens to T lymphocytes. In this process (antigen processing and presentation), cysteine proteases might have two major roles that could be targeted by nematode cystatins (**Figure 3.27**). Firstly, cysteine proteases are involved in the degradation of proteins into antigenic peptides within the endosomal-lysosomal compartment of APCs and the peptides are linked to MHC class II molecules and transferred to the membrane. The cysteine proteases, cathepsin B, cathepsin S and cathepsin L, are involved in the degradation of internalized antigens. Secondly, cysteine proteases participate in the degradation of the MHC chaperone invariant chain (Ii) that plays an important role in intracellular trafficking and peptide loading of MHC class II molecules. Ii has to be progressively degraded within endosomes, in smaller fragments from Ii to Lip 23, Lip 10 and finally in a 3-kDa peptide called CLIP (class II-associated invariant chain peptide). Clip fragment which bound to the MHC class II groove is released and allows the peptides to bind the MHC class II molecule.[215] Subsequently, MHC class II with bound antigen is transported to the cell surface for T cells presentation. Ii degradation is performed by various cathepsins depending on the APC types for example the cysteine protease cathepsin L is active in thymus epithelial cells[130,216] while cathepsin F is active in macrophages.[217] Moreover, cathepsin S participates in the production of the Clip fragment in DCs and B cells.[216,218] The inhibition of cysteine proteases that are important for antigen processing and presentation by nematode cystatins could lead to an inefficient antigen-specific T cell response by suppressing APCs to process antigen, generate and

load MHC class II molecules and subsequently reduction of T cell proliferation as described for cystatins from *O. volvulus*, *A. viteae*, *L. sigmodontis*, *N. brasiliensis* and *B. malayi* (CPI-2) (**Section 3.3.1.4**). This would allow the parasites to evade from the host immune system.[16,17,20,21,213]
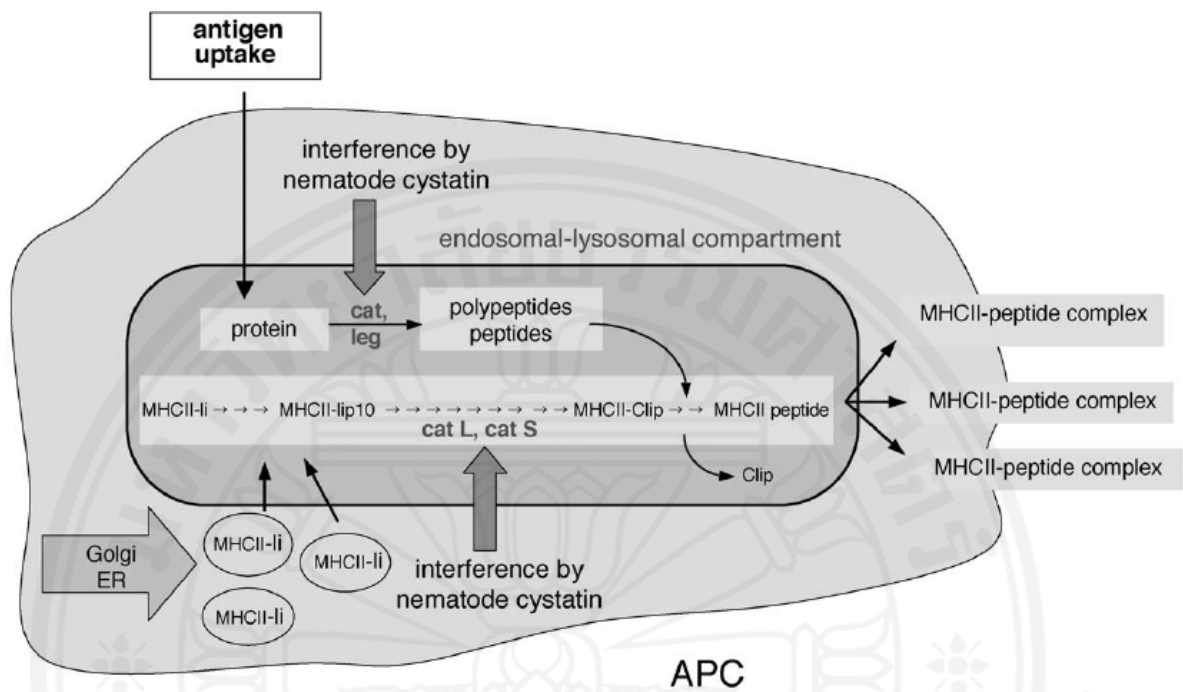
Figure 3.27 Immune response to exogenous antigens requires the formation of peptide–MHC class II complexes in antigen presenting cells (APCs).[203]

    - cat: cathepsin

    - leg: legumain

    - Ii: invariant chain

3.4.2 Modulation of the cytokine production

Nematode cystatins might have effect on the production of cytokines. Filarial cystatins have been described to induce anti-inflammatory cytokine responses such as an increased level of IL-10 and a decreased level of IL-12. The most important feature is the induction of a Th2 response. The contact of macrophages with bacterial lipopolysaccharide (LPS), peptidoglycan or lipoarabinomannan (LAM) and related substances leads to a characteristic pattern that is generated by upregulation of TNF-**α** followed by increase of the cytokine IL-10.[19,20] IL-10, a cytokine that causes immunosuppressive effects, is predominantly upregulated and that leads among others to the downregulation of costimulatory surface molecules of macrophages (CD86 and the HLA-DR receptor) and reduced T-cell activation. There have been several studies about the immunomodulatory properties of filarial cystatin such as onchocystatin (*O. volvulus* cystatin) that demonstrated that human PBMC exposed to this cystatin induced TNF-**α** production, followed by a strong upregulation of IL-10 and downregulation of IL-12.[21] Furthermore, *A. viteae* cystatin (Av17) enhanced the production of IL-10 and led to down-regulation of IL-4 but had no effect on IFN-**γ** and IL-2 production.[14] Therefore, these data suggest that IL-10 might be an essential component associated with inhibition of T cell proliferation after exposure of mononuclear cells to filarial cystatin and high levels of IL-10 are a characteristic feature of filarial infections and this is related to T cell hyporeactivity.[22]

3.4.3 Effects on the inducible nitric oxide production

Nitric oxide (NO), a short living molecule, is essential in several physiological and biological processes including cytostasis, inhibition of tissue invasion, reduced growth, smooth muscle regulation, neurotransmission and vasodilatation and also involved in a major defense molecule of immune cells with effects on protozoans and helminth parasites.[219,220] The upregulation of NO from IFN-**γ** activated macrophages was observed when exposed to members of three cystatin families. The natural cysteine protease inhibitors could increase the NO production while the synthetic inhibitors such as E64 failed to up-regulate the level of NO. Furthermore, the inhibitors of aspartyl, serine proteases and aprotinin (a

trypsin-like serine protease inhibitor) are also without effect on the production of NO.[23]   NO is synthesized by macrophages from L-arginine by NO-synthase (NOS) which has three isoforms (NOS-1, NOS-2 and NOS-3) with tissue-specific distribution and regulation.[221]   NOS-1 (neuronal NOS or n NOS) and NOS -3 (endothelial NOS or eNOS) are calcium dependent and found in neurons and endothelial cells, respectively while NOS2 (inducible NOS or iNOS) is calcium independent, present in macrophages, fibroblasts and hepatocytes and induced by IFN-γ that lead to synthesis of substantial amounts of NO.   Moreover, NO has been shown to be involved in the inhibition of lymphocyte proliferation and the expression of cytokines in several cell types.[222,223]   Many nematode parasites such as *B. malayi*, *O. volvulus*, *O. lienalis L. sigmodontis* and *A. viteae* were shown to be significantly affected by NO released from IFN-γ activated macrophages, although some filarial worms were affected in *in vivo* experiments.[203,212]   In filarial infection, the upregulation of NO production seems to be involved in the increase of IL-10 and TNF-α that might play a role in concert to suppress the immune response or polarize the host T cell responses toward Th2/Th3 responses that are characteristic for nematode infection and also related with the suppression of T cell proliferation in a murine model of filariasis.[20,212,224,225]

CHAPTER IV

MATERIALS AND METHODS

4.1 Molecular cloning and sequence analysis of FgStefin-2

4.1.1 Molecular cloning of FgStefin-2 cDNA
4.1.1.1 PCR amplification of FgStefin-2 cDNA

A cDNA was amplified by RT-PCR from total RNA of adult *F. gigantica* using primers (forward 5' -GAT TTG TGA AGG TGA AGC-3', reverse 5'-TGC ATG TGC AGA GAT AGC-3') based on an EST sequence from an adult stage cDNA of *F. gigantica*. The components in the RT-PCR and PCR mixture are shown below.

The reverse transcription reaction was set following the instruction manual of RevertAid™ M-MuLV Reverse Transcriptase (Thermo Scientific, Lithuania).

Components	Volume (µl)
Total RNA	1.0
Reverse primer (10µM)	2.0
DEPC-treated DW	10.0
Mix all above components by pipetting, briefly spin and add following components	
5× RevertAid™ reaction buffer	4.0
Mixed dNTPs (2.5mM each)	2.0
RiboLock™ RNase Inhibitor	0.5
RevertAid™ M-MuLV Reverse Transcriptase	0.5
Total volume	20.0

The mixture was incubated at 42°C for 1 h. The reaction was terminated by heating at 70°C for 10 min. The reverse transcription product was stored on ice until used as template of PCR.

Components	Volume (µl)
Template (RT-PCR product)	2.0
Forward primer (10µM)	1.0
Reverse primer (10µM)	1.0
$10\times(NH_4)_2SO_4$ buffer	5.0
$MgCl_2$ (25mM)	3.0
Mixed dNTPs (2.5mM each)	1.0
Taq DNA polymerase (5U/µl)	0.5
DW	36.5
Total volume	50.0

The PCR reaction was performed using following conditions: pre-denaturation at 95℃ for 5 min, 35 cycles of denaturation at 95℃ for 1 min, annealing at 45℃ for 1 min and extension at 72℃ for 1 min then one cycle of final extension at 72℃ for 10 min and hold at 4℃. The PCR product was resolved on a 0.7% (w/v) agarose gel.

4.1.1.2 Agarose gel electrophoresis

The PCR product was separated by electrophoresis in a 0.7% (w/v), 1% (w/v) or 1.2% (w/v) agarose gel. Agarose gel was prepared by dissolving Ultrapure™ agarose power (Invitrogen, Carlsbad, CA, USA) at the required final concentration in 0.5× TBE electrophoresis buffer (22.5 mM Tris-base, 22.5 mM boric acid, 1mM EDTA, pH8.0) containing 0.5 µg ethidium bromide per one ml of agarose gel. The agarose was fully dissolved by heating in a microwave oven until the solution became homogeneous and it was allowed to cool down to 60℃ before pouring into a gel tray (Horizon®, Gibco-BRL, USA). An appropriate comb was inserted and the gel was allowed to harden for 30–60 min before it was submersed into the gel electrophoresis chamber (Horizon®, Gibco-BRL, USA) containing 0.5× TBE and 0.5 µg/ml ethidium bromide buffer. The samples were mixed with 10× DNA loading buffer (0.25% [w/v] bromophenol blue, 0.25% [w/v] xylene cyanol FF, and 50% [v/v]

glycerol) to yield a final concentration of 1× loading buffer. The samples were loaded to the wells of the gel with an appropriate DNA marker (DNA ladder, Thermo Scientific, Lithuania) in an adjacent lane. Electrophoresis was performed at 80 V until the bromophenol blue dye front had migrated about 2/3 of the gel length. The nucleic acid pattern on the gel was directly visualized under an UV transilluminator (Gel Doc 2000, BIO-RAD, Milan, Italy).

4.1.1.3 Isolation of PCR product from agarose gel by using QIA quick® Gel Extraction Kit

The DNA band of interest was excised from the agarose gel with a clean and sharp scalpel and transferred into a 1.5 ml microcentrifuge tube. The gel was extracted by using a QIA quick® Gel Extraction Kit (QIAGEN, Limburg, Netherlands) according to the manufacturer's instructions. The weight of the gel slice was measured in a tube and 3 volume of QG buffer was added to 1 volume of gel (300 μl buffer QG/100 mg gel). The sample was heated at 50°C for 10 min and mixed by vortexing every 2 min. Isopropanol was added at a ratio 1:1 of gel slice volume (100 μl isopropanol per 100 mg of gel) after the gel was completely dissolved. The solution was mixed and loaded to a QIAquick column followed by centrifugation at 13,000 rpm for 1 min. The flow-through was discarded and PE buffer 0.75 ml was added into the column for washing step. The sample was centrifuged at 13,000 rpm for 1 min and the flow-through was discarded. The QIAquick column was placed into a fresh 1.5 ml microcentrifuge tube, 50 μl of DW was added and incubated at room temperature for 1 min followed by centrifugation at 13,000 rpm for 1 min to elute the bound DNA. The extracted DNA was resolved by 0.7% (w/v) agarose gel electrophoresis and stored at −20°C.

4.1.2 **Molecular cloning of the PCR-amplified FgStefin-2 cDNA and transformation of the bacterial host cells with the recombinant plasmid**

4.1.2.1 **Ligation of FgStefin-2 PCR product into the pGEM® -T Easy vector**

The gel-extracted FgStefin-2 PCR product (**Section 4.1.1.3**) was inserted into the pGEM®–T Easy vector (Promega, USA) using the conditions as described below.

Ingredients	Volume (μl)
Rapid ligation buffer (2×)	5.0
pGEM®–T Easy vector (50 ng/μl)	1.0
PCR product	3.0
T4 DNA ligase (3 Weiss units/μl)	1.0
Total volume	10.0

All of the ingredients were mixed in a 1.5 ml microcentrifuge tube, briefly spun and incubated at 4°C overnight. The ligation product was introduced into *E. coli* XL1-Blue competent cells by chemical transformation as described in **Section 4.1.2.2**.

4.1.2.2 **Preparation and storage of chemical competent *E. coli* cells**

E. coli XL1-Blue, *E. coli* M15 and *E. coli* Top10 bacteria were grown on LB-agar containing 15 μg/ml tetracycline, 25 μg/ml kanamycin and no antibiotics, respectively at 37°C for 16-18 h. A single isolated colony was selected for inoculation of 5 ml LB broth and the culture was grown at 37°C overnight with shaking at 250 rpm. One milliliter of the *E. coli* culture was used to inoculate 100 ml fresh LB broth and the culture was incubated until an OD_{600} value of 0.5 had been reached. The bacterial culture was cooled down to 0°C by vigorously swirling the flask in a salt-ice water bath for 3 min and centrifuged at 6,000×g, 4°C for 8 min to harvest the bacterial cells. The supernatant was discarded and the bacterial pellet

was gently resuspended in 20 ml ice-cold 0.1 M $MgCl_2$ by agitation. The mixture was centrifuged again at 6,000×g, 4°C for 8 min and the supernatant was discarded. The pellet was gently resuspended in 20 ml ice-cold 0.1 M $CaCl_2$ and kept on ice for 20 min. The cells were pelleted as above, the supernatant was discarded and the cell pellet was gently resuspended in 4.3 ml 0.1 M $CaCl_2$ and mixed with 0.7 ml glycerol. The competent *E. coli* XL1-Blue cells and *E. coli* M15 were distributed into 100 µl aliquots, shock frozen in liquid nitrogen for 5 min and stored at −80°C.

4.1.2.3 Chemical transformation of competent *E. coli* with recombinant the pGEM® -T Easy DNA

The ligation product (**Section 4.1.2.1**) at amounts of 50–100 pg was pipetted into a 15 ml prechilled polypropylene tube. Competent *E. coli* XL1-blue cells were thawed on ice, 100 µl of the competent cells were added to the tube containing the recombinant plasmid DNA solution and gently mixed by pipetting up and down several times. Following incubation on ice for 20 min the transformation reaction was heat shocked by placing the tube into a 42°C water bath for 45 s and then immediately incubated on ice for 2 min before 900 µl LB broth was added. The sample was incubated at 37°C for 1 h with shaking at 250 rpm. The transformed cells (10 µl to 100 µl aliquots) were spread on 37°C-prewarmed LB agar containing 100 µg/ml ampicillin and incubated at 37°C overnight. Several single colonies were checked for positive transformants using colony PCR.

4.1.2.4 Colony PCR to screen for positive transformants

The bacterial colonies from **Section 4.1.2.3** were picked and suspended in 10 µl DW and used as template for PCR amplification. The FgStefin-2 fragment was amplified by using specific forward and reverse primers as described in **Section 4.1.1.1**. The reaction mixture was prepared as shown next page.

Components	Volume (µl)
Template (bacterial colony in 10 µl of DW)	2.0
Forward primer (10µM)	1.0
Reverse primer (10µM)	1.0
10×$(NH_4)_2SO_4$ buffer	5.0
$MgCl_2$ (25mM)	3.0
Mixed dNTPs (2.5mM each)	1.0
Taq DNA polymerase (5U/µl)	0.5
DW	36.5
Total volume	50.0

The PCR reaction was set using following conditions: pre-denaturation at 95°C for 5 min, 35 cycles of denaturation at 95°C for 1 min, annealing at 45°C for 1 min and extension at 72°C for 1 min then one cycle of final extension at 72°C for 10 min and hold at 4°C. The PCR product was resolved on a 0.7% (w/v) agarose gel.

4.1.2.5 Plasmid DNA purification by using quick preparation (for screening of many positive clones)

Isolated single bacterial colonies carrying recombinant pGEM®–T Easy plasmid was picked from the selective agar plate and used to inoculate 5 ml LB broth containing 100 µg/ml ampicillin. The culture was incubated at 37°C with shaking at 250 rpm overnight. The bacterial cells were pelleted by centrifugation at 4,000×g for 5 min. The pellet was resuspended in 200 µl solution I (25 mM Tris, pH 8.0, 50 mM glucose, 10 mM EDTA) and the mixture was transferred to a microcentrifuge tube. Afterwards, 400 µl of freshly prepared solution II (0.1 N NaOH, 1% [w/v] SDS) was added to the bacterial suspension, mixed by tube inversion and incubated on ice for 5 min. After that, 300 µl solution III (2.7 M Potassium acetate, pH 4.8) was added, mixed again by inverting and incubated on ice for 5 min. The mixture was subsequently centrifuged at 12,000×g, room temperature for 5 min

and the clear supernatant containing nucleic acids was transferred to a new microcentrifuge tube. Isopropanol at 0.6 volume of the transferred supernatant was added and mixed by inverting. The precipitated DNA was pelleted by centrifugation at 12,000×g, room temperature for 5 min and the supernatant was removed. The DNA pellet was washed with 70% (v/v) ethanol, centrifuged at 12,000×g, room temperature for 2 min and the supernatant was discarded. The pellet was air dried, resuspended in 50 μl DW and treated with 0.5 μl RNase A (10mg/ml, Fermentas Life Sciences, Vilnius, Lithuania). The extracted plasmid DNA was digested with the restriction endonuclease *Eco*R I (Fermentas Life Sciences, Vilnius, Lithuania). The reaction mixture is shown below.

Ingredients	Volume (μl)
Plasmid DNA	3.0
*Eco*R I buffer (10×)	2.0
*Eco*R I (10 U/μl)	0.5
DW	14.5
Total volume	20.0

The sample was incubated at 37°C for 2 h and then the restriction endonuclease was inactivated at 65°C for 20 min. The product was resolved by 0.7% (w/v) agarose gel electrophoresis (as described in **Section 4.1.1.2**). After electrophoretic analysis, the positive clones were collected and used for further experiments.

  4.1.2.6 Plasmid DNA purification by using the QIAprep® Spin Miniprep Kit (for cloning and DNA sequencing purposes)

  Isolated single bacterial colonies were used to inoculate 5 ml LB broth containing 100 μg/ml ampicillin and the bacteria were grown at 37°C overnight with shaking at 250 rpm. The bacterial cells were harvested by centrifugation at 4,000×g for 5 min at room temperature. The plasmid was purified by using a QIAprep® Spin Miniprep Kit (QIAGEN, Limburg, The Netherlands) according to the manufacturer's instructions. The pelleted bacterial cells were resuspended in

250 µl buffer P1 (50 mM Tris-HCl, 10 mM EDTA, 100 µl RNase A) and transferred to a microcentrifuge tube. The cell suspensions were mixed with 250 µl buffer P2 (200 mM NaOH, 1% [w/v] SDS) by gently inverting the tube 4–6 times. After that, 350 µl buffer N3 (3.0 M Potassium acetate, pH 5.5) was added and immediately mixed by inverting the tube 4–6 times. The mixture was subsequently centrifuged at 12,000×g, room temperature for 10 min. The supernatant containing plasmid DNA was transferred into the QIAprep$^®$ spin column and centrifuged at 12,000×g, room temperature for 30–60 s. The column was washed with 750 µl buffer PE (1.0 M NaCl, 50 mM MOPS, pH 7.0, 15% [v/v] isopropanol) and centrifuged at 12,000×g, room temperature for 30–60 s. The flow-through was discarded from the collecting tube and the spin column was centrifuged for 1 min to remove the remaining PE buffer. Finally, the spin column was placed into a new microcentrifuge tube, added 50 µl sterile DW and incubated at room temperature for 1 min followed by centrifugation at 12,000×g for 30–60 s to elute the plasmid DNA. Plasmid DNA was verified to contain the correct insert by restriction analysis as described in **Section 4.1.2.5** and the nucleotide sequence was determined by using commercial services (1st Base Asia, Singapore). The positive clone was collected and used for further experiments.

4.1.3 Sequencing and sequence analysis

Recombinant plasmid DNA of the *E. coli* XL1-Blue clone carrying an FgStefin-2 cDNA insert was extracted by using a QIAprep$^®$ Spin Miniprep Kit (QIAGEN, Limburg, The Netherlands) and sent to a commercial services provider for sequencing (1st Base Asia, Singapore). EMBOSS 6.3.0 and SignalP 4.1 were used for editing and analyses of molecular sequences. NCBI-BLASTP (http://blast.ncbi.nlm.nih. gov/Blast/) was used to evaluate classification of FgStefin-2 as a type 1 cystatin. ClustalX was used to calculate a multiple alignment.

4.2 Characterization of FgStefin-2 gene nucleic acids

4.2.1 Preparation of different developmental stages of *F. gigantica*

4.2.1.1 Preparation of newly excysted juveniles

Metacercariae were added into sterile water at room temperature overnight. In the following day, the metacercariae were suspended in 10 ml of solution I (1% [w/v] pepsin [Sigma Aldrich, Steinheim, Germany], 0.4% [v/v] HCl) and incubated at 37°C for 1 h. The supernatant was discarded and the metacercariae were washed with sterile water for 3 times. The metacercariae were incubated in 10 ml of solution II (0.02 M $Na_2O_4S_2$, 0.2% [w/v] taurocholic acid, 1% [w/v] $NaHCO_3$, 0.8% [w/v] NaCl, 0.6% [v/v] HCl) at 37°C for 75 min. The supernatant was discarded and the metacercariae were washed with RPMI-1640 for 3 times. Then the metacercariae were incubated in fresh RPMI-1640 containing 10 µg/ml gentamycin and 10% fetal bovine serum at 37°C for 3–5 h. The excystment process was monitored under the microscope and the newly excysted juveniles were collected and kept at −20°C for further experiments.

4.2.1.2 Preparation of juveniles and collection of sera from infected mice

BALB/c mice were orally infected with 20 *F. gigantica* metacercariae. Juveniles were obtained from the dissected liver parenchyma after sacrificing the infected animals 2, 4, and 6 weeks after infection. The juveniles were washed several times with 0.85% NaCl and stored in liquid nitrogen for further experiments. Serum samples of the infected mice were collected preinfection and weekly postinfection.

4.2.1.3 Preparation of adult parasites

Adult *F. gigantica* were freshly collected from bile ducts and livers of natural infected cattle sacrificed at a slaughterhouse in Pathumthani province, Thailand. The adult parasites were several times washed with 0.85% NaCl to remove the host blood, bile and contaminated microorganisms and kept in liquid nitrogen or processed for further experiments.

4.2.2 Extraction of adult *F. gigantica* genomic DNA

Genomic DNA (gDNA) was extracted from adult *F. gigantica* kept frozen in liquid nitrogen. The frozen parasites were placed in a precooled mortar and liquid nitrogen in small amount was added. Following the parasites were ground to a powder by using a precooled pestle. The frozen powder was transferred into a new tube and resuspended in 500 µl of homogenization buffer (30 mM Tris-HCl, pH 8.0, 0.1 M NaCl, 10 mM EDTA, 0.5% [v/v] Triton X-100). Following centrifugation at 5,000 rpm, room temperature for 5 min the supernatant was discarded and the pellet was resuspended in 500 µl of extraction buffer (0.1 M Tris-HCl, pH 8.0, 0.1 M NaCl, 20 mM EDTA). The suspension was centrifuged at 5,000 rpm for 2 min at room temperature, the supernatant was discarded and the pellet was resuspended in 300 µl of extraction buffer. Three microliters of Proteinase K (10 mg/ml, Fermentas Life Science, Vilnius, Lithuania) and 15 µl of SDS (20% [w/v]) were added to the suspension and incubated at 50°C for 1 h. The degraded and denatured proteins were extracted by added an equal volume of phenol-chloroform solution (phenol: chloroform: isoamyl alcohol – 25:24:1 Ultrapure MB Grade, USB cooperation, OH, USA) and centrifuged at 12,000×g for 5 min. The colorless supernatant was collected. The protein extraction was repeated once with phenol-chloroform and once with chloroform. The supernatant of chloroform extracted was carefully transferred to a new tube and the solution was treated with 10 µl RNase A (10 mg/ml, Fermentas Life Sciences, Lithuania) at 40°C for 1 h to degrade RNA. RNase A was removed by phenol-chloroform and chloroform extraction steps as described previously. The supernatant containing genomic DNA was precipitated by adding 2.5 vol of ethanol (kept at –20°C) and 0.1 vol of 3 M sodium acetate. The sample was mixed and centrifuged at 12,000×g for 20 min at room temperature. The pellet was washed with 70% (v/v) ethanol, air dried and resuspended in 100 µl distilled water. The quality of the genomic DNA was analyzed by 0.7% (w/v) agarose gel electrophoresis and the concentration was determined by comparing the band intensity in the gel to uncut λ phage DNA under UV light. The genomic DNA was kept at -80°C until used in further experiments.

4.2.3 Extraction of total RNA from metacercariae, NEJ, 2-, 4-, 6-week-old juveniles and adult *F. gigantica* using TRIzol^{TM} reagent

Total RNA of metacercariae, juveniles (NEJ, 2-, 4-, and 6-week-old) and adult *F. gigantica* was extracted in TRIzol^{TM} reagent (Invitrogen, Carlsbad, CA, USA). All of the parasites except metacercariae were homogenized by using a tissue homogenizer (Ultra-Turrax® T25 basic, IKA, Germany) at ratio 50–100 mg tissue/1 ml of TRIzol^{TM} reagent. Metacercariae were incubated in 1% (w/v) pepsin, 0.4% (v/v) HCl at 37°C for 1 h and then homogenized in 1 ml TRIzol^{TM} reagent per 50–100 mg weight using a precooled pestle and mortar. Insoluble matter was removed from the homogenate solution by centrifugation at 12,000×*g*, 4°C for 10 min. The cleared supernatant was transferred to a fresh tube and incubated at room temperature for 5 min. Then chloroform at a volume 0.2 ml per 1 ml of TRIzol^{TM} reagent was added, mixed by shaking for 15 s and incubated at room temperature for 2–3 min. The sample was centrifuged at 12,000×*g*, 4°C for 15 min. The mixture was separated into a lower red phenol-chloroform phase, an interphase, and a colorless upper aqueous phase. RNA remained exclusively in the aqueous phase. The aqueous phase was carefully transferred without disturbing the interphase into a new tube. RNA was precipitated by adding isopropyl alcohol (0.5 ml per 1 ml of starting TRIzol^{TM} reagent). The sample was incubated for 10 min at room temperature and centrifuged at 12,000×*g*, 4°C for 10 min. The supernatant was discarded and the RNA pellet was washed once with 1 ml of 75% ethanol and centrifuged at 7,500×*g*, 4°C for 5 min. The pellet was dried and re-dissolved in DEPC-treated DW. The quality of RNA was analyzed by 1% (w/v) agarose gel electrophoresis and the concentration was quantitated by photometrical analysis (Nanodrop® ND-1000, Thermo Scientific, Waltham, MA, USA). The RNA was kept at −80°C until processed in further experiments.

4.2.4 Construction of a digoxigenin (DIG) labeled FgStefin-2 DNA probe

4.2.4.1 Restriction endonuclease digestion of the recombinant pGEM®–T Easy plasmid carrying the FgStefin-2 cDNA

The pGEM®–T Easy plasmid containing the FgStefin-2 encoding sequence as described in **Section 4.1.2.6** and **Section 4.3.1** were digested with an appropriate restriction enzyme for the Southern and Northern hybridization DIG-labeled DNA probe, respectively. The reactions mixture were prepared as shown below.

Components	Volume (μl)
Plasmid DNA	3.0
*Eco*R I buffer (10×)	2.0
*Eco*R I (10 U/μl)	0.5
DW	14.5
Total volume	20.0

Components	Volume (μl)
Plasmid DNA	5.0
BamH I buffer (10×)	2.0
*Bam*H I (10 U/μl)	0.5
Pst I (10 U/μl)	1.0
DW	11.5
Total volume	20.0

The sample was mixed and incubated at 37°C for 2 h and then the restriction endonuclease was inactivated at 65°C, 80°C for 20 min (*Eco*R I and *Bam*H I plus *Pst* I, respectively). The digestion products were resolved on a 0.7% (w/v) agarose gel (as described in **Section 4.1.1.2**). After electrophoresis, the FgStefin-2 DNA fragment was extracted from the agarose gel using a QIA quick® Gel

Extraction Kit (as described in S**ection 4.1.1.3**) and used as template for preparation of DIG-labeled DNA probe.

4.2.4.2 Labeling of the FgStefin-2 cDNA probe

The isolated FgStefin-2 cDNA fragment from **Section 4.2.4.1** was used as template for probe preparation using the PCR DIG-Labeling Kit (Roche Diagnostics, Mannheim, Germany). Two primer pairs were used as described in **Sections 4.1.1.1 and 4.3.1.** The components in the PCR reaction mixture are listed below.

Components	Volume (μl)
Template from Section 4.2.4.1	2.0
Forward primer (10 μM)	1.0
Reverse primer (10 μM)	1.0
10×$(NH_4)_2SO_4$ buffer	10.0
$MgCl_2$ (25 mM)	6.0
PCR DIG Labeling Mix (Dig labeling dNTPs)	10.0
Taq DNA polymerase (5U/μl)	1
DW	69
Total volume	100.0

The PCR reaction sample was mixed and PCR performed using following conditions: pre-denaturation at 95°C for 5 min, 35 cycles of denaturation at 95°C for 1 min, annealing at 55°C, 45°C for 1 min (Northern and Southern hybridization DIG-labeled DNA probe, respectively) and extension at 72°C for 1 min then one cycle of final extension at 72°C for 10 min and hold at 4°C. The synthesized probe was analyzed by 0.7% (w/v) agarose gel electrophoresis (as described in **Section 4.1.1.2**).

4.2.4.3 Probe quantification by spot assay

The concentration of the DIG-labeled DNA probe was determined by a spot test with DIG-labeled control DNA. The DIG-labeled control

DNA (Roche Diagnostics, Mannheim, Germany) and DIG-labeled FgStefin-2 specific DNA probe were diluted to a concentration of 1 µg/ml. The amount of DIG-labeled DNA probe and the dilution series of DIG-labeled DNA probe in DNA dilution buffer provided in the Kit (Roche Diagnostics, Mannheim, Germany) are shown in **Table 4.1**.

Table 4.1 List of the amount and dilution series of DIG-labeled DNA probe.

Tube	DIG-labeled DNA concentration (1µg/ml)/dilution buffer	Final concentration (pg/ µl)	Total dilution
1	1 µl/ 9 µl	100	1:10
2	1 µl (tube1)/ 9 µl	10	1:100
3	3 µl (tube1)/ 7 µl	3	1:330
4	1 µl (tube2)/ 9 µl	1	1:1000
5	1 µl (tube3)/ 9 µl	0.3	1:3300
6	1 µl (tube4)/ 9 µl	0.1	1:10000
7	1 µl (tube5)/ 9 µl	0.03	1:33000
8	1 µl (tube6)/ 9 µl	0.01	1:100000
9	0 µl/ 10 µl	0	Negative control

Probe dilutions ranging from 0 to 100 pg per µl were prepared and 1 µl of each was spotted onto a nylon membrane (Amersham Hybond™ N⁺, GE Healthcare, Buckinghamshire, UK). The membrane was air dried and then rinsed with washing buffer (10 mM PBS [140 mM NaCl, 2.7 mM KCl, 10 mM Na_2HPO_4, 1.8 mM KH_2PO_4], pH 7.2, and 0.05% [v/v] Tween-20) for 5 min. This was followed by incubation in 1× blocking buffer (Blocking Reagent, Roche Diagnostics, Mannheim, Germany) at room temperature for 30 min. The blocking solution was discarded and the membrane incubated in anti-digoxigenin-AP Fab fragments (Roche Diagnostics, Mannheim, Germany) diluted 1:5,000 in 1× blocking solution at room temperature for 30 min. The membrane was washed in washing buffer at room temperature twice, for 15 min each. Afterwards, the detection buffer (0.1 M Tris-HCl, pH 9.5, 0.1 M NaCl, 50 mM $MgCl_2$) was added to equilibrate the membrane for 5 min before adding the freshly prepared BCIP/NBT substrate solution (Amresco, Salon, OH, USA). The membrane was incubated in the dark without shaking until a color precipitate had formed. Color development was stopped by washing the membrane several times with DW. The spot intensive of the control and specific probe were compared to estimate concentration of DIG-labeled FgStefin-2 specific DNA probe.

4.2.5 Southern hybridization analysis

4.2.5.1 Digestion of genomic DNA

Genomic DNA (20 µg) of *F. gigantica* (**Section 4.2.2**) was digested with restriction endonucleases (Thermo Scientific, Lithuania) *Bam*H I, *Hin*d III, or *Bam*H I/*Hin*d III and separated by electrophoresis in a 0.7% (w/v) agarose gel in TBE buffer including ethidium bromide (0.5 µg/ml). All reactions of genomic DNA were separated as described next.

Components	Volume (µl)		
	Tube 1	Tube 2	Tube 3
Genomic DNA	25	25	25
10× *Bam*H I buffer	2	-	2
10× buffer R	-	2	-
*Bam*H I	1	-	1
*Hin*d III	-	1	2
DW	2	2	-
Total volume	30	30	30

The reactions were incubated at 37°C for 6 h in an incubator (Memmert, Germany). The reactions of enzyme were stopped by heat-inactivating at 80°C for 20 min. The digested DNA was resolved on a 0.7% (w/v) agarose gel at 25 V, 12–16 hours. The agarose gel was prepared following the procedure described in **Section 4.1.1.2.** Lambda DNA digested with *Eco*R I and *Hin*d III (Thermo Scientific, Lithuania) was used as a size standard. Subsequently, the marker lane was cut from the gel and the remaining gel was processed for Southern transfer.

4.2.5.2 Southern transfer

The agarose gel containing fragmented genomic DNA from **Section 4.2.5.1** was incubated in 0.25 N HCl for 20 min at room temperature and denatured by soaking the gel in denaturing buffer (3 M NaCl, 0.5 N NaOH) for 30 min. Following this gel was incubated in neutralizing buffer (0.5 M Tris-HCl, pH 7.0, 1.5 M NaCl) twice, for 20 min each and transferred into 10× SSC (3 M NaCl, 0,3 M sodium citrate, pH 7.0) for 30 min. The fragmented DNA was capillary-transferred to a nylon membrane (Hybond-N Plus, Amersham Biosciences). The blotting tower is illustrated in **Figure 4.1**. Two pieces of blotting paper (3MM Chromatography paper, Whatman, UK) were cut 4–6 inches larger than the gel, saturated with transfer buffer (10× SSC) and placed on the gel support plate of the blotting set. The plate was placed in the transfer buffer reservoir with both ends of the gel blotting paper hanging into the

buffer reservoir. The agarose gel (upside-down) was placed on the top of the gel blotting paper (bridge) and covered with the prepared nylon membrane, followed by two pieces of gel blotting paper cut to fit the gel size. A stack of paper towels was placed on top of the blotting paper. Sufficient transfer buffer (10× SSC) was added to the buffer reservoir to ensure a complete transfer. Finally, a light weight was placed on the top of the stacking paper towels. The DNA was allowed to transfer to the membrane overnight. On the following day, the stack was disassembled and the membrane was soaked in 5× SSC for 5 min to remove bits of gel or particles from the membrane and dried at room temperature. The nucleic acid was immobilized on the membrane by baking in a vacuum oven at 80°C for 1 h. The membrane was stored at −20°C until use.

4.2.5.3   Southern hybridization

The nylon membrane containing size-separated genomic DNA was equilibrated in pre-hybridization buffer (5× SSC, 50% [v/v] formamide, 0.1 mg/ml heat-denatured Herring sperm DNA [Promega, Madison, WI, USA], 0.02% [w/v] SDS, 2% [v/v] blocking reagent [Roche Diagnostics, Mannheim, Germany]) in a hybridization tube in a hybridization oven with slow rotation at 42°C for 1 h. The DIG-labeled FgStefin-2 DNA probe (**Section 4.2.4**) was denatured at 95°C for 5 min, cooled on ice and added to fresh hybridization buffer. The pre-hybridization buffer was replaced with fresh hybridization buffer that contained the DIG-labeled FgStefin-2 DNA probe. The membrane was incubated at 42°C for 16–18 hours in a hybridization oven with rotating. In the following day, the hybridization buffer was removed and kept at −20°C for reuse. The membrane was incubated in wash buffer I (2× SSC, 0.1% [w/v] SDS) at room temperature twice, for 5 min each and wash buffer II (0.1× SSC, 0.1% [w/v] SDS) at 50°C twice, for 15 min each. The nylon membrane was then transferred from the hybridization tube to a container for immunological detection.

4.2.5.4   Immunological detection

After the hybridization and washing steps, the membrane was rinsed in maleic acid washing buffer (0.1 M maleic acid, 0.15 M NaCl, pH 7.5, 0.3% [v/v] Tween 20) for 1–5 min. After that, the membrane was incubated in 1×

blocking solution (Roche Diagnostics, Mannheim, Germany) in maleic acid buffer (0.1 M maleic acid, 0.15 M NaCl, pH 7.5) for 30 min at room temperature. Then the blocking solution was discarded and replaced with anti-DIG-AP conjugate (Roche Diagnostics, Mannheim, Germany) diluted 1: 5,000 in 1× blocking solution and the membrane was incubated for 30 min at room temperature. Following this the membrane was washed in maleic acid washing buffer twice, for 15 min each to remove unbound antibodies and equilibrated in detection buffer (0.1 M Tris-HCl, 0.1 M NaCl, 50 mM $MgCl_2$, pH 9.5) for 5 min. The detection buffer was discarded and the membrane was incubated in freshly prepared BCIP/NBT substrate solution (Amresco, Salon, OH, USA) in the dark without shaking until a color precipitate had developed. Color development was stopped by washing the membrane several times with DW. The membrane was dried and kept for analysis of the result.
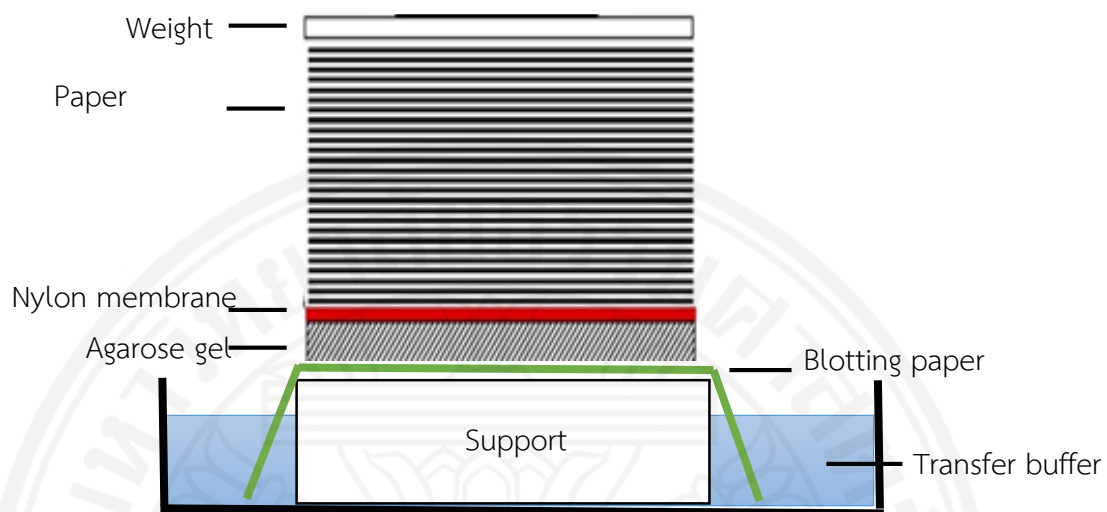
Figure 4.1 Upward capillary transfer tower for Southern blot and Northern blot analysis.

4.2.6 Northern hybridization analysis

4.2.6.1 Preparation of agarose gel containing 2.2 M formaldehyde

A 1.2% denaturing agarose gel containing 2.2 M formaldehyde was prepared under a fume hood. For preparation of 100 ml agarose solution 1.2 g of Ultrapure™ agarose powder was dissolved in 72.5 ml DEPC-treated DW by boiling in a microwave oven. The agarose solution was allowed to cool down to approximately 55℃ before 10 ml of prewarmed 10× MOPS buffer, pH 7.2 (0.2 M MOPS, 50 mM sodium acetate, 10 mM EDTA) and 17.5 ml of 37% formaldehyde were added. The solution was poured into a gel tray and an appropriate comb was inserted. The gel was allowed to polymerize for 30–60 min in a fume hood.

4.2.6.2 Preparation of RNA sample

Total RNA (50 µg) from adult *F. gigantica* (**Section 4.2.3**) was heat-denatured in 50% formaldehyde in 1× MOPS buffer with formamide at 65℃ for 5 min and quickly cooled on ice. The RNA sample was mixed with 10× electrophoresis sample buffer and loaded on a 1.2% (w/v) agarose gel containing 2.2 M formaldehyde in 1× MOPS buffer (**Section 4.2.6.1**). The components of the reaction mixture are shown below.

Components	Volume (µl)
Total RNA	20.0
Formamide	60.0
37% Formaldehyde (2.2 M in final conc.)	22.0
10× MOPS buffer	6.0
10× RNA loading buffer	12.0
Total volume	120.0

Gel electrophoresis was performed in 1× MOPS buffer under the fume hood at 35 V for 8 h. A high range RNA molecular weight marker (Thermo Scientific, Lithuania) was used to determine the sizes of hybridizing RNAs. After electrophoresis the gel was stained in DEPC-treated DW containing 0.5 µg/ml of

ethidium bromide for 15 min and then de-stained in DEPC-treated DW for 5 min. The nucleic acid pattern on the gel was observed under an UV transilluminator (Gel Doc 2000, BIO-RAD, Milan, Italy). Subsequently, the marker lane was cut from the gel and the remaining gel was processed for capillary transfer.

4.2.6.3 Northern transfer, Northern hybridization and immunological detection

The formaldehyde agarose gel was rinsed twice in DEPC-treated DW to remove residual ethidium bromide and equilibrated in 10× SSC. After that, the resolved total RNA was transferred onto a nylon membrane (Amersham Hybond™ N⁺, GE Healthcare, Buckinghamshire, UK) by the capillary transfer method (as described in **Section 4.2.5.2**) and immobilized by baking at 80°C for 1 h. Hybridization and immunological detection were performed as described in **Sections 4.2.5.3 and 4.2.5.4**.

4.2.7 Stage-specific Reverse Transcriptase Polymerase Chain Reaction (RT-PCR)

Total RNA from NEJ, 2-, 4-, 6-week-old juveniles and adult *F. gigantica* (**Section 4.2.3**) was used as template for RT-PCR to verify FgStefin-2 gene expression during development. The first strand cDNA was generated by using RevertAid™ M-MuLV Reverse Transcriptase (Thermo Scientific, Lithuania). The FgStefin-2 specific primer pair used in this experiment and all ingredients were prepared as described in the following lists.

Forward primer: 5'- GGA TCC atc gag ggt cgc ATG CTC GTC GGT GGT TAT ACT G -3'

Reverse primer: 5'- CTG CAG TCA AGT GCA AGA TAC CC-3'

Components	Volume (μl)
Total RNA from each stage (0.5 μg)	X
Reverse primer (10 μM)	2.0
DEPC-treated DW	12.0-X
Mix all above components by pipetting, briefly spin and add following components	
5× RevertAid™ reaction buffer	4.0
Mixed dNTPs (2.5 mM each)	2.0
RiboLock™ RNase Inhibitor	0.5
RevertAid™ M-MuLV Reverse Transcriptase	0.5
Total volume	20.0

The mixture was incubated at 42°C for 1 h and the reaction was terminated by heating at 70°C for 10 min. The reverse transcription product was stored on ice until used as template of PCR.

Components	Volume (µl)
Template (RT-PCR product)	2.0
Forward primer (10 µM)	1.0
Reverse primer (10 µM)	1.0
10×$(NH_4)_2SO_4$ buffer	5.0
$MgCl_2$ (25 mM)	3.0
Mixed dNTPs (2.5 mM each)	1.0
Taq DNA polymerase (5U/µl)	0.5
DW	36.5
Total volume	50.0

The components were mixed and the PCR reaction was performed using following conditions: pre-denaturation at 95°C for 5 min, 35 cycles of denaturation at 95°C for 1 min, annealing at 55°C for 1 min and extension at 72°C for 1 min then one cycle of final extension at 72°C for 10 min and hold at 4°C. The PCR product was analyzed by 0.7% (w/v) agarose gel electrophoresis (as described in **Section 4.1.1.2**).

4.3 Expression and purification of recombinant FgStefin-2 protein in prokaryotic system and production of anti-rFgStefin-2

4.3.1 Generating the PCR products encoding FgStefin-2

The cDNA fragment encoding FgStefin-2 was amplified by PCR using forward primer 5'-<u>GGA TCC</u> atc gag ggt cgc ATG CTC GTC GGT GGT TAT ACT G-3' and reverse primer 5'-<u>CTG CAG</u> TCA AGT GCA AGA TAC CC-3'. *Bam*H I and *Pst* I endonuclease restriction sites (underlined) were added to the forward and reverse primers, respectively, to facilitate the DNA cloning into the pQE30 vector (QIAGEN, Venlo, Netherlands). The reaction mixture was prepared as shown on the next page.

Components	Volume (µl)
Template (RT-PCR product **Section 4.2.7**)	2.0
Forward primer (10 µM)	1.0
Reverse primer (10 µM)	1.0
10×(NH$_4$)$_2$SO$_4$ buffer	5.0
MgCl$_2$ (25mM)	3.0
Mixed dNTPs (2.5 mM each)	1.0
Taq DNA polymerase (5U/µl)	0.5
DW	36.5
Total volume	50.0

The PCR reaction was performed using following conditions: pre-denaturation at 95℃ for 5 min, 35 cycles of denaturation at 95℃ for 1 min, gradient annealing at 50℃-55℃-60℃ for 1 min and extension at 72℃ for 1 min then one cycle of final extension at 72℃ for 10 min and hold at 4℃. The PCR product was resolved on a 0.7% (w/v) agarose gel (as described in **Section 4.1.1.2**). The FgStefin-2 cDNA fragment was extracted from the agarose gel using QIA quick® Gel Extraction Kit (QIAGEN, Limburg, Netherlands) as described in **Section 4.1.1.3.** The extracted PCR product was inserted into the pGEM®-T Easy vector by ligation and competent *E. coli* XL1-Blue was transformed with the ligation product. Positive transformant XL1-Blue *E. coli* clones were verified by PCR, restriction endonuclease digestion (*Bam*H I and *Pst* I) and DNA sequencing as described in **Sections 4.1.2.1** to **4.1.2.6.**

4.3.2 Subcloning of the FgStefin-2 cDNA fragment from pGEM®-T Easy into the expression vector pQE30

4.3.2.1 Restriction endonuclease digestion of FgStefin-2 and pQE30 vector

Recombinant pGEM®-T Easy carrying FgStefin-2 (**Section 4.3.1**) and the pQE30 expression vector (QIAGEN, Limburg, Netherlands) were double-digested with restriction endonucleases *Bam*H I and *Pst* I (Thermo Scientific, Lithuania). The reaction sample was set up as shown below.

Components	Volume (μl)
Plasmid DNA (pGEM®-T Easy carrying FgStefin-2 or pQE-30)	5.0
*Bam*H I buffer (10×)	2.0
*Bam*H I (10 U/μl)	0.5
Pst I (10 U/μl)	1.0
DW	11.5
Total volume	20.0

The sample was incubated at 37°C for 2 h and the restriction enzymes were inactivated at 80°C for 20 min. The product was kept at −20°C until use.

4.3.2.2 Insertion of FgStefin-2 into pQE30 vector and introduction of the recombinant vector into *E. coli* expression hosts

The digested pQE30 expression vector and digested FgStefin-2 cDNA fragments from **Section 4.3.2.1** were resolved on a 0.7% (w/v) agarose gel (as described in **Section 4.1.1.2**) and their concentration was estimated by comparison with 1 kb DNA ladder (Thermo Scientific, Lithuania). The FgStefin-2 cDNA fragment and the linearized pQE30 plasmid were extracted from the agarose using a QIAquick® Gel Extraction Kit (QIAGEN, Limburg, Netherlands) as described in **Section 4.1.1.3** and combined by ligation using T4 DNA ligase (Thermo Scientific, Lithuania). The insert: vector molar ratios (3:1 to 1:3) were optimized by using the following formula:

$$\frac{\text{ng of vector} \times \text{kb size of insert} \times \text{insert: vector molar ratio}}{\text{kb size of vector}} = \text{ng of insert}$$

The ligation reaction was prepared as follows.

Components	Volume (µl)
10× T4 DNA ligase buffer	1.0
Digested pQE30 vector	1.0
Digested FgStefin-2	3.0
T4 DNA ligase (5 Weiss U/µl)	1.0
DW	4.0
Total volume	10.0

The sample was incubated at 4°C, overnight and 1 µl of reaction product were introduced into chemically competent *E. coli* M15 by transformation as described in **Sections 4.1.2.2** to **4.1.2.3**. The bacterial cells were spread on LB agar containing 100 µg/ml ampicillin plus 25 µg/ml kanamycin and incubated overnight at 37°C. Positive clones were identified by using colony PCR and restriction endonuclease digestion (*Bam*H I and *Pst* I) as described in **Sections 4.1.2.4** to **4.1.2.6**.

4.3.3 Expression and purification of recombinant FgStefin-2

4.3.3.1 Small scale culture screening of rFgStefin-2 expression and times course analysis

Single colonies each of two positive transformant clones (**Section 4.3.2**) were cultured in 5 ml LB medium containing antibiotics (100 µg/ml ampicillin and 25 µg/ml kanamycin) at 37°C with shaking 250 rpm, overnight. On the following day, 1 ml of each starter overnight culture was used to inoculate 20 ml LB broth containing antibiotics (100 µg/ml ampicillin and 25 µg/ml kanamycin) and incubated at 37°C with shaking 250 rpm until an OD_{600} of 0.6 had been reached. One milliliter of each culture sample was collected as a non-induced control and then the remaining culture was induced with 1 M IPTG (Sigma Aldrich, Steinheim, Germany) at final concentration of 1 mM. After induction the culture was incubated for 4 h and 1 ml of cell samples were hourly collected for a time course analysis. Both non-induced and induced bacterial cells were centrifuged at 6,000×*g* for 5 min. The supernatants were discarded and the pellets were resuspended in 50 µl denaturing lysis buffer (100 mM NaH_2PO_4, 10 mM Tris-HCl, 8 M urea, pH 8.0). The cell

debris was removed by centrifugation at 6,000×g for 30 min at 4℃. The protein expression was analyzed by 16% SDS-PAGE (as described in **Section 4.3.4**).

4.3.3.2 Analysis of recombinant protein solubility

The solubility of protein was determined by using the clone with highest expression (**Section 4.3.3.1**). A single bacterial colony was cultured in 5 ml LB Broth containing antibiotics (100 μg/ml ampicillin and 25 μg/ml kanamycin) at 37℃ with shaking 250 rpm, overnight. On the next day, 1 ml of starter overnight culture was used to inoculate 20 ml LB broth containing the above mentioned antibiotics and incubated at 37℃ with shaking 250 rpm until an OD_{600} of 0.6 had been reached. A sample of 1 ml of non-induced bacteria was collected as a non-induced control and the remaining culture was induced with 1 M IPTG (Sigma Aldrich, Steinheim, Germany) to a final concentration of 1 mM. After induction the culture was incubated for 4 h and 1 ml of cell sample was collected. The cells were harvested by centrifugation at 6,000×g for 5 min and the supernatant was discarded. The cell pellet was resuspended in 100 μl native lysis buffer (50 mM NaH_2PO_4, 300 mM NaCl, 10 mM imidazole, pH 8.0) and was lysed by sonication 6 × 9 s with 9 s pauses at 30% amplitude using a sonicator (Sonics vibra cell™ VC 750, Newtown, CT, USA). During the sonication process, the cells were kept on ice at all times. The lysate was centrifuged at 12,000×g, 4℃, 10 min. The supernatant (soluble protein fraction) was collected and kept on ice. The pellet was resuspended (insoluble protein fraction) in 100 μl denaturing lysis buffer (100 mM NaH_2PO_4, 10 mM Tris-HCl, 8 M urea, pH 8.0). The protein solubility was analyzed by 16% SDS-PAGE (as described in **Section 4.3.4**).

4.3.3.3 Large scale expression of recombinant FgStefin-2 protein

A single colony of transformant *E. coli* M15 carrying pQE30-FgStefin-2 was cultured in 5 ml LB broth containing antibiotics (100 μg/ml ampicillin and 25 μg/ml kanamycin) at 37℃ with shaking 250 rpm, overnight. In the following day 100 ml LB broth containing antibiotics (100 μg/ml ampicillin and 25 μg/ml kanamycin) were inoculated with 5 ml overnight culture and incubated at 37℃ with shaking 250 rpm until the OD_{600} had reached 0.6. The expression of recombinant

protein was induced by adding 1 M IPTG to a final concentration of 1 mM and the culture was incubated for 4 h. The bacterial cells were harvested by centrifugation at 6,000×g, 4°C, 30 min and the supernatant was discarded. The cell pellet was kept at −20°C or immediately processed for purification of recombinant protein.

4.3.3.4 Purification of recombinant FgStefin-2

The recombinant FgStefin-2 was purified by nickel-nitrilo tri-acetic acid (Ni-NTA) affinity chromatography. The cell pellet in **Section 4.3.3.3** was resuspended in 5 ml native lysis buffer (50 mM NaH_2PO_4, 300 mM NaCl, 10 mM imidazole, pH 8.0) per gram wet weight. The bacterial cells were lysed by sonication 6×9 s with 9 s pauses at 30% amplitude and centrifuged at 6,000×g at 4°C for 30 min to remove the cell debris. The supernatant was transferred into a new sterile tube. A 1 ml of Ni-NTA agarose slurry (QIAGEN, Hilden, Germany) was added to 4 ml cleared lysate and mixed gently on a rotary shaker at 4°C for 1 h. The mixture of proteins and beads was loaded into a polypropylene column and waited until the beads were packed by gravity. The bottom cap was removed and the flow-through was collected. The column was washed twice with 4 ml washing buffer (50 mM NaH_2PO_4, 300 mM NaCl, 20 mM imidazole, pH 8.0) and the washing fractions were collected. The rFgStefin-2 was eluted 4 times with 0.5 ml each elution buffer (50 mM NaH_2PO_4, 300 mM NaCl, 250 mM imidazole, pH 8.0). All protein fractions were analyzed by 12.5% SDS-PAGE (as described in **Section 4.3.4**).

4.3.4 Analysis of recombinant proteins by sodium dodecyl sulfate-polyacrylamide gel electrophoresis (SDS-PAGE)

SAS-PAGE is the method used to separate the proteins by their molecular mass. Smaller proteins migrate faster through the acrylamide mesh and the proteins are separated according to mass (usually measured in kilodaltons, kDa).

4.3.4.1 Preparation of polyacrylamide gel

The protocol to prepare the polyacrylamide gels was modified from the Hoeffer manual (Amersham Biosciences, UK). The separating and stacking gel for 12.5% and 16% acrylamide (Tris-Glycine gel) were prepared as described in **Table 4.2**

4.3.4.2 Preparation of samples and electrophoresis of proteins

The protein samples were mixed with an equal volume of 2× sample electrophoresis buffer (0.125 M Tris-HCl, pH 6.8, 4% [w/v] SDS, 20% [v/v] glycerol, 0.2 M DTT, 0.02% bromophenol blue) and heat-denatured at 95°C for 5 min to denature the protein or mixed with 5× native sample loading buffer (0.313 M Tris-HCl, pH 6.8, 50% [v/v] glycerol, 0.05% [w/v] bromophenol blue). The denatured and non-denatured proteins were loaded into the wells of the stacking gel in the electrophoretic chamber (Amersham Biosciences, Buckinghamshire, UK) containing electrophoresis buffer (0.025 M Tris-HCl, pH 8.9, 0.2 M glycine, 0.1% [w/v] SDS). Broad range molecular weight standard (Bio-Rad, California, USA) was used as standard protein marker. Electrophoresis proceeded at a constant current of 20 mA per gel (Electrophoresis Power Supply EPS 301, Amersham Biosciences, UK) until the front dye marker had reached the bottom of the gel. The gel was removed from the glass plates and placed in a clean staining tray of the appropriate size and then stained with 0.025% (w/v) Coomassie Blue R-250 (Brilliant Blue R-250, USB Corporation, Cleveland, OH, USA) or silver (the SilverQuest™ Silver Staining Kit) as described in **Sections 4.3.4.3** and **4.3.4.4**.

4.3.4.3 Staining of proteins in the polyacrylamide gel with Coomassie Blue R-250

The polyacrylamide gel was fixed and stained in Coomassie blue staining solution (0.025% [w/v] Coomassie Brilliant Blue R-250, 40% [v/v] methanol, and 7% [v/v] glacial acetic acid) with shaking at room temperature, overnight. After staining, the dye solution was replaced with high methanol destaining solution (40% [v/v] methanol, 7% [v/v] glacial acetic acid) followed by low methanol destaining solution (5% [v/v] methanol, 7% [v/v] glacial acetic acid). The destaining solutions were used for decreased the background of stained gel. The gel was subsequently kept in 1% [v/v] glycerol and dried on a cellophane membrane for long-term storage. The protein bands were visualized directly or photographed.

4.3.4.4 Silver staining of proteins in polyacrylamide gels

The polyacrylamide gel was fixed and stained in silver solution using a SilverQuest™ Silver Staining Kit (Invitrogen, Carlsbad, CA, USA)

according to the manufacturer's instructions. The gel was briefly rinsed with DW and then fixed in 50 ml fixative (ethanol 20 ml, acetic acid 5 ml and DW 25 ml) at room temperature for 20 min with gentle agitation to remove interfering ions and detergent from the gel. The fixative solution was discarded and the gel was washed with 30% (v/v) ethanol at room temperature for 10 min before adding 50 ml of sensitizing solution (ethanol 15 ml, sensitizer 5 ml and DW 30 ml) and then incubated at room temperature for 10 min with gentle agitation to increase sensitivity and contrast of the stain. The sensitizing solution was discarded and the gel was washed with DW at room temperature for 10 min. Afterwards, the gel was incubated in 50 ml staining solution (stainer 0.5 ml and DW 49.5 ml) at room temperature for 15 min with gentle agitation to bind silver ions to the proteins. After the staining was achieved, the staining solution was discarded and the gel was washed with DW at room temperature for 30 s. Subsequently, 100 ml of developing solution (developer 10 ml, developer enhancer 1 drop and DW 90 ml) was added and the gel incubated for 4–8 minutes until the desired staining intensity had been reached. Afterwards 10 ml of stopper solution was immediately added to the gel while still submerged in developing solution. The gel was incubated at room temperature with gentle agitation until the color of solution had changed from pink to colorless indicating that the development process had been stopped. Finally, the solution was discarded, the gel was washed with DW for 10 min and dried on a cellophane membrane for long-term storage. The protein bands were visualized directly or photographed.

Table 4.2 Preparation of polyacrylamide gel.

List of components for 12.5% and 16% Tris-Glycine gel (for one gel)

Reagent	12.5%	16%	4%
	Separating gel	Separating gel	Stacking gel
30% Acrylamide stock (ml)	3.13	4.00	0.33
1.5 M Tris-HCl pH 8.8 (ml)	1.88	1.88	-
0.5 M Tris-HCl pH 6.8 (ml)	-	-	0.63
10% SDS (ml)	0.08	0.08	0.03
DW (ml)	2.38	1.51	1.50
10% w/v APS (µl)	37.50	37.50	12.50
TEMED (µl)	2.50	2.50	1.25
Total volume (ml)	7.50	7.50	2.50

Table 4.2 Preparation of polyacrylamide gel (cont.)

List of components for 10% polyacrylamide gel containing 0.1% gelatin

Reagent	10% Separating gel	5% Stacking gel
30% Acrylamide stock (ml)	5.00	0.75
1.5 M Tris-HCl pH 8.8 (ml)	3.75	-
0.5 M Tris-HCl pH 6.8 (ml)	-	1.25
10% SDS (ml)	0.15	0.05
DW (ml)	3.08	2.95
10% w/v APS (μl)	100.00	50.00
TEMED (μl)	15.00	5.00
0.5% Gelatin	3.02	-
Total volume (ml)	15.00	5.00

4.3.5 Dialysis of rFgStefin-2

The recombinant FgStefin-2 in elution buffer (**Section 4.3.3.4**) was dialyzed against 10 mM PBS, pH 7.2 in a dialysis bag (3 Spectral Por® Dialysis Membrane, Rancho Dominiguez, CA, USA) to obtain refolded soluble protein. The dialysis bag was cut into the desired length and washed with DW before use. The bag was tightly closed at one side with a string and rFgStefin-2 in elution buffer was added into the bag by pipetting. The bag was tightly closed with a string and then immersed in 10 mM PBS, pH 7.2 at 4°C with stirring. PBS buffer was changed after 1 h and the dialysis process was continued overnight. The solution was transferred from the dialysis bag into a microtube by pipetting and kept at −20°C until use.

4.3.6 Measurement of protein concentration

Determination of protein concentration was performed by using the Bradford method according to the microtiter plate protocol of the Bio-Rad Protein Assay (Bio-Rad, California, USA). The bovine serum albumin (Sigma Aldrich, St. Louis, MO, USA) was used as protein standard by diluting at a range of 0.05 to 0.5 mg/ml in 10 mM PBS, pH 7.2. Each BSA dilution and the protein sample (10 µl) were added to individual wells of a standard 96-wells non-protein-absorbed plastic plate (NUNC, Roskide, Denmark). The samples were mixed with 200 µl of working dye solution (1 ml Dye Reagent Concentrate plus 4 ml DW). The mixtures were incubated at room temperature for 5 min and then the OD_{595} was measured on a microplate reader (Anthos 2020, Anthos Labtec Instruments, Austria). A protein standard curve was plotted by the concentration of the BSA standards and absorbance. The concentration of protein samples was calculated from equation of the linear standard curve.

4.3.7 Production of polyclonal antibodies against rFgStefin-2

4.3.7.1 Animal immunization

Polyclonal antibodies were produced by immunization of 6–8 week-old BALB/c mice. The rFgStefin-2 (10 µg per well) was analyzed by 12.5% SDS-PAGE (as described in **Section 4.3.4**), the gel was stained with 0.5% Coomassie blue G-250 (Brilliant Blue G-250, USB Corporation, Cleveland, OH, USA) and destained with DW. The band of rFgStefin-2 was carefully cut from the gel to avoid the other

co-purified bacterial proteins and transferred to a microcentrifuge tube. Afterwards, 10 mM PBS, pH 7.2 was added into the tube and then the mixture was ground by a glass homogenizer. Before immunization process, the preimmune sera were collected from three BALB/c mice as negative control. Two weeks later, all of the mice were primary intraperitoneally injected with 100 µl of the gel containing 10 µg rFgStefin-2 as described above. The immunization step was repeated twice in a 3-week interval by the same route. Serum samples were collected every 2 weeks after immunization by collecting the blood from tail using capillary tubes with anticoagulant and then the tubes were centrifuged at 10,000×g for 10 min at room temperature (priming, first and second boost serum). The sera were collected and kept at −20°C for further experiments.

4.3.7.2 Determination of the specific antibody titer by indirect ELISA

Indirect ELISA was used to demonstrate the immune response of all mouse anti-rFgStefin-2 antisera (**Section 4.3.7.1**) against rFgStefin-2. A standard 96-well ELISA plate (NUNC, Roskide, Denmark) was coated with 100 ng rFgStefin-2 in 100 µl of ELISA coating buffer (30 mM Na_2CO_3, 75 mM $NaHCO_3$, pH 9.6). The plate was added into the humidified chamber and incubated at 4°C, overnight. On the next day, the solution was discarded and the plate was washed three times with washing buffer (10 mM PBS, pH 7.2, 0.05% [v/v] Tween$^®$ 20) to remove unbound protein and the unoccupied sites in each well were blocked by adding 200 µl of blocking solution (0.25% [w/v] BSA in coating buffer). The plate was incubated at room temperature for 30 min and then washed with washing buffer for 3 times. The anti-rFgStefin-2 antisera were diluted (1:800) in antibody diluents (0.25% [w/v] BSA in 10 mM PBS, pH 7.2) and then 100 µl of diluted serum was added to each well. The plated was incubated in a humidified chamber at 37°C for 1 h and then washed three times with washing buffer. The secondary antibody (HRP-conjugated goat anti-mouse IgG, Zymed, San Francisco, CA, USA) was diluted 1:10,000 in antibody diluents and added to the wells (100 µl per well). The plate was incubated at 37°C for 1 h and washed three times with washing buffer. Subsequently, 100 µl of OPD substrate (Sigma Aldrich, St. Louis, IL, USA) was added to wells. The plate was incubated in

the dark for 30 min at room temperature and the reaction was stopped by adding 25 µl of 3 M H$_2$SO$_4$ to each well. The absorbance was measured at a wavelength of 492 nm on a microplate reader (Anthos 2020, Anthos Labtec Instruments, Austria).

4.4 Characterization of recombinant FgStefin-2 protein

4.4.1 Preparation of parasite antigen
4.4.1.1 Preparation of crude extract of *F. gigantica* metacercariae

Metacercariae of *F. gigantica* were digested in 1% (w/v) pepsin, 0.4% (v/v) HCl at 37°C for 1 h and then homogenized in 0.1 M sodium acetate buffer pH 5 followed by centrifugation at 20,000×*g* for 1 h, room temperature. The supernatant was collected and used as crude extract. The concentration of protein was measured (as described in **Section 4.3.6**) and the crude extract was stored at −20°C until used.

4.4.1.2 Extraction of crude worm antigens from adult *F. gigantica*

Frozen adult *F. gigantica* (**Section 4.2.1.3**) were mixed with homogenization buffer (10 mM Tris-HCl, pH 7.2, 0.5% [v/v] Triton X-100, 1 mM PMSF, 150 mM NaCl and 1 mM EDTA) at a ratio 1 gram tissue per 2 ml buffer and homogenized by using a tissue homogenizer (IKA, Staufen, Germany). The homogenate was centrifuged at 12,000×g, 4°C for 30 min to remove insoluble material and the supernatant was collected. The concentration of soluble CW was determined (as described in **Section 4.3.6**) and the crude extract was kept at −20°C for further experiments.

4.4.1.3 Preparation of excretory/secretory products

Excretory-secretory product was prepared from freshly collected adult parasites obtained from bile ducts of naturally infected cattle. The parasites were repeatedly washed in 10 mM PBS, pH 7.2 at room temperature with gentle shaking. The cleaned parasites were cultured in 10 mM PBS, pH 7.2 and incubated at 37°C for 4 h. The buffer was collected and fresh PBS was hourly added

for 4 h. The collected buffer was centrifuged at 5,000×g, 4°C for 20 min to eliminate the eggs of the parasites and other insoluble material. The ES products in the supernatant were concentrated using Amicon® Ultra centrifugal filters (3 kDa cut off, Millipore, Carrigtwohill, Ireland). The concentration of protein was measured (as described in **Section 4.3.6)** and the ES product was kept at −20°C until further analysis.

4.4.2 Western analysis

4.4.2.1 Western blot analysis of recombinant and native proteins

CW extract (10 μg), ES product (10 μg) and recombinant FgStefin-2 (100 ng) were resolved by 12.5% SDS-PAGE (as described in **Section 4.3.4**) and then the gel was transferred into semi-dry transfer buffer (50 mM Tris, 40 mM glycine, 0.04% [w/v] SDS, 20% [v/v] methanol). A Hybond™ ECL nitrocellulose membrane (Amersham, GE Healthcare, Buckinghamshire, UK) and 3 MM blotting papers (Whatman®, GE Healthcare, Buckinghamshire, UK) were submersed in transfer buffer for 5 min before use. The semi-dry blotting stack was prepared as follows: 6 pieces of buffer-saturated blotting paper, nitrocellulose membrane, gel and 6 pieces blotting paper as shown in **Figure 4.2** and placed in the middle of a Fastblot B33 instrument (Whatman Biometra, Goettingen, Germany). The air bubbles were removed by rolling a glass pipette carefully over the blotting stack. The protein transfer was performed at 60 mA for 45 min. After blotting, the nitrocellulose membrane was stained with Ponceau S solution (0.1% [w/v] Ponceau S (Sigma Aldrich, Steinheim, Germany), 5% [v/v] acetic acid) for 5 min and washed with DW until the protein bands were observable. The blotted membrane was dried and stored at −20°C or immediately processed for immunological detection (as described in **Section 4.4.2.2**).

4.4.2.2 Western immunological detection

The blotted membrane was washed in DW for 10 min and then equilibrated in 1× TBS (20 mM Tris-base, 150 mM NaCl) for 5 min at room temperature. Subsequently, the equilibration buffer was replaced with blocking solution (5% [w/v] Skim milk [Oxiod, Hampshire, England] in 1× TBS, pH 7.5) at room

temperature for 1 h with gentle agitated. Mouse anti-rFgStefin-2 antiserum was diluted 1:1,000 (pre-immune serum was used as negative control) in antibody diluent (1% [w/v] Skim milk in TBS, pH 7.5) and used to probe the membrane-bound antigens followed by incubation at 4°C, overnight. Afterwards, the membrane was washed three times for 5 min each in washing buffer (1× TBS, 0.05% [v/v] Tween® 20). The membrane was incubated with goat anti-mouse IgG (whole molecule)-alkaline phosphatase (Sigma Aldrich, Steinheim, Germany) diluted 1:30,000 in antibody diluent with gentle shaking at room temperature for 1 h. The wash step as mentioned above was repeated to remove the unbound antibodies and the membrane was equilibrated in detection buffer (0.1 M Tris-HCl, pH 9.5, 0.1 M NaCl, 50 mM $MgCl_2$) for 5 min. The colorimetric signal was detected in the dark by using the chromogenic substrate mix BCIP/NBT (Amresco, Salon, OH, USA) until the signal was observed. The reaction was stopped by washing the membrane several times with DW.

Figure 4.2 The semi-dry blotting stack for western blot analysis.

4.4.2.3 Cross reactivity of mouse anti-rFgStefin-2 antisera against rFgStefin-1, multi-domain cystatin (FgMDC) and crude worm extracts of other trematodes

Western analysis was used to analyze cross-reactivity of anti-rFgStefin-2 antisera (**Section 4.3.7.1**) to CW extracts of other trematodes. CW extracts from *Opisthorchis viverrini* (10 µg), *Paramphistomum* spp. (10 µg), *Eurytrema pancreaticum* (10 µg), *Schistosoma mansoni* (10 µg), *Fischoederius elongates* (10 µg), *Fasciola gigantica* (10 µg), rFgStefin-1 (100 ng), multi-domain cystatin (100 ng) and rFgStefin-2 (100 ng) were resolved by 12.5% SDS-PAGE (as described in **Section 4.3.4**). All proteins were electrotransferred to nitrocellulose membrane by semi-dry blotting using a Fastblot B33 instrument and then processed for immunological detection as described in **Sections 4.4.2.1** and **4.4.2.2**.

4.5 Analysis of native FgStefin-2 distribution in parasite tissue sections

4.5.1 Preparation of paraffin-embedded tissue sections

The 2- and 4-week-old juveniles and adult *F. gigantica* were freshly collected and processed (as described in **Sections 4.2.1.2** and **4.2.1.3**) for immunolocalization. The adult parasites were cut into several smaller pieces before fixation. All stages of the parasite were fixed with freshly prepared fixative solution (4% [w/v] paraformaldehyde in 10 mM PBS, pH 7.2) at 4°C for 4 h. Subsequently, the fixative solution was discarded and the tissue was dehydrated three times with 50%, 70%, 80%, 95% and absolute ethanol, respectively for 20 min each. The absolute ethanol was replaced with xylene for three times, 10 min each and then the worms were transferred to 60°C incubator. Afterwards, prewarmed xylene:paraplast at a ratio 1:1 was added followed by incubation at 60°C for 30 min and this step was repeated for three times. The parasites were immersed in melted paraplast (Q Path Paraffin Normal, LABONORD SAS, Templemars, France), incubated at 60°C for 1 h and this step was repeated for three times. Thereafter, the tissue was embedded in fresh molten paraplast and the paraffin was allowed to harden at room temperature, overnight. On the following day, the embedded tissue was cut at 8 µm thick by a

microtome (LEICA RM 2235, Nussloch, Germany) and placed on gelatin coated slides (as described in **Section 4.5.2**). The tissue sections were completely dried on a 42°C heating plate and stored in a dry place until used.

4.5.2 Preparation of gelatin-coated microscope glass slides

The gelatin-coating solution was prepared by dissolving 3 g of gelatin (Sigma Aldrich, St. Louis, IL, USA) in DW at 45°C and then 0.05 g of chromium potassium sulfate (Fluka chemika, Steinheim, USA) was added. The glass slides were cleaned with detergent and washed several times with water. The cleaned slides were placed into a staining rack and then the rack was immersed into the gelatin-coating solution for 5 min. Afterwards, the rack containing the slides was slowly removed from the solution. The wet slides were air dried at 37°C in a hot air oven (Memmert, Germany) for 1 h. Dried slides were kept in the box at room temperature until used.

4.5.3 Immunohistochemical detection of native FgStefin-2 in tissue sections

The tissue sections on the gelatin coated slides were dewaxed twice in xylene for 10 min each and then rehydrated in serial alcohol dilutions including absolute, 95%, 90%, 80%, 70% (v/v) ethanol for two times, 5 min each. The slides were rinsed with DW and non-specific binding sites were blocked by incubation in glycine blocking solution (0.1% [w/v] glycine in 10 mM PBS, pH 7.2) and 4% BSA in PBS each for 30 min at room temperature, respectively. Afterwards, the blocking solution was discarded and mouse anti-rFgStefin-2 antiserum diluted 1:400 in antibody diluents (1% [w/v] BSA in 10 mM PBS, pH 7.2) was added followed by incubation in a humid chamber at 4°C overnight. On the next day, the sections were washed three times with washing buffer (10 mM PBS, pH 7.2 and 0.1% Tween®20) for 5 min each with gentle shaking to remove unbound antibodies and then incubated twice with 3% (v/v) H_2O_2 (prepared from 30% [v/v] H_2O_2, Merck, Hohenbrunn, Germany) in the dark at room temperature for 10 min each to suppress endogenous peroxidase activity. The sections were rinsed with DW and washed three times with washing buffer for 5 min each. Subsequently, the sections were incubated with biotinylated rabbit anti-mouse immunoglobulins (Dako™, Agilent Technologies, USA)

diluted 1:200 in PBS at room temperature for 30 min. The wash step as mentioned above was repeated and then the sections were incubated with avidin–biotin peroxidase (ABComplex Kit, Thermo Scientific, Rockford, IL, USA) in a humid chamber at room temperature for 30 min. The sections were washed as above and then incubated with AEC substrate solution (Invitrogen, Carlsbad, CA, USA) for the colorimetric detection. The color development was stopped by washing several times with washing buffer. After the reaction had been stopped only the sections of adult parasite were counterstained with modified hematoxylin solution at room temperature for 1 min and destained with DW. The tissue sections were mounted in 10% (v/v) glycerol in PBS. Mouse preimmune serum (1:400) was used as negative control.

4.6 Functional analysis of recombinant FgStefin-2

4.6.1 Determination of *Km*

The Michaelis-Menten constant (K_m) is defined as the substrate concentration at which the reaction velocity is equal to half-maximal velocity for the enzymatic reaction. K_m was determined from initial velocities (v_0) over a range of substrate concentrations [S] at a fixed enzyme concentration. The ranging concentration of fluorogenic substrate (Z-Arg-Arg-AMC, Sigma Aldrich, St. Louis, IL, USA) from 0-512 µM was mixed with 1 ng of native bovine cathepsin B (Sigma Aldrich, St. Louis, IL, USA) in 2× CatB-cystatin assay buffer (100 mM MES, 400 mM NaCl, 2 mM EDTA, 2 mM DTT, pH 6.0. Afterwards, the fluorescence released by substrate hydrolysis was measured at excitation wavelengths of 390 nm and emission wavelengths of 460 nm on a Varioskan Flash spectral scanning multimode reader (Thermo Scientific, Waltham, MA, USA). Non-linear regression was used to plot initial velocity versus substrate concentration according to equation 1 by using GraphPad Prism 6.0.

Equation 1: $v_0 = Vmax \, [S] / (K_m+[S])$

4.6.2 Determination of the inhibition coefficients (IC$_{50}$)

The inhibitory activities of rFgStefin-2, rFgStefin-1 and native human cystatin C (Calbiochem, USA) on several proteases were determined by analyzing residual enzyme activity after incubation of each enzyme with all inhibitors. The IC$_{50}$ of purified rFgStefin-2, rFgStefin-1 and native human cystatin C were determined for ES product (**Section 4.4.4.3**) and native bovine cathepsins B and L (Sigma Aldrich, St. Louis, IL, USA).

Cathepsin L activity and cysteine protease activity in ES product were measured by a modified method from Barrett and Kirschke (1981). Native bovine cathepsin L (1 ng/reaction) and ES product (10 ng/reaction) were activated in CatL assay buffer (340 mM sodium acetate, 60 mM acetic acid, 4 mM EDTA, 8 mM DTT, pH 5.5) containing 1 M cysteine for 5 min at room temperature. Subsequently, rFgStefin-2, rFgStefin-1 and human cystatin C at the final concentrations of 20–500 nM were added and then pre-incubated at room temperature for 5 min. The substrate solution (Z-Phe-Arg-AMC, Sigma Aldrich, St. Louis, IL, USA) at final concentration of 10 µM was added.

Native bovine cathepsin B (1 ng/reaction) was incubated in CatB assay buffer (100 mM MES, 400 mM NaCl, 2 mM EDTA, 2 mM DTT, pH 6.0) at room temperature for 5 min to activate the enzyme. Afterwards, different amount of inhibitors at the final concentrations of 100–1,200 nM were added and pre-incubated for 5 min at room temperature. The substrate solution (Z-Arg-Arg-AMC, Sigma Aldrich, St. Louis, IL, USA) at final concentration of 10 µM was added.

All of the mixture samples (proteases, inhibitors, and substrates) were incubated in black 96-well microtiter plates (Thermo Scientific, Denmark) at 37°C for 30 min. Subsequently, the fluorescence was measured on a Varioskan Flash spectral scanning multimode reader (Thermo Scientific, Waltham, MA, USA) at excitation and emission wavelengths of 355 nm and 460 nm, respectively. Assays were performed in triplicate for duplicate samples. The data was normalized between 0% to 100% activities and nonlinear fitted according to a sigmoidal dose-response (variable slope) to obtain the IC$_{50}$ values using GraphPad Prism 6.0.

4.6.3 Determination of the equilibrium inhibition constant (K_i)

The equilibrium inhibition constant (K_i) of purified rFgStefin-2, rFgStefin-1 and human cystatin C for native bovine cathepsins B (Sigma Aldrich, St. Louis, IL, USA) was determined from the equilibrium rates of fluorogenic substrate hydrolysis by enzyme at different amount of inhibitors. The enzyme protease at the final concentration 25 pg was incubated with different concentration (final concentration 20 to 1,000 nM) of rFgStefin-2, rFgStefin-1 and human cystatin C in cathepsin B assay buffer (100 mM MES, 400 mM NaCl, 2 mM EDTA, 2 mM DTT, pH 6.0) at room temperature for 5 min. Subsequently, the substrate solution (Z-Arg-Arg-AMC, Sigma Aldrich, St. Louis, IL, USA) at final concentration of 10 µM was added. The fluorescence of released product was continuously monitored at 37°C, 60 s intervals for 30 min on a Varioskan Flash spectral scanning multimode reader (Thermo Scientific, Waltham, MA, USA) at excitation and emission wavelengths of 355 nm and 460 nm, respectively. The recorded values were fitted using nonlinear regression with the Morrison equation for tight competitive inhibition using GraphPad Prism 6.0.

4.6.4 Zymography

The inhibitory activity of rFgStefin-2 and rFgStefin-1 against the proteolytic activity of ES products, CW extracts from metacercariae and adults (**Section 4.4.1**) was visualized on non-denaturing gels containing gelatin substrate. ES product, CW metacercariae and CW adult (2 µg) were incubated in assay buffer (0.1 M sodium acetate, pH 5.5, 1 mM EDTA) in the presence or absence of rFgStefin-2 and rFgStefin-1 (1–20 µM) at 37°C for 30 min. The samples were mixed with 5× native sample loading buffer (0.313 M Tris-HCl, pH 6.8, 50% [v/v] glycerol, 0.05% [w/v] bromophenol blue) and analyzed by a non-denaturing 10% polyacrylamide gel containing 0.1% gelatin (as described in **Section 4.3.4**). After electrophoresis, the gel was twice washed in 2.5% Triton X-100 with gentle agitation for 30 min each to remove the SDS from the gel. The washing buffer was discarded and the developing buffer (0.1 M sodium acetate, 1 mM EDTA, 2 mM DTT, pH 5.5) was added followed by incubation at room temperature for 10 min with gentle agitation. Subsequently, the developing buffer was replaced with fresh developing buffer and the gel was

further incubated at 37°C, overnight. On the following day, the gel was washed with DW and stained with 0.5% Coomassie blue G-250 followed by incubation at room temperature, overnight. On the next day, the gel was destained with high methanol destaining solution (40% [v/v] methanol, 7% [v/v] glacial acetic acid) until clear bands were observed. Finally, the gel was incubated in 50% methanol for 3 h and dried on a cellophane membrane.

4.6.5 Temperature stability of rFgStefin-2

Analysis of thermal stability of rFgStefin-2 was analyzed by incubation of rFgStefin-2 (1 µM) in cathepsin L assay buffer (340 mM sodium acetate, 60 mM acetic acid, 4 mM EDTA, pH 5.5) containing 1 M cysteine at 100°C for 30 to 180 min. The mixture was rapidly cooled on ice and the residual inhibitory activity of rFgStefin-2 at 250 nM final concentration against bovine cathepsin L (Sigma Aldrich, St. Louis, IL, USA) was determined as described in **Section 4.6.2** in duplicate measurements. The percentage of residual inhibitory activity of rFgStefin-2 against cathepsin L was calculated in comparison with cathepsin L activity in the absence of inhibitor.

4.6.6 pH dependency of rFgStefin-2

Analysis of pH dependency of rFgStefin-2 was performed by incubation of rFgStefin-2 (1 µM) in different pH assay buffers (20 mM sodium acetate buffer [pH 3.0–6.0], sodium phosphate buffer [pH 7.0–8.0], and Tris-HCl buffer [pH 9.0] for 30 min at 37°C. Subsequently, the residual inhibitory activity against bovine cathepsin L (Sigma Aldrich, St. Louis, IL, USA) was determined at 250 nM final concentration of rFgStefin-2 as described in **Section 4.6.2** in duplicate measurements. The percentage of residual inhibitory activity of rFgStefin-2 against cathepsin L was calculated in comparison with cathepsin L activity in the absence of inhibitor.

4.6.7 RT-PCR and western blot analysis of FgStefin1 and FgStefin-2 genes products in metacercariae and adult *F. gigantica*

Total RNA from metacercariae and adult *F. gigantica* (**Section 4.2.3**) was used as template in RT-PCR to verify FgStefin-1 and FgStefin-2 gene expression during development. The first strand cDNA was generated by using

RevertAid™ M-MuLV Reverse Transcriptase (Thermo Scientific, Lithuania). The rFgStefin-1 and rFgStefin-2 specific primer pair used in this experiment and all of the ingredients are detailed in the following lists.

FgStefin-1

Forward primer: 5'-AAT CAC TAA AAA TGA TGT GC-3'

Reverse primer: 5'-ATA GGA GTA CCG GTC ATG-3'

FgStefin-2

Forward primer: 5'-GGA TCC atc gag ggt cgc ATG CTC GTC GGT GGT TAT ACT G-3'

Reverse primer: 5'-TGC ATG TGC AGA GAT AGC-3'

Components	Volume (µl)
Total RNA from each stage (2 µg)	X
Reverse primer (10 µM)	2.0
DEPC-treated DW	12.0-X
Mix all above components by pipetting, briefly spin and add following components	
5× RevertAid™ reaction buffer	4.0
Mixed dNTPs (2.5 mM each)	2.0
RiboLock™ RNase Inhibitor	0.5
RevertAid™ M-MuLV Reverse Transcriptase	0.5
Total volume	20.0

The mixture was incubated at 42°C for 1 h and the reaction was terminated by heating at 70°C for 10 min. The reverse transcription product was stored on ice until used as template of PCR.

Components	Volume (μl)
Template (RT-PCR product)	2.0
Forward primer (10μM)	1.0
Reverse primer (10μM)	1.0
10×$(NH_4)_2SO_4$ buffer	5.0
$MgCl_2$ (25mM)	3.0
Mixed dNTPs (2.5mM each)	1.0
Taq DNA polymerase (5U/μl)	0.5
DW	36.5
Total volume	50.0

The components were mixed and the PCR reaction was performed using the following conditions: pre-denaturation at 95°C for 5 min, 35 cycles of denaturation at 95°C for 1 min, annealing at 55°C for 1 min and extension at 72°C for 1 min then one cycle of final extension at 72°C for 10 min and hold at 4°C. The PCR product was analyzed by 0.7% (w/v) agarose gel electrophoresis (as described in **Section 4.1.1.2**).

For the western blot analysis, ES products, CW extracts from metacercariae and adults (**Section 4.4.1**) were electrotransferred to a nitrocellulose membrane and the membrane was processed for immunological detection as described in **Sections 4.4.2.1–4.4.2.2.**

4.6.8 Reactivity of sera from *F. gigantica*–infected mice to rFgStefin1 and rFgStefin-2

The pre-infection sera and 2-, 4-, 6-week postinfection sera of 14 *F. gigantica*-infected mice (**Section 4.2.1.2**) were used to detect rFgStefin-1 and rFgStefin-2 by ELISA as described in **Section 4.3.7.2**.

4.7 Analysis of immunomodulatory properties of recombinant FgStefin-2

4.7.1 Isolation of murine spleen cells

Naïve BALB/c mice were sacrificed by euthanasia method (cervical dislocation) to collect the spleens. Each spleen was placed in a sterile glass petri dish containing a few milliliters of complete RPMI medium (RPMI-1640 supplemented with 1% antibiotic-antimycotic, 2 mM glutamine, and 10% fetal bovine serum). The splenocytes were separated by crushing the tissue between sterile frosted-end slides. The suspension was transferred to a sterile tube and the splenocytes were recovered by centrifugation at 1,000×g for 5 min. The supernatant was discarded by pipetting and the cell pellet was resuspended in 2 ml of RBC lysis buffer (ammonium chloride and 0.1 M Tris-HCl) followed by incubation at room temperature for 5 min. Subsequently, 5 ml of complete RPMI medium was added and the cells were recovered by centrifugation at 1,000×g for 5 min. The supernatant was discarded by pipetting and the cell pellet was washed three times with 5 ml complete RPMI medium followed by centrifugation at 1,000×g for 5 min. Finally, the splenocytes were resuspended in 5 ml complete RPMI medium and the cells were stained with trypan blue solution to determine the cell viability by using a hemocytometer. The cell viability was counted within 10 min to avoid false cell staining.

4.7.2 Isolation of murine PBMC

The peripheral blood mononuclear cells (PBMC) of naïve BALB/c mice were isolated from EDTA-treated venous blood by Ficoll-Paque™ PREMIUM density gradient media (GE Healthcare, Buckinghamshire, UK). The sample was prepared in a sterile tube by adding 2 ml of EDTA-treated venous blood and equal volume of balanced salt solution (**Appendix A**). Afterwards, the blood and buffer

(final volume 4 ml) were mixed several times by inverting the tube or pipetting. The Ficoll-Paque media was added in the fresh sterile tube and then the diluted blood sample (4 ml) was carefully added onto the Ficoll-Paque media solution followed by centrifugation at 400×g for 30 min at room temperature. The upper layer containing plasma and platelets was removed by pipetting and the mononuclear cells layer was transferred to a new sterile tube by pipetting (**Figure 4.3**). Subsequently, the volume of transferred mononuclear cells was estimated and 3 vol of balanced salt solution was added to 1 vol of the mononuclear cells. The sample was mixed by pipetting and centrifuged at 400×g for 15 min at room temperature. The supernatant was removed and the pellet was resuspended in 6 ml of balanced salt solution. The mixture was centrifuged at 400×g for 10 min at room temperature and the supernatant was removed by pipetting. Finally, the cell pellet was resuspended in RPMI 1640, supplemented with 1% antibiotic-antimycotic, 2 mM glutamine, and 10% fetal bovine serum.
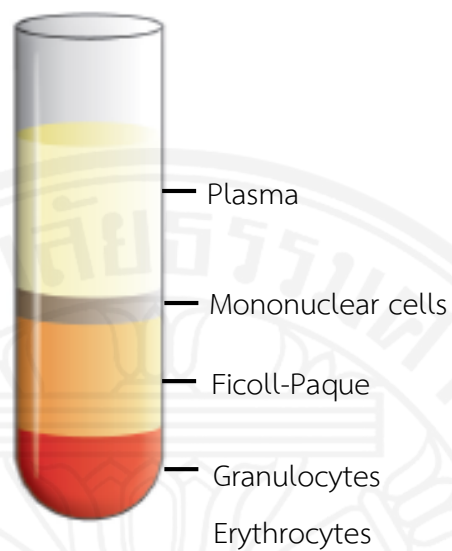
Figure 4.3 Mononuclear cell isolation using Ficoll-Paque™ PREMIUM density gradient media.

4.7.3 MTT cell proliferation

MTT (3-[4,5-dimethylthiazol-2-yl-2, 5-diphenyltetrazolium bromide, Invitrogen, Carlsbad, CA, USA) was diluted in 0.1 mM PBS, pH 7.4 at the final concentration 5 mg/ml. Subsequently, 10 µl of MTT reagent was added to each well and the plate was incubated at 37 °C for 4 hr. At the end of the incubation period, 100 µl DMSO (Dimethyl sulfoxide, Sigma Aldrich, St. Louis, IL, USA) was added and mixed by pipetting to ensure complete solubilization. The absorbance was recorded at 570 nm on a Varioskan Flash spectral scanning multimode reader (Thermo Scientific, Waltham, MA, USA).

4.7.4 Polyclonally stimulated proliferation of murine spleen cells

Spleen cells of naïve BALB/c mice were prepared as described in **Section 4.7.1** and cultured in 96-well flat-bottomed plates (NUNC, Roskide, Denmark) at a density of 3.5×10^5 cells/well. Subsequently, concanavalin A at 2 µg per ml in complete RPMI medium (RPMI-1640 supplemented with 1% antibiotic-antimycotic, 2 mM glutamine, and 10% fetal bovine serum) was added to stimulate the proliferation and then purified rFgStefin-1 and rFgStefin-2 were added at concentrations of 0.2–0.5 µM to the spleen cells. The plate was incubated at 37°C for 72 h. Proliferation of cells was quantified by MTT cell proliferation assay as described in **Section 4.7.3**. Assays were performed in triplicate for duplicate samples.

4.7.5 Polyclonally stimulated proliferation of murine PBMC

The peripheral blood mononuclear cells (PBMC) of naïve BALB/c mice as described in **Section 4.7.2** were cultured in 96-well flat-bottomed plates (NUNC, Roskide, Denmark) at a density of 3.5×10^5 cells/well. The proliferation was stimulated with 2 µg of concanavalin A per ml in complete RPMI medium (RPMI-1640 supplemented with 1% antibiotic-antimycotic, 2 mM glutamine, and 10% fetal bovine serum). Afterwards, rFgStefin-1 and rFgStefin-2 were added at concentrations of 0.2–0.5 µM to the murine PBMCs. The plate was incubated at 37°C for 72 h and the proliferation of cells was quantified by MTT cell proliferation assay as described in **Section 4.7.3**. Assays were performed in triplicate for duplicate samples.

4.8 Expression of recombinant *F. gigantica* cathepsin B5 (rFgCatB5) in eukaryotic system

4.8.1 Generating the PCR products encoding FgCatB5

The cDNA fragment encoding FgCatB5 was amplified by PCR using forward primer 5'-<u>CTG CAG</u> CAA CAC CAA GCC TCA AAA CAG G-3' and reverse primer 5'-<u>TCT AGA</u> GCC AAA CGC GGC ATA CCC GTC-3'. *Pst* I and *Xba* I endonuclease restriction sites (underlined) were added to the forward and reverse primers, respectively, to facilitate the fragment cloning into the pPicZαB vector (QIAGEN, Venlo, Netherlands). The reaction mixture was prepared as shown below.

Components	Volume (µl)
Template (plasmid FgCatCB5)	2.0
Forward primer (10 µM)	1.0
Reverse primer (10 µM)	1.0
$10\times(NH_4)_2SO_4$ buffer	5.0
$MgCl_2$ (25 mM)	3.0
Mixed dNTPs (2.5 mM each)	1.0
Taq DNA polymerase (5U/µl)	0.5
DW	36.5
Total volume	50.0

The PCR reaction was performed using the following conditions: pre-denaturation at 95℃ for 5 min, 35 cycles of denaturation at 95℃ for 1 min, gradient annealing at 60–65℃ for 1 min and extension at 72℃ for 1 min then one cycle of final extension at 72℃ for 10 min and hold at 4℃. The PCR product was resolved on a 0.7% (w/v) agarose gel (as described in **Section 4.1.1.2**). The FgCatB5 fragment was extracted from the agarose gel using a QIAquick® Gel Extraction Kit (QIAGEN, Limburg, Netherlands) as described in **Section 4.1.1.3.** The extracted PCR product was inserted into the pGEM®-T Easy vector by ligation and competent *E. coli* XL1-Blue was transformed with the ligation product. Positive transformant bacteria

were identified by PCR, restriction endonuclease digestion (*Pst* I and *Xba* I) as described in **Sections 4.1.2.1–4.1.2.6.**

4.8.2 Subcloning of the FgCatB5 cDNA fragment from pGEM®-T Easy into the expression vector pPicZαB

4.8.2.1 Restriction endonuclease digestion of FgCatB5 and pPicZαB vector

Recombinant pGEM®-T Easy carrying FgCatB5 (**Section 4.8.1**) and the pPicZαB expression vector (QIAGEN, Limburg, Netherlands) were double-digested with restriction endonucleases *Pst* I and *Xba* I (Thermo Scientific, Lithuania). The reaction sample was set up as shown below.

Components	Volume (µl)
Plasmid DNA (pGEM®-T Easy carrying FgCatB5 or pPicZα B)	5.0
Tango buffer (10×)	2.0
Xba I (10 U/µl)	0.5
Pst I (10 U/µl)	1.0
DW	11.5
Total volume	20.0

The sample was incubated at 37°C for 2 h and the restriction enzymes were inactivated at 80°C for 20 min. The product was kept at −20°C until used.

4.8.2.2 Insertion of FgCatB5 into the pPicZαB vector and introduction of the recombinant vector into the *E. coli* expression host

The digested pPicZαB expression vector and digested FgCatB5 cDNA fragments from **Section 4.8.2.1** were resolved on a 0.7% (w/v) agarose gel (as described in **Section 4.1.1.2**) and their concentration was estimated by comparison with 1 kb DNA ladder (Thermo Scientific, Lithuania). The FgCatB5 cDNA fragment and the linearized pPicZαB plasmid were extracted from the agarose using

the QIAquick® Gel Extraction Kit (QIAGEN, Limburg, Netherlands) as described in **Section 4.1.1.3** and combined by ligation using T4 DNA ligase (Thermo Scientific, Lithuania). The insert:vector molar ratios (3:1 to 1:3) were optimized by using the following formula:

$$\frac{\text{ng of vector} \times \text{kb size of insert} \times \text{insert: vector molar ratio}}{\text{kb size of vector}} = \text{ng of insert}$$

The content of the ligation reaction was as follows.

Components	Volume (µl)
10× T4 DNA ligase buffer	1.0
Digested pPicZαB vector	1.0
Digested FgCatB5 cDNA	3.0
T4 DNA ligase (5 Weiss U/µl)	1.0
DW	4.0
Total volume	10.0

The sample was incubated at 4°C, overnight and 1 µl of reaction product were used for transformation of chemically competent *E. coli* Top10 as described in **Sections 4.1.2.2–4.1.2.3.** The transformed cells were spread on LB agar containing 100 µg/ml of Zeocin™ (Life Technology, California, USA) and incubated overnight at 37°C. Positive clones were checked by using colony PCR and restriction endonuclease digestion (*Pst* I and *Xba* I) as described in **Sections 4.1.2.4–4.1.2.6.**

4.8.3 Transformation of *Pichia pastoris* (strain X33) with recombinant pPicZαB-FgCatB5

4.8.3.1 Linearization of recombinant pPicZαB-FgCatB5

The vector containing the FgCatB5 cDNA was linearized with *Sac* I using the digestion conditions below.

Components	Volume (µl)
Plasmid DNA (Section 4.8.2.2)	45.0
Buffer B (10×)	6.0
Sac I (10 U/µl)	3.0
DW	6.0
Total volume	60.0

The sample was incubated at 37°C for 2 h and the restriction enzymes were inactivated at 65°C for 20 min. Subsequently, DW was added to adjust the volume to 100 µl and then phenol-chloroform (100 µl) was added, mixed followed by centrifugation at 12,000×g, 4°C for 15 min. The upper aqueous phase was transferred into a new tube and then 0.1 vol of 3 M sodium acetate and 2.5 vol of absolute ethanol were added to precipitate the DNA. The mixture was incubated at −70°C for 1 h and then centrifuged at 12,000×g, 4°C for 15 min. The supernatant was discarded and the pellet was washed with 80% ethanol followed by centrifugation at 12,000×g, 4°C for 15 min. The pellet was air dried and resuspended in 20 µl DW. The linearized plasmid DNA was kept at −20°C until used.

4.8.3.2 Preparation and storage of electrocompetent *Pichia* cells

Pichia pastoris (strain X33) was grown on YPD agar (1% [w/v] yeast extract, 2% [w/v] peptone, 2% [w/v] glucose and 2% agar) at 30°C for 16–18 h. A single isolated colony was selected for inoculation of 5 ml YPD medium (1% [w/v] yeast extract, 2% [w/v] peptone and 2% [w/v] glucose) and the culture was grown at 30°C, overnight with shaking at 250 rpm. The overnight culture (500 µl) was used to inoculate 500 ml fresh YPD medium and the culture was incubated at 30°C, overnight with shaking at 250 rpm until an OD_{600} value of 1.3-1.5 had been reached. The cultured medium was centrifuged at 1,500×g, 4°C for 5 min to harvest the cells. The supernatant was discarded and the cell pellet was resuspended in 500 ml of ice-cold DW. The mixture was centrifuged at 1,500×g, 4°C for 5 min and the supernatant was discarded. The pellet was resuspended in 250 ml of ice-cold DW and the centrifugation step was repeated. The supernatant was discarded and the cell pellet

was resuspended in 20 ml of ice-cold 1 M sorbitol. Finally, the cells were pelleted as above and resuspended in 1 ml of ice-cold 1 M sorbitol. The competent *Pichia pastoris* cells were kept on ice and used within the same day.

4.8.3.3 Transformation by electroporation

The competent *Pichia pastoris* strain X33 cells (80 µl) from **Section 4.8.3.2** were mixed with 10 µg of linearized DNA (**Section 4.8.3.1**). Subsequently, the mixture was transferred into an ice-cold 0.2 cm electroporation cuvette (Eppendorf, Hamburg, Germany) and incubated on ice for 5 min. The cells were pulsed at 2,000 V using an electroporator 2510 instrument (Eppendorf, Hamburg, Germany). After electroporation, 1 ml of ice-cold 1 M sorbitol was immediately added to the cuvette and mixed by pipetting. Afterwards, the mixture was transferred to a sterile tube and incubated at 30°C without shaking for 2h. The yeast cells (100 µl to 200 µl aliquots) were spread on 30°C-prewarmed YPDS agar (1% [w/v] yeast extract, 2% [w/v] peptone, 2% [w/v] glucose, 1 M sorbitol and 2% agar) containing 100 µg/ml of Zeocin™ (Life Technology, California, USA) and incubated at 30°C for 3–10 days until colonies had formed. Several single colonies were checked for positive transformants using MMH and MDH agar selection and PCR analysis.

4.8.3.4 Determination of the Mut phenotype by using MMH and MDH agar

Several isolated colonies of the transformant clones from **Section 4.8.3.3** were picked and streaked on a MMH plate (1.34% [w/v] yeast nitrogen base, 4×10^{-5}% [w/v] biotin and 0.5% [v/v] methanol) and a MMD plate (1.34% [w/v] yeast nitrogen base, 4×10^{-5}% [w/v] biotin and 2% [w/v] glucose). The plate was incubated at 30°C for 2–5 days. Mut$^+$ cells will grow normally on both plates, while Mut^S cells will grow normally on the MDH plate but show little or no growth on the MMH plate.

4.8.3.5 Genomic DNA extraction

The positive clones (**Section 4.8.3.4**) were cultured in 20 ml YPD medium containing 100 µg/ml Zeocin™ in a sterile tube and incubated at 30°C for 48 h with shaking at 250 rpm. The cultured cells were harvested by centrifugation at 6,000×g, room temperature for 10 min. Subsequently, the

supernatant was discarded and the pellet was resuspended in 1 ml STES buffer (0.2 M Tris-HCl, pH 7.6, 0.5 M NaCl, 0.1% [w/v] SDS and 10 mM EDTA). The suspension (350 µl) was transferred into a fresh tube and acid washed glass beads (50 µl), TE buffer pH 7.6 (140 µl) and phenol/chloroform (450 µl) were added to the suspension. The cells were broken by vortexing for 2 min and then centrifuged at 13,000 rpm for 5 min at room temperature to remove the cell debris and denatured proteins. The upper aqueous phase containing the nucleic acids was transferred to a new tube and then 0.1 vol of 3 M sodium acetate, pH 5.2 and 2 vol of absolute ethanol were added to precipitate the DNA. Afterwards, the mixture was centrifuged at 13,000 rpm, 4°C for 10 min and the pellet was twice washed with 80% ethanol followed by centrifugation at 13,000 rpm, 4°C for 5 min. The pellet was air dried and resuspended in 50 µl DW followed by incubation at room temperature for 15 min. The solution was treated with 0.5 µl RNase A (10 mg/ml, Fermentas Life Sciences, Lithuania) to degrade co-purified RNA and the genomic DNA was kept at −20°C until used.

4.8.3.6 PCR analysis for positive clones

The genomic DNA from **Section 4.8.3.5** was used as template for PCR amplification. The FgCatB5 cDNA fragment was amplified by using specific forward and reverse primers as described in **Section 4.8.1.** The reaction mixture was prepared as shown next page.

Components	Volume (µl)
Template (genomic DNA)	5.0
Forward primer (10µM)	1.0
Reverse primer (10µM)	1.0
$10\times(NH_4)_2SO_4$ buffer	5.0
$MgCl_2$ (25 mM)	2.5
Mixed dNTPs (2.5 mM each)	2.5
Taq DNA polymerase (5U/µl)	0.5
DW	32.5
Total volume	50.0

The PCR reaction was set using following conditions: pre-denaturation at 95°C for 5 min, 35 cycles of denaturation at 95°C for 1 min, annealing at 60°C for 1 min and extension at 72°C for 1 min then one cycle of final extension at 72°C for 10 min and hold at 4°C. The PCR product was resolved on a 0.7% (w/v) agarose gel.

4.8.4 Expression and purification of rFgCatB5 in *Pichia pastoris* (strain X33)

4.8.4.1 Small scale culture screening of rFgCatB5 expression and time course analysis

Single colonies of positive transformant clones (**Section 4.8.3.6**) were cultured in 25 ml BMGY (1% [w/v] yeast extract, 2% [w/v] peptone, 100 mM potassium phosphate, pH 6.0, 1.34% [w/v] yeast nitrogen base, 4×10^{-5}% [w/v] biotin and 1% [v/v] glycerol) at 30°C, 250 rpm, overnight until an OD_{600} of 2–6 had been reached. On the following day, the cells were centrifuged at 3,000×g, room temperature for 5 min and the pellet was resuspended in BMMY (1% [w/v] yeast extract, 2% [w/v] peptone, 100 mM potassium phosphate, pH 6.0, 1.34% [w/v] yeast nitrogen base, 4×10^{-5}% [w/v] biotin and 0.5% [v/v] methanol) to an OD_{600} of 1.0 (approximately 100–200 ml) to induce expression. The induction of recombinant protein expression was maintained by adding absolute methanol at a final

concentration of 0.5% methanol every 24 h.   After induction the culture was incubated for 96 h and 1 ml of cell samples were collected at 0, 12, 24, 48, 72 and 96 h for a time course analysis.   The collected samples were centrifuged at 12,000×g for 5 min and the supernatants were transferred to a new tube.   The supernatants were analyzed for protein expression by western blot as described in **Sections 4.4.2.1**–**4.4.2.2** or kept at −80℃.

4.8.4.2   Large scale expression of rFgCatB5 protein

A single colony of a transformant clone was cultured in 100 ml BMGY at 30℃, 250 rpm, overnight until an OD_{600} of 2–6 had been reached.   On the next day, the cells were centrifuged at 3,000×g, room temperature for 5 min and the pellet was resuspended in BMMY medium (approximately 700–1,000 ml) to an OD_{600} of 1.0 to induce expression.   The induction of recombinant protein expression was maintained by adding absolute methanol at a final concentration of 0.5% methanol every 24 h.   After induction the culture was incubated for 72 h and centrifuged at 5,000×g, 4℃ for 30 min.   The supernatant was kept at −20℃ until used in purification assay.

4.8.4.3   Purification of rFgCatB5

The rFgCatB5 was purified by nickel-nitrilo tri-acetic acid (Ni-NTA) affinity chromatography.   The supernatant collected in **Section 4.8.4.2** was mixed with 10× native lysis buffer (0.5 M NaH_2PO_4, 3 M NaCl and 0.1 M imidazole, pH 8.0) to a final concentration of 1× lysis buffer.   Five milliliters of Ni-NTA agarose slurry (QIAGEN, Hilden, Germany) was mixed with 15 ml of medium and gently rotated on a rotary shaker at 4℃ for 1 h.   The mixture of proteins and beads was loaded onto a polypropylene column and the beads were packed by gravity.   The bottom cap was removed and the flow-through was collected.   The remaining medium was continuously added to the column.   The column was washed twice with 20 ml washing buffer (50 mM NaH_2PO_4, 300 mM NaCl, 20 mM imidazole, pH 8.0) and the washing fractions were collected.   The rFgCatB5 was eluted with 15 ml of elution buffer (50 mM NaH_2PO_4, 300 mM NaCl, 250 mM imidazole, pH 8.0) and then the eluted protein was concentrated and dialyzed against 10 mM PBS, pH 7.2 using Amicon® Ultra centrifugal filters (10 kDa cut off, Millipore, Carrigtwohill, Ireland).   The

concentration of protein was measured (as described in **Section 4.3.6**) and the purified protein was analyzed by western blot as described in **Sections 4.4.2.1– 4.4.2.2** or kept at −20°C.

4.9 Western blot analysis of rFgCatB5, CW extract and ES product with mouse anti-rFgCatB5 antisera

CW extract (10 µg), ES product (10 µg) and rFgCatB5 (100 ng) were resolved by 12.5% SDS-PAGE (as described in Section 4.3.4). All proteins were electrotransferred to a nitrocellulose membrane by semi-dry blotting using a Fastblot B33 instrument and then processed for western immunological detection as described in **Sections 4.4.2.1** and **4.4.2.2**.

4.10 Reactivity of sera from *F. gigantica*-infected mice to rFgCatB5

The pre-infection sera and 2-, 4-, 6-week postinfection sera of 10 *F. gigantica*-infected mice (**Section 4.2.1.2**) were used to detect rFgCatB5 by ELISA as described in **Section 4.3.7.2**.

4.11 Characterization of recombinant *F. gigantica* cathepsin B5

4.11.1 Autoprocessing of rFgCatB5

Purified rFgCatB5 (800 ng) was incubated in AMT buffer (100 mM sodium acetate, 100 mM MES, 200 mM Tris-HCl, 4 mM EDTA) containing 50 µg/ml dextran sulfate (DS 500K) and 10 mM DTT at a pH range of 4.0–5.5 for 0, 0.5, 1.5, 4 and 19 h to analyze autoprocessing. All samples were analyzed by 12.5% SDS-PAGE under reducing conditions and visualized by silver staining as described in **Sections 4.3.4** and **4.3.4.4**. Experiments were done in duplicate.

4.11.2 Determination of K_m values

The K_m value of rFgCatB5 for Z-Arg-Arg-AMC was determined as described in **Section 4.6.1**.

4.11.3 Determination of the inhibition coefficients (IC_{50})

The inhibitory activity of rFgStefin-2, rFgStefin-1 and human cystatin C (Calbiochem, USA) for rFgCatB5 (**Section 4.8.2**) were determined as the inhibition coefficients (IC_{50}) by measuring the loss of enzymatic activity at increasing concentrations of inhibitor in the presence of a fluorogenic substrate in large excess. The IC_{50} of purified rFgStefin-1, rFgStefin-2 and human cystatin C were determined for rFgCatB5. rFgCatB5 (1 ng/reaction) was incubated in CatB assay buffer (100 mM sodium acetate, 2 mM EDTA, 1 mM DTT, pH 6.0) at room temperature for 5 min to activate the enzyme and then different amounts of inhibitors were added to final concentrations between 100–1,200 nM followed by pre-incubation at room temperature for 5 min. Afterwards, the substrate solution (Z-Arg-Arg-AMC, Sigma Aldrich, St. Louis, IL, USA) was added to the mixture at final concentration of 10 µM. The samples were incubated in black 96-well microtiter plates (Thermo Scientific, Denmark) at 37°C for 30 min and then the residual enzyme activity was measured by the release of fluorescence (excitation and emission wavelengths of 355 nm and 460 nm, respectively) on a Varioskan Flash spectral scanning multimode reader (Thermo Scientific, Waltham, MA, USA). Assays were performed in triplicate for duplicate samples. The data was normalized between 0% to 100% activity and nonlinear fitted according to a sigmoidal dose-response (variable slope) to obtain the IC_{50} values using GraphPad Prism 6.0.

4.11.4 Determination of the equilibrium inhibition constant (K_i)

The equilibrium inhibition constant (K_i) of purified rFgStefin-2, rFgStefin-1 and human cystatin C for rFgCatB5 was determined in **Section 4.6.3.**

4.11.5 Temperature stability of rFgCatB5

The thermal stability of rFgCatB5 was analyzed by incubation of rFgCatB5 (800 ng) in AMT buffer containing 50 µg/ml DS 500K, 200 mM NaCl and 10 mM DTT pH.4.5 at 37°C between 1–5 h and after 24 h. The residual activity was measured simultaneously against the substrate solution (Z-Arg-Arg-AMC, Sigma Aldrich, St. Louis, IL, USA) at a final concentration of 10 µM as described in **Section 4.9.3**.

4.11.6 pH dependency of rFgCatB5

The pH dependency of rFgCatB5 was performed by incubation of rFgCatB5 (800 ng) in AMT buffer containing 50 µg/ml DS 500K, 200 mM NaCl and 10 mM DTT at a pH range of 3.0–8.0 for 2 h at 37℃. The residual activity was measured simultaneously against the substrate solution (Z-Arg-Arg-AMC, Sigma Aldrich, St. Louis, IL, USA) at a final concentration of 10 µM as described in **Section 4.9.3**.

4.11.7 Degradation of host proteins by rFgCatB5

The degradation of various host proteins was assessed by incubation of rFgCatB5 (500 and 700 nM) with 500 µg/ml of bovine serum albumin, hemoglobin, human IgG and 1,000 µg/ml of fibronectin, laminin, collagen type IV (all Sigma Aldrich, USA except fibronectin: Calbiochem, USA) in AMT buffer containing 50 µg/ml DS 500K, 200 mM NaCl and 10 mM DTT at pH 4.5 and 5.5 for 4 h at 37℃. Afterwards, the reactions were stopped by adding reducing sample buffer and heated at 95℃ for 5 min. Samples were analyzed by 12.5% SDS-PAGE under reducing conditions and stained with Coomassie Brilliant Blue R-250 as described in **Sections 4.3.4** and **4.3.4.3**.

4.11.8 Activity of rFgCatB5 against exopeptidase substrate

The exopeptidase activity of rFgCatB5 and human cathepsin B (Sigma Aldrich, St. Louis, IL, USA) against the substrate (Abz-Phe-Arg-Ala-Lys[Dnp]-OH), was analyzed in assay buffer (50 mM NaH_2PO_4, 200 mM NaCl, 5 mM EDTA and 1 mM DTT, pH 4.5). All cathepsin B enzymes (75 nM) were activated in the assay buffer and then the exopeptidase substrate solution (Exo-OH) was added at 20 µM final concentration. The exopeptidase activity was determined by continuously monitoring the released fluorescence at 30 s intervals, 37℃ for 20 min on a Varioskan Flash spectral scanning multimode reader (Thermo Scientific, Waltham, MA, USA) at excitation and emission wavelengths of 320 nm and 420 nm, respectively. Assays were performed in triplicate for duplicate samples.

CHAPTER V

RESULTS

5.1 Molecular cloning and sequence analysis of FgStefin-2

5.1.1 Nucleic acid sequence analysis

An adult stage *F. gigantica* EST database was searched for uncharacterized parasite cystatins by TBLASTN with FgStefin-1 as a query sequence. EST A00363 (857 bp) was identified as a transcript encoding a novel uncharacterized single domain cystatin of *Fasciola* which was termed FgStefin-2. This cDNA was re-isolated by RT-PCR from adult stage *F. gigantica* total RNA with a specific primer pair as described in **Section 4.1.1.1**. The product was size-separated by 0.7% agarose gel electrophoresis and the fragment of expected 836 bp size was observed (**Figure 5.1**). Subsequently, the PCR product was extracted from the agarose gel and subcloned into the pGEM®-T Easy vector. Positive transformant *E. coli* XL1-Blue were identified by colony PCR and restriction analysis of the extracted plasmid DNA with *Eco*R I for presence of the expected insert (**Figure 5.2**). The nucleic acid sequence was determined using the services of 1st base Pte Ltd, Singapore. The nucleotide sequence data is available in the GenBank database under the accession number JX838801 (**Figure 5.3**). The FgStefin-2 cDNA encodes a protein of 116 amino acid residues.

5.1.2 Amino acid sequence characterization

The FgStefin-2 amino acid sequence was analyzed by EMBOSS pepstat for general protein properties. FgStefin-2 has a calculated molecular mass of 12.56 kDa and a pI of 7.0 (**Figure 5.4**). SignalP 4.1 predicted the presence of a N-terminal signal peptide in the FgStefin-2 sequence (**Figure 5.5**).

A multiple amino acid sequence alignment of FgStefin-2 with other cystatins, namely, *F. gigantica* Stefin-1 (ACS35603.1), *F. hepatica* cystatin (AAV68752.1), *Opisthorchis viverrini* hypothetical protein T265_11270 (XP_009164067.1), *S. mansoni* cystatin (AAQ16180.1), *Brugia malayi* cystatin

(XP_001895476.1), *Onchocerca volvulus* cystatin-type cysteine protease inhibitor CPI-1 (AAD51087.1), human cystatin B (AAA99014.1) and human cystatin A (NP_005204.1) is shown in **Figure 5.6**. FgStefin-2 contains a characteristic conserved glycine residue in the N-terminal region and the QVVAG motif (amino acid residues 70–74) that is involved in binding to proteases.

NCBI-BLASTP was used to find related sequences in the NCBI non-redundant protein database. The sequence identity and similarity values (%) of FgStefin-2 with other cystatins are shown in **Table 5.1**. The identity values are 92.2%, 22.3%, 26.5%, 18.2%, 13.3%, 13.2%, 23.3% and 16.7% for *F. hepatica* cystatin, *F. gigantica* Stefin-1, *Opisthorchis viverrini* hypothetical protein T265_11270, *S. mansoni* cystatin, *Brugia malayi* cystatin, *Onchocerca volvulus* cystatin-type cysteine protease inhibitor CPI-1, human cystatin B and human cystatin A, respectively. The similarity values were 94.0%, 35.5%, 42.6%, 29.7%, 26.6%, 26.5%, 33.3% and 25.4% for *F. hepatica* cystatin, *F. gigantica* Stefin-1, *Opisthorchis viverrini* hypothetical protein T265_11270, *S. mansoni* cystatin, *Brugia malayi* cystatin, *Onchocerca volvulus* cystatin-type cysteine protease inhibitor CPI-1, human cystatin B and human cystatin A, respectively.
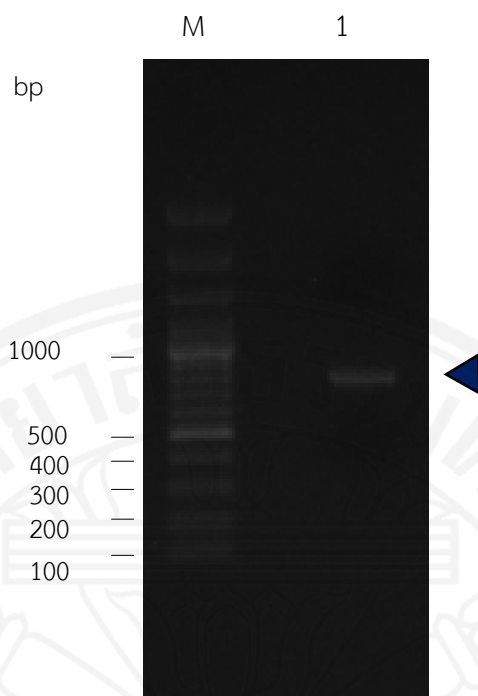
Figure 5.1 Agarose gel electrophoresis of the FgStefin-2 cDNA. Lane 1: PCR amplified 836 bp FgStefin-2 cDNA fragment (arrowhead). Lane M: GeneRuler™ 100 bp DNA ladder (Thermo Scientific, Lithuania).
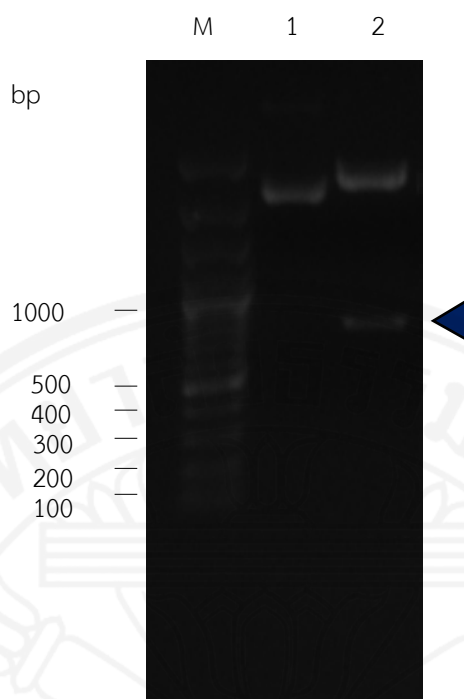
Figure 5.2 Agarose gel electrophoresis of recombinant pGEM®-T Easy carrying FgStefin-2 digested with restriction endonuclease *Eco*R I. Lane 1: uncut plasmid DNA, lane 2: cut plasmid DNA. The position of the FgStefin-2 is indicated by an arrowhead, lane M: GeneRuler™ 100 bp DNA ladder (Thermo Scientific, Lithuania).

```
      d  l  *  r  *  s  i  M  F  R  I  L  F  G  I  C  I  L  H  L
   1 GATTTGTGAAGGTGAAGCATAATGTTTCGCATATTATTTGGGATTTGCATTTTACATCTC 60
     ----:----|----:----|-***:----|----:----|----:----|----:----|

      M  S  C  D  V  F  G  E  M  A  L  V  G  G  Y  T  E  P  R  S  V
  61 ATGAGCTGTGATGTTTTTGGTGAAATGCTCGTCGGTGGTTATACTGAGCCGAGATCAGTT 120
     ----:----|----:----|----:----|----:----|----:----|----:----|

      T  S  E  E  R  S  V  F  R  P  M  I  L  S  K  F  L  T  T  G
 121 ACATCAGAGGAACGATCTGTATTCCGACCAATGATACTTTCCAAATTTCTCACAACTGGC 180
     ----:----|----:----|----:----|----:----|----:----|----:----|

      S  V  E  S  S  C  E  L  E  L  L  Q  V  S  T  Q  V  V  A  G
 181 TCTGTGGAAAGCTCGTGTGAGTTAGAGTTGCTCCAAGTGTCAACTCAAGTTGTTGCGGGG 240
     ----:----|----:----|----:----|----:----|----:----|----:----|

      T  N  Y  K  F  K  V  S  G  G  A  T  C  P  G  C  W  E  V  V
 241 ACAAATTATAAGTTCAAAGTCTCAGGTGGTGCAACGTGTCCGGGATGTTGGGAAGTTGTC 300
     ----:----|----:----|----:----|----:----|----:----|----:----|

      V  F  V  P  L  Y  S  S  K  A  A  T  S  V  G  T  P  T  R  V
 301 GTATTTGTTCCACTCTACTCGAGCAAAGCTGCCACCAGTGTAGGCACACCGACTCGGGTA 360
     ----:----|----:----|----:----|----:----|----:----|----:----|

      S  C  T  *  c  l  t  r  c  i  l  l  r  p  t  s  *  k  f  e
 361 TCTTGCACTTGATGTTTGACCAGATGTATTCTTTTACGTCCGACATCTTGAAAATTCGAG 420
     ----:----###--:----|----:----|----:----|----:----|----:----|

      i  i  q  n  i  i  n  n  q  *  n  i  l  n  y  s  n  p  i  t
 421 ATCATTCAAAACATTATCAACAATCAATGAAACATTTTGAATTATTCGAACCCGATTACT 480
     ----:----|----:----|----:----|----:----|----:----|----:----|

      v  p  t  *  n  n  f  i  f  v  g  p  k  t  m  n  v  h  l  t
 481 GTTCCTACCTGAAATAACTTCATTTTTGTGGGACCGAAGACAATGAACGTTCACCTGACA 540
     ----:----|----:----|----:----|----:----|----:----|----:----|

      g  l  t  s  s  e  v  l  c  l  q  a  l  c  f  t  w  f  h  t
 541 GGTTTAACTTCTAGTGAGGTTTTATGTTTGCAAGCACTATGTTTCACATGGTTTCATACA 600
     ----:----|----:----|----:----|----:----|----:----|----:----|

      r  *  v  r  r  s  r  a  f  h  t  f  s  c  n  s  k  l  v  c
 601 CGCTGAGTAAGGCGTTCTCGCGCGTTTCACACGTTTTCATGCAACTCCAAATTGGTATGC 660
     ----:----|----:----|----:----|----:----|----:----|----:----|

      h  h  s  n  f  i  h  p  *  q  v  c  c  h  c  r  l  i  v  r
 661 CACCACTCAAATTTCATACATCCTTAACAAGTGTGCTGTCATTGCAGACTGATTGTCCGT 720
     ----:----|----:----|----:----|----:----|----:----|----:----|

      s  v  l  r  q  t  v  t  r  i  r  t  i  r  m  h  r  l  i  t
 721 TCCGTCCTCCGACAGACTGTTACTCGCATACGTACAATTCGAATGCATCGACTCATTACT 780
     ----:----|----:----|----:----|----:----|----:----|----:----|

      d  f  f  c  h  s  w  i  f  t  e  *  m  l  s  l  h  m  x
 781 GATTTTTTCTGTCACTCTTGGATTTTTACTGAGTAAATGCTATCTCTGCACATGCA 836
     ----:----|----:----|----:----|----:----|----:----|----:-
```

Figure 5.3 Nucleotide and deduced amino acid sequences of the isolated FgStefin-2 cDNA (GenBank accession JX838801). The FgStefin-2 amino acid sequence is indicated by bold uppercase lettering. Start (***) and stop (###) codons are indicated.

Molecular mass [Da]	12559.64
Residues	116
Average residue mass [Da]	108.273
Charge	0.5
Isoelectric point	7.0431
A280 Molar extinction coefficients	9970 (reduced) 10345 (cystine bridges)
A280 Extinction coefficients 1mg/ml	0.794 (reduced) 0.824 (cystine bridges)
Improbability of expression in inclusion bodies	0.802

```
Residue   Number  Mole%   DayhoffStat
A = Ala      4     3.448   0.401
B = Asx      0     0.000   0.000
C = Cys      6     5.172   1.784
D = Asp      1     0.862   0.157
E = Glu      8     6.897   1.149
F = Phe      7     6.034   1.676
G = Gly     10     8.621   1.026
H = His      1     0.862   0.431
I = Ile      4     3.448   0.766
J = ---      0     0.000   0.000
K = Lys      4     3.448   0.522
L = Leu     10     8.621   1.165
M = Met      4     3.448   2.028
N = Asn      1     0.862   0.200
O = ---      0     0.000   0.000
P = Pro      5     4.310   0.829
Q = Gln      2     1.724   0.442
R = Arg      5     4.310   0.880
S = Ser     14    12.069   1.724
T = Thr     11     9.483   1.555
U = ---      0     0.000   0.000
V = Val     15    12.931   1.959
W = Trp      1     0.862   0.663
X = Xaa      0     0.000   0.000
Y = Tyr      3     2.586   0.761
Z = Glx      0     0.000   0.000

Property   Residues                     Number  Mole%
Tiny       (A+C+G+S+T)                    45     38.793
Small      (A+B+C+D+G+N+P+S+T+V)          67     57.759
Aliphatic  (A+I+L+V)                      33     28.448
Aromatic   (F+H+W+Y)                      12     10.345
Non-polar  (A+C+F+G+I+L+M+P+V+W+Y)        69     59.483
Polar      (D+E+H+K+N+Q+R+S+T+Z)          47     40.517
Charged    (B+D+E+H+K+R+Z)                19     16.379
Basic      (H+K+R)                        10      8.621
Acidic     (B+D+E+Z)                       9      7.759
```

Figure 5.4 Protein and amino acid properties of FgStefin-2 calculated by EMBOSS pepstats.
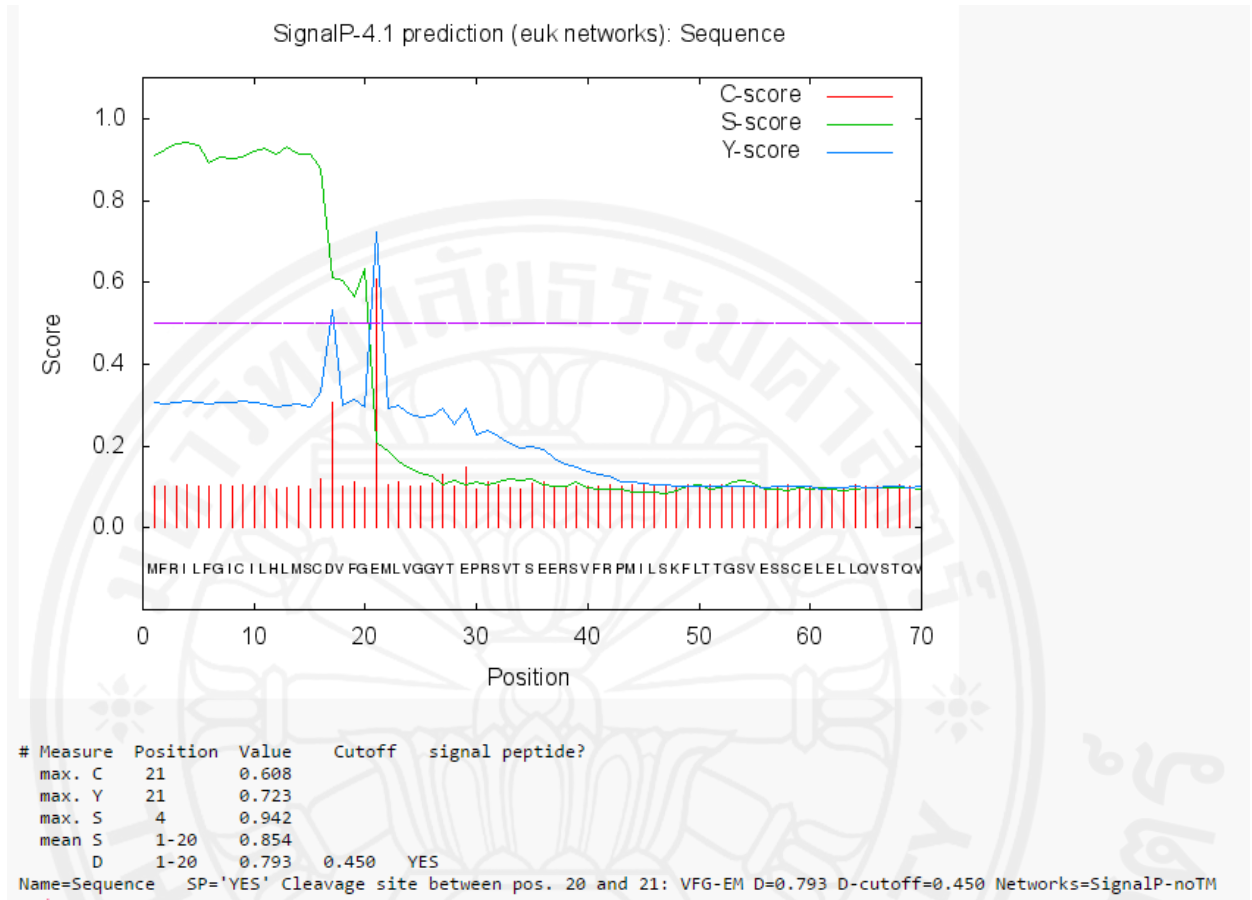
Figure 5.5 SignalP 4.1 signal peptide prediction for FgStefin-2.

Table 5.1 Sequence identity and similarity values of FgStefin-2 with other cystatins.

	Identity (%)	Similarity (%)
FgStefin2: Cystatin [*Fasciola hepatica*]	92.2	94.0
FgStefin2: FgStefin-1	22.3	35.4
FgStefin2: Cystatin of hypothetical protein [*Opisthorchis viverrini*]	26.5	42.6
FgStefin2: Cystatin [*Schistosoma mansoni*]	18.2	29.7
FgStefin2: Cystatin [*Brugia malayi*]	13.3	26.6
FgStefin2: Cystatin [*Onchocerca volvulus*]	13.2	26.5
FgStefin2: Cystatin-A [*Homo sapiens*]	23.3	33.3
FgStefin2: Cystatin-B [*Homo sapiens*]	16.7	25.4

The identity and similarity values (%) were calculated by global pairwise alignment (EMBOSS needle, BLOSUM62 matrix with gap penalty: 10 and extend penalty: 0.5) of the protein sequences. *F. hepatica* cystatin (AAV68752.1), *F. gigantica* Stefin-1 (ACS35603.1), Hypothetical protein T265_11270 [*Opisthorchis viverrini*] (XP_009164067.1), *Schistosoma mansoni* cystatin (AAQ16180.1), *Brugia malayi* cystatin (XP_001895476.1), Cystatin-type cysteine protease inhibitor CPI-1 [*Onchocerca volvulus*] (AAD51087.1), human cystatin B (AAA99014.1) and human cystatin A (NP_005204.1).

```
gi|410061138|gb|AFV53480.1|   MFRILFGICILHLMSCDVFGEMLVGGYTEPRSVTSEERSVFRPMILSKFL   50
gi|55978577|gb|AAV68752.1|    MLRILLGICILHFMSCDVFGEMLVGGYTEPRSVTPEERSVFQPMILSKLL   50
gi|239937595|gb|ACS35603.1|   --------------------MMCGGCTQTRAPSAEEKTELETVLREQLE    29
gi|33355623|gb|AAQ16180.1|    --------------------MPLCCGGIGTPREPSAEEKEKLKTLLESKLE   31
gi|4885165|ref|NP_005204.1|   --------------------MIPGGLSEAK-PATPEIQEIVDKVKPQLE    28
gi|1235678|gb|AAA99014.1|     --------------------MMCGAPSATQ-PATAETCHIADQVRSQLE    28
gi|170580954|ref|XP_001895476.1|   -MFFPIVWLSVLLIISKSFAREIRLSRATY-NEDDEEIQEVAEKAMEQVN   48
gi|5759315|gb|AAD51087.1|AF177194_1   -MFYLIIWFSAFAIISKSFAREIRLGKLTNDNEDDEEIQEVABKAMIQVN   49
gi|684410664|ref|XP_009176144.1|   --MLLEVLCLCLIFCLPASPQVAVGGYTPFRCPTANEIRTFTSLLNAEIS   48
                              1.......10........20........30........40........50
```

```
gi|410061138|gb|AFV53480.1|   TTGSVESSC---ELELLQVSTQVVAGTNYKFKVSGGAT-------CPGCW   90
gi|55978577|gb|AAV68752.1|    TAGSVESSC---ELELLQVSTQVVAGINYKFKVSGGAT-------CPGCW   90
gi|239937595|gb|ACS35603.1|   SH-IGHKPQ---IIEVVEICTQVVAGINYFAKVKIGN---------DNYI   66
gi|33355623|gb|AAQ16180.1|    SH-IGRKPR---SFEIVQITSQVVAGTNHFVKVKLDN---------GEYI   68
gi|4885165|ref|NP_005204.1|   EK-TNETYG---KLEAVQYKTQVVAGTNYYIKVRAGD---------NKYM   65
gi|1235678|gb|AAA99014.1|     EK-ENKKFP---VFKAVSFKSQVVAGTNYFIKVHVGD---------EDFV   65
gi|170580954|ref|XP_001895476.1|   DQTRYRNLYK--LVRVISAQTQVVAGIKYYLTILAAPTTCRKGAVGMNPM   96
gi|5759315|gb|AAD51087.1|AF177194_1   EKMKYDNLYK--LVKVINARTQVVAGMKYYLTILTAPTTCRK-NSGMSPA   96
gi|684410664|ref|XP_009176144.1|   NYLGTESVSGQ-EIQILEVSTQVVAGTNYRIKVGFCPMSYYMTPSTSRPA   97
                              ........60........70........80........90.......100
```

```
gi|410061138|gb|AFV53480.1|   EVVVFVPLYSSKAATSVGTPTRVSCT-------   116
gi|55978577|gb|AAV68752.1|    EVVVFVPLYSSKSATSVGTPTRVSCT-------   116
gi|239937595|gb|ACS35603.1|   HARIFQDLPCNGGKKKVHSVLKDKSATDSLKYF    99
gi|33355623|gb|AAQ16180.1|    HARIFEPLPCHGKELQHSVVKDKKESDALEYF   101
gi|4885165|ref|NP_005204.1|   HLKVFKSLPGQNEDLVLTGYQVDKNKDDELTGF    98
gi|1235678|gb|AAA99014.1|     HLRVFQSLPHENKPLTLSNYQTNKAKHDELTYF    98
gi|170580954|ref|XP_001895476.1|   KCTIDSSKPTKQFKIEVWSAPWQNTFKVTLT--   127
gi|5759315|gb|AAD51087.1|AF177194_1   NCAIDHSKPKKKVILEVWSAPWQNIFKVTMA--   127
gi|684410664|ref|XP_009176144.1|   LLTANVILLKCIKVFLLLKMAALRSGSPV----   126
                              .......110.......120.......130...
```

Figure 5.6 Multiple alignment of *F. gigantica* Stefin-2 (AFV53480.1), *F. gigantica* Stefin-1 (ACS35603.1), *F. hepatica* cystatin (AAV68752.1), Hypothetical protein T265_11270 [*Brugia malayi* cystatin] (XP_009164067.1), *Schistosoma mansoni* cystatin (AAQ16180.1), *Brugia malayi* cystatin (XP_001895476.1), Cystatin-type cysteine protease inhibitor CPI-1 [*Onchocerca volvulus*] (AAD51087.1), human cystatin B (AAA99014.1) and human cystatin A (NP_005204.1) generated by ClustalX version2.1.

(✽) indicates fully conserved positions

(:) indicates strongly conserved positions

(.) indicates weakly conserved positions

5.2 Characterization of FgStefin-2 nucleic acids

5.2.1 Probe quantification by spot assay

The concentration of the DIG-labeled DNA probe was determined by a spot test with DIG-labeled standard DNA as described in **Section 4.2.4.3**. The standard was diluted to the final concentrations 10, 3, 1, 0.3, 0.1, 0.03, 0.01 and 0 pg/μl. The DIG-labeled FgStefin-2 cDNA fragment was diluted 1:10, 1:100, 1:300, 1:1,000, 1:3,300, 1:10,000, 1:33,000 and 1:100,000 in DNA dilution buffer. From each sample 1 μl was taken 1 and spotted side by side onto a nylon membrane. Immunological detection was performed with anti-DIG-AP Fab fragments and the results are shown in **Figures 5.7–5.8**.

$$
\begin{aligned}
\text{Probe concentration} \quad &= 0.1 \text{ pg/μl} \times \text{dilution factor} \\
&= 0.1 \times 10^{3} \\
&= 1,000 \text{ pg/μl} \\
&= 1 \text{ ng/μl} \\
&= 1 \text{ μg/ml}
\end{aligned}
$$
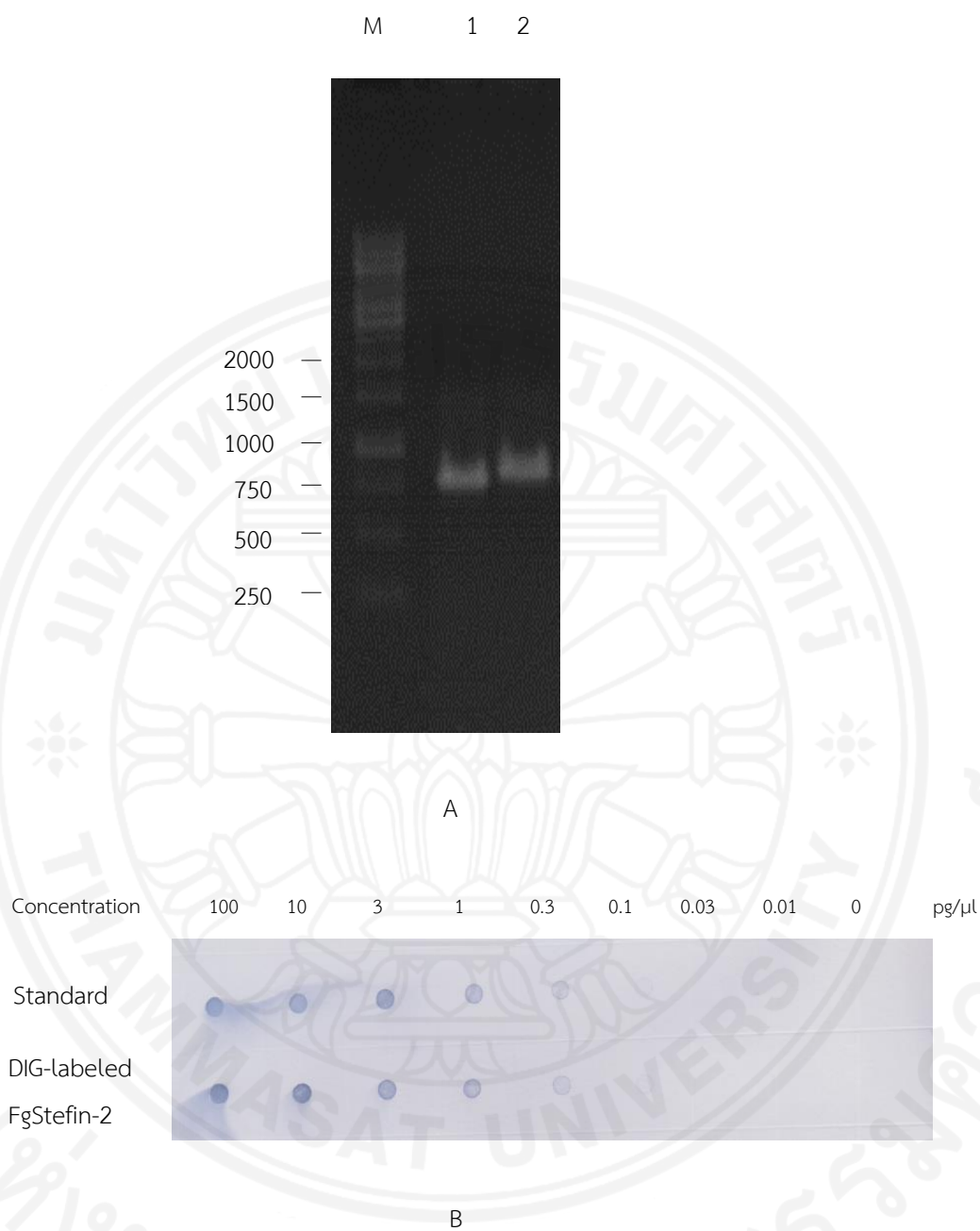
Figure 5.7 Analysis of the DIG-labeled DNA probe used for Southern hybridization. Panel A: Agarose gel electrophoresis of amplified FgStefin-2 cDNA fragment. Lane 1: unlabeled cDNA fragment, lane 2: DIG-labeled cDNA fragment. Lane M: 1 kb DNA ladder (Thermo Scientific, Lithuania). Panel B: Spot assay of DIG-labeled FgStefin-2 cDNA fragment.
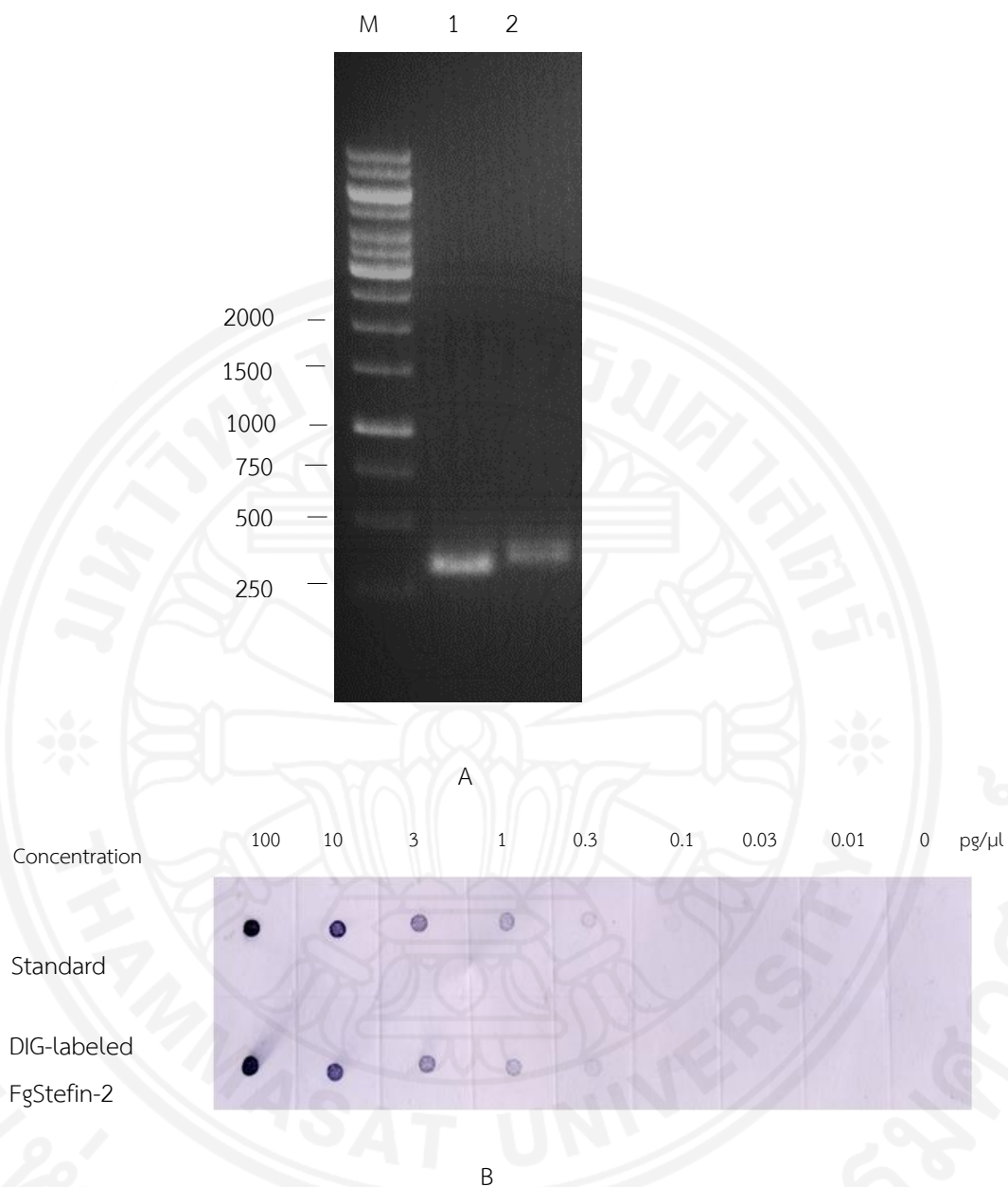
Figure 5.8 Analysis of the DIG-labeled DNA probe used for Northern hybridization. Panel A: Agarose gel electrophoresis of amplified FgStefin-2 cDNA fragment. Lane 1: unlabeled cDNA fragment, lane 2: DIG-labeled cDNA fragment. Lane M: 1 kb DNA ladder (Thermo Scientific, Lithuania). Panel B: Spot assay of DIG-labeled FgStefin-2 cDNA fragment.

5.2.2 Southern analysis hybridization of genomic DNA from adult *F. gigantica*

Genomic DNA was extracted from adult *F. gigantica* and digested separately with restriction endonucleases *Bam*H I (B), *Hin*d III (H), and *Bam*H I/*Hin*d III (B/H). The products were size-separated by 0.7% agarose gel electrophoresis in TBE buffer including ethidium bromide (0.5 µg/ml) and transferred to a nylon membrane and hybridized with a DIG-labeled FgStefin-2 DNA probe. Several hybridizing fragments were detected in the *F. gigantica* genomic DNA at sizes of 10.81 kb in lane 1, 8.09 and 10.96 kb in lane 2 and 8.57, 3.71 and 10.96 kb in lane 3 (**Figure 5.9**). The sizes of these fragments were calculated based on the standard curve created from the λ DNA double-digested with *Eco*R I/*Hin*d III standard marker.

5.2.3 Northern hybridization analysis

Northern hybridization analysis was performed to investigate the presence and size of FgStefin-2 transcripts in adult *F. gigantica*. Total RNA extracted from adult parasites (as described in **Section 4.2.3**) was size-separated in a 1.2% agarose gel containing 2.2 M formaldehyde. After electrophoresis, the total RNA was transferred to a nylon membrane by capillary transfer and hybridized with a DIG-labeled FgStefin-2 DNA probe. A single hybridization signal was detected at an approximate size of 1,000 nucleotides (**Figure 5.10**).
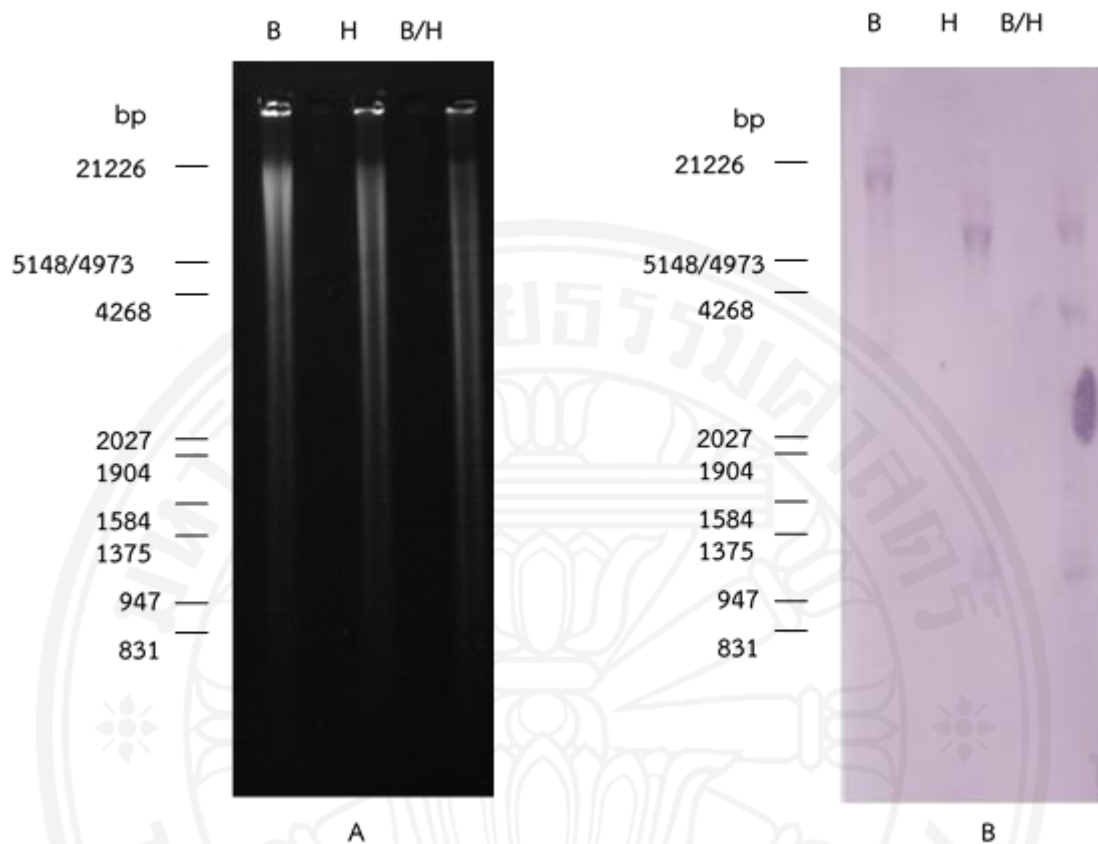
Figure 5.9 Southern hybridization analysis. Panel A: Agarose gel electrophoresis of *F. gigantica* genomic DNA digested with *Bam*H I (B), *Hin*d III (H), and *Bam*H I/*Hin*d III (B/H). Panel B: Nylon membrane showing the presence of hybridizing DNA fragments in the *F. gigantica* genome after detection with the FgStefin-2 probe. Positions and sizes of λ *Eco*R I/*Hin*d III standard marker fragments (Thermo Scientific, Lithuania) are indicated at the left.
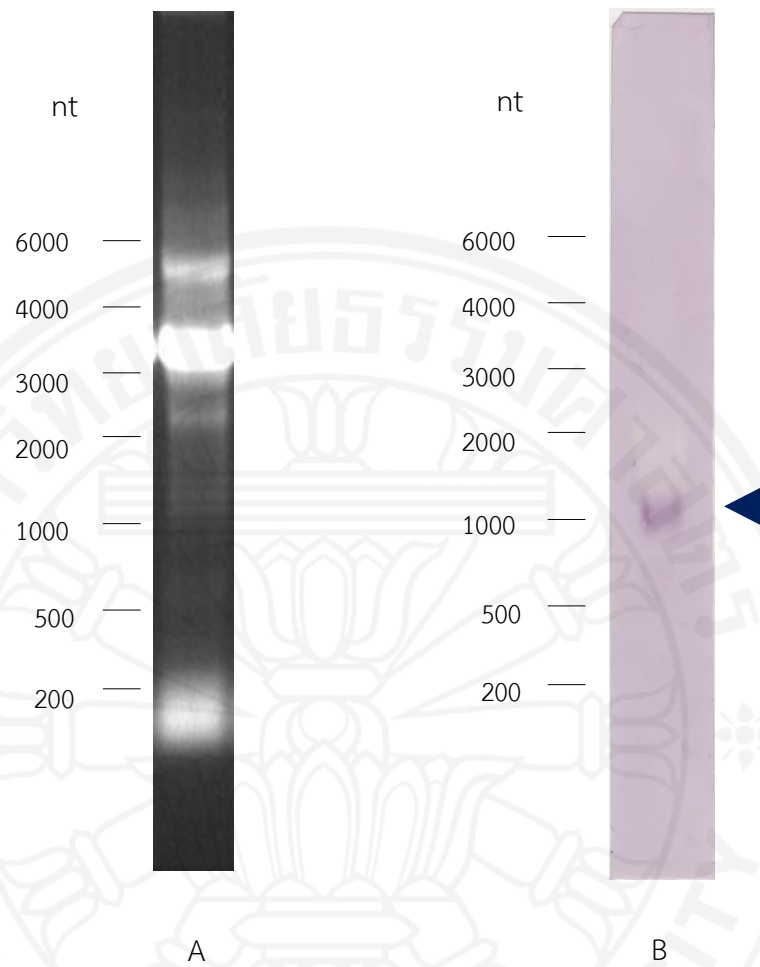
Figure 5.10 Northern hybridization analysis. Panel A: formaldehyde denaturing agarose gel electrophoresis of 50 µg total RNA. Panel B: Northern hybridization of the membrane-bound total RNA with the DIG-labeled FgStefin-2 DNA probe detected a product (arrowhead) at approximately 1,000 nucleotides size. Positions and fragment sizes of the RiboRuler™ High range RNA Ladder (Thermo Scientific, Lithuania) standard marker are indicated at the left.

5.2.4 Stage-specific reverse transcriptase polymerase chain reaction (RT-PCR)

The presence of FgStefin-2 during development was investigated by RT-PCR. This method was used to detect its transcript in various stages. Total RNA was isolated from different stages (newly excysted juveniles, 2-, 4-, 6-week-old juveniles and adult parasites), reverse transcribed, and the FgStefin-2 cDNA amplified with FgStefin-2 specific primers (**Section 4.2.7**). The RT-PCR products were size separated by 0.7% agarose gel electrophoresis and visualized by ethidium bromide staining. FgStefin-2 cDNA fragments were obtained from all developmental stages of the parasite (**Figure 5.11**) suggesting that FgStefin-2 is transcribed in NEJ, immature and mature parasites.
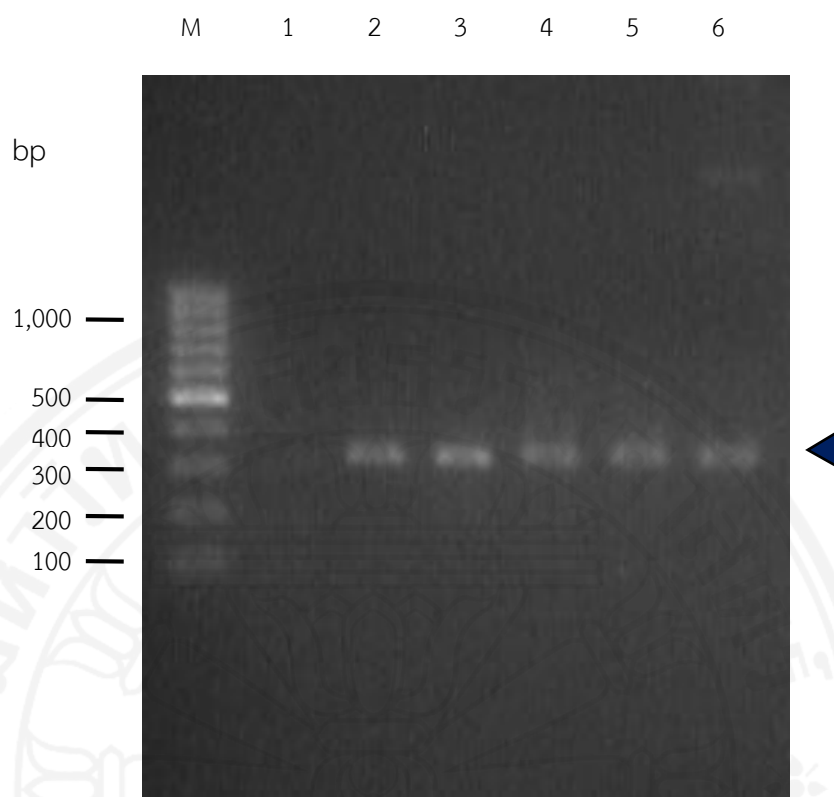
Figure 5.11 Agarose gel electrophoresis showing the FgStefin-2 RT-PCR products (arrowhead) obtained from different stages of *F. gigantica* with FgStefin-2-specific primers. Lane 1: negative control without RNA template, lane 2: newly excysted juveniles, lane 3: 2-week-old juveniles, lane 4: 4-week-old juveniles, lane 5: 6-week-old juveniles and lane 6: adult parasites. Lane M: GeneRuler™ 100 bp DNA ladder (Thermo Scientific, Lithuania).

5.3 Preparation of recombinant FgStefin-2 (rFgStefin-2) and mouse polyclonal antibody against rFgStefin-2

   5.3.1 Subcloning of the FgStefin-2 coding sequence into the expression vector pQE-30 and introduction of the recombinant plasmid into the *E. coli* M15 expression host

    The 288 bp cDNA fragment encoding FgStefin-2 was amplified with specific primers as described in **Section 4.3.1** containing recognition sizes for restriction endonucleases *Bam*H I and *Pst* I at the 5′ and 3′ end, respectively. The PCR product was resolved on a 0.7% agarose gel and then extracted from the gel as described in **Section 4.1.1.3** (**Figure 5.12**). The purified PCR product was firstly inserted into pGEM®-T Easy and the resulting recombinant plasmid introduced into *E. coli* XL-1 blue. Positive transformants were verified by sequence determination of the FgStefin-2 cDNA fragment using the service of 1st base Pte Ltd, Singapore. The pGEM®-T Easy-FgStefin-2 and pQE30 expression vector were digested with restriction endonucleases *Bam*H I and *Pst* I and resolved by 0.7% agarose gel electrophoresis. The linearized pQE30 DNA and FgStefin-2 coding DNA were extracted from the gel, combined by ligation, and introduced into *E. coli* M15. Eleven transformants were checked for pQE30 carrying the FgStefin-2 insert by direct colony PCR using the specific primers as above. All of the clones contained the FgStefin-2 cDNA insert (**Figure 5.13**).
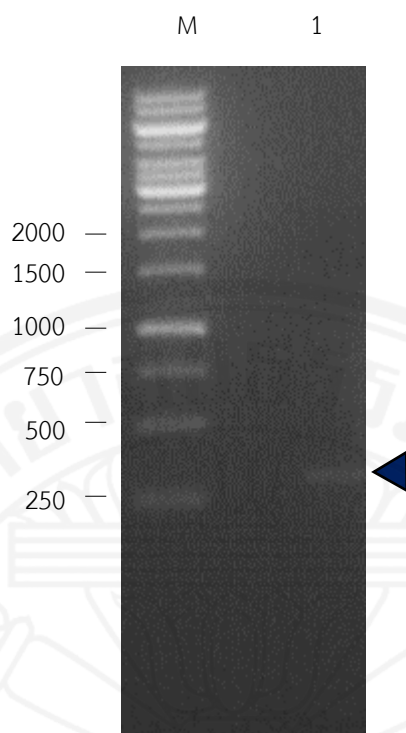
Figure 5.12 Agarose gel electrophoresis of FgStefin-2 PCR product. Lane 1: PCR product after extracted from the gel. Lane M: 1 kb DNA ladder (Thermo Scientific, Lithuania). The position of FgStefin-2 is indicated by an arrowhead.
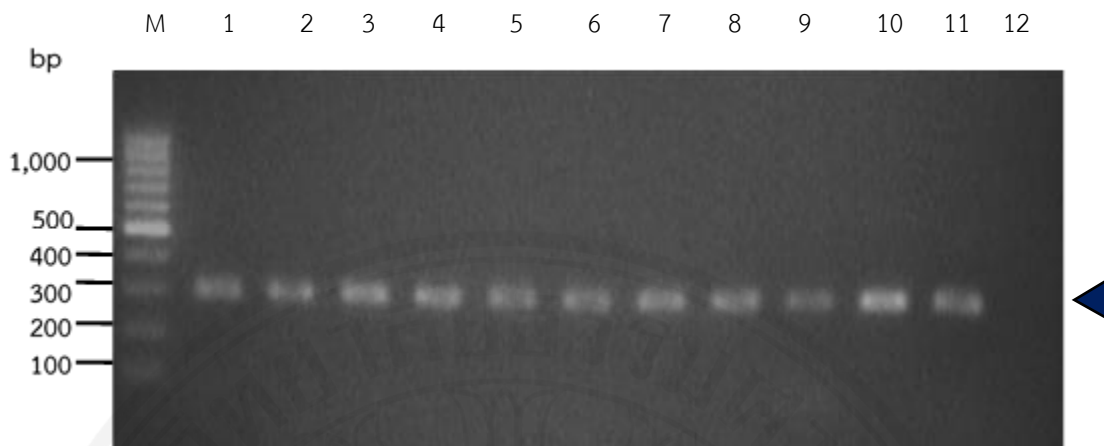
Figure 5.13 Agarose gel electrophoresis of direct colony PCR products obtained from the tested transformant *E. coli* carrying pQE30-FgStefin-2 with FgStefin-2 primers. Lanes: 1-11: PCR products of eleven transformants, lane 12: negative control without template. Lane M: GeneRuler™ 100 bp DNA ladder (Thermo Scientific, Lithuania). The position of FgStefin-2 is indicated by an arrowhead.

5.3.2 Expression and purification of recombinant FgStefin-2 protein in *E. coli* M15

Recombinant FgStefin-2 was expressed in transformant *E. coli* M15 carrying pQE30-FgStefin-2. Transformant bacterial cells were grown in LB medium for several hours until an OD_{600} of 0.6 had been reached and induced with 1mM IPTG to stimulate expression of rFgStefin-2. The culture samples were collected at 0 (non-induced control), 1, 2, 3 and 4 h to determine the time point with highest amount of recombinant protein expression. Total bacterial proteins were extracted from all samples and resolved on 12.5% SDS-PAGE and visualized by 0.025% Coomassie Blue R-250 staining. The results showed that the protein was highly expressed at 4 h after induction. During the observation time, the amount of protein was steadily increasing following induction (**Figure 5.14**).

The solubility of rFgStefin-2 was tested by protein extraction from transformant bacteria in native lysis buffer (soluble protein) and denaturing lysis buffer (insoluble protein). The protein fractions were resolved by 12.5% SDS-PAGE and stained with 0.025% Coomassie Blue R-250. The recombinant FgStefin-2 was found in the soluble and the insoluble protein fraction (**Figure 5.15**). The expression results suggested that rFgStefin-2 could be expressed in the prokaryotic expression system pQE30/*E. coli* M15.

Following time-course and solubility analyses a large scale expression of recombinant FgStefin-2 was performed and the expressed protein was purified by using Ni-NTA affinity chromatography (QIAGEN, Germany) under native conditions. The collected protein fractions were analyzed by 12.5% SDS-PAGE and Coomassie Brilliant Blue R-250 staining. Purified rFgStefin-2 was present in fractions E1 to E4 but most abundant in fraction E2 with the expected molecular masses of 13 kDa (**Figure 5.16**). All of the eluted fractions were pooled and dialyzed against 10 mM PBS, pH 7.2 for further experiments.
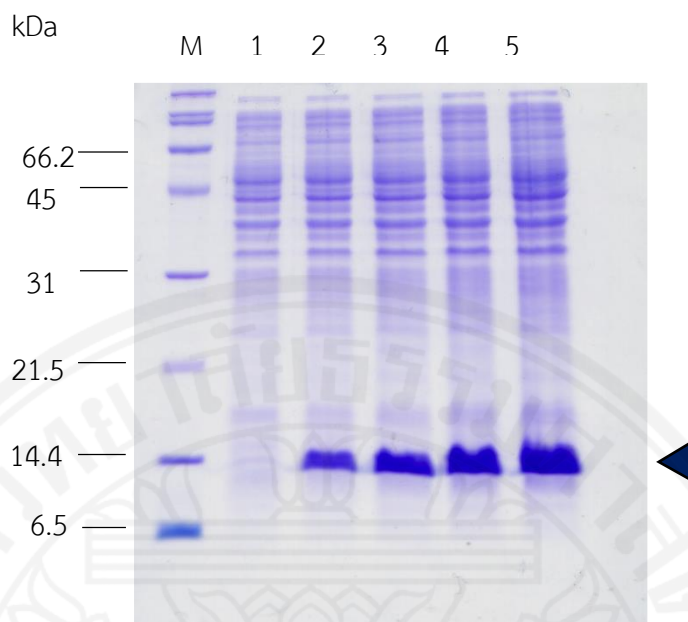
Figure 5.14 SDS-PAGE analysis of time-course analysis of rFgStefin-2 expression. Lane 1: 0 h = non-induced, lane 2-5: after induction with IPTG for 1 h, 2 h, 3 h and 4 h, respectively. Lane M: broad range protein standard marker (Bio-Rad, USA). The position of rFgStefin-2 is indicated by an arrowhead.
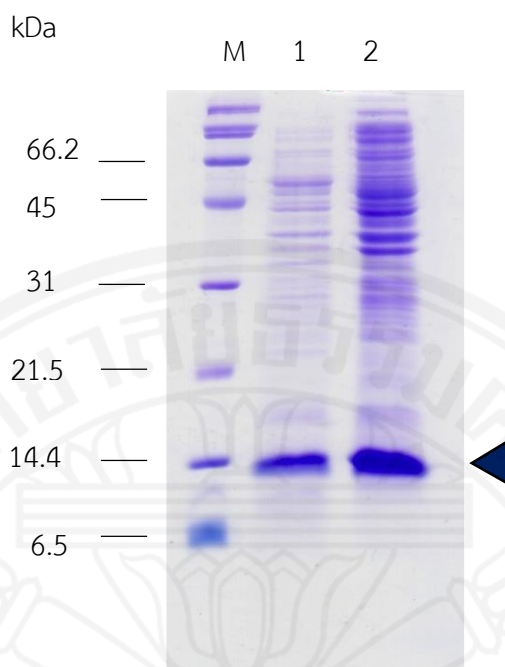
Figure 5.15 SDS-PAGE analysis of protein solubility shows that rFgStefin-2 is expressed in soluble and insoluble form. Lane: 1 soluble protein, Lane 2: insoluble protein. Lane M: broad range protein standard marker (Bio-Rad, USA). The position of rFgStefin-2 is indicated by an arrowhead.
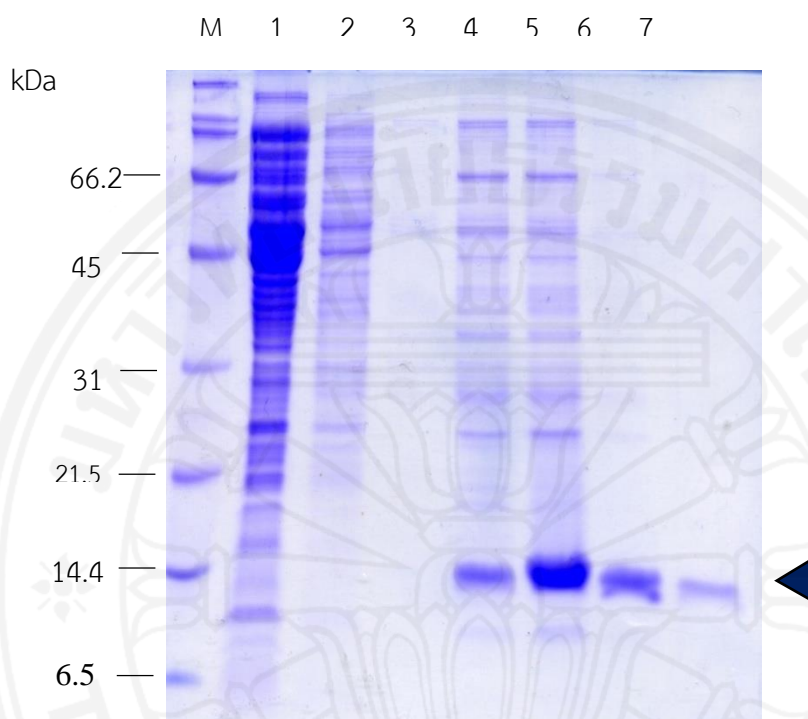
Figure 5.16 SDS-PAGE of rFgStefin-2 purified under native conditions. Lane 1: flow through fraction, lane 2, 3: wash fractions, lane 4-7: elution fractions. Lane M: broad range protein standard marker (Bio-Rad, USA). Purified rFgStefin-2 was most abundant in the E2 elution fraction and migrated in SDS-PAGE at the expected mass of approximately 13 kDa. Lane M: broad range protein standard marker (Bio-Rad, USA). The position of rFgStefin-2 is indicated by an arrowhead.

5.3.3 Production of polyclonal antibodies against rFgStefin-2

The anti-rFgStefin-2 antibodies were produced by immunization of three female BALB/c mice with 10 µg gel-embedded rFgStefin-2. Serum samples were collected before immunization (pre-immune serum) and after immunization (priming, 1st boost and 2nd boost serum). The polyclonal antibodies were analyzed by indirect ELISA against rFgStefin-2 to test the specificity and titer as described in **Section 4.3.7.2**. Antibody titers of 1st boost and 2nd boost sera were found to be increased in all mice (**Figure 5.17**). The polyclonal antibodies were stored at −20°C and used for immunological detection, e.g. immunohistochemistry, western analyses.

OD.492
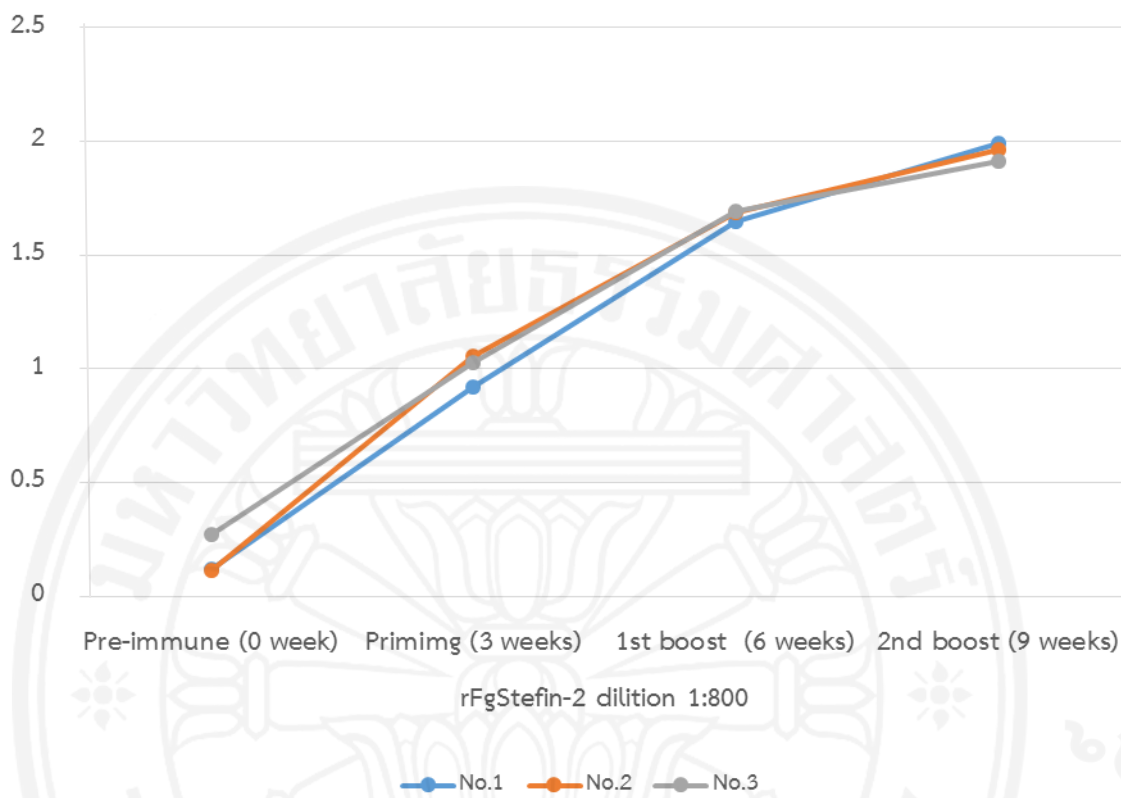
Figure 5.17 Indirect ELISA of immune responses in 3 BALB/c mice immunized with rFgStefin-2. The blue, orange and gray lines indicate the absorbance values from mouse number 1, 2 and 3, respectively.

5.4 Western blot analysis

    5.4.1 **Western blot analysis of mouse anti-rFgStefin-2 antisera against rFgStefin-2, CW extract and ES product**

Excretory/secretory product (ES products), crude worm extract (CW) and rFgStefin-2 were prepared as described in **Section 4.4.1** and resolved on 12.5% SDS-PAGE. All fractions were transferred onto a nitrocellulose membrane by semi-dry transfer and the membrane was probed with the anti-rFgStefin-2 antisera (1:1,000) as described in **Sections 4.4.2.1** and **4.2.2.2**. Western blot analysis showed that the mouse anti-rFgStefin-2 antisera reacted specifically rFgStefin-2 and with antigens in CW extract, ES product at the expected molecular mass of native FgStefin-2 (**Figure 5.18**).

    5.4.2 **Cross reactivity of mouse anti-rFgStefin-2 antisera against rFgStefin-1, multi-domain cystatin (FgMDC) and crude worm extracts of other trematodes**

The mouse anti-rFgStefin-2 antisera were tested for cross reactivity with rFgStefin-1, multi-domain cystatin and crude worm extracts of other trematodes (*Opisthorchis viverrini*, *Paramphistomum* spp., *Eurytrema pancreaticum*, *Schistosoma mansoni*, and *Fischoederius elongates*) by western blot analysis. Crude worm extract of *Fasciola gigantica* and rFgStefin-2 was used as a positive control. In the western blot analysis the antisera (1:1,000) did not cross-react with rFgStefin-1, multi-domain cystatin and CW extracts from other trematodes but specifically detected rFgStefin-2 and CW extract from *F. gigantica* at the expected mass of approximately 13 kDa (**Figures 5.19** and **5.20**).
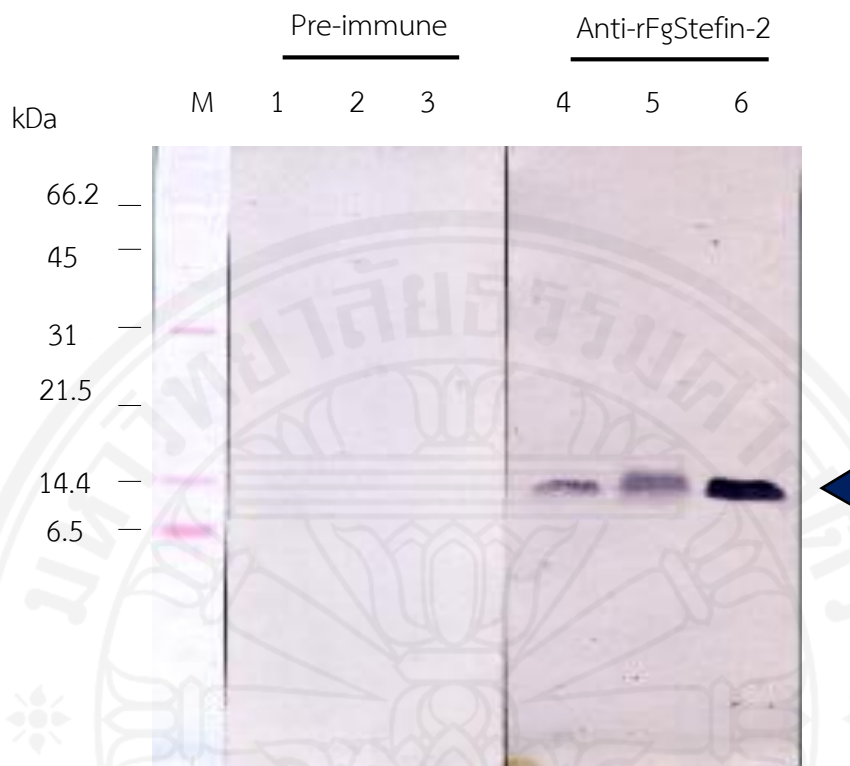
Figure 5.18 Western blot analysis of CW extract, ES product and rFgStefin-2 with mouse preimmune serum or anti-rFgStefin-2 antiserum (1:1,000) as indicated on the top. Lane 1, 4: 10 μg CW extract, lane 2, 5: 10 μg ES product and lane 3, 6: 100 ng rFgStefin-2. Lane M: broad range protein standard marker (Bio-Rad, USA). The position of rFgStefin-2 is indicated by the arrowhead.
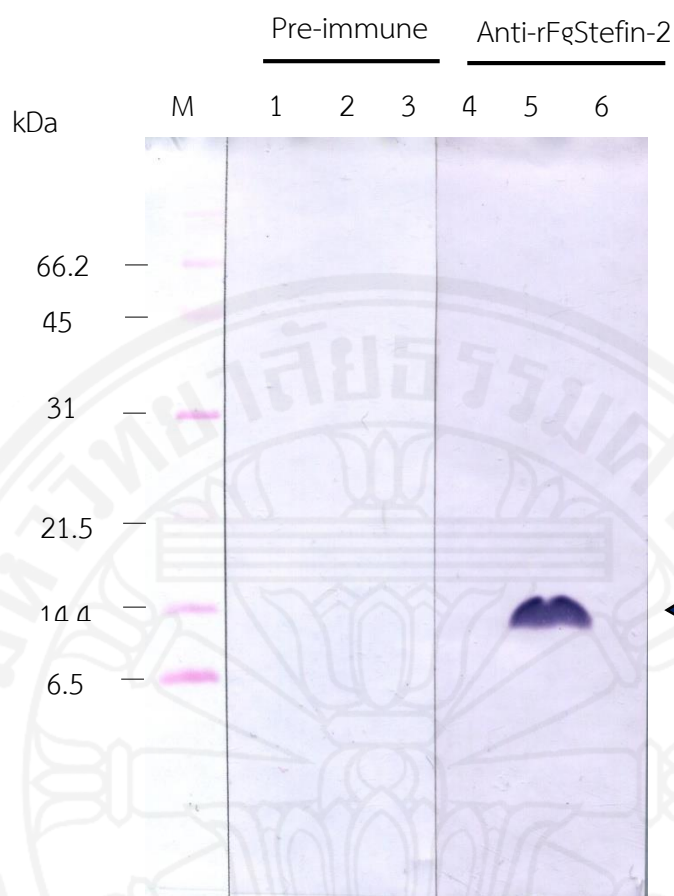
Figure 5.19 Western blot analysis of rFgStefin-1, rFgStefin-2 and multi-domain cystatin with mouse preimmune serum or anti-rFgStefin-1 antiserum (1:1,000) as indicated on the top. Lane 1, 4**:** 100 ng rFgStefin-1, lane 2, 5: 100 ng rFgStefin-2 and lane 3, 6: 100 ng multi-domain cystatin. Lane M: broad range protein standard marker (Bio-Rad, USA). The position of rFgStefin-2 is indicated by the arrowhead.
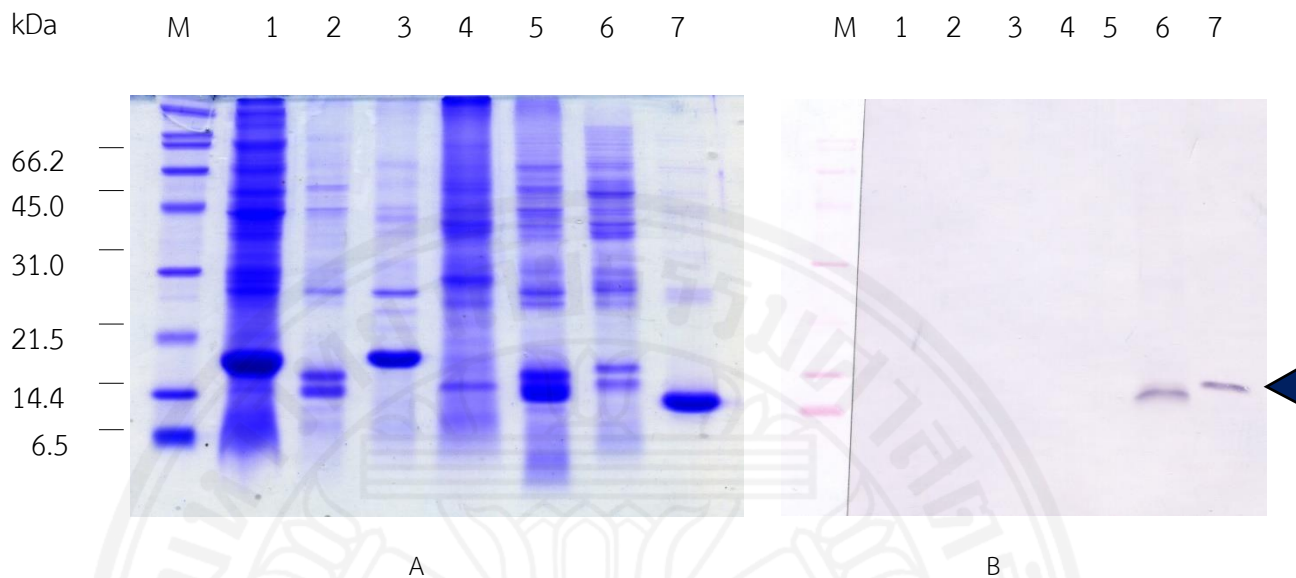
Figure 5.20 Cross-reactivity analysis of anti-rFgStefin-2 antiserum with CW extracts of other trematodes. Panel A: CW extracted of other trematodes and rFgStefin-2 were separated by SDS-PAGE and visualized by Coomassie Blue Staining; lane 1: *Opisthorchis viverrini*, lane 2: *Paramphistomum* spp., lane 3: *Eurytrema pancreaticum*, lane 4: *Schistosoma mansoni*, lane 5: *Fischoederius elongates*, lane 6: *F. gigantica* and lane 7: rFgStefin-2. Panel B: the blotted proteins were probed with anti-rFgStefin-2 antiserum. Lane M: broad range protein standard marker (Bio-Rad, USA). The position of rFgStefin-2 is indicated by an arrowhead.

5.5 Immunolocalization of FgStefin-2 in tissue sections of 2-, 4-week-old juveniles and adults *F. gigantica*

The polyclonal mouse anti-rFgStefin-2 antisera (diluted 1:400) was used to analyze the distribution of FgStefin-2 in 2-, 4-week-old juveniles and adult parasites by immunohistochemical detection. The native FgStefin-2 protein was localized in the intestinal epithelium in 2-, 4-week-old juveniles (**Figure 5.21**) and in adult parasites this protein was detected in several tissue types of the parasite including the prostate gland, gut epithelium and intrauterine eggs (**Figure 5.22**). This result indicates that FgStefin-2 is important for regulation of cysteine proteases in the digestive system and the reproductive system. Preimmune serum (diluted 1:400) was used as negative control and all tissue sections that were incubated with preimmune serum showed negative staining.
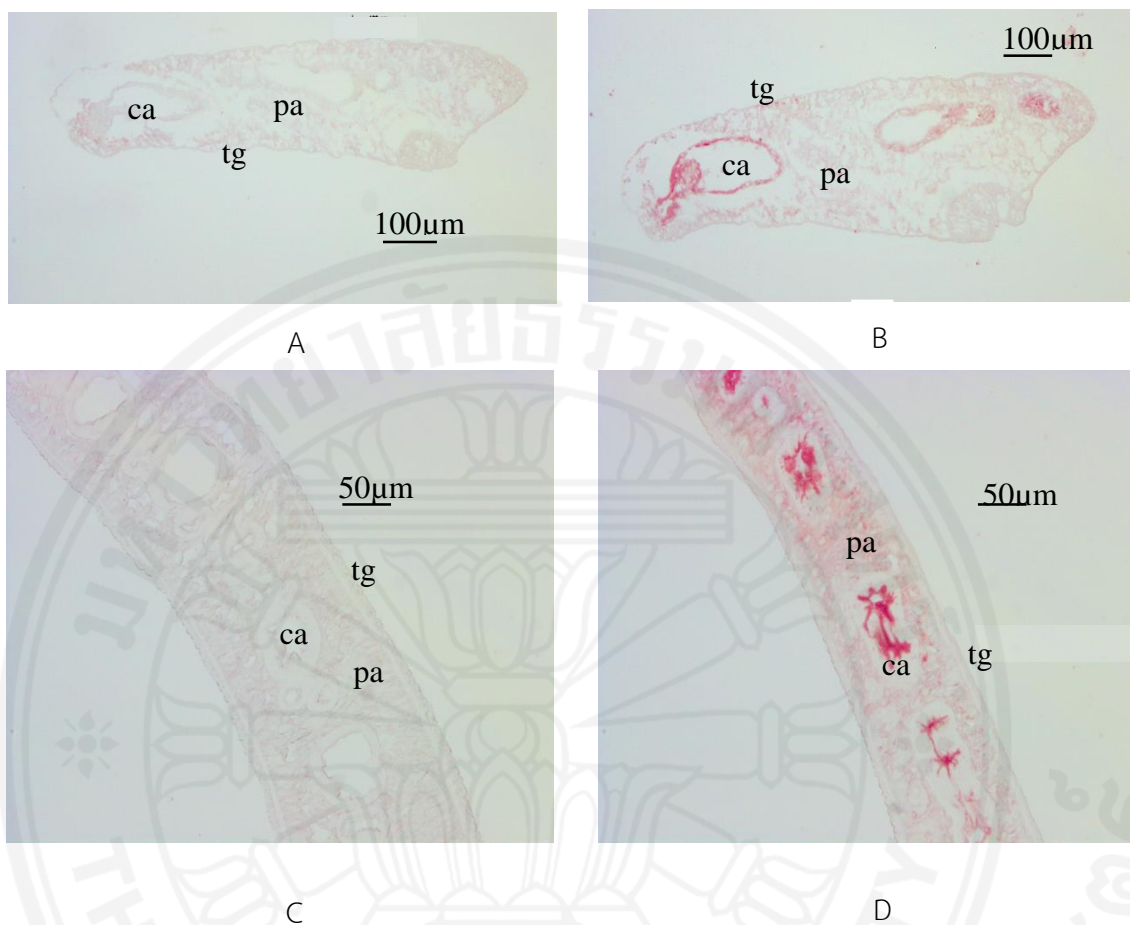
Figure 5.21 Immunohistochemical detection of FgStefin-2 in 2- and 4-week-old juveniles by mouse anti-rFgStefin-2 antiserum using AEC substrate (red color) for visualization. A, B: 2-week-old juvenile. C, D: 4-week-old juvenile. Mouse preimmune serum (negative control) was used in A and C and mouse anti-rFgStefin-2 antiserum was used in B and D. ca, cecum; pa, parenchyma and tg, tegument.
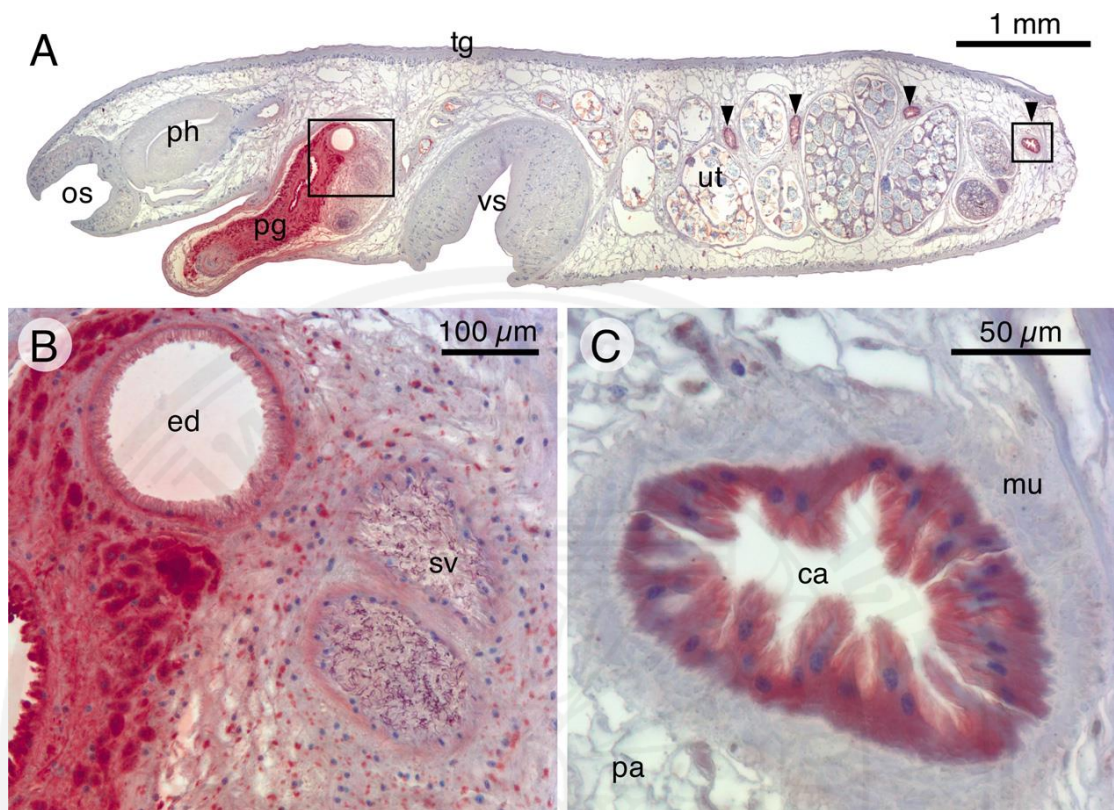
Figure 5.22 Immunohistochemical detection of FgStefin-2 in a sagittal section of the anterior region of adult *F. gigantica* by mouse anti-rFgStefin-2 antiserum using AEC substrate (red color) for visualization and hematoxylin (blue color) as counterstain. (A) Overview at low magnification. (B) Details at high magnification of the cirrus sac and (C) a cecum. ca, cecum; ed, ejaculatory duct; mu, muscle layers; os, oral sucker; pa, parenchyma; pg, prostate gland; ph, pharynx; sv, seminal vesicle; tg, tegument; ut, uterus and vs, ventral sucker.

5.6 Functional analysis of recombinant FgStefin-2

5.6.1 Determination of K_m values

The K_m value of bovine cathepsin B for the substrate Z-Arg-Arg-AMC was determined by measuring the reaction velocity at different substrate concentrations [S] from 0 to 512 μM at a fixed enzyme concentration. The data was analyzed by nonlinear regression with the Michaelis-Menten equation using GraphPad Prism 6.0 (**Figure 5.23**). The K_m value is shown in **Table 5.2**.
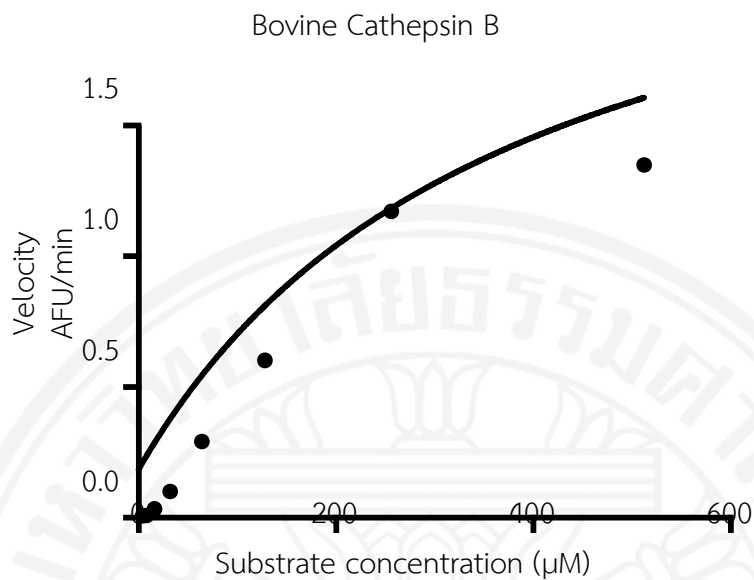
Bovine Cathepsin B

Figure 5.23 Substrate concentration versus initial velocity plots for cleavage of fluorogenic substrate, Z-Arg-Arg-AMC, by native bovine cathepsin B (1 ng).

Table 5.2 K_m values of bovine cathepsin B.

Protease	K_m (µM)
Bovine cathepsin B	375.9 ± 128.9

5.6.2 Determination of the inhibition coefficients (IC_{50})

The cysteine protease inhibitory profiles of rFgStefin-1, rFgStefin-2 and human cystatin C were investigated. The purified recombinant FgStefin-1 and FgStefin-2, and native human cystatin C were tested for inhibitory activity against native bovine cathepsins B and L and cysteine protease activity in adult *F. gigantica* ES product by incubation of the enzymes with increasing concentrations of the inhibitors and the activity was measured in the presence of fluorogenic substrates. The inhibition coefficients (IC_{50}) values for rFgStefin-2 against native bovine cathepsins B and L and *F. gigantica* ES product in comparison with rFgStefin-1 and human cystatin C are shown in **Figure 5.24**. In case of native bovine cathepsin L human cystatin C was slightly more effective while rFgStefin-1 and 2 showed similar inhibition curves. The enzyme inhibition by the three cystatins was hardly different for the parasite ES product, although rFgStefin-1, rFgStefin-2 were slightly more effective than human cystatin C. Significant differences of the inhibition curves were observed when the cystatins were tested with native bovine cathepsin B. The lowest IC_{50} value was observed for rFgStefin-2, followed by human cystatin C and finally rFgStefin-1. The IC_{50} values and substrate details are shown in **Table 5.3**. A higher IC_{50} value indicates a lower affinity of the inhibitor towards the enzyme.

Table 5.3 IC_{50} values of human cystatin C, *F. gigantica* Stefin-1 and Stefin-2 against bovine cathepsin L and B and parasite ES product.

Enzyme [ng/100μl]	Substrate (10 μM)	IC_{50} (95% confidence interval) [nm]		
		rFgStefin-1	rFgStefin-2	Human cystatin C
Bovine cathepsin B [1]	Z-Arg-Arg-AMC	775.2 (758.5–792.2)	178.8 (167.4–191.1)	482.8 (472.4–493.4)
Bovine cathepsin L [1]	Z-Phe-Arg-AMC	229.8 (226.7–232.9)	218.3 (214.8–221.9)	174.3 (170.1–178.6)
F. gigantica ES product [10]	Z-Phe-Arg-AMC	210.0 (206.6–213.5)	213.8 (211.0–216.6)	196.0 (193.1–198.9)
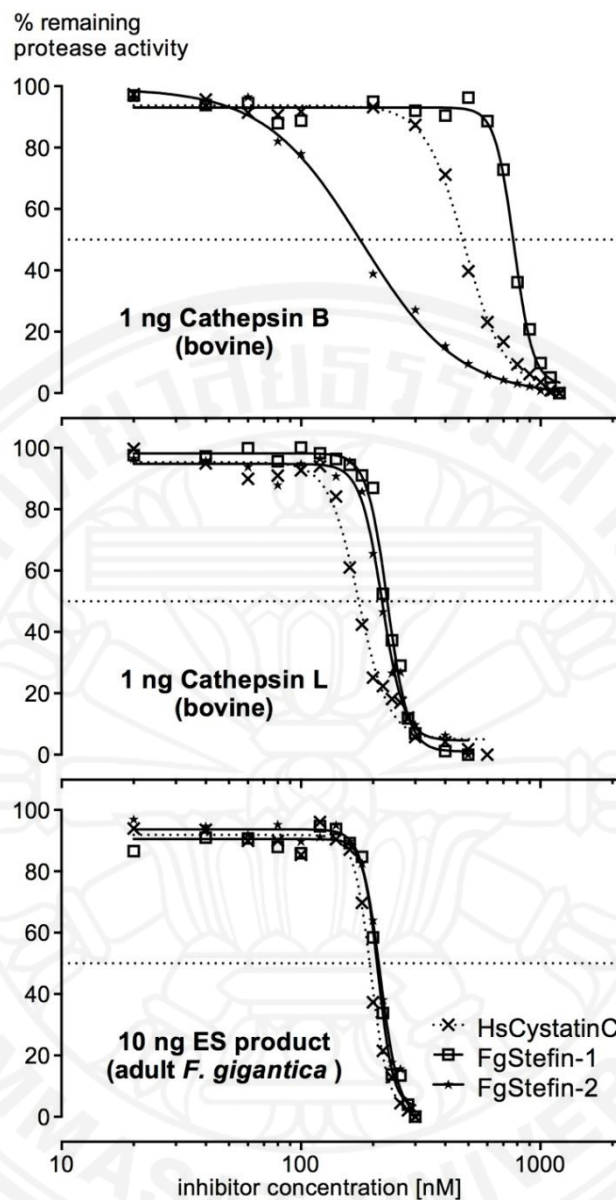
Figure 5.24 Inhibitory activity of rFgStefin-1, rFgStefin-2 and human cystatin C against bovine cathepsin B, L, and *F. gigantica* ES product. The IC_{50} values and substrate details are shown in **Table 5.3.**

5.6.3 Determination of the equilibrium inhibition constant (K_i)

The equilibrium inhibition constant (K_i) was calculated using the Morrison equation to determine the level of inhibition of bovine cathepsin B by rFgStefin-1, rFgStefin-2 and human cystatin C as described in **Section 4.6.1**. The recorded data was fitted using nonlinear regression and the Morrison equation for tight competitive binding at fixed concentrations of enzyme and substrate with varying concentrations of inhibitors. Each experiment was performed in triplicate with duplicate samples. The K_i values of rFgStefin-1, rFgStefin-2 and human cystatin C for bovine cathepsin B are shown in **Table 5.4**. It was found that rFgSteFin-2 had the lowest K_i value (56.6 nM), followed by human cystatin C (234.5 nM) and finally rFgStefin-1 (422.1 nM). The K_i values of the three cystatins for bovine cathepsin B supported the IC$_{50}$ results of the previous experiment.

Table 5.4 K_i values of rFgStefin-1, rFgStefin-2 and human cystatin C for bovine cathepsin B.

Inhibitor	K_i (95% confidence interval) [nm]
rFgStefin-1	422.1 (308.7–535.6)
rFgStefin-2	56.6 (43.9–69.4)
HsCystatin C	234.5 (174.9–294.1)

5.6.4 Zymography

Zymography is an electrophoretic technique used for detection of proteolytic activity in a sample by incubation of the gel-resolved sample with a substrate and observed proteolytic cleavage of the substrate. The inhibitory activity of rFgStefin-1 and rFgStefin-2 against gelatinolytic activity of adult stage ES product and CW extracts from metacercariae and adult parasites was determined. Adult stage ES product and CW extracts from metacercariae and adult parasites (2 μg/reaction) were incubated in assay buffer in the presence and absence of rFgStefin-1 and rFgStefin-2 and then separated by electrophoresis on a non-denaturing 10% polyacrylamide gel containing 0.1% gelatin substrate. The gel was subsequently stained with Coomassie Blue G-250 and the areas of digestion were determined. The results of the gelatinolytic activity showed that the inhibitory activity of rFgStefin-2 against the cysteine proteases in CW extract from metacercariae and adult parasites was higher than the one of rFgStefin-1 (**Figures 5.25** and **5.26**), but no difference was observed for rFgStefin-1 and rFgStefin-2 in inhibition of cysteine proteases in ES product (**Figure 5.27**).
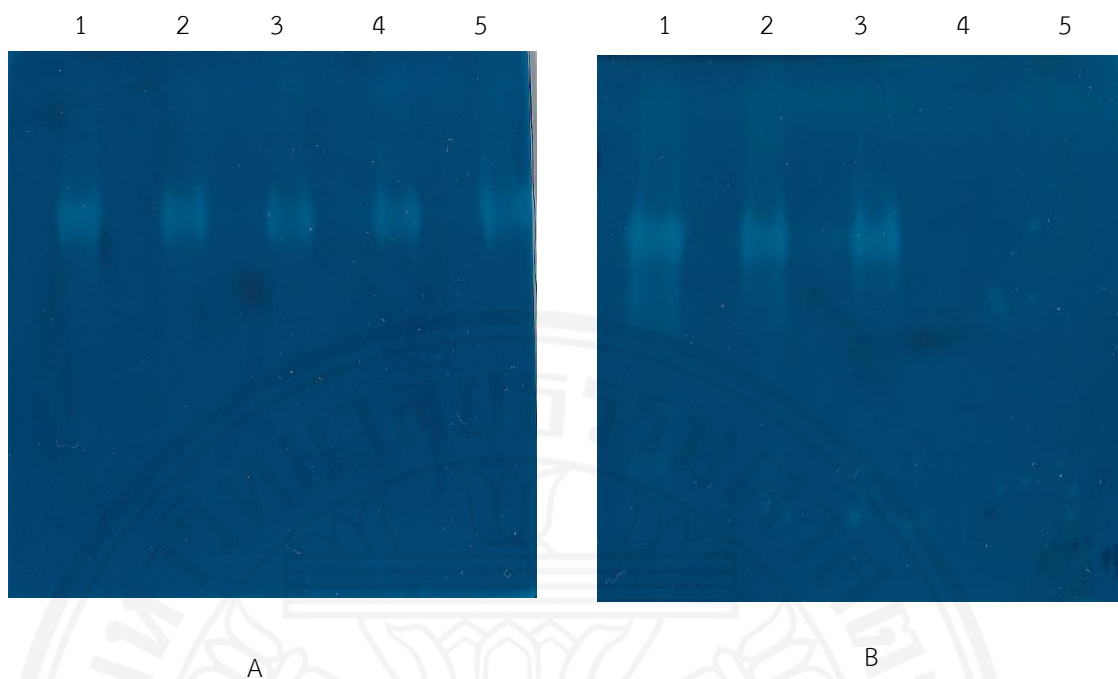
Figure 5.25 Analysis of the inhibitory activity of rFgStefin-1 and rFgStefin-2 with CW extract from metacercariae by zymography. Metacercariae CW extract (2 μg) was incubated in the absence and presence of rFgStefin-1 (Panel A) and rFgStefin-2 (Panel B) then separated on a non-denaturing polyacrylamide gel containing gelatin substrate. Lane 1: Metacercariae extract tested in the absence of inhibitors, lanes 2–5: metacercariae CW extract tested at different concentrations of inhibitors 1, 5, 10 and 20 μM, respectively. The gel was incubated overnight and then stained with Coomassie Blue G-250 to observe the gelatinolytic activity of metacercariae CW extract.
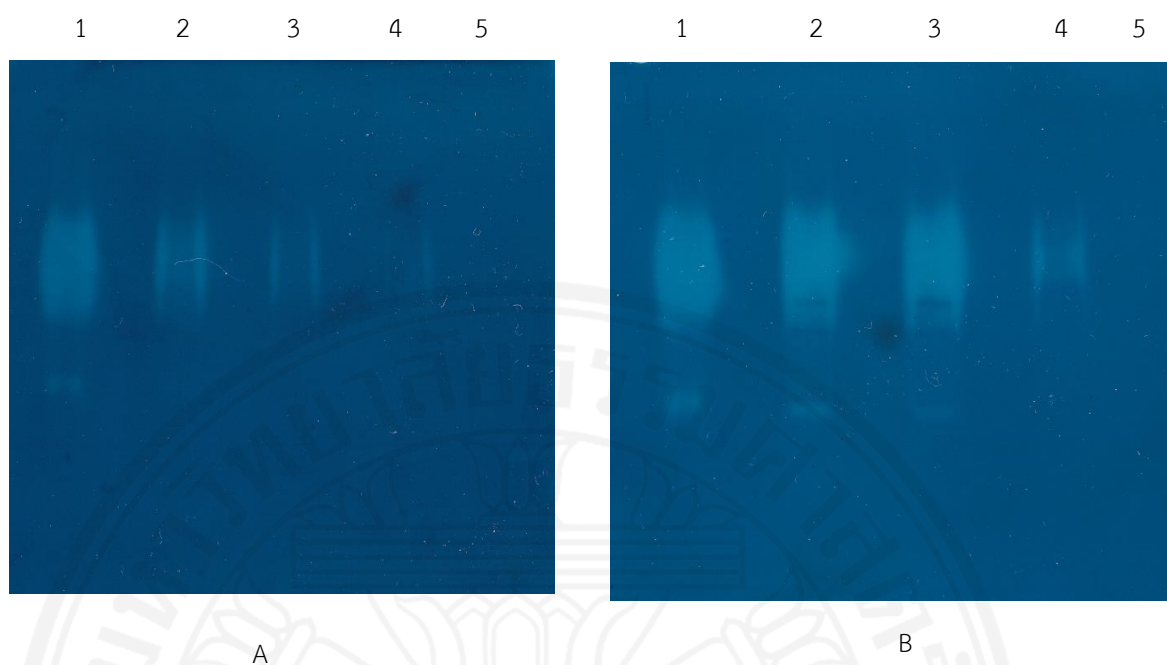
Figure 5.26 Analysis of the inhibitory activity of rFgStefin-1 and rFgStefin-2 with CW extract from adult parasites by zymography. Adult CW extract (2 μg) was incubated in the absence and presence of rFgStefin-1 (Panel A) and rFgStefin-2 (Panel B) then separated on a non-denaturing polyacrylamide gel containing gelatin substrate. Lane 1: Adult CW extract tested without inhibitors, lanes 2–5: adult CW extract tested at different concentrations of inhibitors 1, 5, 10 and 20 μM, respectively. The gel was incubated overnight and then stained with Coomassie Blue G-250 to observe the gelatinolytic activity of adult CW extract.
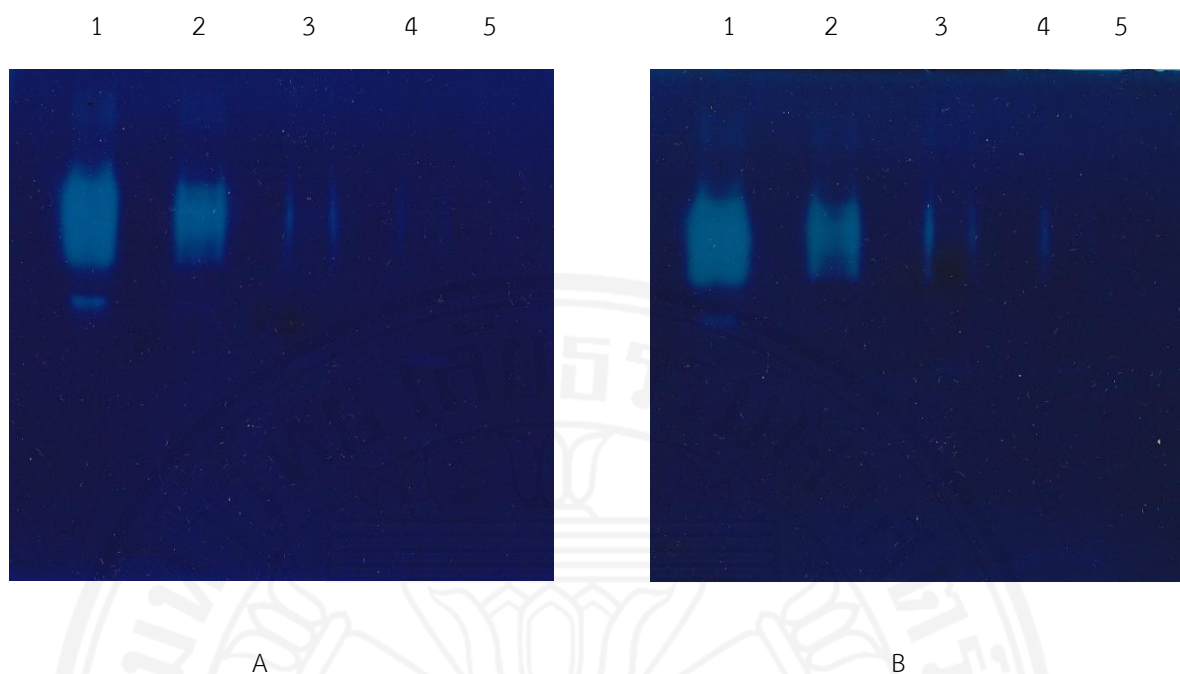
Figure 5.27 Analysis of the inhibitory activity of rFgStefin-1 and rFgStefin-2 with adult stage ES product by zymography. ES product (2 μg) was incubated in the absence and presence of rFgStefin-1 (Panel A) and rFgStefin-2 (Panel B) then separated on a non-denaturing polyacrylamide gel containing gelatin substrate. Lane 1: ES product tested without inhibitors, lanes 2–5: ES product tested at different concentrations of inhibitors 1, 5, 10 and 20 μM, respectively. The gel was incubated overnight and then stained with Coomassie Blue G-250 to observe the gelatinolytic activity of ES product.

5.6.5 pH dependency of recombinant FgStefin-2

The pH profile of rFgStefin-2 was evaluated by pre-incubating rFgStefin-2 in buffers of different pH values (pH 3.0–9.0) and then the remaining inhibitory activity against bovine cathepsin L (1 ng/100 µl) was determined. The result showed that rFgStefin-2 was stable in the pH range 3.0–9.0 and maintained over 95% inhibitory activity (**Figure 5.28**). Pre-incubation of rFgStefin-2 for 30 min at pH 3.0–9.0 had no effect on its inhibitory activity.

5.6.6 Temperature stability of recombinant FgStefin-2

The thermal stability of rFgStefin-2 was estimated using bovine cathepsin L (1 ng/100 µl) and rFgStefin-2 in 2× Cat-L buffer at 100℃ for 0–180 min. This result showed that rFgStefin-2 was stable at 100℃ and maintained over 85% activity from 0–180 min (**Figure 5.29**).
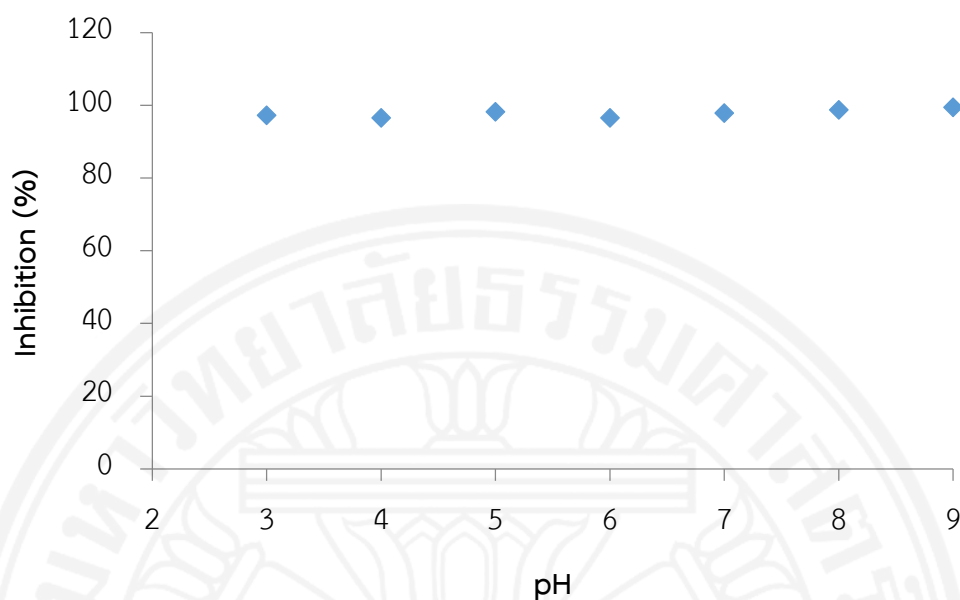
Figure 5.28 pH dependence assay. The remaining inhibitory activity (%) of rFgStefin-2 was analyzed against bovine cathepsin L (1 ng/100 µl) after pre-incubation in buffer pH 3.0–9.0 for 30 min.
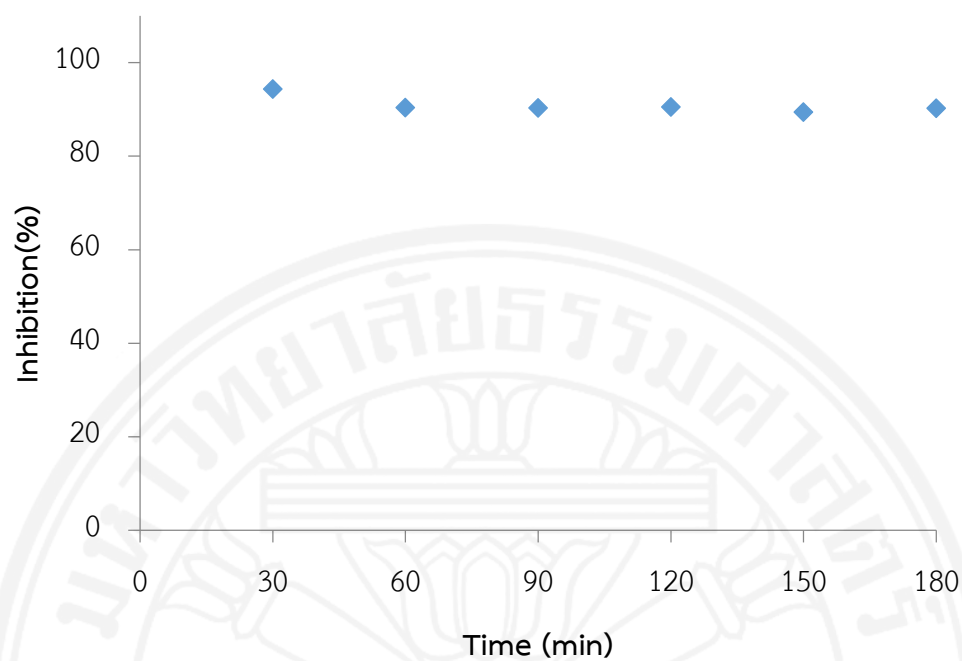
Figure 5.29 Temperature stability assay. The remaining inhibitory activity (%) of rFgStefin-2 was analyzed against bovine cathepsin L (1 ng/100 μl) after pre-incubation 100℃ for 0–180 min.

5.6.7 RT-PCR and western blot analysis of FgStefin1 and FgStefin-2 genes products in metacercariae and adult *F. gigantica*

Total RNA was isolated from metacercarial stage and adult parasites and then reverse transcribed with FgStefin-1, FgStefin-2-specific reverse primers. The RT-products were used as template with FgStefin-1 and FgStefin-2 primers in multiplex RT-PCR (**Section 4.6.7**). The RT-PCR products were size separated by 0.7% agarose gel electrophoresis and visualized by ethidium bromide staining. The 752 bp FgStefin-2 cDNA product was observed in all investigated stages of the parasite and the 333 bp FgStefin-1 cDNA product was observed at the adult stage but only weakly detected at the metacercarial stage (**Figure 5.30**).

Metacercarial, adult crude worm extract (CW) and excretory/secretory product (ES product) were prepared as described in **Section 4.4.1**. All fractions were resolved on 12.5% SDS-PAGE and electrotransferred to a nitrocellulose membrane by semi-dry blotting. Western blot analysis showed that the mouse anti-rFgStefin-2 antiserum reacted with native FgStefin-2 at the expected mass of about 13 kDa in the metacercarial extract, adult CW extract and ES product (**Figure 5.31B**) and anti-rFgStefin-1 antiserum reacted with native FgStefin-1 at the expected mass of 11–12 kDa in adult CW extract and ES product but only weakly in metacercarial extract (**Figure 5.31A**).

RT-PCR and immunoblots showed that the FgStefin-2 gene products were found to be more abundant in the metacercarial stage than the FgStefin-1 gene products.
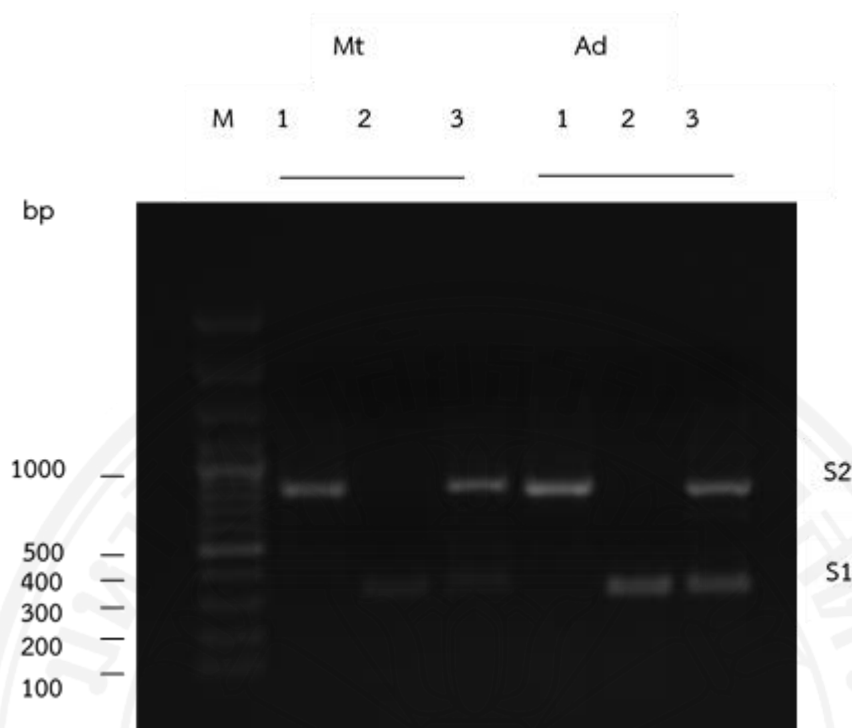
Figure 5.30 Agarose gel electrophoresis showing the resolved RT-PCR products of *F. gigantica* total RNA from metacercariae (Mt) and adults (Ad) by using FgStefin-2 primers (lane1), FgStefin-1 primers (lane 2), FgStefin-1 and 2 primers (multiplex RT-PCR, lane 3). S1: 333 bp FgStefin-1 product, S2: 752 bp FgStefin-2 product. Lane M: GeneRuler™ 100 bp DNA ladder (Thermo Scientific, Lithuania).
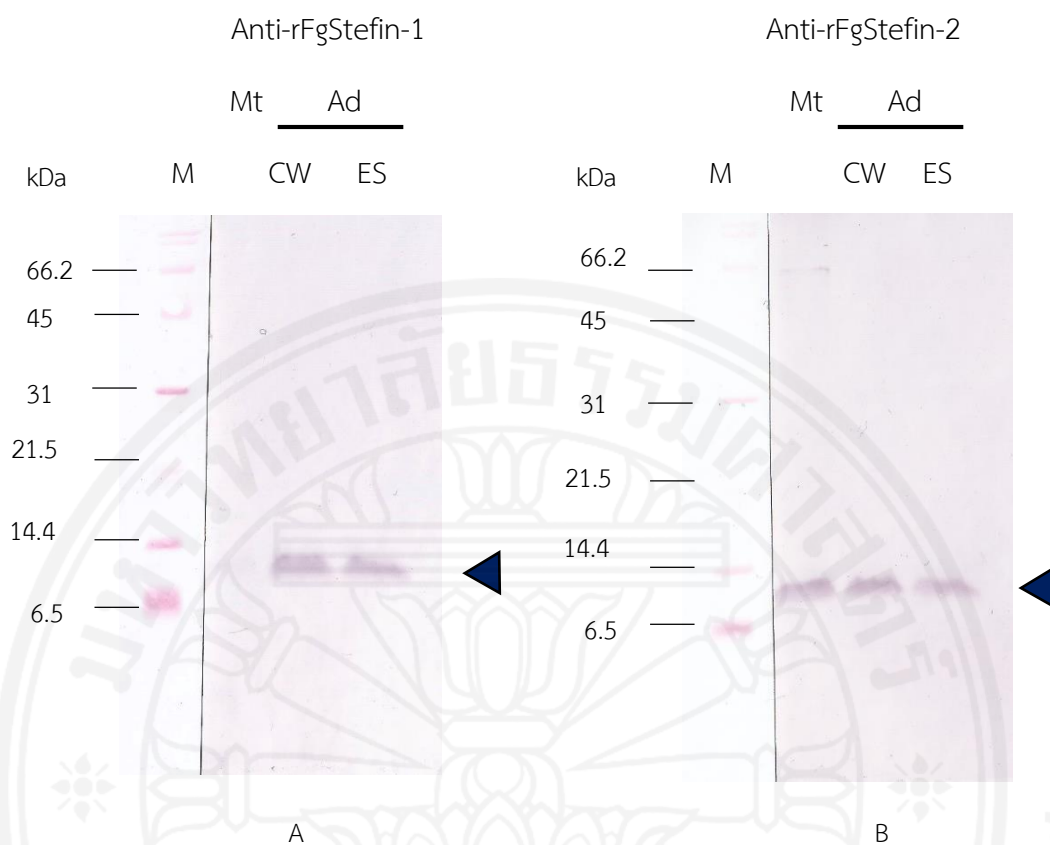
Figure 5.31 Western blot analysis of 2 μg each metacercarial extract, adult CW extract and ES product. Panel A: the blotted proteins were probed with anti-rFgStefin-1 antiserum. Panel B: the blotted proteins were probed with anti-rFgStefin-2 antiserum. Lane M: broad range protein standard marker (Bio-Rad, USA). The position of the rFgStefin-1 and rFgStefin-2 are indicated by an arrowhead.

5.6.8 Specific immune responses to FgStefin-1 and FgStefin-2 in sera of *F. gigantica*–infected mice

The pre-infection sera and 2-, 4-, 6-week post-infection sera of *F. gigantica*-infected mice (n=14) were tested for specific immune responses by indirect ELISA against rFgStefin-1 and rFgStefin-2. The absorbance values at OD_{492} of *F. gigantica*-infected sera against rFgStefin-1 and rFgStefin-2 were recorded and plotted (**Figure 5.32**). The results showed that a slightly higher reactivity towards rFgStefin-2 by the 4-, 6-week post-infection sera of *F. gigantica*-infected compared to rFgStefin-1.
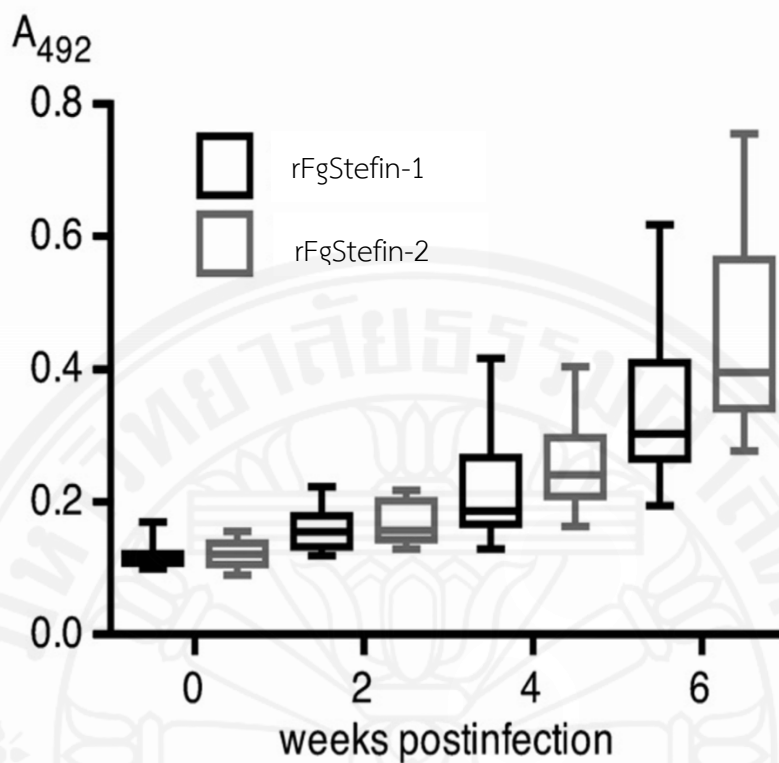
Figure 5.32 Box and whiskers graph showing the ELISA results obtained with mouse *F. gigantica*-infected sera (n=14) probed against rFgStefin-1 and rFgStefin-2. The boxes extend from the 25th to the 75th percentile and have a line at the median. The whiskers indicate highest and lowest values.

5.7 Analysis of immunomodulatory properties of recombinant FgStefin-2

5.7.1 Polyclonally stimulated proliferation of murine spleen cells

The effects of rFgStefin-1 and rFgStefin-2 on polyclonal T-cell proliferation from murine spleen cells were investigated. Spleen cells of native BALB/c mice were prepared as described in **Section 4.7.1**, cultured in 96-well flat-bottomed plates at a density of 3.5×10^5 cells/well and stimulated with concanavalin A in the presence of 0.2 to 0.5 µM rFgStefin-1 and rFgStefin-2. The plate was incubated at 37°C for 72 h. Proliferation of cells was quantified by MTT assay as described in **Section 4.7.3**. The result showed that rFgStefin-1 and rFgStefin-2 inhibited cellular proliferation by 40-61% and 30-63%, respectively at 0.2-0.5 µM of the concentrations (**Figure 5.33**). The data suggest that rFgStefin-1 and rFgStefin-2 had some effect on the polyclonally stimulated proliferation of BALB/c spleen cells.

5.7.2 Polyclonally stimulated proliferation of murine PBMC

The effect of rFgStefin-1 and rFgStefin-2 on polyclonal T-cell proliferation in murine peripheral blood mononuclear cells (PBMCs) was determined. PBMCs of native BALB/c mice were prepared as described in **Section 4.7.2**, cultured in 96-well flat-bottomed plates at a density of 3.5×10^5 cells/well and stimulated with concanavalin A in the presence of 0.2 to 0.5 µM rFgStefin-1 and rFgStefin-2. The plate was incubated at 37°C for 72 h and the proliferation of cells was quantified by MTT assay as described in **Section 4.7.3**. The result showed that rFgStefin-1 and rFgStefin-2 inhibited cellular proliferation by 25-50% and 21-50%, respectively at 0.2–0.5 µM concentration (**Figure 5.34**). The data suggest that rFgStefin-1 and rFgStefin-2 had some effect on the polyclonally stimulated proliferation of BALB/c PBMC cells.
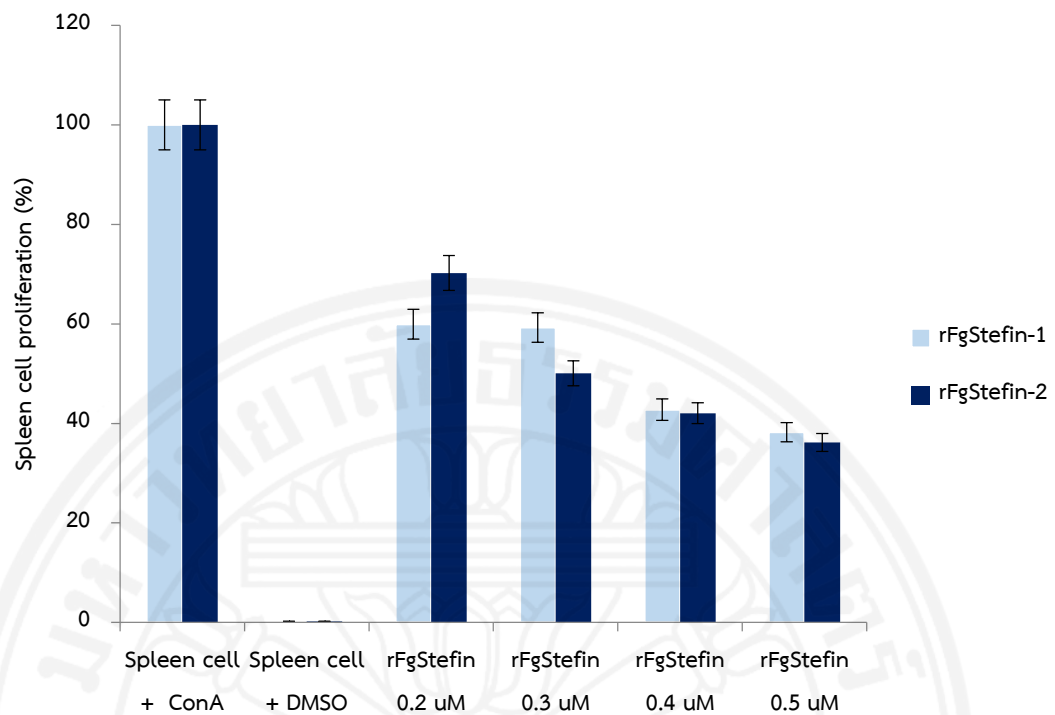
Figure 5.33 Mitogen-induced murine T-cell proliferation in the presence of rFgStefin-1 and rFgStefin-2. Concanavalin A (0.5 µg/ml)-stimulated proliferation of BALB/c spleen cells in the presence of 0.2 to 0.5 µM rFgStefin-1 and rFgStefin-2. Each bar represents the mean data of triplicate experiments obtained with 3.5×10^5 spleen cells from two mice. Proliferation of T-cells in the presence of only Con A was set at 100%. DMSO was used as the negative control.
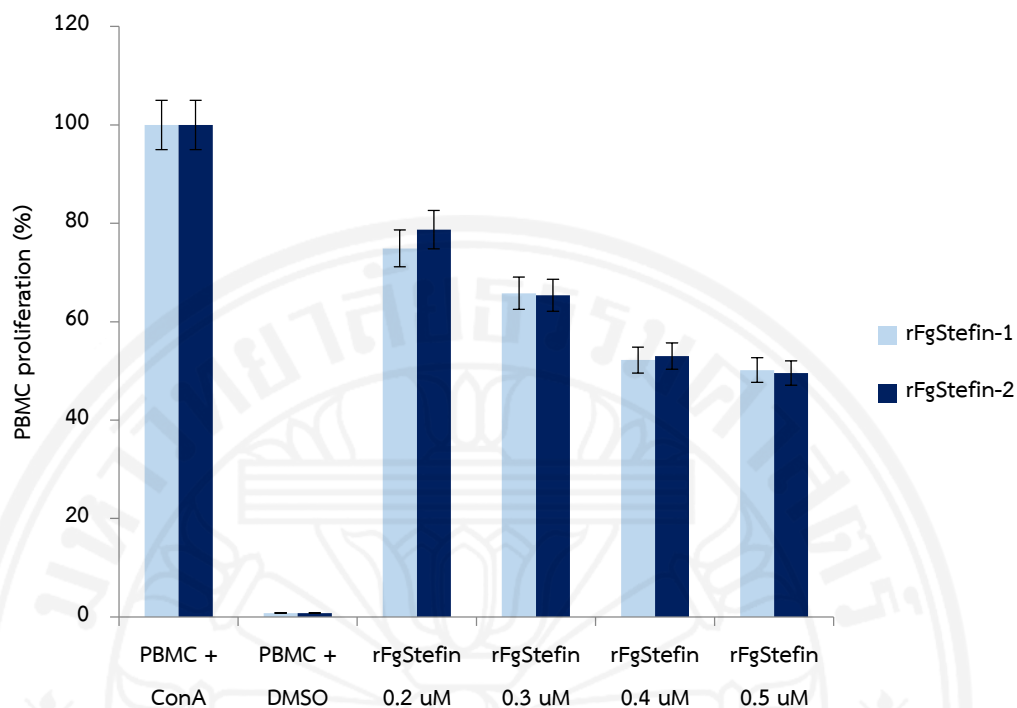
Figure 5.34 Mitogen-induced murine T-cell proliferation in the presence of rFgStefin-1 and rFgStefin-2. Concanavalin A (0.5 μg/ml)-stimulated proliferation of BALB/c PBMC cells in the presence of 0.2 to 0.5 μM rFgStefin-1 and rFgStefin-2. Each bar represents the mean data of triplicate experiments obtained with 3.5×10^5 spleen cells from three mice. Proliferation of T-cells in the presence of only Con A was set at 100%. DMSO was used as the negative control.

5.8 Expression and purification of recombinant *F. gigantica* cathepsin B5 (rFgCB5) in the yeast *Pichia pastoris* (strain X33)

  5.8.1 Cloning of FgCB5 encoding cDNA fragment into the eukaryotic expression vector pPicZαB and introduction into the yeast expression host *Pichia pastoris* (strain X33)

    The FgCB5 encoding cDNA fragment was amplified by PCR with specific primers carrying *Pst* I and *Xba* I restriction sites. The FgCB5 cDNA fragment was inserted into the *Pst* I and *Xba* I digested vector pPicZαB by ligation. The ligation product was used for transformation of *E. coli* Top10. Positive clones were checked by PCR, restriction analysis, and DNA sequencing. The plasmid DNA (pPicZαB-FgCB5) was linearized with *Sac* I and used for transformation of *Pichia pastoris* strain X33 by electroporation. Genomic DNA was extracted from eleven transformants and used as template for PCR to check the integration of FgCB5. The result showed that six of eleven clones contained a genomic FgCB5 insertion (**Figure 5.35**).

  5.8.2 Expression and purification of rFgCB5 in *Pichia pastoris* (strain X33)

    Culture medium was collected at 0, 12, 24, 48, 72 and 96 h and tested by western blot for a time point analysis of the expression of rFgCB5. The result showed that rFgCB5 was expressed at 72 and 96 h after induction (**Figure 5.36**). The recombinant protein was secreted into the yeast culture medium and purified by Ni-NTA affinity sepharose chromatography. The elution fraction containing soluble rFgCB5 was concentrated on a 3 kDa cut off filter column and dialyzed against 10 mM PBS, pH 7.2. In western blot analysis, the purified protein showed the expected molecular mass of approximately 39.2 kDa and was expressed without glycosylation at 100 ng protein/ml medium (**Figure 5.37**).

Figure 5.35 Agarose gel electrophoresis of direct colony PCR obtained from checked transformant *E. coli* carrying pPicZαB-FgCB5 with FgCB5 primers. Lanes: 1: negative control without template, lanes 2–12: PCR products of eleven transformants. Lane M: 1 kb DNA ladder (Thermo Scientific, Lithuania). The position of FgCB5 is indicated by an arrowhead.

Figure 5.36 Western blot analysis of rFgCB5 expression in *Pichia pastoris* (strain X33). Lane 1: 0 h (non-induced), lanes 2–6: after induction for 12 h, 24 h, 48 h, 72 h and 96h. Lane M: Broad range protein standard marker (Bio-Rad, USA). The position of rFgCB5 is indicated by an arrowhead.
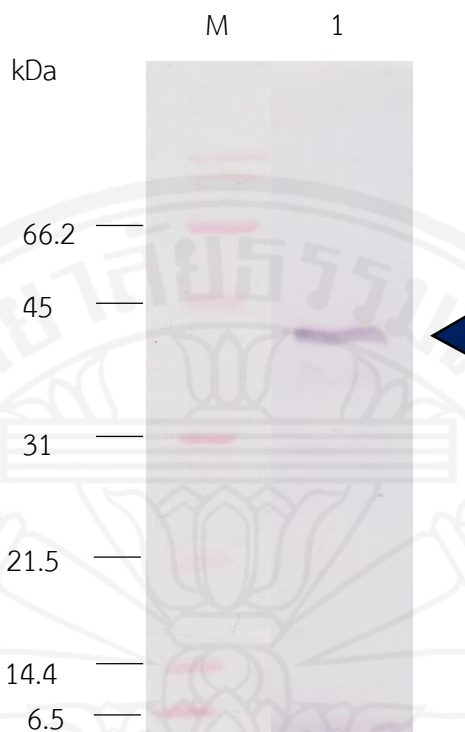
Figure 5.37 Western blot analysis of purified rFgCB5 after concentration and dialysis against 10 mM PBS, pH 7.2. Lane M: Broad range protein standard marker (Bio-Rad, USA), lane 1: purified rFgCB5. The position of rFgCB5 is indicated by an arrowhead.

5.9 Western blot analysis of mouse anti-rFgCB5 antisera against rFgCB5, CW extract and ES product

Excretory/secretory product (ES product), crude worm extract (CW) and rFgCB5 were prepared as described in **Section 4.4.1** and resolved on 12.5% SDS-PAGE. All fractions were transferred onto a nitrocellulose membrane by semi-dry transfer and the membrane was probed with the mouse anti-rFgCB5 antisera (1:100) as described in **Sections 4.4.2.1** and **4.2.2.2**. Western blot analysis showed that anti-rFgCB5 antiserum reacted with rFgCB5 at the expected mass of the recombinant proprotease at approximately 39.2 kDa (this includes the C-terminal myc-His-tag). In CW extract the antiserum detected a doublet of antigens migrating slightly faster than rFgCB5 at the approximate size of the native proprotease (36.4 kDa) and in the ES product of adult *F. gigantica* the antiserum detected very faintly an antigen migrating at the lower position of the CW extract doublet (**Figure 5.38**).
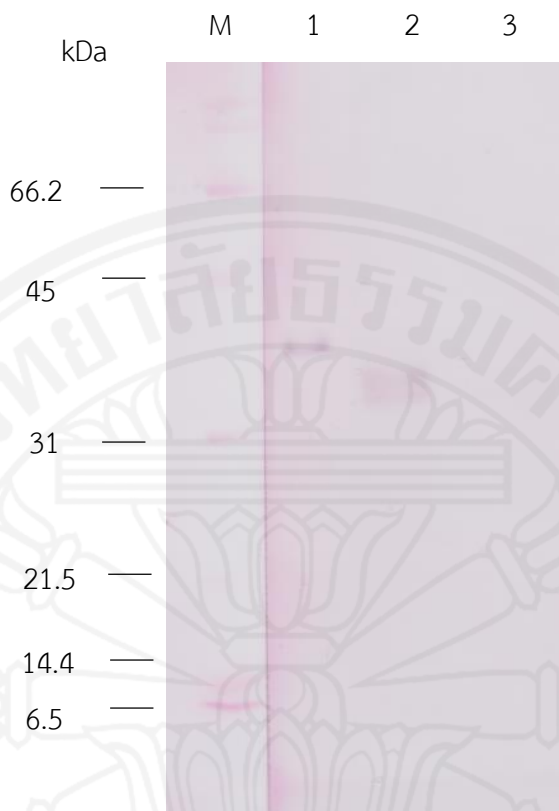
Figure 5.38 Western blot analysis of rFgCB5, CW extract and ES product with mouse anti-rFgCB5 antiserum (1:100). Lane 1: 100 ng rFgCB5, lane 2: 60 µg CW extract and lane 3: 60 µg ES product. Lane M: broad range protein standard marker (Bio-Rad, USA).

5.10 Specific immune responses of rFgCB5 in mouse *F. gigantica* – infected serum

The pre-infection sera and 2-, 4-, 6-week post-infection sera of *F. gigantica*-infected mice (n=10) were tested for specific immune responses by indirect ELISA against yeast-expressed rFgCB5. The absorbance values at OD_{492} of *F. gigantica*-infected sera against rFgCB5 were recorded and plotted (**Figure 5.39**). The results showed that the sera of *F. gigantica*-infected mice 4-, 6-week postinfection were significantly different from the pre-infection sera with the 6-week postinfection sera again significantly different from the 4-week sera.
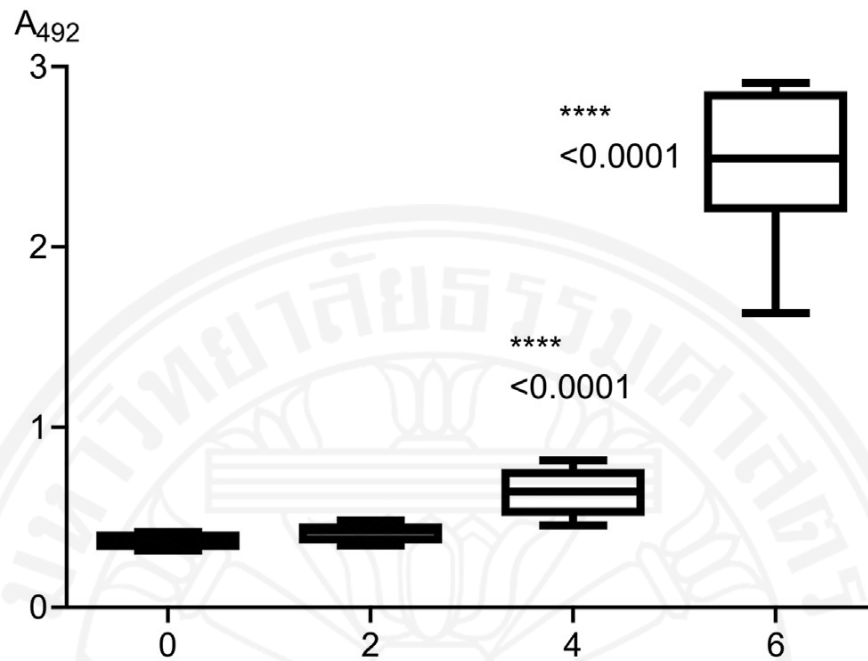
Figure 5.39 Box and whiskers graph showing ELISA results obtained with mouse *F. gigantica*-infected sera (n = 10) probed against yeast-expressed rFgCB5. The boxes extend from the 25th to the 75th percentile and have a line at the median. The whiskers indicate highest and lowest values. Statistically significant differences between the means of pre-infection sera and 2- and 4-week postinfection sera are indicated.

5.11 Functional analysis of recombinant *F. gigantica* Cathepsin B5 (rFgCB5)

5.11.1 Determination of K_m values

The K_m value of rFgCB5 for Z-Arg-Arg-AMC was determined by measuring the rate of reaction velocity at different substrate concentrations [S] from 0 to 512 µM at a fixed enzyme concentration. The recorded data was for nonlinear regression analysis with the Michaelis-Menten equation using GraphPad Prism 6.0 (**Figure 5.40**). The K_m value is shown in **Table 5.5**.

5.11.2 Determination of the inhibition coefficients (IC_{50})

Purified rFgStefin-1, rFgStefin-2 and human cystatin C were tested for inhibitory activity against rFgCB5. The inhibition of rFgCB5 by the three cystatins was most effective with rFgStefin-2 which showed the lowest IC_{50} value, followed by human cystatin C and finally rFgStefin-1 (**Figure 5.41**). The IC_{50} values are shown in **Table 5.6**. A higher IC_{50} value indicates a lower affinity of the inhibitor towards the enzyme.
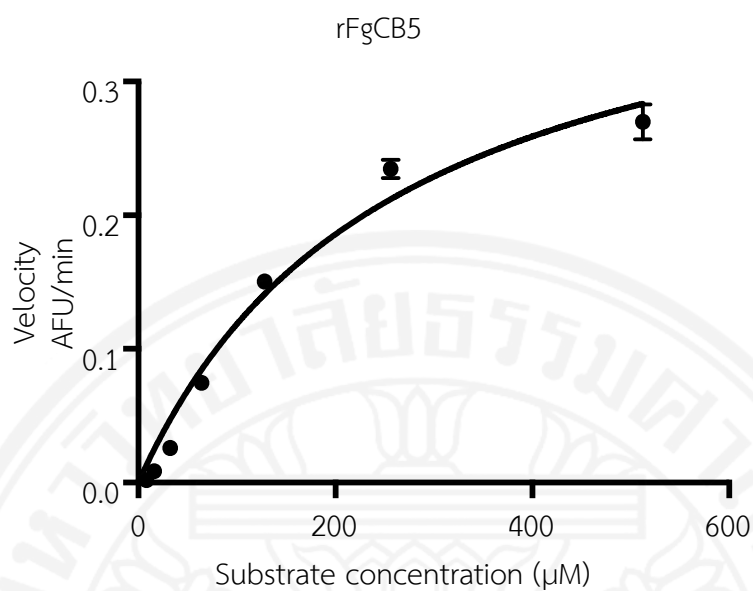
rFgCB5

Figure 5.40 Substrate concentration versus initial velocity plots for cleavage of fluorogenic substrate (Z-Arg-Arg-AMC) by rFgCB5.

Table 5.5 K_m value for recombinant *F. gigantica* cathepsin B5.

Protease	K_m (μM)
rFgCB5	262.2 ± 69.35

Table 5.6 IC_{50} values of human cystatin C, *F. gigantica* Stefin-1 and Stefin-2 against recombinant *F. gigantica* cathepsin B5 with substrate Z-Arg-Arg-AMC.

rFgCatB5 [ng/100µl]	Z-Arg-Arg-AMC [µM]	IC_{50} (95% confidence interval) [nM]		
		rFgStefin-1	rFgStefin-2	Human cystatin C
1	10	679.8 (668.9-691.0)	130.7 (108.3-157.6)	486.5 (476.4-496.7)
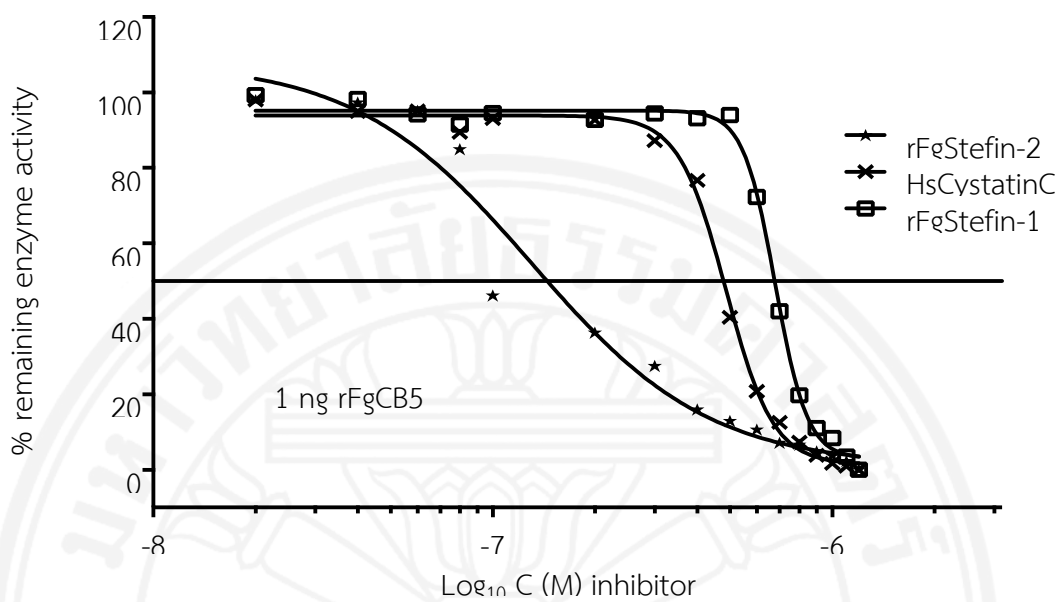
Figure 5.41 Inhibitory activity of rFgStefin-1, rFgStefin-2 and human cystatin C against rFgCB5 (1 ng). The IC_{50} values and substrate details are shown in **Table 5.6.**

5.11.3 Determination of the equilibrium inhibition constant (K_i)

The equilibrium inhibition constant (K_i) was calculated according to the Morrison equation to determine the level of inhibition of rFgCB5 by rFgStefin-1, rFgStefin-2 and human cystatin C as described in **Section 4.9.4**. The Morrison equation determines the K_i value of a tight binding enzyme inhibitor at fixed concentrations of enzyme and substrate with varying concentrations of inhibitor. Each experiment was performed in triplicate with duplicate samples. The K_i values of rFgStefin-1, rFgStefin-2 and human cystatin C for rFgCB5 are shown in **Table 5.7**. The results demonstrate that rFgSteFin-2 the lowest K_i value (57.18 nM), followed by human cystatin C (229.3 nM) and finally rFgStefin-1 (373.2 nM). The K_i values of the three cystatins for rFgCB5 confirmed the previous IC_{50} results.

Table 5.7 K_i values of FgStefin-1, FgStefin-2 and human cystatin C for rFgCB5.

Inhibitor	Ki (95% confidence interval) [nm]
rFgStefin-1	373.2
rFgStefin-2	57.18
HsCystatin C	229.3

5.11.4 Autoprocessing of rFgCB5

Recombinant FgCB5 (proprotein, 39.2 kDa) was incubated 0, 0.5, 1.5, 4 and 19 h at acid pH ranging from 4.0 to 5.5 in AMT buffer containing 50 μg/ml DS 500K, 200 mM NaCl and 10 mM DTT to analyze autoprocessing of the enzyme. Following incubation, all samples were analyzed by 12.5% SDS-PAGE and visualized by silver staining. Optimal autoprocessing was observed after incubation of rFgCB5 at pH 4.5 for 0.5 h. Autoprocessing was slow and the enzyme appeared unstable at pH 5.0 and 5.5. Degradation of rFgCB5 was observed at pH 4.0 after 1.5 h incubation time (**Figure 5.42**).
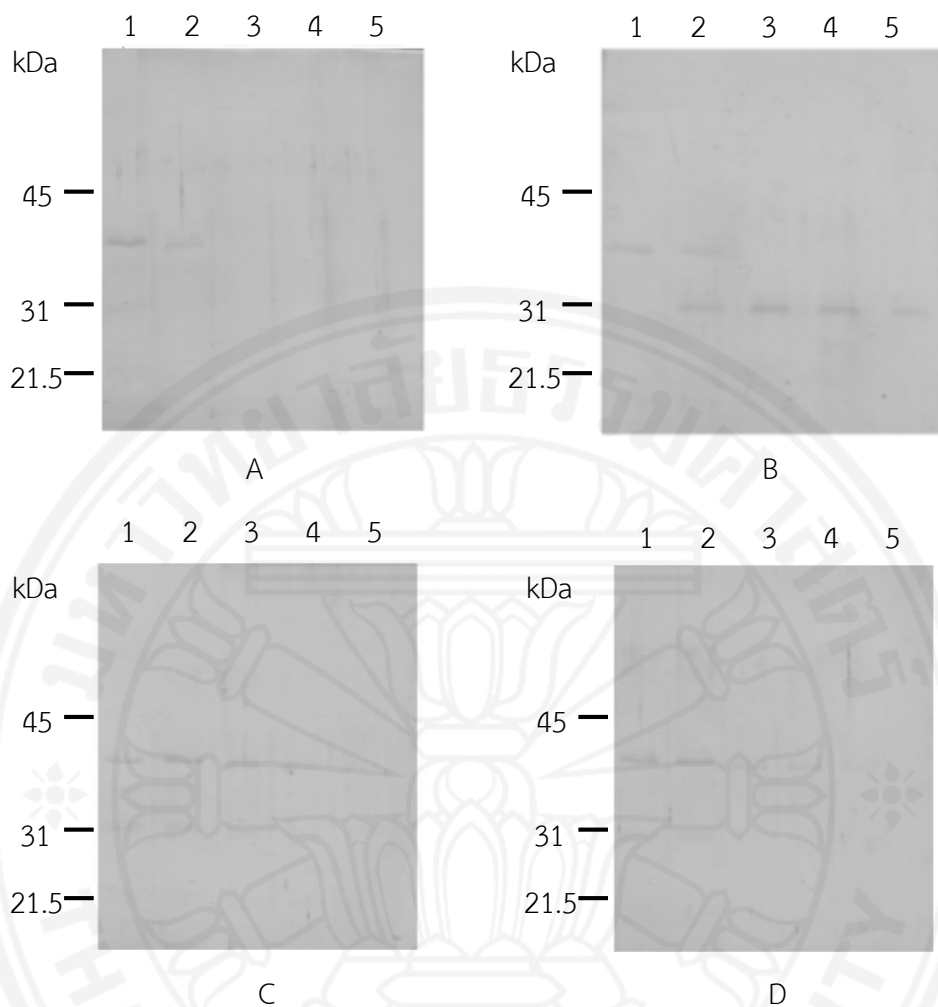
Figure 5.42 SDS-PAGE of products generated after autoprocessing of rFgCB5 (proprotein) at various pH values in AMT buffer (panel A = pH 4.0, panel B = pH 4.5, panel C = pH 5.0 and panel D = pH 5.5) in the presence of DTT and DS (500 K) for 0, 0.5, 1.5, 4 and 19 h (lanes: 1–5). The products were analyzed by reducing 12.5% SDS-PAGE and visualized by silver staining. Positions and sizes of the broad range protein standard marker (Bio-Rad, USA) are indicated at the left.

5.11.5 Temperature stability of rFgCB5

The stability of rFgCB5 was estimated against Z-Arg-Arg-AMC in AMT buffer containing 50 µg/ml DS 500K, 200 mM NaCl and 10 mM DTT pH.4.5 at 37°C. The enzyme maintained high activity against Z-Arg- Arg-AMC for 3 h (over 90% activity) but activity decreased to 68%, 56% and 25% activity after 4 h, 5h and 24 h incubation time, respectively (**Figure 5.43**).

5.11.6 pH dependency of rFgCB5

The pH profiles of rFgCB5 were evaluated by incubating rFgCB5 in AMT buffer containing 50 µg/ml DS 500K, 200 mM NaCl and 10 mM DTT adjusted to different pH values (pH 3.0–8.0) for 2 h at 37°C. The results showed that the optimal pH for the maximum activity of rFgCB5 was 4.5 (**Figure 5.44**).
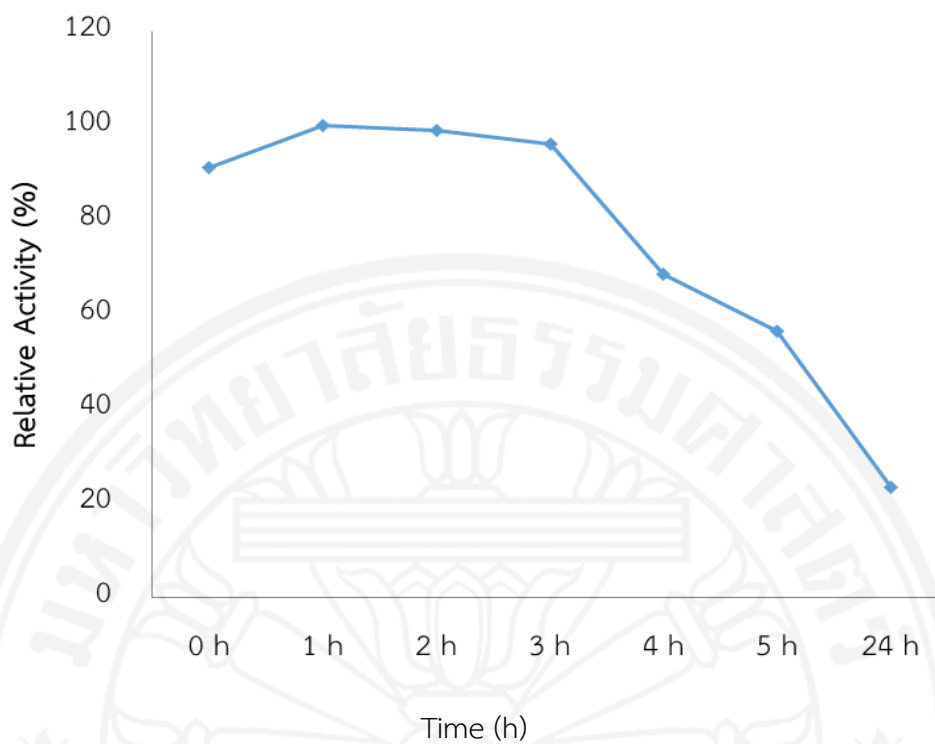
Figure 5.43 Temperature stability assay, the activity of rFgCB5 was measured after incubation in the presence of Z-Arg-Arg-AMC at 37°C for 0–5 h and 24 h.
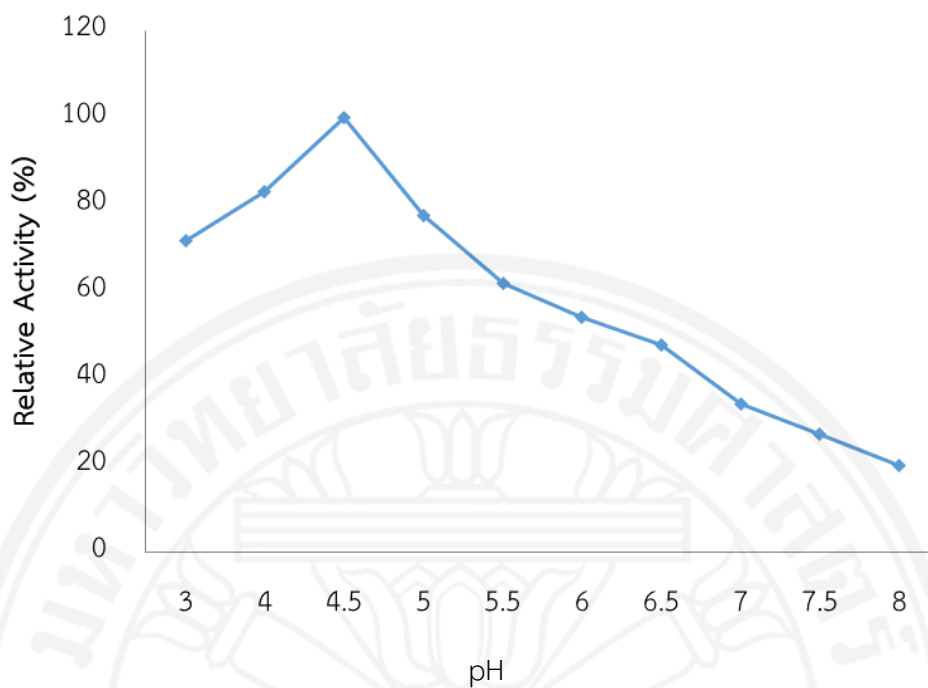
Figure 5.44 pH stability assay, the activity of rFgCB5 was measured after incubation in the presence of Z-Arg-Arg-AMC for 2 h, 37°C in AMT buffer at pH 3.0–8.0.

5.11.7 Degradation of host proteins by rFgCB5

The degradation of various host substrates by proteolytic activity of rFgCB5 is shown in **Figure 5.45**. The enzyme was able to hydrolyze bovine serum albumin, human IgG, fibronectin, laminin, collagen type IV at substantial amounts and showed weak activity against hemoglobin at pH 4.5 and pH 5.5, 37°C for 4 h.
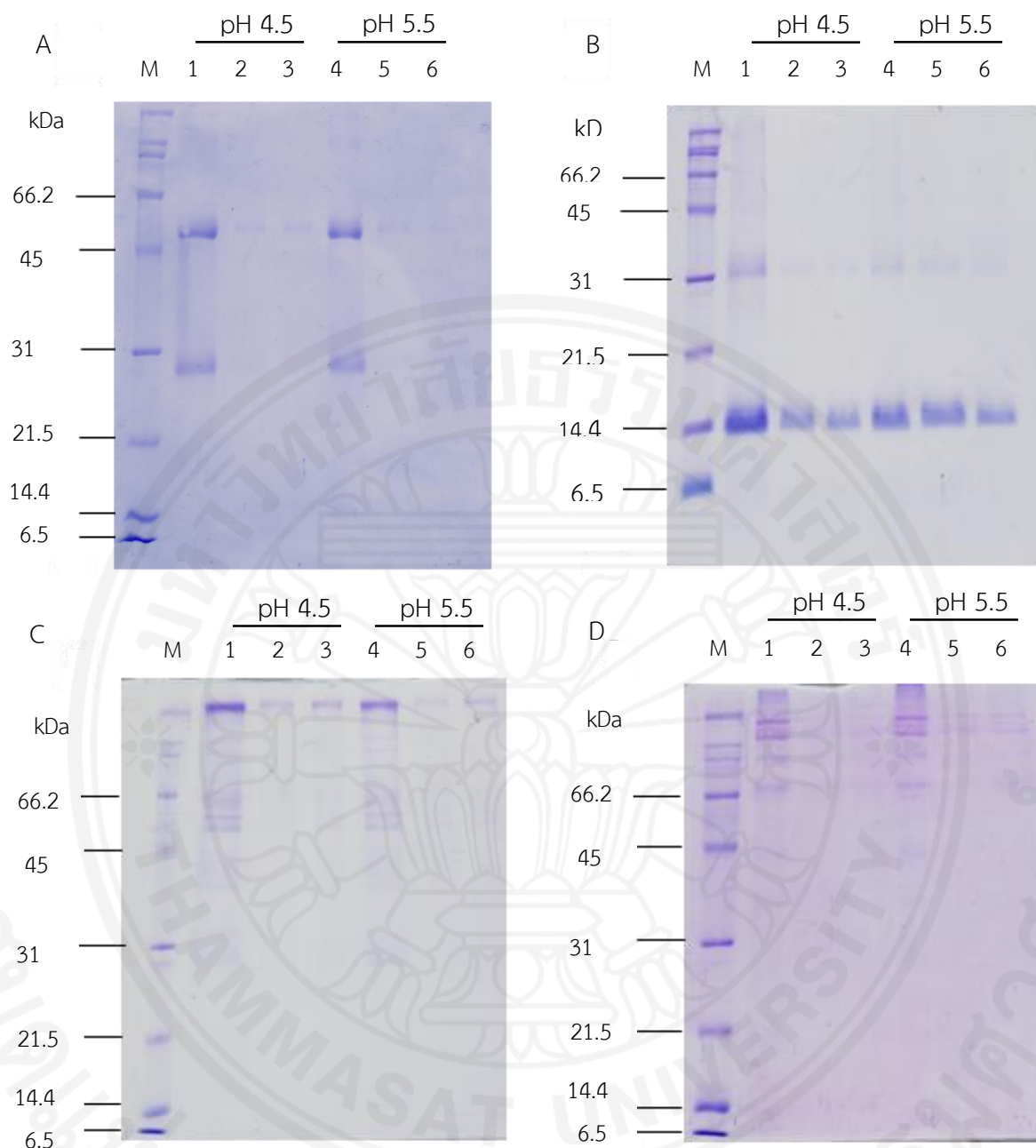
Figure 5.45 Degradation of various host proteins by proteolytic activity of FgCB5. (A) human IgG, (B) hemoglobin, (C) fibronectin, (D) collagen type IV were incubated with rFgCB5 (lanes 2, 5: 500 nM, lanes 3, 6: 700 nM) for 4 h at 37°C and analyzed by SDS-PAGE and stained with Coomassie blue R-250. Lanes M: Broad range protein standard marker (Bio-Rad, USA), lanes 1, 4: control protein without any enzymes.
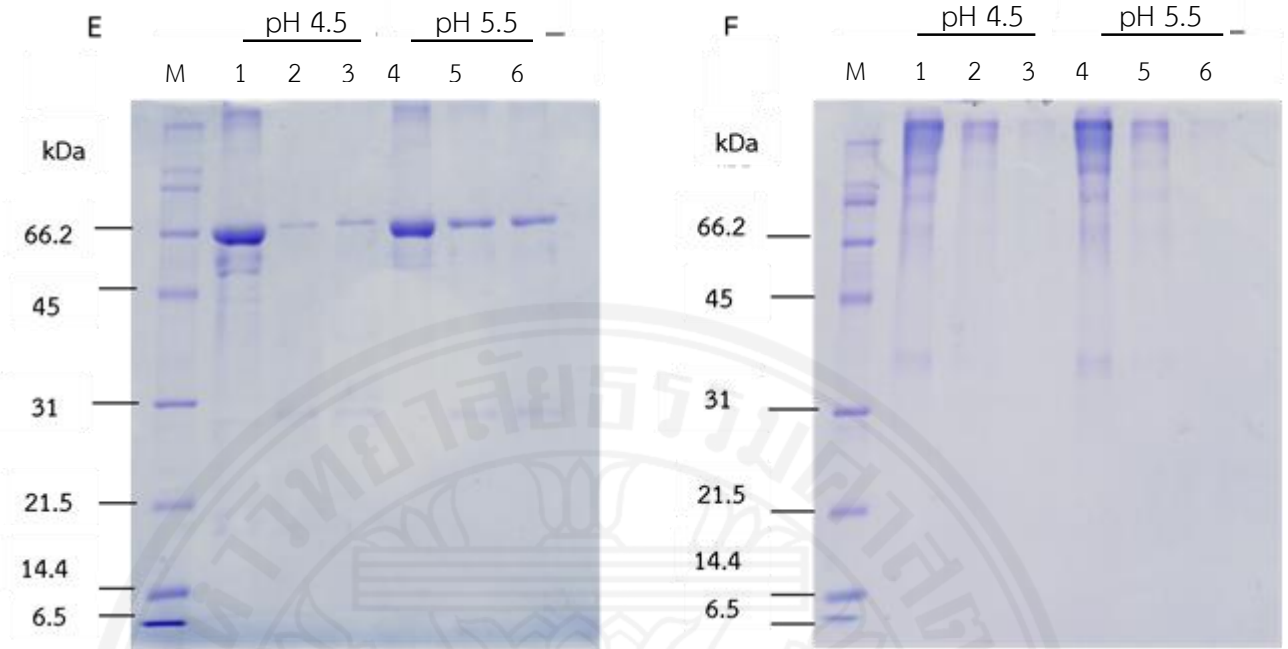
Figure 5.45 Degradation of various host proteins by proteolytic activity of FgCB5. (E) bovine serum albumin, (F) laminin were incubated with rFgCB5 (lanes 2, 5: 500 nM, lanes 3, 6: 700 nM) for 4 h at 37°C and analyzed by SDS-PAGE and stained with Coomassie blue R-250. Lanes M: Broad range protein standard marker (Bio-Rad, USA), lanes 1, 4: control protein without any enzymes. (cont.)

5.11.8 Exopeptidase activity

The exopeptidase activity of rFgCB5 was investigated using the synthetic substrate Abz-Phe-Arg-Ala-Lys(Dnp)-OH [Exo-OH] which was selected according to the substrate preferences of human cathepsin B. The proteolytic activity of activated human cathepsin B and rFgCB5 to Abz-Phe-Arg-Ala-Lys(Dnp)-OH [Exo-OH] in assay buffer (50 mM NaH$_2$PO$_4$, 200 mM NaCl, 5mM EDTA and 1 mM DTT, pH 4.5) at 37°C for 20 min is shown in **Figures 5.46** and **5.47**. The results of this analysis demonstrated that rFgCB5 showed substantial exopeptidase activity at a relative rate of 34.26% compared to human cathepsin B (17.31 ± 0.7766 AFU/min/nM to 50.53 ± 0.7729 AFU/min/nM) (**Figure 5.48**). Plots demonstrating the carboxydipeptidyl exopeptidase activity of rFgCB5 in comparison to human cathepsin B (HsCB) against Abz-Phe-Arg-Ala-Lys[Dnp]-OH at pH 4.5, 37°C, 20 min is shown in **Figure 5.49**.
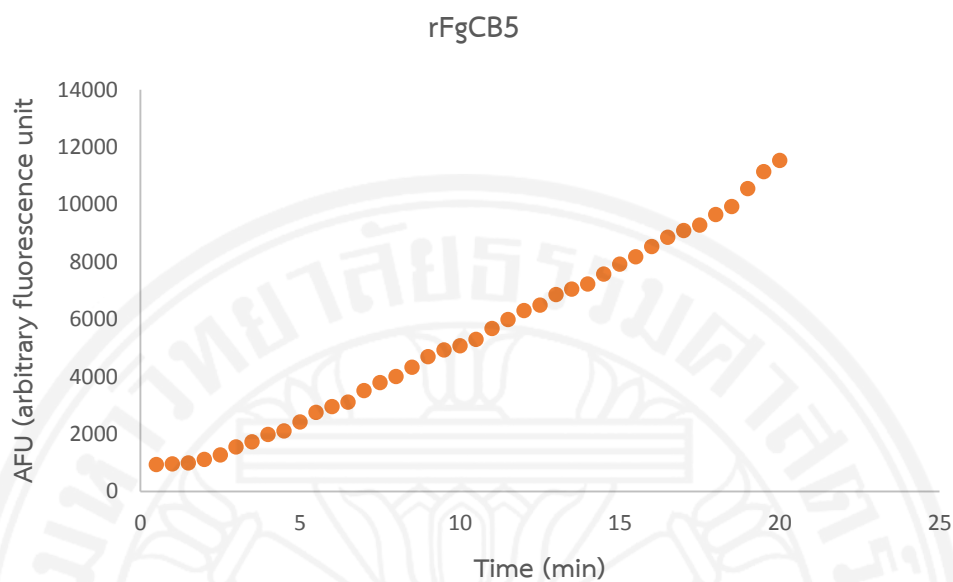
Figure 5.46 Processing of the synthetic fluorometric substrate Abz-Phe-Arg-Ala-Lys (Dnp)-OH by activated rFgCB5 at pH 4.5, 37°C for 20 min. Direct correlation could be observed between fluorescence units and time incubation.
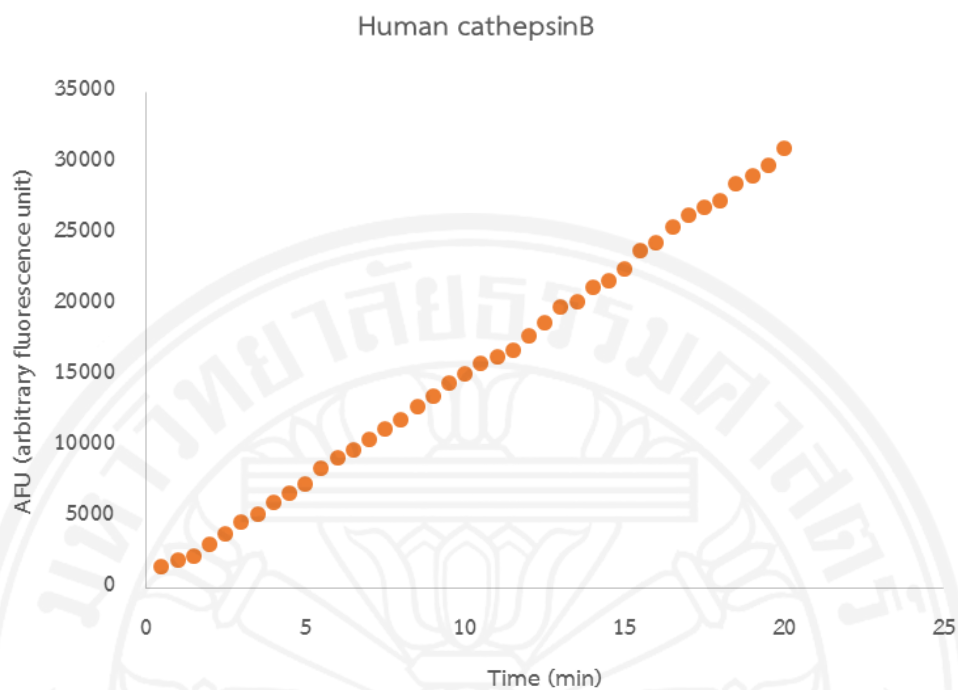
Figure 5.47 Processsing of the synthetic fluorometric substrate Abz-Phe-Arg-Ala-Lys (Dnp)-OH with activated human cathepsin B at pH 4.5, 37°C for 20 min. Direct correlation could be observed between fluorescence units and time incubation.
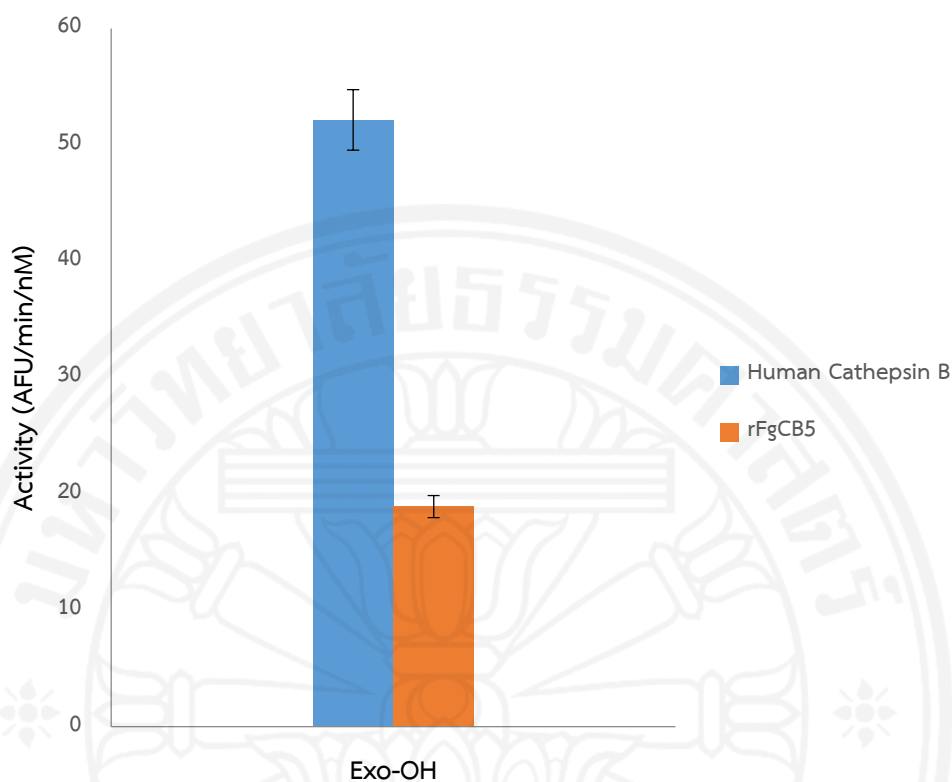
Figure 5.48 Processing of synthetic fluorometric substrate Abz-Phe-Arg-Ala-Lys (Dnp)-OH by the activated human cathepsin B and rFgCB5 at pH 4.5, 37°C for 20 min. The initial velocities for human cathepsin B (blue bars) and rFgCB5 (orange bar) are plotted as AFU/ (min nM)$^{-1}$ enzyme.
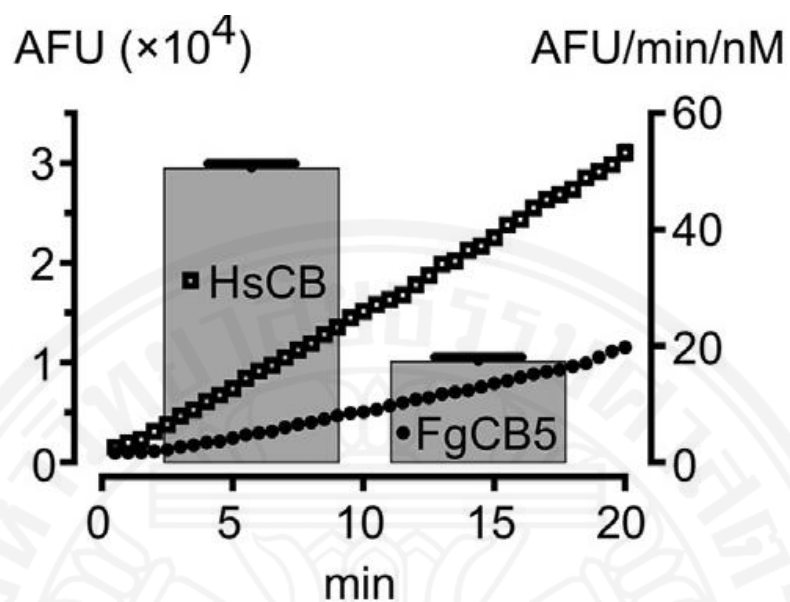
Figure 5.49 Plots demonstrating the carboxydipeptidyl exopeptidase activity of rFgCB5 in comparison to human cathepsin B (HsCB) against Abz-Phe-Arg-Ala-Lys[Dnp]-OH at pH 4.5, 37°C, 20 min. The averaged activities (AFU/min/nM) of the enzymes are shown in the column plot.

CHAPTER VI

DISCUSSION

6.1 Molecular cloning and sequence analysis of *F. gigantica* cDNAs encoding cystatin (FgStefin-2)

Cysteine proteases exist in all living organisms and are involved in biochemical and pathological processes.[203] Cystatins, the inhibitors of cysteine proteases, participate in various biological processes by regulating the activity of these proteases, for example to protect cells from inappropriate endogenous or extraneous proteolysis. The functions of several cystatins in higher animals and human have been studied. They are present in body fluids and a variety of tissues depending on their specific functions.[193] Cystatins are also found in plants, as exemplified by inhibitors isolated from wheat, corn, soybean and rice seeds.[226-229] Many cystatins have been isolated from filarial nematodes for example, Bm-CPI-2 of *Brugia malayi*, cystatin of *Acanthocheilonema viteae*, Onchocystatin of *Onchocerca volvulus*, nippocystatin of *Nippostrongylus brasiliensis* and cystatin of *Litomosoides sigmodontis* and were found to be involved in immunomodulatory activities.[17,219] Cystatins in trematodes especially in *Fasciola* spp. have been described in only a few publications. In the present study a novel type 1 cystatin (stefin) of the liver fluke *F. gigantica* was molecular and biochemically characterized. A full length cDNA of FgStefin-2 was cloned by RT-PCR from total RNA of adult *F. gigantica*. The FgStefin-2 cDNA has 836 bp size and its deduced amino acid sequence carries the typical features of type 1 cystatins with the characteristic conserved glycine residue in the N-terminal region, low molecular mass, absence of C-terminal located extended loops with disulfide bond-forming conserved cysteine residues, and the QVVAG motif in the active site-binding loop.[202,215] The protein contained 116 amino acid residues with a calculated molecular mass of 12.56 kDa and had a pI of 7.0. FgStefin-2 contained a putative N-terminal signal peptide which is unusual for stefins but the remaining sequence features clearly indicate homology to stefins. Sequence similarity between

FgStefin-2 and human stefins A, B is low in the C-terminal region (β-strand 4, active site-binding loop 2, β-strand 5 and unordered tail in structure-resolved human stefins A and B) (**Figure 5.6**). NCBI-BLASTP was used to find related sequences in the NCBI non-redundant protein database. The result revealed a high identity value (92.2%) with the uncharacterized *Fasciola hepatica* ortholog (GenBank accession AAV68752) and the identity and similarity values of FgStefin-2 and other cystatins are shown in **Table 5.1**. FgStefin-2 orthologs could not be detected in *Schistosoma*, *Opisthorchis* and *Clonorchis* transcriptome/genome data by use TBLASTN.

6.2 Characterization of FgStefin-2 nucleic acids

Genomic Southern analysis was done to confirm the presence of FgStefin-2 from a nuclear gene in the parasite. The nucleic acid patterns of cystatin genes analyzed by Southern blot analysis have previously only been published for FgStefin-1 from *F. gigantica* and a multi-domain cystatin from *F. hepatica*. Southern blot analysis had demonstrated that FgStefin-1 is encoded by a single copy gene in the parasite genome[10] while the analysis of multi-domain cystatin from *F. hepatica* observed two hybridizing fragments at different intensity in the parasite genome.[11] Results of the RT-PCR analysis suggest that the FgStefin-2 gene is transcribed in all developmental stages of the parasites (NEW, 2-, 4-, 6-week-old juveniles and adult parasites). Northern blot analysis suggests that the gene is transcribed at only one size, 1,000 nucleotides, in adults (**Figure 5.10 and 5.11**). The presence of FgStefin-2 in all developmental stages suggests an important function of this protein for the parasite which generally will be the control of cysteine protease activity.

6.3 Expression and purification of recombinant FgStefin-2

Recombinant FgStefin-2 (rFgStefin-2) was expressed in *Escherichia coli* M15 using pQE30 as expression vector. Expression of N-terminal His-tagged rFgStefin-2 was induced with IPTG and recombinant protein was observed 1 h after induction and the amount of this protein steadily increased over 4 h. Recombinant protein

was highly abundant at 4 h after induction and it was expressed in both, soluble and insoluble form (**Figures 5.14** and **5.15**). The 13 kDa soluble protein was purified by Ni-NTA-sepharose affinity chromatography (**Figure 5.16**). The expression results demonstrate that rFgStefin-2 can be expressed in the prokaryotic expression system and that it is not toxic to the expression host *E. coli* M15. After purification, the recombinant protein was used for immunization of BALB/c mice by intraperitoneal injection to produce specific antisera. The polyclonal anti-rFgStefin-2 antisera were checked for the specificity and sensitivity against the recombinant protein before used in further experiments.

6.4 Characterization and immunolocalization of recombinant FgStefin-2

The anti-rFgStefin-2 antisera reacted with rFgStefin-2 and antigens of the expected 13 kDa mass in crude worm (CW) extract and excretory/secretory (ES) product of the adult parasites (**Figure 5.18**). Furthermore, the antisera did not cross-react with rFgStefin-1, multi-domain cystatin and CW extracts of other trematodes including *Opisthorchis viverrini*, *Paramphistomum* spp., *Eurytrema pancreaticum*, *Schistosoma mansoni*, and *Fischoederius elongates* (**Figures 5.19** and **5.20**). The distribution of native FgStefin-2 in the tissues of 2-, 4-week-old juvenile and adult *F. gigantica* was analyzed by immunohistochemistry with the mouse anti-rFgStefin-2 antisera (**Figures 5.21** and **5.22**). The results demonstrated that FgStefin-2 is expressed in the intestinal epithelium in all developmental stages. In adults, FgStefin-2 is expressed and released from the prostate gland cells into ejaculatory duct and its targets in ejaculate or, following insemination, the uterus are presently unknown as parasite cysteine proteases have not been investigated in these locations yet. Immunolocalization of FgStefin-2 is different from FgStefin-1 which was present in intestinal epithelium and tegumental cells.[10] Cathepsin L is a major protease in the cecal epithelial cells[169] while cathepsin B is not only found in cecal epithelial cells but also in the tegumental cells and the reproductive system such as prostate gland, vitelline cells through which it becomes incorporated in the parasite's eggs, Mehlis' gland, testis, and eggs[176]. The expression of FgStefin-2

associated with the cysteine proteases in gut and reproductive tissues suggests that the inhibitor has important roles in regulation of the proteases in these tissues to ensure appropriate proteolytic processes. The expression of FgStefin-2 in the gut epithelium where the cathepsin L proteases are expressed supports a regulatory role for this inhibitor within the cytoplasm prior to release of active proteases at the luminal surface of the gut if they are leaking from their storage vesicles. Several type 2 cystatins are expressed in male reproductive tissues in Mammalia[230] and FgStefin-2 may have analogous functionality.

6.5 Functional analysis of recombinant FgStefin-2

Purified recombinant FgStefin-2 was tested for its inhibitory activity against native bovine cathepsin B and L and the ES product of *Fasciola gigantica*. A previous study had demonstrated that the N-terminal His-tag of rFgStefin-1 had only slight influence on the inhibition of cathepsin B and L.[10] Therefore, the His-tags of rFgStefin-1 and 2 were not removed in this study. Recombinant FgStefin-2 has an inhibition profile comparable to homologs described from other organisms with highest activity towards ES product, followed by cathepsin L, and then cathepsin B. Remarkably, it shows a significantly lower IC_{50} and K_i value to bovine cathepsin B compared to rFgStefin-1 and human cystatin C, a type 2 cystatin that is one of the most effective inhibitors of cathepsin B (**Tables 5.3** and **5.4**, **Figure 5.24**).[231] These results are related to the RT-PCR and immunoblots experiments in which FgStefin-2 was found to be more abundant than FgStefin-1 in the metacercariae, the stage in which cathepsin B is most abundant (**Figures 5.30** and **5.31**).[176,179,210,232] The efficient inhibition of the parasite's endogenous cathepsin B isoforms by FgStefin-2 is also indirectly supported by the zymography analyses (**Figures 5.25–5.27**). CW extract from metacercariae containing abundant cathepsin B is blocked by rFgStefin-2 but not rFgStefin-1 at similar concentration. Comparable, CW extract from adult parasites which contains a mixture of cathepsin B and L isoforms is again more effectively blocked by rFgStefin-2. The ES product of adult parasites with its high cathepsin L content is equally inhibited by rFgStefin-2 and rFgStefin-1. Cathepsin B is released in

the early infectious phase of fascioliasis[175] and the parallel release of an inhibitor optimized to recognize this protease could be important for the protection of newly excysted juveniles, which should be sensitive due to their minute size, from autolytic tissue damage. Primary damage could cause escalating harm through a cascade of suddenly released proteases which again damage nearby cells.

The pH dependency and temperature stability of rFgStefin-2 activity were determined. Recombinant FgStefin-2 is active over a wide range of pH values (pH 3.0–9.0) and would effectively work in slightly alkaline bile and more neutral liver parenchyma of host and in the acidic gut lumen of the parasite (**Figure 5.28**). This property of rFgStefin-2 relates to cathepsin B and L of *Fasciola* spp. that also active over a broad pH range.[166,211] The rFgStefin-2 is also remarkably heat stable at 100°C for 3 h (**Figure 5.29**) similar to rFgStefin-1[10] and other cystatins such as chicken cystatin[233], human stefins A and B[101].

The sera from *F. gigantica*-infected mice reacted with rFgStefin-2 with the mean immune response being slightly higher compared to rFgStefin-1 starting four weeks postinfection (**Figure 5.32**).

6.6 Analysis of immunomodulatory properties of recombinant FgStefin-2

A preliminary study of the immunomodulatory properties of FgStefin-2 analyzed the inhibition of polyclonal T-cell proliferation from murine spleen cells and PBMC by recombinant FgStefin-2 as had been described in parasitic nematodes.[20] The result showed that rFgStefin-2 inhibited cellular proliferation by 30-63% of murine spleen cells and 21-50% of murine PBMC at 0.2-0.5 µM inhibitor concentrations (**Figures 5.33** and **5.34**). The effect of rFgStefin-2 was similar to *A. viteae* (rAv17), which reported significantly suppressed mitogen-induced T cell proliferation by 63.5% and 45.5%.[14,20] These preliminary data suggest that rFgStefin-2 may interfere with an immune response mechanism that is involved in polyclonal T-cell proliferation.

6.7 Expression and purification of recombinant FgCB5

Recombinant FgCB5 (rFgCB5) was expressed in the *Pichia pastoris* (strain X33) yeast expression system with pPicZαB as expression vector. A transformant yeast clone carrying the expression construct integrated in the genome was cultured in BMMY medium to induce expression. The 39.2 kDa rFgCB5 (proprotein) was found expressed at 72 and 96 h after induction (**Figure 5.36**) and was purified by Ni-NTA-sepharose affinity chromatography (**Figure 5.37**). The results demonstrate that rFgCB5 can be successfully expressed as a non-toxic His-tagged protein in the eukaryotic expression system. A denatured form of rFgCB5 expressed in *E. coli* was used to immunize BALB/c mice by intraperitoneal injection to produce specific antisera. The obtained polyclonal anti-rFgCB5 antisera were tested against the yeast-expressed recombinant protein to confirm their specificity and sensitivity before used in further experiments.

6.8 Characterization of recombinant FgCB5

The anti-rFgCB5 antiserum reacted with yeast-expressed 39.2 kDa rFgCB5 (proFgCB5), detected native cathepsin B in CW extract as a doublet of antigens that migrated slightly faster than proFgCB5 at the approximate size of the native proprotease (36.4 kDa) and in the ES product of the adult parasite very faintly as an antigen migrating at the lower position of the CW extract doublet (**Figure 5.38**). The anti-rFgCB5 antiserum has high probability to cross-react with FgCB4, FgCB7 and other similar high conserved isoforms. Therefore, the bands that were detected in the CW extract might represent a complex of co-migrating CB4, CB5 and CB7. Previous studies showed that anti-bovine cathepsin B antiserum cross-reacted with cathepsin B of *F. hepatica* in NEJ and with cathepsin B in the intestinal tract of the fluke in the juvenile stage.[177,179] Antiserum raised against rFgCB2 was reactive with CW extract from metacercariae, NEJ, and 2-week-old juveniles while 3-week-old juveniles or later stages were not observed and anti-rFgCB3 antiserum was reactive with CW

extract from metacercariae and NEJ whereas, 4-week-old juveniles or later stages were not detected.[234,235]

The sera from *F. gigantica*-infected mice reacted with rFgCB5 starting four weeks postinfection. The reactivity in 4- and 6-week postinfection sera was significantly different from the reactivity of sera from earlier weeks (**Figure 5.39**) and increased over time. In a previous study it had been demonstrated that the sera from *F. hepatica*-infected rats and sheep reacted with rFhCB2 indicating a steady release of cathepsin B from the flukes.[232]

6.9 Functional analysis of recombinant FgCB5

Purified rFgStefin-1, rFgStefin-2 and human cystatin C were tested for inhibitory activity against yeast-expressed FgCB5. The enzyme inhibition by the three cystatins showed some differences with rFgStefin-2 exhibiting the lowest IC_{50} and K_i values, followed by human cystatin C and finally rFgStefin-1 (**Figure 5.41, Tables 5.6 and 5.7**). A higher IC_{50} value indicates a lower affinity of the inhibitor towards the enzyme and the K_i values of the three cystatins for yeast-expressed FgCB5 confirmed the IC_{50} results. As previously observed rFgStefin-2 showed higher inhibition against bovine cathepsin B than rFgStefin-1 and human cystatin C. Therefore, the results of this experiment confirm that rFgStefin-2 is a potent inhibitor of cathepsin B.[236] In a previous study it had been demonstrated that stefin A, stefin B and cystatin C weakly inhibited FhCB2.[211]

Autoprocessing of rFgCB5 (39.2 kDa proprotein) was analyzed at an acid pH range from 4.0 to 5.5 in AMT buffer containing 50 µg/ml DS 500K, 200 mM NaCl and 10 mM DTT at different time points (0, 0.5, 1.5, 4 and 19 h incubation). The results showed that the enzyme underwent optimal processing to the mature form at pH 4.5 for 0.5 h. At pH 5.0 and 5.5 autoprocessing was slow and the enzyme appeared unstable while degradation of rFgCB5 was observed at pH 4.0 after 1.5 h incubation time (**Figure 5.42**). Importantly, the result of this experiment is comparable to the described autoprocessing of human procathepsin B.[237]

The pH profiles and temperature stability of rFgCB5 activity were determined. As observed in the autoprocessing experiment, rFgCB5 showed maximum activity at an acidic pH of 4.5 like lysosomal hydrolases that would efficiently work in the acidic gut lumen of the parasite (**Figure 5.44**). Fully activated rFgCB5 was incubated in AMT buffer, pH 4.5 and >90% enzyme activity was recorded after 3 h incubation time and 25% activity after 24 h incubation time (**Figure 5.43**). This property of rFgCB5 is similar to cathepsin B1 and B2 of *S. mansoni* (SmCB1 and SmCB2) that also showed optimum activity at acid pH but not at pH 6.5 or higher.[238] Furthermore, cathepsin B and cathepsin B-like cysteine proteases of *Naegleria fowleri* (rNfCPB and rNfCPB-L) have similar properties to rFgCB5 with maximum activity at pH 4.5.[239]

The degradation of several host proteins by rFgCB5 was observed. This included mammalian proteins such as bovine serum albumin, human IgG, fibronectin, laminin, collagen type IV and hemoglobin at pH 4.5 and pH 5.5, 37°C for 4 h and all substrates were readily hydrolyzed by rFgCB5 at substantial amounts at both pH values (**Figure 5.45**). Therefore, rFgCB5 might be involved in parasite migration in the host tissues, evasion of the host immune system and nutrient uptake. The protein digestion properties of rFgCB5 are similar to those of *N. fowleri* rNfCPB and rNfCPB-L that also digested human IgA, IgG and IgM and other human proteins including fibronectin, collagen, albumin and hemoglobin.[239] Moreover, cathepsin B3 of *F. gigantica* (FgCatB3) and cathepsin B of *Angiostrongylus cantonensis* (AcCPB) also showed the ability to degrade host substrates.[235,240]

The suspected exopeptidase activity of rFgCB5 due to the presence of two His residues at positions 109 and 110 (mature form, equivalent human His[110] and His[111]) in the occluding loop was investigated using fluorescence substrate Abz-Phe-Arg-Ala-Lys (Dnp)-OH [Exo-OH] based on the substrate preferences of human cathepsin B. The results of dipeptidyl peptidase activity demonstrated that rFgCB5 has substantial exopeptidase activity at a relative rate of 34.26% compared to human cathepsin B (**Figures 5.46–5.49**). In a previous study, C-terminal dipeptidyl activity was reported for *S. mansoni* SmCB1, SmCB2 and mammalian cathepsin B

(first reported) while FhCB2 that is missing the equivalent of human cathepsin B residue His[111] does not show this activity.[211,241,242]

CHAPTER VII

CONCLUSION

This section summarizes the findings of the molecular, biochemical and immunological characterization of type 1 cystatin (stefin) and cathepsin B5 of *Fasciola gigantica*. The major findings are concluded as the following:

1. A 836 bp *Fasciola gigantica* cDNA containing the complete coding sequence of an uncharacterized cystatin (FgStefin-2) was generated by RT-PCR from total RNA of mature *F. gigantica*.

2. Sequence analysis showed that the FgStefin-2 cDNA encoded a protein of 116 amino acid residues with a molecular mass of 12.56 kDa and a pI of 7.0. Sequence comparison strongly suggested that this protein was a novel parasite type 1 cystatin (stefin). While the predicted N-terminal signal peptide is unusual for stefins the remaining sequence features, e.g. characteristic conserved glycine residue in the N-terminal region, absence of C-terminal located extended loops with disulfide bond-forming conserved cysteine residues, low molecular mass and QVVAG motif in the active site-binding loop are key signatures of the type 1 cystatin family.

3. The amino acid sequence of FgStefin-2 showed the highest identity to the orthologous uncharacterized *F. hepatica* cystatin at 92.2% identity and 94.0% similarity.

4. Southern and Northern hybridization of nucleic acids isolated from adult *F. gigantica*, suggest that FgStefin-2 is expressed by a single copy gene as a single transcriptional product of 1,000 nucleotides.

5. FgStefin-2 RNA is present in all analyzed developmental stages of *F. gigantica* including NEJ, 2-, 4-, 6-week-old immature parasites and mature parasites.

6. Recombinant FgStefin-2 was abundantly produced in both soluble and insoluble form in *Escherichia coli* M15 at the predicted mass of 13 kDa. The recombinant protein was purified by Ni-NTA sepharose affinity chromatography under native conditions.

7. The purified rFgStefin-2 was used to immunize BALB/c mice by intraperitoneal injection to produce polyclonal anti-rFgStefin-2 antisera.

8. In western blot analysis, anti-rFgStefin-2 antisera reacted strongly with rFgStefin-2, and with native antigens at the expected mass in CW extract and ES product of adult *F. gigantica*. Moreover, we observed no cross-reactivity of the anti-rFgStefin-2 antisera to rFgStefin-1, *F. gigantica* multi-domain cystatin and CW extracts of other trematodes such as *Opisthorchis viverrini*, *Paramphistomum* spp., *Eurytrema pancreaticum*, *Schistosoma mansoni*, and *Fischoederius elongates*.

9. Immunohistochemical analysis revealed that native FgStefin-2 was localized in the intestinal epithelium in 2-, 4-week-old juveniles and in adult parasites. The protein was detected in several tissue types of the parasite including the prostate gland, gut epithelium and intrauterine eggs.

10. Purified recombinant FgStefin-2 showed an inhibition profile comparable to homologs described from other organisms with highest activity towards endogenous cathepsin L in the ES product, followed by bovine cathepsin L and then cathepsin B. In comparison to human cystatin C and rFgStefin-1 it showed the lowest IC_{50} and K_i values to bovine cathepsin B.

11. Recombinant FgStefin-2 is active over a wide pH range (pH 3.0–9.0) and is a heat stable at 100℃ for at least 3 h.

12. Analysis of cystatin inhibitory activity by zymography with parasite protein preparations suggested again that rFgStefin-2 is more effective against cathepsin B. CW extract from metacercariae that have stored abundant cathepsin B and CW extract from adult parasites that express a mixture of lysosomal cathepsin B and secreted cathepsin L isoforms was more efficiently blocked by rFgStefin-2 than rFgStefin-1. Contrary, rFgStefin-1 and rFgStefin-2 showed no difference in the inhibition of cysteine proteases in adult stage ES product that contains only cathepsin L.

13. RT-PCR and immunoblots showed that rFgStefin-2 was more abundant in the metacercarial stage than rFgStefin-1. This result and the better inhibition of cathepsin B by rFgStefin-2 as shown by inhibition coefficients (IC_{50}), the

equilibrium inhibition constants (K_i), and zymography experiments allow to conclude that rFgStefin-2 was evolutionary adapted to regulate endogenous cathepsin B.

14. Sera of *F. gigantica*-infected mice showed a higher reactivity to rFgStefin-2 than to rFgStefin-1 at 4-, 6- week postinfection by indirect ELISA possibly because of the higher abundance of rFgStefin-2 in the early juvenile.

15. A preliminary study of the immunomodulatory properties suggests that rFgStefin-2 negatively interferes with an immune response mechanism that is involved in polyclonal T-cell proliferation.

16. Recombinant FgCB5 was expressed in insoluble form in *Escherichia coli* and was used to immunize BALB/c mice by intraperitoneal injection to produce polyclonal anti-rFgCB5 antisera.

17. Recombinant FgCB5 was expressed in soluble form in the yeast *Pichia pastoris* strain X33 at the predicted size of 39.2 kDa (proprotein). The recombinant protein was purified by Ni-NTA sepharose affinity chromatography.

18. In immunoblots anti-rFgCB5 antiserum detected yeast-expressed rFgCB5 (positive control) and in adult stage CW extract it detected a doublet of antigens at the expected 36.4 kDa mass of the native proprotease. In the ES product, the antigen migrating at the lower position of the CW extract doublet was faintly observed.

19. Sera of *F. gigantica*-infected mice showed significantly increasing reactivity to rFgCB5 four and six week postinfection suggesting continued release of cathepsin B isoforms in the immature parasite.

20. Inhibition of rFgCB5 by three cystatins, i.e. rFgStefin-1, rFgStefin-2 and human cystatin C demonstrated that the protease is more efficiently blocked by rFgStefin-2 is (lowest IC_{50} and K_i values) than by human cystatin C and rFgStefin-1.

21. Optimal autoprocessing of soluble yeast-expressed rFgCB5 (proprotein) to the mature form was observed at pH.4.5 after 30 min incubation time. The protein was degraded and could not be detected after incubation at pH 4.0 for 1.5 h while autoprocessing was slow and the enzyme appeared unstable at pH 5.0 and 5.5.

22. Recombinant FgCB5 exhibited the highest activity at pH 4.5, at this pH value it also retained >90% activity for 3 h and 25% activity after 24 h incubation time.

23. Several host substrates including fibronectin, laminin, collagen type IV, human IgG, hemoglobin and bovine serum albumin were hydrolyzed by rFgCB5 at substantial amounts at pH 4.5 and pH 5.5.

24. Recombinant FgCB5 showed substantial carboxydipeptidyl exopeptidase activity. It can be concluded that FgCB5 is a typical lysosomal hydrolase that will have a role in the digestion of proteins/peptides taken up in the endolysosomal pathway.
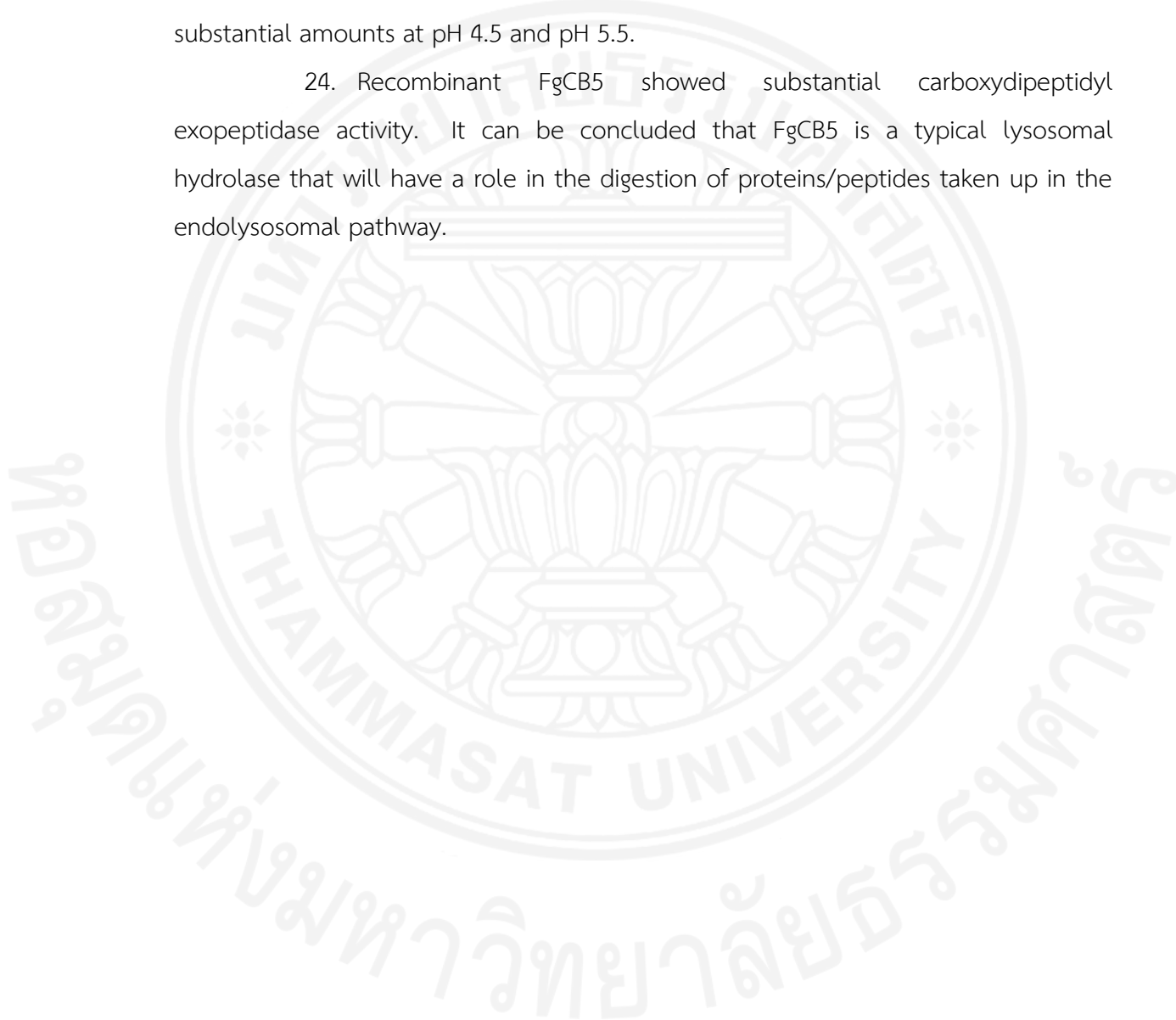
REFERENCES

1.   Robinson MW, Dalton JP. Zoonotic helminth infections with particular emphasis on fasciolosis and other trematodiases. Philos Trans R Soc Lond B Biol Sci. 2009;364(1530):2763-76.

2.   Control of foodborne trematode infections. Report of a WHO Study Group. World Health Organ Tech Rep Ser. 1995;849:1-157.

3.   Brennan GP, Fairweather I, Trudgett A, Hoey E, McCoy, McConville M, et al. Understanding triclabendazole resistance. Exp Mol Pathol. 2007;82(2):104-9.

4.   Overend DJ, Bowen FL. Resistance of *Fasciola hepatica* to triclabendazole. Aust Vet J. 1995;72(7):275-6.

5.   Robinson MW, Dalton JP, Donnelly S. Helminth pathogen cathepsin proteases: it's a family affair. Trends Biochem Sci. 2008;33(12):601-8.

6.   Kabanda A, Goffin E, Bernard A, Lauwerys R, van Ypersele de Strihou C. Factors influencing serum levels and peritoneal clearances of low molecular weight proteins in continuous ambulatory peritoneal dialysis. Kidney Int. 1995;48(6):1946-52.

7.   Delaisse JM, Ledent P, Vaes G. Collagenolytic cysteine proteinases of bone tissue. Cathepsin B, (pro)cathepsin L and a cathepsin L-like 70 kDa proteinase. Biochem J. 1991;279 (Pt 1):167-74.

8.   Trabandt A, Gay RE, Fassbender HG, Gay S. Cathepsin B in synovial cells at the site of joint destruction in rheumatoid arthritis. Arthritis Rheum. 1991;34(11):1444-51.

9.   Morales FC, Furtado DR, Rumjanek FD. The N-terminus moiety of the cystatin SmCys from *Schistosoma mansoni* regulates its inhibitory activity *in vitro* and *in vivo*. Mol Biochem Parasitol. 2004;134(1):65-73.

10. Tarasuk M, Vichasri Grams S, Viyanant V, Grams R. Type I cystatin (stefin) is a major component of *Fasciola gigantica* excretion/secretion product. Mol Biochem Parasitol. 2009;167(1):60-71.

11. Khaznadji E, Collins P, Dalton JP, Bigot Y, Moire N. A new multi-domain member of the cystatin superfamily expressed by *Fasciola hepatica*. Int J Parasitol. 2005;35(10):1115-25.

12. Geadkaew A, Kosa N, Siricoon S, Grams SV, Grams R. A 170kDa multi-domain cystatin of *Fasciola gigantica* is active in the male reproductive system. Mol Biochem Parasitol. 2014;196(2):100-7.

13. Lustigman S, Brotman B, Huima T, Prince AM, McKerrow JH. Molecular cloning and characterization of onchocystatin, a cysteine proteinase inhibitor of *Onchocerca volvulus*. J Biol Chem. 1992;267(24):17339-46.

14. Hartmann S, Kyewski B, Sonnenburg B, Lucius R. A filarial cysteine protease inhibitor down-regulates T cell proliferation and enhances interleukin-10 production. Eur J Immunol. 1997;27(9):2253-60.

15. Gregory WF, Maizels RM. Cystatins from filarial parasites: evolution, adaptation and function in the host-parasite relationship. Int J Biochem Cell Biol. 2008;40(6-7):1389-98.

16. Pfaff AW, Schulz-Key H, Soboslay PT, Geiger SM, Hoffmann WH. The role of nitric oxide in the innate resistance to microfilariae of *Litomosoides sigmodontis* in mice. Parasite Immunol. 2000;22(8):397-405.

17. Dainichi T, Maekawa Y, Ishii K, Himeno K. Molecular cloning of a cystatin from parasitic intestinal nematode, *Nippostrongylus brasiliensis*. J Med Invest. 2001;48(1-2):81-7.

18. Dainichi T, Maekawa Y, Ishii K, Zhang T, Nashed BF, Sakai T, et al. Nippocystatin, a cysteine protease inhibitor from *Nippostrongylus brasiliensis*, inhibits antigen processing and modulates antigen-specific immune response. Infect Immun. 2001;69(12):7380-6.

19. Meisel C, Vogt K, Platzer C, Randow F, Liebenthal C, Volk HD. Differential regulation of monocytic tumor necrosis factor-alpha and interleukin-10 expression. Eur J Immunol. 1996;26(7):1580-6.

20. Schierack P, Lucius R, Sonnenburg B, Schilling K, Hartmann S. Parasite-specific immunomodulatory functions of filarial cystatin. Infect Immun. 2003;71(5):2422-9.

21. Schonemeyer A, Lucius R, Sonnenburg B, Brattig N, Sabat R, Schilling K, et al. Modulation of human T cell responses and macrophage functions by onchocystatin, a secreted protein of the filarial nematode *Onchocerca volvulus*. J Immunol. 2001;167(6):3207-15.

22. Knox DP. Proteinase inhibitors and helminth parasite infection. Parasite Immunol. 2007;29(2):57-71.

23. Mukherjee S, Ukil A, Das PK. Immunomodulatory peptide from cystatin, a natural cysteine protease inhibitor, against leishmaniasis as a model macrophage disease. Antimicrob Agents Chemother. 2007;51(5):1700-7.

24. Kuchai JA, Chishti MZ, Zaki MM, Rasool SADM, Ahmad J, Tak H. Some Epidemiological Aspects of Fascioliasis Among Cattle of Ladakh. Global Veterinaria. 2011;7(4):342-6.

25. Mas-Coma S, Bargues MD, Valero MA. Fascioliasis and other plant-borne trematode zoonoses. Int J Parasitol. 2005;35(11-12):1255-78.

26. Mas-Coma S, Valero MA, Bargues MD. Chapter 2. *Fasciola*, lymnaeids and human fascioliasis, with a global overview on disease transmission, epidemiology, evolutionary genetics, molecular epidemiology and control. Adv Parasitol. 2009;69:41-146.

27. J.G. ESTEBA MDBSM-C. GEOGRAPHICAL DISTRIBUTION, DIAGNOSIS AND TREATMENT OF HUMAN FASCIOLIASIS: A REVIEW. Research and Reviews in Parasitology. 1998;58(1):13-42.

28. Srihakim S, Pholpark M. Problem of fascioliasis in animal husbandry in Thailand. Southeast Asian J Trop Med Public Health. 1991;22 Suppl:352-5.

29. Torgerson P, Claxton J. Epidemiology and control. In: Dalton JP (Ed) Fasciolosis CABI publishing, Oxon, UK. 1999:113-49.

30. Department of Livestock Development [Internet]. [updated December 2009; cited 2015 30 December]. Available from: http://www.dld.go.th/.

31. Dangprasert T, Khawsuk W, Meepool A, Wanichanon C, Viyanant V, Upatham ES, et al. *Fasciola gigantica*: surface topography of the adult tegument. J Helminthol. 2001;75(1):43-50.

32. Boray JC. The ecology of *Fasciola hepatica* with particular reference to its intermediate host in Australia. Proceedings of the 17th World Veterinary Congress. 1963;1:709 - 15.

33. Andrews N. The life cycle of *Fasciola hepatica*. In: Dalton JP (Ed) Fasciolosis CABI publishing, Oxon, UK. 1999:1-20.

34. FLUKE DRUG PROTOCOL: Praziquantel & Albendazole [Internet]. [updated 11 April 2010; cited 2015 29 December]. Available from: http://www.curezone.org/forums/am.asp?i=1667673.

35. Sheep Liver Fluke (*Fasciola hepatica*) miracidium larva. LM [Internet]. [updated 21 June 2010; cited 2015 30 December]. Available from: http://www.corbisimages.com/stock-photo/rights-managed/42-26623908/sheep-liver-fluke-fasciola-hepatica-miracidium-larva.

36. Zoology Lab Pratical #2 [Internet]. [updated 28 October 2013; cited 2015 30 December]. Available from: https://www.studyblue.com/notes/note/n/zoology-lab-pratical-2/deck/8330842.

37. Laboratory 6 TREMATODES [Internet]. [updated 16 August 2004; cited 2015 30 December]. Available from: http://cal.vet.upenn.edu/projects/paralab/labs/lab6.htm.

38. metacercaria of *Fasciola hepatica* [Internet]. [updated 26 May 2007; cited 2015 30 December]. Available from: http://workforce.calu.edu/Buckelew/Fasciola%20hepatica%20metacercaria.htm.

39. *Fasciola hepatica* [Internet]. [cited 2015 30 December]. Available from: http://ruby.fgcu.edu/courses/davidb/50249/web/fh180.htm.

40. Bargues MD, Vigo M, Horak P, Dvorak J, Patzner RA, Pointier JP, et al. European *Lymnaeidae* (Mollusca: Gastropoda), intermediate hosts of trematodiases, based on nuclear ribosomal DNA ITS-2 sequences. Infect Genet Evol. 2001;1(2):85-107.

41. Dreyfuss G, Moukrim A, Rondelaud D, Vareille-Morel C. Field observations concerning infection of *Lymnaea palustris* by *Fasciola hepatica*. J Helminthol. 1994;68(2):115-8.

42. Dreyfuss G, Abrous M, Rondelaud D. The susceptibility of *Lymnaea fuscus* to experimental infection with *Fasciola hepatica*. J Parasitol. 2000;86(1):158-60.

43. Rana MAA, Roohi N, Khan MA. FASCIOLIASIS IN CATTLE- A REVIEW. The Journal of Animal & Plant Sciences. 2014;24(3):668-75.

44. Marden P, Warren K. Tropical and geographical medicine. New York: Fascioliasis; 1984.

45. DPDx - Laboratory Identification of Parasitic Diseases of Public Health Concern [Internet]. [updated 9 December 2015; cited 2015 30 December]. Available from: http:www.dpd.cdc.gov/dpdx.

46. *Lymnaea truncatula* [Internet]. [updated 19 April 2013; cited 2015 30 December]. Available from: https://www.flickr.com/photos/cladoniophile/86739671 44/in/photostream/.

47. *Lymnaea stagnalis* [Internet]. [updated 23 November 2015; cited 2015 30 December]. Available from: http://en.wikipedia.org/wiki/Lymnaea_stagnalis.

48. Shell Encyclopedia [Internet]. [updated 30 December 2015; cited 2015 30 December]. Available from: http://www.conchology.be/?t=68&u=362721&g=da3 d046939d55b0a5ce09a88273dfade&q=4303f36004ade1b200940cb012741d0e.

49. *Radix auricularia* [Internet]. [updated 30 November 2015; cited 2015 30 December]. Available from: http://en.wikipedia.org/wiki/Radix_auricularia.

50. *Radix natalensis* [Internet]. [updated 26 May 2007; cited 2015 30 December]. Available from: http://www.conchology.be/?t=68&u=805993&g=0c891a0d5610a95e cb101b228b58a477&q=9428886a7a1a56e2b9e6dd123ca7915a.

51. Hanna RE. *Fasciola hepatica*: an electron microscope autoradiographic study of protein synthesis and secretion by gut cells in tissue slices. Exp Parasitol. 1975;38(2):167-80.

52. Fairweather I, Threadgold L, Hanna R. Development of *Fasciola hepatica* in the mammalian host. In: Dalton JP (Ed) Fasciolosis CABI publishing, Oxon, UK. 1999:47–112.

53. Robinson G, Threadgold L. Electron microscope studies of *Fasciola hepatica* XIII. The fine structure of the gastrodermis. Exp Parasitol. 1975;37:20-36.

54. Meepool A, Sobhon P. Oogenesis of the liver fluke *Fasciola gigantica*. J Microsc Soc Thailand. 2009;23:15-9.

55. Grove AJ, Newell GE. Animal Biology: University Tutorial 2013.

56. Mas-Coma S, Rodrigue Z, Bargues MD, Valero MA, Coello JR, Angles R. SECONDARY RESERVOIR ROLE OF DOMESTIC ANIMALS OTHER THAN SHEEP AND CATTLE IN FASCIOLIASIS TRANSMISSION IN THE NORTHERN BOLIVIAN ALTIPLANO. Research and Reviews in Parasitology. 1997;57(1):39-46.

57. Unit WHOSC. Progress in assessment of morbidity due to *fasciola hepatica* infection : a review of recent literature Geneva : World Health Organization; 1990.

58. Horstmann H, Pedersen OM. [Heart infarct; etiology, pathology, pathophysiology and clinical aspects]. Dtsch Krankenpflegez. 1971;24(7):310-6.

59. Boray JC. Experimental fascioliasis in Australia. Adv Parasitol. 1969;7:95-210.

60. Nithiuthai S, Anantaphruti MT, Waikagul J, Gajadhar A. Waterborne zoonotic helminthiases. Vet Parasitol. 2004;126(1-2):167-93.

61. Marcos LA, Tagle M, Terashima A, Bussalleu A, Ramirez C, Carrasco C, et al. Natural history, clinicoradiologic correlates, and response to triclabendazole in acute massive fascioliasis. Am J Trop Med Hyg. 2008;78(2):222-7.

62. Marcos LA, Terashima A, Gotuzzo E. Update on hepatobiliary flukes: fascioliasis, opisthorchiasis and clonorchiasis. Curr Opin Infect Dis. 2008;21(5):523-30.

63. Marcos Raymundo LA, Maco Flores V, Terashima Iwashita A, Samalvides Cuba F, Gotuzzo Herencia E. [Clinical characteristics of chronic infection by *Fasciola hepatica* in children]. Rev Gastroenterol Peru. 2002;22(3):228-33.

64. Rana SS, Bhasin DK, Nanda M, Singh K. Parasitic infestations of the biliary tract. Curr Gastroenterol Rep. 2007;9(2):156-64.

65. Sezgin O, Altintas E, Tombak A, Ucbilek E. *Fasciola hepatica*-induced acute pancreatitis: report of two cases and review of the literature. Turk J Gastroenterol. 2010;21(2):183-7.

66. Kaya M, Bestas R, Cetin S. Clinical presentation and management of *Fasciola hepatica* infection: single-center experience. World J Gastroenterol. 2011;17(44):4899-904.

67. Turhan O, Korkmaz M, Saba R, Kabaaliogu A, Inan D, Mamikoglu L. Seroepidemiology of fascioliasis in the Antalya region and uselessness of eosinophil count as a surrogate marker and portable ultrasonography for epidemiological surveillance. Infez Med. 2006;14(4):208-12.

68. Gilberto BT, Angélica TI, Ciro MV, V.L. L, Humberto AB, Raúl TC. Fasciolosis humana y compromiso gastrointestinal. REV GASTROENTEROL PERU. 2004;24:143-57.

69. Luis AMR, Vicente MF, Angélica TI, Frine SC, Eduardo GH. Características clínicas de la infección crónica por *Fasciola hepática* en niños. Rev gastroenterol Perú. 2002;22.

70. Khalil G, Haddad C, Otrock ZK, Jaber F, Farra A. Halzoun, an allergic pharyngitis syndrome in Lebanon: the trematode *Dicrocoelium dendriticum* as an additional cause. Acta Trop. 2013;125(1):115-8.

71. Saleha AA. Liver fluke disease (fascioliasis): epidemiology, economic impact and public health significance. Southeast Asian J Trop Med Public Health. 1991;22 Suppl:361-4.

72. Marcos L, Maco V, Samalvides F, Terashima A, Espinoza JR, Gotuzzo E. Risk factors for *Fasciola hepatica* infection in children: a case-control study. Trans R Soc Trop Med Hyg. 2006;100(2):158-66.

73. Marcos LA, Terashima A, Leguia G, Canales M, Espinoza JR, Gotuzzo E. [*Fasciola hepatica* infection in Peru: an emergent disease]. Rev Gastroenterol Peru. 2007;27(4):389-96.

74. Zumaquero-Rios JL, Sarracent-Perez J, Rojas-Garcia R, Rojas-Rivero L, Martinez-Tovilla Y, Valero MA, et al. Fascioliasis and intestinal parasitoses affecting schoolchildren in Atlixco, Puebla State, Mexico: epidemiology and treatment with nitazoxanide. PLoS Negl Trop Dis. 2013;7(11):e2553.

75. Espinoza JR, Maco V, Marcos L, Saez S, Neyra V, Terashima A, et al. Evaluation of Fas2-ELISA for the serological detection of *Fasciola hepatica* infection in humans. Am J Trop Med Hyg. 2007;76(5):977-82.

76. Tantrawatpan C, Maleewong W, Wongkham C, Wongkham S, Intapan PM, Nakashima K. Serodiagnosis of human fascioliasis by a cystatin capture enzyme-linked immunosorbent assay with recombinant *Fasciola gigantica* cathepsin L antigen. Am J Trop Med Hyg. 2005;72(1):82-6.

77. Fagbemi BO, Guobadia EE. Immunodiagnosis of fasciolosis in ruminants using a 28-kDa cysteine protease of *Fasciola gigantica* adult worms. Vet Parasitol. 1995;57(4):309-18.

78. Diab TM, Rabia I, Komy WEL, Amir AEL. Efficacy of sandwich and dot-ELISA in diagnosis of fascioliasis using a pair of polyclonal antibodies against cathepsin L antigen in naturally infected sheep. Res J Parasitol. 2011;6:90-100.

79. Gupta A, Dixit AK, Dixit P, Mahajan C, Sharma RL. Evaluation of dipstick-ELISA using 28 kDa *Fasciola gigantica* cathepsin l cysteine proteinase (FgCL3) for serodiagnosis of fasciolosis in naturally infected goats. Vet Parasitol. 2011;176(2-3):165-9.

80. Ali NM. Development and evaluation of a dipstick assay in diagnosis of human fasciolosis. Parasitol Res. 2012;110(5):1649-54.

81. Martinez-Sernandez V, Muino L, Perteguer MJ, Garate T, Mezo M, Gonzalez-Warleta M, et al. Development and evaluation of a new lateral flow immunoassay for serodiagnosis of human fasciolosis. PLoS Negl Trop Dis. 2011;5(11):e1376.

82. Cevikol C, Karaali K, Senol U, Kabaalioglu A, Apaydin A, Saba R, et al. Human fascioliasis: MR imaging findings of hepatic lesions. Eur Radiol. 2003;13(1):141-8.

83. Van Beers B, Pringot J, Geubel A, Trigaux JP, Bigaignon G, Dooms G. Hepatobiliary fascioliasis: noninvasive imaging findings. Radiology. 1990;174(3 Pt 1):809-10.

84. Cosme A, Ojeda E, Cilla G, Torrado J, Alzate L, Beristain X, et al. [*Fasciola hepatica*. study of a series of 37 patients]. Gastroenterol Hepatol. 2001;24(8):375-80.

85. el-Shazly AM, Soliman M, Gabr A, Haseeb AN, Morsy AT, Arafa MA, et al. Clinico-epidemiological study of human fascioliasis in an endemic focus in Dakahlia Governorate, Egypt. J Egypt Soc Parasitol. 2001;31(3):725-36.

86. Bacq Y, Besnier JM, Duong TH, Pavie G, Metman EH, Choutet P. Successful treatment of acute fascioliasis with bithionol. Hepatology. 1991;14(6):1066-9.

87. Fairweather I. Triclabendazole: new skills to unravel an old(ish) enigma. J Helminthol. 2005;79(3):227-34.

88. Mitchell GB, Maris L, Bonniwell MA. Triclabendazole-resistant liver fluke in Scottish sheep. Vet Rec. 1998;143(14):399.

89. Moll L, Gaasenbeek CP, Vellema P, Borgsteede FH. Resistance of *Fasciola hepatica* against triclabendazole in cattle and sheep in The netherlands. Vet Parasitol. 2000;91(1-2):153-8.

90. Olaechea F, Lovera V, Larroza M, Raffo F, Cabrera R. Resistance of *Fasciola hepatica* against triclabendazole in cattle in Patagonia (Argentina). Vet Parasitol. 2011;178(3-4):364-6.

91. Ortiz P, Scarcella S, Cerna C, Rosales C, Cabrera M, Guzman M, et al. Resistance of *Fasciola hepatica* against Triclabendazole in cattle in Cajamarca (Peru): A clinical trial and an *in vivo* efficacy test in sheep. Vet Parasitol. 2013.

92. McConville M, Brennan GP, McCoy M, Castillo R, Hernandez-Campos A, Ibarra F, et al. Immature triclabendazole-resistant *Fasciola hepatica*: tegumental responses to *in vitro* treatment with the sulphoxide metabolite of the experimental fasciolicide compound alpha. Parasitol Res. 2007;100(2):365-77.

93. Hernandez-Campos A, Ibarra-Velarde F, Vera-Montenegro Y, Rivera-Fernandez N, Castillo R. Synthesis and fasciolicidal activity of 5-chloro-2-methylthio-6-(1-naphthyloxy)-1H-benzimidazole. Chem Pharm Bull (Tokyo). 2002;50(5):649-52.

94. Keiser J, Utzinger J, Vennerstrom JL, Dong Y, Brennan G, Fairweather I. Activity of artemether and OZ78 against triclabendazole-resistant *Fasciola hepatica*. Trans R Soc Trop Med Hyg. 2007;101(12):1219-22.

95. Rollinson D. Control of foodborne trematode infections. Report of a WHO Study Group: Geneva: World Health Organization. Transactions of the Royal Society of Tropical Medicine and Hygiene. 1995;89(6).

96. Esteban J, Flores A, Aguirre C, Strauss W, Angles R, Mas-Coma S. Presence of very high prevalence and intensity of infection with *Fasciola hepatica* among Aymara children from the Northern Bolivian Altiplano. Acta Trop. 1997;66(1):1-14.

97. Bjorland J, Bryan RT, Strauss W, Hillyer GV, McAuley JB. An outbreak of acute fascioliasis among Aymara Indians in the Bolivian Altiplano. Clin Infect Dis. 1995;21(5):1228-33.

98. Esteban JG, Flores A, Angles R, Mas-Coma S. High endemicity of human fascioliasis between Lake Titicaca and La Paz valley, Bolivia. Trans R Soc Trop Med Hyg. 1999;93(2):151-6.

99. Copland RS, Skerratt LF. Options for the control of liver fluke. approaches to extension for fasciolosis Control.56-89.

100. Hillyer GV. *Fasciola* antigens as vaccines against fascioliasis and schistosomiasis. J Helminthol. 2005;79(3):241-7.

101. Barrett AJ, McDonald JK. Nomenclature: protease, proteinase and peptidase. Biochem J. 1986;237(3):935.

102. Rao MB, Tanksale AM, Ghatge MS, Deshpande VV. Molecular and biotechnological aspects of microbial proteases. Microbiol Mol Biol Rev. 1998;62(3):597-635.

103. Rawlings ND, Barrett AJ, Bateman A. MEROPS: the peptidase database. Nucleic Acids Res. 2010;38(Database issue):D227-33.

104. Johnson SL, Pellecchia M. Structure- and fragment-based approaches to protease inhibition. Curr Top Med Chem. 2006;6(4):317-29.

105. Nogaroto V, Tagliavini S, Gianotti A, Mikawa A, Barros NT, Puzer L, et al. Recombinant expression and characterization of a *Xylella fastidiosa* cysteine protease differentially expressed in a nonpathogenic strain. FEMS Microbiol Lett. 2006;261(2):187-93.

106. Chemical digestion is the process of breakdown of large macronutrients into smaller molecules by enzyme-mediated hydrolysis. [Internet]. [updated 21 June 2015; cited 2015 30 December]. Available from: https://www.boundless.com/physiology/textbooks/boundless-anatomy-and-physiology-textbook/the-digestive-system-23/chemical-digestion-224/mechanisms-of-chemical-digestion-1103-8914/.

107. Adeliana SO, Jose XF, Mauricio PS. Cysteine Proteinase and Cystatins. Brazilian Archives of Biology and Technology. 2003;46(1):91-104.

108. Podolin PL, Bolognese BJ, Carpenter DC, Davis TG, Johanson RA, Fox JH, et al. Inhibition of invariant chain processing, antigen-induced proliferative responses, and the development of collagen-induced arthritis and experimental autoimmune encephalomyelitis by a small molecule cysteine protease inhibitor. J Immunol. 2008;180(12):7989-8003.

109. Vasiljeva O, Reinheckel T, Peters C, Turk D, Turk V, Turk B. Emerging roles of cysteine cathepsins in disease and their potential as drug targets. Curr Pharm Des. 2007;13(4):387-403.

110. Rzychon M, Chmiel D, Stec-Niemczyk J. Modes of inhibition of cysteine proteases. Acta Biochim Pol. 2004;51(4):861-73.

111. Lemere CA, Munger JS, Shi GP, Natkin L, Haass C, Chapman HA, et al. The lysosomal cysteine protease, cathepsin S, is increased in Alzheimer's disease and Down syndrome brain. An immunocytochemical study. Am J Pathol. 1995;146(4):848-60.

112. Jedinak A, Maliar T. Inhibitors of proteases as anticancer drugs - Minireview. Neoplasma. 2005;52(3):185-92.

113. Layton GT, Harris SJ, Bland FA, Lee SR, Fearn S, Kaleta J, et al. Therapeutic effects of cysteine protease inhibition in allergic lung inflammation: inhibition of allergen-specific T lymphocyte migration. Inflamm Res. 2001;50(8):400-8.

114. Katunuma N, Kominami E. Abnormal expression of lysosomal cysteine proteinases in muscle wasting diseases. Rev Physiol Biochem Pharmacol. 1987;108:1-20.

115. Yasuda Y, Kaleta J, Bromme D. The role of cathepsins in osteoporosis and arthritis: rationale for the design of new therapeutics. Adv Drug Deliv Rev. 2005;57(7):973-93.

116. Grzonka Z, Jankowska E, Kasprzykowski F, Kasprzykowska R, Lankiewicz L, Wiczk W, et al. Structural studies of cysteine proteases and their inhibitors. Acta Biochim Pol. 2001;48(1):1-20.

117. Otto HH, Schirmeister T. Cysteine Proteases and Their Inhibitors. Chem Rev. 1997;97(1):133-72.

118. Sajid M, McKerrow JH. Cysteine proteases of parasitic organisms. Mol Biochem Parasitol. 2002;120(1):1-21.

119. Bode W, Huber R. Structural basis of the endoproteinase-protein inhibitor interaction. Biochim Biophys Acta. 2000;1477(1-2):241-52.

120. Rawlings ND, Barrett AJ. Chapter 404 - Introduction: The Clans and Families of Cysteine Peptidases. In: Salvesen NDR, editor. Handbook of Proteolytic Enzymes: Academic Press; 2013. p. 1743-73.

121. Schechter I, Berger A. On the size of the active site in proteases. I. Papain. 1967. Biochem Biophys Res Commun. 2012;425(3):497-502.

122. Turk D, Guncar G. Lysosomal cysteine proteases (cathepsins): promising drug targets. Acta Crystallogr D Biol Crystallogr. 2003;59(Pt 2):203-13.

123. Turk D, Guncar G, Podobnik M, Turk B. Revised definition of substrate binding sites of papain-like cysteine proteases. Biol Chem. 1998;379(2):137-47.

124. Turk V, Turk B, Guncar G, Turk D, Kos J. Lysosomal cathepsins: structure, role in antigen processing and presentation, and cancer. Adv Enzyme Regul. 2002;42:285-303.

125. Chapman HA, Riese RJ, Shi GP. Emerging roles for cysteine proteases in human biology. Annu Rev Physiol. 1997;59:63-88.

126. Goulet B, Baruch A, Moon NS, Poirier M, Sansregret LL, Erickson A, et al. A cathepsin L isoform that is devoid of a signal peptide localizes to the nucleus in S phase and processes the CDP/Cux transcription factor. Molecular Cell. 2004;14(2):207-19.

127. Duncan EM, Muratore-Schroeder TL, Cook RG, Garcia BA, Shabanowitz J, Hunt DF, et al. Cathepsin L proteolytically processes histone H3 during mouse embryonic stem cell differentiation. Cell. 2008;135(2):284-94.

128. Santos-Rosa H, Kirmizis A, Nelson C, Bartke T, Saksouk N, Cote J, et al. Histone H3 tail clipping regulates gene expression. Nat Struct Mol Biol. 2009;16(1):17-22.

129. Buck MR, Karustis DG, Day NA, Honn KV, Sloane BF. Degradation of extracellular-matrix proteins by human cathepsin B from normal and tumour tissues. Biochem J. 1992;282 (Pt 1):273-8.

130. Nagaya T, Murata Y, Yamaguchi S, Nomura Y, Ohmori S, Fujieda M, et al. Intracellular proteolytic cleavage of 9-cis-retinoic acid receptor alpha by cathepsin L-type protease is a potential mechanism for modulating thyroid hormone action. J Biol Chem. 1998;273(50):33166-73.

131. Dickinson DP. Cysteine peptidases of mammals: their biological roles and potential effects in the oral cavity and other tissues in health and disease. Crit Rev Oral Biol Med. 2002;13(3):238-75.

132. Alvarez-Fernandez M, Barrett AJ, Gerhartz B, Dando PM, Ni J, Abrahamson M. Inhibition of mammalian legumain by some cystatins is due to a novel second reactive site. J Biol Chem. 1999;274(27):19195-203.

133. Salminen-Mankonen HJ, Morko J, Vuorio E. Role of cathepsin K in normal joints and in the development of arthritis. Curr Drug Targets. 2007;8(2):315-23.

134. Kakegawa H, Nikawa T, Tagami K, Kamioka H, Sumitani K, Kawata T, et al. Participation of cathepsin L on bone resorption. FEBS Lett. 1993;321(2-3):247-50.

135. Ishidoh K, Kominami E. Procathepsin L degrades extracellular matrix proteins in the presence of glycosaminoglycans in vitro. Biochem Biophys Res Commun. 1995;217(2):624-31.

136. Kirschke H. Chapter 410 - Cathepsin L. In: Salvesen NDR, editor. Handbook of Proteolytic Enzymes: Academic Press; 2013. p. 1808-17.

137. Barrett AJ, Kirschke H. Cathepsin B, Cathepsin H, and cathepsin L. Methods Enzymol. 1981;80 Pt C:535-61.

138. Esser RE, Angelo RA, Murphey MD, Watts LM, Thornburg LP, Palmer JT, et al. Cysteine proteinase inhibitors decrease articular cartilage and bone destruction in chronic inflammatory arthritis. Arthritis Rheum. 1994;37(2):236-47.

139. Yagel S, Warner AH, Nellans HN, Lala PK, Waghorne C, Denhardt DT. Suppression by cathepsin L inhibitors of the invasion of amnion membranes by murine cancer cells. Cancer Res. 1989;49(13):3553-7.

140. Stachowiak K, Tokmina M, Karpinska A, Sosnowska R, Wiczk W. Fluorogenic peptide substrates for carboxydipeptidase activity of cathepsin B. Acta Biochim Pol. 2004;51(1):81-92.

141. Mordier SB, Bechet DM, Roux MP, Obled A, Ferrara MJ. The structure of the bovine cathepsin B gene. Genetic variability in the 3' untranslated region. Eur J Biochem. 1995;229(1):35-44.

142. Kazunori H, T. M, Y. M, O. S, S. J, T. I. Isolation and Characterization of E–64, a New Thiol Protease Inhibitor. Agricultural and Biological Chemistry. 2014;42(3):523-8.

143. JOHN SM, J.B. D. MOLECULES IN FOCUS Cathepsin B. Int J Biochem Cd Bid. 1997;29(5):715-20.

144. Koblinski JE, Ahram M, Sloane BF. Unraveling the role of proteases in cancer. Clin Chim Acta. 2000;291(2):113-35.

145. Podgorski I, Sloane BF. Cathepsin B and its role(s) in cancer progression. Biochem Soc Symp. 2003(70):263-76.

146. Lang A, Horler D, Baici A. The relative importance of cysteine peptidases in osteoarthritis. J Rheumatol. 2000;27(8):1970-9.

147. Hashimoto Y, Kakegawa H, Narita Y, Hachiya Y, Hayakawa T, Kos J, et al. Significance of cathepsin B accumulation in synovial fluid of rheumatoid arthritis. Biochem Biophys Res Commun. 2001;283(2):334-9.

148. Kukor Z, Mayerle J, Kruger B, Toth M, Steed PM, Halangk W, et al. Presence of cathepsin B in the human pancreatic secretory pathway and its role in trypsinogen activation during hereditary pancreatitis. J Biol Chem. 2002;277(24):21389-96.

149. Hook V, Toneff T, Bogyo M, Greenbaum D, Medzihradszky KF, Neveu J, et al. Inhibition of cathepsin B reduces beta-amyloid production in regulated secretory vesicles of neuronal chromaffin cells: evidence for cathepsin B as a candidate beta-secretase of Alzheimer's disease (vol 386, pg 931, 2005). Biological Chemistry. 2005;386(12):1325-.

150. Cataldo AM, Nixon RA. Enzymatically active lysosomal proteases are associated with amyloid deposits in Alzheimer brain. Proc Natl Acad Sci U S A. 1990;87(10):3861-5.

151. Nagai A, Murakawa Y, Terashima M, Shimode K, Umegae N, Takeuchi H, et al. Cystatin C and cathepsin B in CSF from patients with inflammatory neurologic diseases. Neurology. 2000;55(12):1828-32.

152. Kennett CN, Cox SW, Eley BM. Ultrastructural localization of cathepsin B in gingival tissue from chronic periodontitis patients. Histochem J. 1997;29(10):727-34.

153. Berasain P, Goni F, McGonigle S, Dowd A, Dalton JP, Frangione B, et al. Proteinases secreted by *Fasciola hepatica* degrade extracellular matrix and basement membrane components. J Parasitol. 1997;83(1):1-5.

154. Fagbemi BO, Hillyer GV. Partial purification and characterisation of the proteolytic enzymes of *Fasciola gigantica* adult worms. Vet Parasitol. 1991;40(3-4):217-26.

155. Dalton JP, Caffrey CR, Sajid M, Stack C, Donnelly S, Loukas A, et al. Parasitic flatworms: molecular biology, biochemistry, immunology and physiology.2005.

156. Li Z, Yasuda Y, Li W, Bogyo M, Katz N, Gordon RE, et al. Regulation of collagenase activities of human cathepsins by glycosaminoglycans. J Biol Chem. 2004;279(7):5470-9.

157. McKerrow JH, McGrath ME, Engel JC. The cysteine protease of *Trypanosoma cruzi* as a model for antiparasite drug design. Parasitol Today. 1995;11(8):279-82.

158. Ultaigh SN, Carolan JC, Britton C, Murray L, Ryan MF. A cathepsin L-like protease from *Strongylus vulgaris*: an orthologue of *Caenorhabditis elegans* CPL-1. Exp Parasitol. 2009;121(4):293-9.

159. Dalton JP, Clough KA, Jones MK, Brindley PJ. Characterization of the cathepsin-like cysteine proteinases of *Schistosoma mansoni*. Infect Immun. 1996;64(4):1328-34.

160. Molina-Hernandez V, Mulcahy G, Perez J, Martinez-Moreno A, Donnelly S, O'Neill SM, et al. *Fasciola hepatica* vaccine: we may not be there yet but we're on the right road. Vet Parasitol. 2015;208(1-2):101-11.

161. Dalton JP, Neill SO, Stack C, Collins P, Walshe A, Sekiya M, et al. *Fasciola hepatica* cathepsin L-like proteases: biology, function, and potential in the development of first generation liver fluke vaccines. Int J Parasitol. 2003;33(11):1173-81.

162. Robinson MW, Tort JF, Lowther J, Donnelly SM, Wong E, Xu W, et al. Proteomics and phylogenetic analysis of the cathepsin L protease family of the helminth pathogen *Fasciola hepatica*: expansion of a repertoire of virulence-associated factors. Mol Cell Proteomics. 2008;7(6):1111-23.

163. Collins PR, Stack CM, O'Neill SM, Doyle S, Ryan T, Brennan GP, et al. Cathepsin L1, the major protease involved in liver fluke (*Fasciola hepatica*) virulence: propetide cleavage sites and autoactivation of the zymogen secreted from gastrodermal cells. J Biol Chem. 2004;279(17):17038-46.

164. Yamasaki H, Mineki R, Murayama K, Ito A, Aoki T. Characterisation and expression of the *Fasciola gigantica* cathepsin L gene. Int J Parasitol. 2002;32(8):1031-42.

165. Harmsen MM, Cornelissen JB, Buijs HE, Boersma WJ, Jeurissen SH, van Milligen FJ. Identification of a novel *Fasciola hepatica* cathepsin L protease containing protective epitopes within the propeptide. Int J Parasitol. 2004;34(6):675-82.

166. Dowd AJ, Dooley M, Fagain C, Dalton JP. Stability studies on the cathepsin L proteinase of the helminth parasite, *Fasciola hepatica*. Enzyme Microb Technol. 2000;27(8):599-604.

167. Dowd AJ, Smith AM, McGonigle S, Dalton JP. Purification and characterisation of a second cathepsin L proteinase secreted by the parasitic trematode *Fasciola hepatica*. Eur J Biochem. 1994;223(1):91-8.

168. Dowd AJ, Tort J, Roche L, Ryan T, Dalton JP. Isolation of a cDNA encoding *Fasciola hepatica* cathepsin L2 and functional expression in *Saccharomyces cerevisiae*. Mol Biochem Parasitol. 1997;88(1-2):163-74.

169. Grams R, Vichasri-Grams S, Sobhon P, Upatham ES, Viyanant V. Molecular cloning and characterization of cathepsin L encoding genes from *Fasciola gigantica*. Parasitol Int. 2001;50(2):105-14.

170. Carmona C, Dowd AJ, Smith AM, Dalton JP. Cathepsin L proteinase secreted by *Fasciola hepatica in vitro* prevents antibody-mediated eosinophil attachment to newly excysted juveniles. Mol Biochem Parasitol. 1993;62(1):9-17.

171. Prowse RK, Chaplin P, Robinson HC, Spithill TW. *Fasciola hepatica* cathepsin L suppresses sheep lymphocyte proliferation *in vitro* and modulates surface CD4 expression on human and ovine T cells. Parasite Immunol. 2002;24(2):57-66.

172. Smith AM, Dowd AJ, Heffernan M, Robertson CD, Dalton JP. *Fasciola hepatica*: a secreted cathepsin L-like proteinase cleaves host immunoglobulin. Int J Parasitol. 1993;23(8):977-83.

173. Alcala-Canto Y, Ibarra-Velarde F, Sumano-Lopez H, Gracia-Mora J, Alberti-Navarro A. Effect of a cysteine protease inhibitor on *Fasciola hepatica* (liver fluke) fecundity, egg viability, parasite burden, and size in experimentally infected sheep. Parasitol Res. 2007;100(3):461-5.

174. Hawthorne SJ, Pagano M, Halton DW, Walker B. Partial characterization of a novel cathepsin L-like protease from *Fasciola hepatica*. Biochem Biophys Res Commun. 2000;277(1):79-82.

175. Smooker PM, Jayaraj R, Pike RN, Spithill TW. Cathepsin B proteases of flukes: the key to facilitating parasite control? Trends Parasitol. 2010;26(10):506-14.

176. Meemon K, Grams R, Vichasri-Grams S, Hofmann A, Korge G, Viyanant V, et al. Molecular cloning and analysis of stage and tissue-specific expression of cathepsin B encoding genes from *Fasciola gigantica*. Mol Biochem Parasitol. 2004;136(1):1-10.

177. Creaney J, Wilson L, Dosen M, Sandeman RM, Spithill TW, Parsons JC. *Fasciola hepatica*: irradiation-induced alterations in carbohydrate and cathepsin-B protease expression in newly excysted juvenile liver fluke. Exp Parasitol. 1996;83(2):202-15.

178. Yang Y, Qin W, Wei H, Ying J, Zhen J. Characterization of cathepsin B proteinase (AcCP-2) in eggs and larvae stages of hookworm *Ancylostoma caninum*. Exp Parasitol. 2011;129(3):215-20.

179. Wilson LR, Good RT, Panaccio M, Wijffels GL, Sandeman RM, Spithill TW. *Fasciola hepatica*: characterization and cloning of the major cathepsin B protease secreted by newly excysted juvenile liver fluke. Exp Parasitol. 1998;88(2):85-94.

180. Malagon D, Diaz-Lopez M, Benitez R, Adroher FJ. Cathepsin B- and L-like cysteine protease activities during the *in vitro* development of *Hysterothylacium aduncum* (Nematoda: Anisakidae), a worldwide fish parasite. Parasitol Int. 2010;59(1):89-92.

181. McGonigle L, Mousley A, Marks NJ, Brennan GP, Dalton JP, Spithill TW, et al. The silencing of cysteine proteases in *Fasciola hepatica* newly excysted juveniles using RNA interference reduces gut penetration. Int J Parasitol. 2008;38(2):149-55.

182. Jayaraj R, Piedrafita D, Dynon K, Grams R, Spithill TW, Smooker PM. Vaccination against fasciolosis by a multivalent vaccine of stage-specific antigens. Vet Parasitol. 2009;160(3-4):230-6.

183. Liu YH, Han YP, Li ZY, Wei J, He HJ, Xu CZ, et al. Molecular cloning and characterization of cystatin, a cysteine protease inhibitor, from *Angiostrongylus cantonensis*. Parasitol Res. 2010;107(4):915-22.

184. Kang JM, Lee KH, Sohn WM, Na BK. Identification and functional characterization of CsStefin-1, a cysteine protease inhibitor of *Clonorchis sinensis*. Mol Biochem Parasitol. 2011;177(2):126-34.

185. He B, Cai G, Ni Y, Li Y, Zong H, He L. Characterization and expression of a novel cystatin gene from *Schistosoma japonicum*. Mol Cell Probes. 2011;25(4):186-93.

186. Cox SW, Eley BM. Detection of cathepsin B- and L-, elastase-, tryptase-, trypsin-, and dipeptidyl peptidase IV-like activities in crevicular fluid from gingivitis and periodontitis patients with peptidyl derivatives of 7-amino-4-trifluoromethyl coumarin. J Periodontal Res. 1989;24(6):353-61.

187. Köppel P, Baici A, Keist R, Matzku S, Keller R. Cathepsin B-Like Proteinase as a Marker for Metastatic Tumor Cell Variants. Expl Cell Biol. 1984;52(5):293-9.

188. Buttle DJ, Burnett D, Abrahamson M. Levels of neutrophil elastase and cathepsin B activities, and cystatins in human sputum: relationship to inflammation. Scand J Clin Lab Invest. 1990;50(5):509-16.

189. Assfalg-Machleidt I, Jochum M, Klaubert W, Inthorn D, Machleidt W. Enzymatically active cathepsin B dissociating from its inhibitor complexes is elevated in blood plasma of patients with septic shock and some malignant tumors. Biol Chem Hoppe Seyler. 1988;369 Suppl:263-9.

190. Rashid F, Sharma S, Bano B. Detailed biochemical characterization of human placental cystatin (HPC). Placenta. 2006;27(8):822-31.

191. Turk V, Bode W. The cystatins: protein inhibitors of cysteine proteinases. FEBS Lett. 1991;285(2):213-9.

192. Pol E, Olsson SL, Estrada S, Prasthofer TW, Bjork I. Characterization by spectroscopic, kinetic and equilibrium methods of the interaction between recombinant human cystatin A (stefin A) and cysteine proteinases. Biochem J. 1995;311 (Pt 1):275-82.

193. Dubin G. Proteinaceous cysteine protease inhibitors. Cell Mol Life Sci. 2005;62(6):653-69.

194. Turk B, Turk D, Salvesen GS. Regulating cysteine protease activity: essential role of protease inhibitors as guardians and regulators. Curr Pharm Des. 2002;8(18):1623-37.

195. Freije JP, Balbin M, Abrahamson M, Velasco G, Dalboge H, Grubb A, et al. Human cystatin D. cDNA cloning, characterization of the *Escherichia coli* expressed inhibitor, and identification of the native protein in saliva. J Biol Chem. 1993;268(21):15737-44.

196. Shaw PA, Yu WH. Sympathetic and parasympathetic regulation of cystatin S gene expression. Life Sci. 2001;70(3):301-13.

197. Zeeuwen PL, Van Vlijmen-Willems IM, Jansen BJ, Sotiropoulou G, Curfs JH, Meis JF, et al. Cystatin M/E expression is restricted to differentiated epidermal keratinocytes and sweat glands: a new skin-specific proteinase inhibitor that is a target for cross-linking by transglutaminase. J Invest Dermatol. 2001;116(5):693-701.

198. Cappello F, Gatti E, Camossetto V, David A, Lelouard H, Pierre P. Cystatin F is secreted, but artificial modification of its C-terminus can induce its endocytic targeting. Exp Cell Res. 2004;297(2):607-18.

199. Salvesen G, Parkes C, Abrahamson M, Grubb A, Barrett AJ. Human low-Mr kininogen contains three copies of a cystatin sequence that are divergent in structure and in inhibitory activity for cysteine proteinases. Biochem J. 1986;234(2):429-34.

200. Schmaier AH. The plasma kallikrein-kinin system counterbalances the renin-angiotensin system. J Clin Invest. 2002;109(8):1007-9.

201. Bjork I, Brieditis I, Abrahamson M. Probing the functional role of the N-terminal region of cystatins by equilibrium and kinetic studies of the binding of Gly-11 variants of recombinant human cystatin C to target proteinases. Biochem J. 1995;306 (Pt 2):513-8.

202. Hall A, Dalboge H, Grubb A, Abrahamson M. Importance of the evolutionarily conserved glycine residue in the N-terminal region of human cystatin C (Gly-11) for cysteine endopeptidase inhibition. Biochem J. 1993;291 (Pt 1):123-9.

203. Hartmann S, Lucius R. Modulation of host immune responses by nematode cystatins. Int J Parasitol. 2003;33(11):1291-302.

204. Magister S, Kos J. Cystatins in immune system. J Cancer. 2013;4(1):45-56.

205. Bode W, Engh R, Musil D, Laber B, Stubbs M, Huber R, et al. Mechanism of interaction of cysteine proteinases and their protein inhibitors as compared to the serine proteinase-inhibitor interaction. Biol Chem Hoppe Seyler. 1990;371 Suppl:111-8.

206. Fujisaki K, Kawazu S, Kamio T. The taxonomy of the bovine *Theileria* spp. Parasitol Today. 1994;10(1):31-3.

207. Jongejan F, Uilenberg G. The global importance of ticks. Parasitology. 2004;129 Suppl:S3-14.

208. Kotsyfakis M, Sa-Nunes A, Francischetti IM, Mather TN, Andersen JF, Ribeiro JM. Antiinflammatory and immunosuppressive activity of sialostatin L, a salivary cystatin from the tick *Ixodes scapularis*. J Biol Chem. 2006;281(36):26298-307.

209. Zhou J, Ueda M, Umemiya R, Battsetseg B, Boldbaatar D, Xuan X, et al. A secreted cystatin from the tick *Haemaphysalis longicornis* and its distinct expression patterns in relation to innate immunity. Insect Biochem Mol Biol. 2006;36(7):527-35.

210. Cancela M, Acosta D, Rinaldi G, Silva E, Duran R, Roche L, et al. A distinctive repertoire of cathepsins is expressed by juvenile invasive *Fasciola hepatica*. Biochimie. 2008;90(10):1461-75.

211. Beckham SA, Piedrafita D, Phillips CI, Samarawickrema N, Law RH, Smooker PM, et al. A major cathepsin B protease from the liver fluke *Fasciola hepatica* has atypical active site features and a potential role in the digestive tract of newly excysted juvenile parasites. Int J Biochem Cell Biol. 2009;41(7):1601-12.

212. Hartmann S, Schonemeyer A, Sonnenburg B, Vray B, Lucius R. Cystatins of filarial nematodes up-regulate the nitric oxide production of interferon-gamma-activated murine macrophages. Parasite Immunol. 2002;24(5):253-62.

213. Manoury B, Gregory WF, Maizels RM, Watts C. Bm-CPI-2, a cystatin homolog secreted by the filarial parasite *Brugia malayi*, inhibits class II MHC-restricted antigen processing. Curr Biol. 2001;11(6):447-51.

214. Pfaff AW, Schulz-Key H, Soboslay PT, Taylor DW, MacLennan K, Hoffmann WH. *Litomosoides sigmodontis* cystatin acts as an immunomodulator during experimental filariasis. Int J Parasitol. 2002;32(2):171-8.

215. Ochieng J, Chaudhuri G. Cystatin superfamily. J Health Care Poor Underserved. 2010;21(1 Suppl):51-70.

216. Nakagawa TY, Rudensky AY. The role of lysosomal proteinases in MHC class II-mediated antigen processing and presentation. Immunol Rev. 1999;172:121-9.

217. Shi GP, Bryant RA, Riese R, Verhelst S, Driessen C, Li Z, et al. Role for cathepsin F in invariant chain processing and major histocompatibility complex class II peptide loading by macrophages. J Exp Med. 2000;191(7):1177-86.

218. Riese RJ, Wolf PR, Bromme D, Natkin LR, Villadangos JA, Ploegh HL, et al. Essential role for cathepsin S in MHC class II-associated invariant chain processing and peptide loading. Immunity. 1996;4(4):357-66.

219. Vray B, Hartmann S, Hoebeke J. Immunomodulatory properties of cystatins. Cell Mol Life Sci. 2002;59(9):1503-12.

220. James SL. Role of nitric oxide in parasitic infections. Microbiol Rev. 1995;59(4):533-47.

221. Marletta MA. Nitric oxide synthase structure and mechanism. J Biol Chem. 1993;268(17):12231-4.

222. Denham S, Rowland IJ. Inhibition of the reactive proliferation of lymphocytes by activated macrophages: the role of nitric oxide. Clin Exp Immunol. 1992;87(1):157-62.

223. Kawabe T, Isobe KI, Hasegawa Y, Nakashima I, Shimokata K. Immunosuppressive activity induced by nitric oxide in culture supernatant of activated rat alveolar macrophages. Immunology. 1992;76(1):72-8.

224. Verdot L, Lalmanach G, Vercruysse V, Hoebeke J, Gauthier F, Vray B. Chicken cystatin stimulates nitric oxide release from interferon-gamma-activated mouse peritoneal macrophages via cytokine synthesis. Eur J Biochem. 1999;266(3):1111-7.

225. O'Connor RA, Jenson JS, Devaney E. NO contributes to proliferative suppression in a murine model of filariasis. Infect Immun. 2000;68(11):6101-7.

226. Corr-Menguy F, Cejudo FJ, Mazubert C, Vidal J, Lelandais-Briere C, Torres G, et al. Characterization of the expression of a wheat cystatin gene during caryopsis development. Plant Mol Biol. 2002;50(4-5):687-98.

227. Abe M, Abe K, Domoto C, Arai S. Two distinct species of corn cystatin in corn kernels. Biosci Biotechnol Biochem. 1995;59(4):756-8.

228. Botella MA, Xu Y, Prabha TN, Zhao Y, Narasimhan ML, Wilson KA, et al. Differential expression of soybean cysteine proteinase inhibitor genes during development and in response to wounding and methyl jasmonate. Plant Physiol. 1996;112(3):1201-10.

229. Kondo H, Abe K, Nishimura I, Watanabe H, Emori Y, Arai S. Two distinct cystatin species in rice seeds with different specificities against cysteine proteinases. Molecular cloning, expression, and biochemical studies on oryzacystatin-II. J Biol Chem. 1990;265(26):15832-7.

230. Cornwall GA, Hsia N. A new subgroup of the family 2 cystatins. Mol Cell Endocrinol. 2003;200(1-2):1-8.

231. Turk V, Stoka V, Vasiljeva O, Renko M, Sun T, Turk B, et al. Cysteine cathepsins: from structure, function and regulation to new frontiers. Biochim Biophys Acta. 2012;1824(1):68-88.

232. Law RH, Smooker PM, Irving JA, Piedrafita D, Ponting R, Kennedy NJ, et al. Cloning and expression of the major secreted cathepsin B-like protein from juvenile *Fasciola hepatica* and analysis of immunogenicity following liver fluke infection. Infect Immun. 2003;71(12):6921-32.

233. Saxena I, Tayyab S. Protein proteinase inhibitors from avian egg whites. Cell Mol Life Sci. 1997;53(1):13-23.

234. Chantree P, Wanichanon C, Phatsara M, Meemon K, Sobhon P. Characterization and expression of cathepsin B2 in *Fasciola gigantica*. Exp Parasitol. 2012;132(2):249-56.

235. Sethadavit M, Meemon K, Jardim A, Spithill TW, Sobhon P. Identification, expression and immunolocalization of cathepsin B3, a stage-specific antigen expressed by juvenile *Fasciola gigantica*. Acta Trop. 2009;112(2):164-73.

236. Siricoon S, Grams SV, Grams R. Efficient inhibition of cathepsin B by a secreted type 1 cystatin of *Fasciola gigantica*. Mol Biochem Parasitol. 2012;186(2):126-33.

237. Rozman J, Stojan J, Kuhelj R, Turk V, Turk B. Autocatalytic processing of recombinant human procathepsin B is a bimolecular process. FEBS Lett. 1999;459(3):358-62.

238. Caffrey CR, Salter JP, Lucas KD, Khiem D, Hsieh I, Lim KC, et al. SmCB2, a novel tegumental cathepsin B from adult *Schistosoma mansoni*. Mol Biochem Parasitol. 2002;121(1):49-61.

239. Lee J, Kim JH, Sohn HJ, Yang HJ, Na BK, Chwae YJ, et al. Novel cathepsin B and cathepsin B-like cysteine protease of *Naegleria fowleri* excretory-secretory proteins and their biochemical properties. Parasitol Res. 2014;113(8):2765-76.

240. Han YP, Li ZY, Li BC, Sun X, Zhu CC, Ling XT, et al. Molecular cloning and characterization of a cathepsin B from *Angiostrongylus cantonensis*. Parasitol Res. 2011;109(2):369-78.

241. Sajid M, McKerrow JH, Hansell E, Mathieu MA, Lucas KD, Hsieh I, et al. Functional expression and characterization of *Schistosoma mansoni* cathepsin B and its trans-

activation by an endogenous asparaginyl endopeptidase. Mol Biochem Parasitol. 2003;131(1):65-75.

242. Aronson NN, Jr., Barrett AJ. The specificity of cathepsin B. Hydrolysis of glucagon at the C-terminus by a peptidyldipeptidase mechanism. Biochem J. 1978;171(3):759-65.

APPENDICES

APPENDIX A

REAGENT PREPARATIONS

1. Preparation of antibiotic solution stock

1.1   Tetracycline (1000×)

Tetracycline 150 mg was dissolved in 10 ml of absolute ethanol, mixed until the solution become clear and sterilized by filtration through a 0.22 μm filter. The solution was separated into aliquots of 1 ml and then stored at −20℃ in light-tight containers.

1.2   Ampicillin (2000×)

Ampicillin 1000 mg was dissolved in 10 ml of DW, mixed until the solution become clear and sterilized by filtration through a 0.22 μm filter. The solution was separated into aliquots of 1 ml and then stored at −20℃.

1.3   Kanamycin (500×)

Kanamycin 250 mg was dissolved in 10 ml of DW, mixed until the solution become clear and sterilized by filtration through a 0.22 μm filter. The solution was separated into aliquots of 1 ml and then stored at −20℃.

2. Media for culture of *E. coli* bacteria

2.1 LB broth (1,000 ml)

Bacto peptone	10	g
Bacto yeast extract	5	g
NaCl	5	g

All components were dissolved in DW to a final volume of 1 liter, mixed until the solution become clear and then sterilized by autoclaving. The solution was stored at room temperature.

2.2 LB agar plates

Bacto peptone	10	g
Bacto yeast extract	5	g
NaCl	5	g
Agar	15	g

All components were dissolved in DW to a final volume of 1 liter, and then sterilized by autoclaving. The solution was cooled down to 60°C, poured into petri dishes, allowed to harden at room temperature for 1–2 h and stored at 4°C.

2.3 LB/Tetracycline agar plates

Bacto peptone	10	g
Bacto yeast extract	5	g
NaCl	5	g
Agar	15	g

All components were dissolved in DW to a final volume of 1 liter, and then sterilized by autoclaving. The solution was cooled down to 60°C, tetracycline stock solution was added to a final concentration of 12.5 μg/ml, poured into petri dishes, allowed to harden at room temperature for 1–2 h and stored at 4°C (protected from light).

2.4 LB/Ampicillin agar plates

Bacto peptone	10	g
Bacto yeast extract	5	g

NaCl	5	g
Agar	15	g

All components were dissolved in DW to a final volume of 1 liter, and then sterilized by autoclaving. The solution was cooled down to 60°C, ampicillin stock solution was added to a final concentration of 100 µg/ml, poured into petri dishes, allowed to harden at room temperature for 1–2 h and stored at 4°C.

2.5   LB/Ampicillin+Kanamycin agar plates

Bacto peptone	10	g
Bacto yeast extract	5	g
NaCl	5	g
Agar	15	g

All components were dissolved in DW to a final volume of 1 liters, and then sterilized by autoclaving. The solution was cooled down to 60°C, ampicillin stock solution was added to a final concentration of 100 µg/ml and kanamycin to a final concentration of 25 µg/ml, poured into petri dishes, allowed to harden at room temperature for 1–2 h and stored at 4°C.

3. Reagents for agarose gel electrophoresis

3.1   Ethidium bromide stock (10 mg/ml)

One gram of ethidium bromide was dissolved in 100 ml of DW and stored at 4°C (protected from light).

3.2   TBE buffer (5×)

Tris base	52.00	g
Boric acid	27.50	g
Disodium EDTA·2H$_2$O	4.65	g

All components were dissolved in DW to a final volume of 1 liter and mixed until the solution become clear.

3.3   TBE running buffer (0.5×)

5× TBE buffer	100	ml
10 mg/ml ethidium bromide	50	µl

All solutions were diluted in DW to a final volume of 1 liter and mixed until the solution become homogeneous.

3.4   Agarose gel electrophoresis (100 ml)

Agarose powder	0.7–1.2	g
0.5× TBE running buffer	100	ml

The amount of agarose powder depended on the percentage of agarose gel in the experiments. The agarose suspension was heated in a microwave until the agarose was completely dissolved and then DW was added to adjust the volume back to 100 ml. Pour mixture into the gel cassette after solution is cooled to 50–60°C. Allow gel to harden for at least 45 min before use.

3.5   Sample loading solution (10×)

Bromophenol blue	0.025	g
Xylene cyanol FF	0.025	g
Glycerol	5	ml
DW	5	ml

All components were mixed by inverting the closed tube until the mixture became homogeneous before the solution was stored at 4°C. One microliter

of 10× sample loading solution was mixed with 9 µl DNA sample (final concentration 1×) before loading into the well of an agarose gel.

4. Reagents for isolation of plasmid DNA from *E. coli* (quick preparation)

4.1 Tris-HCl, pH 8.0 stock solution (2 M, 100 ml)

Tris-HCl   24.23   g

This component was dissolved in DW, adjusted to pH 8.0 by using HCl and added DW up to a final volume of 100 ml. The solution was sterilized by autoclaving and stored at room temperature.

4.2 Glucose stock solution (1 M, 100 ml)

Glucose   18   g

This component was dissolved in DW to a final volume of 100 ml and mixed until the solution become clear. The solution was sterilized by filtration through a 0.22 µm filter and stored at 4°C.

4.3 EDTA, pH 8.0 stock solution (0.5 M, 100 ml)

EDTA·Na$_2$·H$_2$O   18.6   g

This component was dissolved in DW, adjusted to pH 8.0 by using NaOH and added DW up to a final volume of 100 ml. The solution was sterilized by autoclaving and stored at room temperature.

4.4 NaOH stock solution (1 N, 100 ml)

NaOH   4   g

This component was dissolved in DW to a final volume of 100 ml. The solution was sterilized by autoclaving and stored at room temperature.

4.5 20% SDS stock solution (100 ml)

Sodium dodecyl sulfate (SDS)   20   g

This component was dissolved in DW to a final volume of 100 ml, mixed until the solution become clear and stored at room temperature.

4.6 Solution I (25 mM Tris-HCl, pH 8.0, 50 mM glucose and 10 mM EDTA pH 8.0)

2 M Tris-HCl pH 8.0   1.25   ml

2 M Glucose 2.50 ml

0.5 M EDTA pH 8.0 200 µl

All components were dissolved in DW to a final volume of 100 ml.

4.7 Solution II (0.1 N NaOH and 1% SDS)

1 N NaOH 1.0 ml

20% (w/v) SDS 0.5 ml

All solutions were diluted in DW to a final volume of 10 ml and mixed until the solution became homogeneous. The solution was freshly prepared before use.

4.8 Solution III (2.7 M potassium acetate, pH 4.8)

Potassium acetate 26.5 g

This component was dissolved in DW, adjusted to pH 4.8 by using acetic acid and added DW up to a final volume of 100 ml. The solution was sterilized by autoclaving and stored at room temperature.

4.9 70% Ethanol

Absolute ethanol 70 ml

The ethanol was mixed with DW to a final volume of 100 ml.

5. Reagents for preparation of competent cell and transformation

5.1 MgCl$_2$ stock solution (1 M, 100 ml)

MgCl$_2$ (anhydrous)   9.5   g

This component was dissolved in DW to a final volume of 100 ml and mixed until the solution become clear. The solution was sterilized by filtration through a 0.22 μm filter and stored at room temperature.

5.2 CaCl$_2$ stock solution (1 M, 100 ml)

CaCl$_2$ (anhydrous)   11   g

This component was dissolved in DW to a final volume of 100 ml and mixed until the solution become clear. The solution was sterilized by filtration through a 0.22 μm filter and stored at room temperature.

5.3 0.1 M MgCl$_2$

1 M MgCl$_2$ 10   ml

This solution was diluted in DW to a final volume of 100 ml and mixed until the solution become homogeneous.

5.4 0.1 M CaCl$_2$

1 M CaCl$_2$ 10   ml

This solution was diluted in DW to a final volume of 100 ml and mixed until the solution become homogeneous.

5.5 Glycerol (100%)

Glycerol   100   ml

The solution was sterilized by autoclaving and stored at room temperature.

6. Reagents for preparation of newly excysted juveniles excystment

6.1 Solution I (1% pepsin and 0.4% HCl)

Pepsin   1   g

HCl   400   µl

All components were dissolved in DW to a final volume of 100 ml.

6.2 Solution II (20 mM $Na_2O_4S_2$, 0.2% Taurocholic acid, 1% $NaHCO_3$, 0.8% NaCl and 0.6% HCl)

$Na_2O_4S_2$ 0.35   g

Taurocholic acid   0.2   g

$NaHCO_3$ 1   g

NaCl   0.8   g

HCl   600   µl

All components were dissolved in DW to a final volume of 100 ml.

7. Reagents for genomic DNA extraction

7.1 NaCl stock solution (5 M, 100 ml)

NaCl   29.2   g

This component was dissolved in DW to a final volume of 100 ml and mixed until the solution become clear. The solution was sterilized by autoclaving and stored at room temperature.

7.2 Tris-HCl, pH 8.0 stock solution (2 M, 100 ml)

Tris-HCl   24.23   g

This component was dissolved in DW, adjusted to pH 8.0 by using HCl and added DW up to a final volume of 100 ml. The solution was sterilized by autoclaving and stored at room temperature.

7.3 EDTA, pH 8.0 stock solution (0.5 M, 100 ml)

EDTA·Na_2·H_2O 18.6   g

This component was dissolved in DW, adjusted to pH 8.0 by using NaOH and added DW up to a final volume of 100 ml. The solution was sterilized by autoclaving and stored at room temperature.

7.4   Homogenization buffer (30 mM Tris-HCl, pH 8.0, 0.1 mM NaCl, 10 mM EDTA and 0.5% Triton X-100)

2 M Tris-HCl pH 8.0   1.5   ml

5 M NaCl   2.0   ml

0.5 M EDTA pH 8.0   2.0   ml

All solutions were diluted in DW to a final volume of 100 ml and then added 0.5 ml of Triton X-100 to the solution. The solution was mixed until become homogeneous.

7.5   Extraction buffer (0.1 M Tris-HCl, pH 8.0, 0.1 mM NaCl, 20 mM EDTA)

2 M Tris-HCl pH 8.0   5   ml

5 M NaCl   2   ml

0.5 M EDTA, pH 8.0   4   ml

All solutions were diluted in DW to a final volume of 100 ml and mixed until become homogeneous.

8. Reagent for Southern hybridization and Northern hybridization

8.1 Tris-HCl, pH 8.0 stock solution (2 M, 100 ml)

Tris-HCl 24.23 g

This component was dissolved in DW, adjusted pH to 8.0 by using HCl and added DW up to a final volume of 100 ml. The solution was sterilized by autoclaving and stored at room temperature.

8.2 NaOH stock solution (5 N, 100 ml)

NaOH 20 g

This component was dissolved in DW to a final volume of 100 ml and mixed until the solution become clear. The solution was sterilized by autoclaving and stored at room temperature.

8.3 NaCl stock solution (5 M, 100 ml)

NaCl 29.2 g

This component was dissolved in DW to a final volume of 100 ml and mixed until the solution become clear. The solution was sterilized by autoclaving and stored at room temperature.

8.4 Sodium acetate stock solution pH 7.0 (1 M, 100 ml)

Sodium acetate 29.4 g

This component was dissolved in DW, adjusted pH to 7.0 by using citric acid and added DW up to a final volume of 100 ml. The solution was sterilized by autoclaving and stored at room temperature.

8.5 Sodium acetate stock solution (3 M, 100 ml)

Sodium acetate 24.6 g

This component was dissolved in DW, adjusted pH to 7.0 by using glacial acetic acid and added DW up to a final volume of 100 ml. The solution was sterilized by autoclaving and stored at room temperature.

8.6 20% SDS stock solution (100 ml)

Sodium dodecyl sulfate (SDS) 20 g

This component was dissolved in DW to a final volume of 100 ml, mixed until the solution become clear and stored at room temperature.

8.7 EDTA, pH 8.0 stock solution (0.5 M, 100 ml)

EDTA·Na$_2$·H$_2$O   18.6   g

This component was dissolved in DW, adjusted pH to 8.0 by using NaOH and added DW up to a final volume of 100 ml. The solution was sterilized by autoclaving and stored at room temperature.

8.8 Glycerol (100%)

Glycerol   100   ml

The solution was sterilized by autoclaving and stored at room temperature.

8.9 DEPC-treated water

One milliliter of DEPC was added into 1,000 ml DW and mixed well by shaking. The open bottle was incubated in fume hood overnight to remove CO$_2$, sterilized by autoclaving and stored at room temperature.

8.10 20× Saline-Sodium citrate (SSC) stock solution (3 M NaCl and 0.3 M sodium citrate pH 7.0)

NaCl   175.3   g

1 M Sodium citrate, pH 7.0   300.0   ml

All component were dissolved in DW to a final volume of 1,000 ml and mixed until the solution become clear.

8.11 Maleic acid buffer (0.1 M Maleic acid and 0.15 M NaCl, pH 7.5)

Maleic acid   11.6   g

5 M NaCl   30.0   ml

All component were dissolved in DW, adjusted to pH 7.5 by using NaOH (pellets) and added DW up to a final volume of 1,000 ml. The solution was sterilized by autoclaving and stored at room temperature.

8.12 Maleic acid washing buffer (0.1 M Maleic acid, 0.15 M NaCl, pH 7.5 and 0.3% Tween® 20)

Maleic acid buffer   100   ml

Tween® 20   0.3   ml

All solutions were mixed until become homogeneous and the solution was freshly prepared before use.

8.13 Blocking reagent (10×)

The solution was prepared by dissolving 10 g of blocking powder (Roche, Germany) in maleic acid buffer up to a final volume of 100 ml with constantly stirring on a heating block (65°C) or in a microwave. The solution was sterilized by autoclaving and stored at −20°C.

8.14 Blocking reagent (1×)

10× Blocking reagent   10   ml

Maleic acid buffer   90   ml

All solutions were mixed until become homogeneous.

8.15 3-Morpholinopropane acid stock solution (1 M MOPS, pH 7.0)

MOPS   209.26   g

This component was dissolved in DW, adjusted to pH 7.0 by using NaOH and added DW up to a final volume of 1,000 ml. The solution was sterilized by autoclaving and stored at room temperature (protected from light).

8.16 10× MOPS buffer (0.2 M MOPS, pH 7.0, 50 mM sodium acetate, 10 mM EDTA)

1 M MOPS, pH 7.0   200.00   ml

3 M Sodium acetate   16.67   ml

0.5 M EDTA   20.00   ml

All solutions were diluted in DW to a final volume of 1,000 ml and mixed until the solution was homogeneous. The solution was sterilized by autoclaving and stored at room temperature (protected from light).

8.17 Denaturing solution (0.5 N NaOH and 3 M NaCl)

5 N NaOH   10   ml

5 M NaCl   30   ml

All solutions were diluted in DW to a final volume of 100 ml and mixed until the solution was homogeneous.

8.18 Neutralizing solution (0.5 M Tris-HCl, pH 7.0 and 1.5 M NaCl)

2 M Tris-HCl, pH 7.0   25   ml

5 M NaCl   30   ml

All solutions were diluted in DW to a final volume of 100 ml and mixed until the solution was homogeneous.

8.19 **Hybridization solution (50% formamide, 5× SSC, 2% (v/v) blocking solution, 100 µg/ml herring sperm and 0.02% SDS)**

100% Formamide	50	ml
20× SSC	25	ml
10× Blocking solution	20	ml
10 mg/ml Herring sperm DNA	0.1	ml
(Heat-denatured 5 min at 100°C)		
20% SDS	2.5	ml

All solutions were diluted in DW to a final volume of 100 ml and mixed until the solution was homogeneous.

8.20 **Washing buffer I (2× SSC and 0.1% SDS)**

20× SSC	100	ml
20% SDS	5	ml

All solutions were diluted in DW to a final volume of 1,000 ml and mixed until the solution was homogeneous.

8.21 **Washing buffer II (0.1× SSC and 0.1% SDS)**

20× SSC	5	ml
20% SDS	5	ml

All solutions were diluted in DW to a final volume of 1,000 ml and mixed until the solution was homogeneous.

8.22 **Detection buffer (0.1 M Tris-HCl, 0.1 M NaCl and 50 mM MgCl$_2$, pH 9.5)**

Tris-HCl	12.1	g
NaCl	5.8	g
MgCl$_2$	5.8	g

All component were dissolved in DW, adjusted to pH 9.5 by using HCl and added DW up to a final volume of 1,000 ml. The solution was sterilized by autoclaving and stored at room temperature.

8.23 RNA sample loading buffer (2x)

Bromophenol blue	30	mg
Glycerol	5	ml
DEPC-treated water	5	ml

All component were mixed until the solution become clear and sterilized by filtration through a 0.22 μm filter. The solution was separated into aliquots of 1 ml and then stored at −20°C in light-tight containers.

8.24 Formaldehyde-denaturing agarose gel (2.2 M Formaldehyde and 1.2% agarose gel)

1.2 g of agarose power was dissolved in 72.58 ml DEPC-treated water by heating in a microwave oven, 10 ml of 10× MOPS buffer was added and 17.42 ml of 38% formaldehyde (12.6 M) after the solution had cooled down to 50–55°C. The solution was mixed well and immediately poured into the gel cassette under a fume hood, allowed to harden at room temperature for at least 45 min before use.

9. Reagents for protein purification by Ni-NTA affinity chromatography under native conditions

9.1 NaCl stock solution (5 M, 100 ml)

NaCl   29.2   g

This component was dissolved in DW to a final volume of 100 ml and mixed until the solution become clear.   The solution was sterilized by autoclaving and stored at room temperature.

9.2 $NaH_2PO_4 \cdot H_2O$ stock solution (1 M, 100 ml)

$NaH_2PO_4 \cdot H_2O$ 13.8   g

This component was dissolved in DW to a final volume of 100 ml and mixed until the solution become clear.   The solution was sterilized by autoclaving and stored at room temperature.

9.3 Imidazole stock solution (1 M, 100 ml)

Imidazole   6.8   g

This component was dissolved in DW to a final volume of 100 ml and mixed until the solution become clear. The solution was sterilized by filtration through a 0.22 μm filter and stored at room temperature.

9.4 Denaturing lysis buffer (100 mM NaH_2PO_4, 10 mM Tris-HCl and 8 M urea, pH 8.0)

$NaH_2PO_4 \cdot H_2O$	13.8	g
Tris-HCl	1.2	g
Urea	480.5	g

All component were dissolved in DW, adjusted to pH 8.0 by using NaOH and DW was added to a final volume of 1,000 ml. The solution was sterilized by autoclaving and stored at room temperature.

9.5 Native lysis buffer (50 mM NaH_2PO_4, 300 mM NaCl and 10 mM imidazole, pH 8.0)

1 M NaH_2PO_4	5	ml
2 M NaCl	15	ml
1 M Imidazole	1	ml

All solutions were diluted in DW, adjusted to pH 8.0 with NaOH and then DW was added to a final volume of 100 ml. The solution was mixed well, sterilized by filtration through a 0.22 μm filter and stored at room temperature.

9.6   Washing buffer (50 mM NaH$_2$PO$_4$, 300 mM NaCl and 20 mM imidazole, pH 8.0)

1 M NaH$_2$PO$_4$	5	ml
2 M NaCl	15	ml
1 M Imidazole	2	ml

All solutions were diluted in DW, adjusted to pH 8.0 with NaOH and then DW was added to a final volume of 100 ml. The solution was mixed well, sterilized by filtration through a 0.22 μm filter and stored at room temperature.

9.7   Elution buffer (50 mM NaH$_2$PO$_4$, 300 mM NaCl and 250 mM imidazole, pH 8.0)

1 M NaH$_2$PO$_4$	5	ml
2 M NaCl	15	ml
1 M Imidazole	25	ml

All solutions were diluted in DW, adjusted to pH 8.0 with NaOH and then DW was added to a final volume of 100 ml. The solution was mixed well, sterilized by filtration through a 0.22 μm filter and stored at room temperature.

10. Reagents for Sodium Dodecyl Sulfate Polyacrylamide Gel Electrophoresis (SDS-PAGE), Tris-Glycine system for 1 gel

     10.1 Acrylamide stock solution (30% w/v)

        Acrylamide   30.0 g

        Bis-acrylamide   0.8 g

        All components were dissolved in DW to a final volume of 100 ml.
The solution was mixed until solution become clear and stored at 4°C (protected from light).

     10.2 Preparation of acrylamide gel

	Separating gel		Stacking gel	
	12.5%	16%	4%	
30% Acrylamide stock	3.13	4.00	0.33	ml
1.5 M Tris-HCl, pH 8.8	1.88	1.88	-	ml
0.5 M Tris-HCl, pH 6.8	-	-	0.63	ml
DW	2.38	1.51	1.50	ml
10% SDS	0.08	0.08	0.03	ml
10% Ammonium persulfate	37.50	37.50	12.50	µl
TEMED	2.50	2.50	1.25	µl

     10.3 2x Sample buffer (125 mM Tris-HCl, pH 6.8, 4% SDS, 20% glycerol, 0.2 M DTT and 0.02% bromophenol blue)

        1 M Tris-HCl, pH 6.8   1.25 ml

        20% SDS   2.00 ml

        Glycerol   2.00 ml

        DTT   0.30 g

        1% Bromophenol blue   0.20 ml

        All components were dissolved in DW to a final volume of 10 ml.
The solution was mixed well, separated into aliquots of 1 ml and then stored at −20°C.

10.4 Electrophoresis buffer (0.1 M Tris, 0.1 M Tricine, and 0.1% [w/v] SDS)

Tris-base   3.03   g

Glycine   15.20   g

SDS   1.00   g

All components were dissolved in DW to a final volume of 1,000 ml. The solution was mixed until it was clear and stored at 4°C.
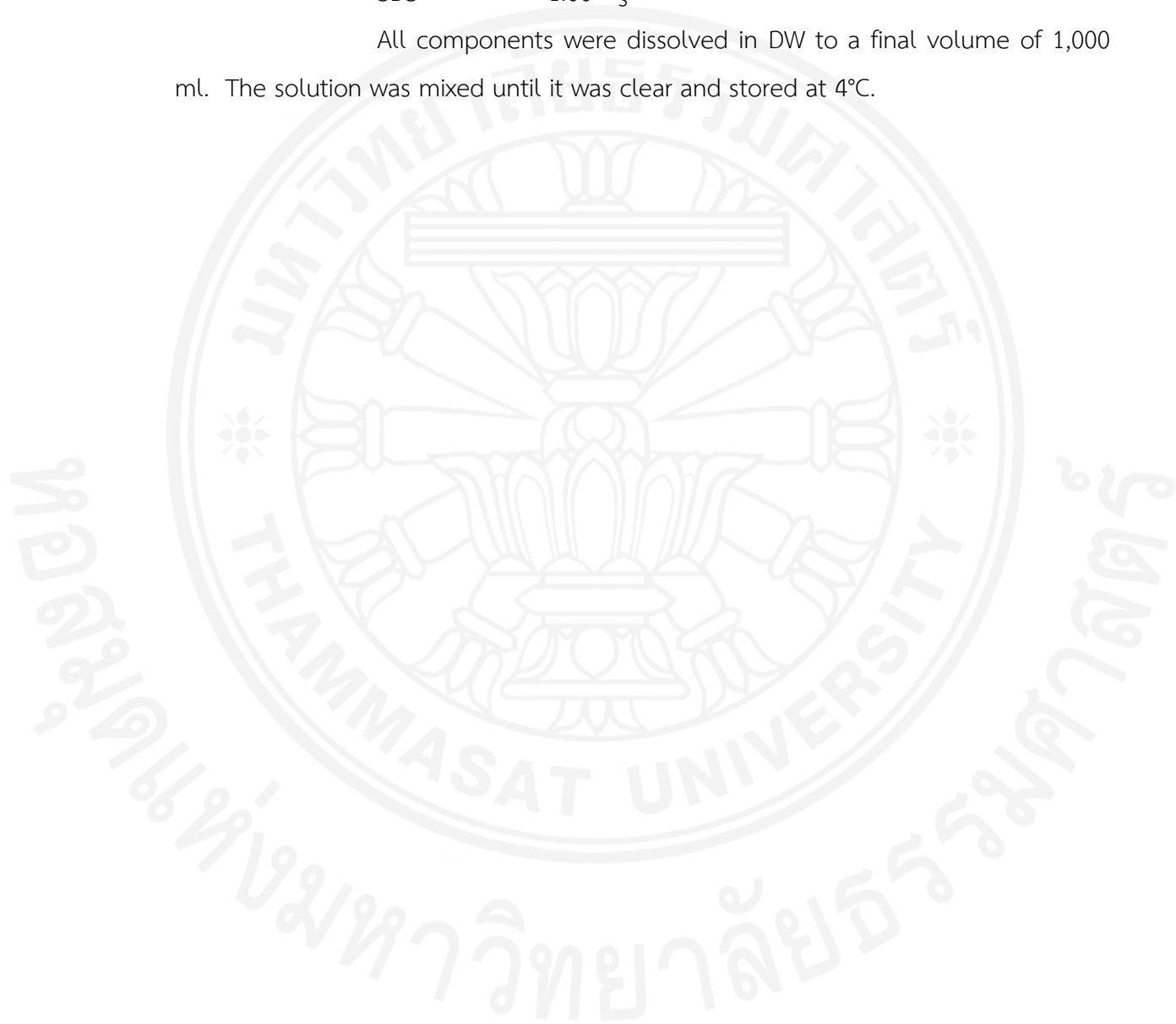
11. Reagent for SDS polyacrylamide gel staining

11.1 0.025% Coomassie Blue R-250

Coomassie Blue R-250	0.25	g
Methanol	400	ml
DW	530	ml
Acetic acid	70	ml

All components except acetic acid were mixed until the solution was homogeneous, filtered through Whatman filter paper and added acetic acid.

11.2 0.5% Coomassie Blue G-250

Coomassie Blue G-250	0.5	g
Methanol	40	ml
DW	53	ml
Acetic acid	7	ml

All components except acetic acid were mixed until the solution was homogeneous, filtered through Whatman filter paper and added acetic acid.

11.3 High methanol destaining solution I

Methanol	400	ml
Acetic acid	70	ml

All solutions were diluted in DW to a final volume of 1,000 ml and mixed well.

11.4 Low methanol destaining solution II

Methanol	50	ml
Acetic acid	70	ml

All solutions were diluted in DW to a final volume of 1,000 ml and mixed well.

11.5 Glycerol (1%)

Glycerol	10	ml
DW	990	ml

All solutions were mixed well, sterilized by autoclaving and stored at room temperature.

12. Reagents for immunoblot and immunodetection

12.1 MgCl$_2$ stock solution (5 M, 100 ml)

MgCl$_2$ (anhydrous)   47.5   g

This component was dissolved in DW to a final volume of 100 ml and mixed until the solution became clear. The solution was sterilized by filtration through a 0.22 µm filter and stored at room temperature.

12.2 NaCl stock solution (5 M, 100 ml)

NaCl   29.2   g

This component was dissolved in DW to a final volume of 100 ml and mixed until the solution became clear. The solution was sterilized by autoclaving and stored at room temperature.

12.3 Tris-HCl, pH 7.5 stock solution (2 M, 100 ml)

Tris-HCl   24.23   g

This component was dissolved in DW, adjusted to pH 7.5 by using HCl and added DW up to a final volume of 100 ml. The solution was sterilized by autoclaving and stored at room temperature.

12.4 TBS (20 mM Tris, pH 7.5, 150 mM NaCl)

2 M Tris-base, pH 7.5   10   ml

5 M NaCl   30   ml

All solutions were diluted in DW to a final volume of 1,000 ml and mixed well.

12.5 Semi-dry transfer buffer

Glycine   2.93   g

Tris-base   5.81   g

SDS   0.375   g

Methanol   200.00   ml

All solutions were diluted in DW to a final volume of 1,000 ml, mixed until the solution became clear and stored at 4°C.

12.6 Ponceau S staining solution (0.1% w/v Ponceau S dye and 5% v/v acetic acid)

Ponceau S	0.25	g
Acetic acid	12.5	ml
DW	237.5	ml

Ponceau S was dissolved in DW until the solution became homogeneous, acetic acid was added and the solution was stored at room temperature.

12.7 Blocking solution (5% Skim milk)

Skim milk 5 g

This component was dissolved in TBS, pH 7.5, to a final volume of 100 ml and mixed until the solution became homogeneous.

12.8 Antibody diluent (1% Skim milk)

Skim milk 0.5 g

This component was dissolved in TBS, pH 7.5, to a final volume of 50 ml and mixed until the solution became homogeneous.

12.9 Washing buffer (TBS, pH 7.5 and 0.5% Tween 20)

TBS, pH 7.5	999.5	ml
Tween® 20	0.5	ml

All components were mixed until the solution became homogeneous. The solution was freshly prepared before use.

12.10 Substrate buffer for BCIP/NBT dilution (0.1 M Tris-HCl, pH 9.5, 0.1 M NaCl and 50 mM $MgCl_2$)

2 M Tris-base pH 9.5	20	ml
5 M NaCl	8	ml
5 M $MgCl_2$	20	ml

All solutions were diluted in DW to a final volume of 400 ml, mixed until the solution became clear and stored at room temperature.

13. Reagents for preparation of crude worm protein extract and excretory-secretory product

13.1 10× PBS (0.1 M)

$NaH_2PO_4 \cdot H_2O$	4.55	g
$Na_2HPO_4 \cdot 2H_2O$	11.85	g
NaCl	85.00	g

All components were dissolved in DW, adjusted to pH 7.2 and DW was added to a final volume of 1,000 ml. The solution was sterilized by autoclaving and stored at room temperature.

13.2 Tris-HCl, pH 7.2 stock solution (2 M, 100 ml)

Tris-HCl   24.23 g

This component was dissolved in DW, adjusted to pH 7.2 by using HCl and DW was added to a final volume of 100 ml. The solution was sterilized by autoclaving and stored at room temperature.

13.3 NaCl stock solution (5 M, 100 ml)

NaCl   29.2 g

This component was dissolved in DW to a final volume of 100 ml and mixed until the solution became clear. The solution was sterilized by autoclaving and stored at room temperature.

13.4 EDTA, pH 8.0 stock solution (0.5 M, 100 ml)

$EDTA \cdot Na_2 \cdot H_2O$ 18.6 g

This component was dissolved in DW, adjusted to pH 8.0 by using NaOH and DW was added to a final volume of 100 ml. The solution was sterilized by autoclaving and stored at room temperature.

13.5 0.85%NaCl

NaCl   8.5 g

All components were dissolved in DW to a final volume of 1,000 ml. The solution was sterilized by autoclaving and stored at room temperature.

13.6 Lysis buffer (10 mM Tris-HCl, pH 7.2, 150 mM NaCl, 0.5% Triton X-100, 1 mM PMSF, and 1 mM EDTA)

2 M Tris-HCl, pH 7.2	0.5	ml
Triton-X 100	1.0	ml
PMSF	0.17	mg
5 M NaCl	3	ml
0.5 M EDTA	0.1	ml

All components were dissolved in DW to a final volume of 100 ml. The solution was mixed until it became clear and stored at room temperature.

13.7 Sodium acetate (0.1 M, 100 ml)

Sodium acetate   0.82   g

This component was dissolved in DW, adjusted to pH 5.0 by using glacial acetic acid and added DW up to a final volume of 100 ml. The solution was sterilized by autoclaving and stored at room temperature.

13.8 Lysis buffer for preparation of crude extract of *F. gigantica* metacercariae (1% (w/v) pepsin and 0.4% (v/v) HCl)

Pepsin	1	g
HCl	0.4	ml

All components were dissolved in DW to a final volume of 100 ml. The solution was mixed until it became clear and stored at room temperature.

14. Reagents for immunohistochemistry buffers

14.1 Fixative solution (4% w/v paraformaldehyde)

Paraformaldehyde   4   g

This component was dissolved in 10 ml 0.1 M PBS, pH 7.2 and 70 ml DW by adding 1 drop of 2 N NaOH and heating at 65°C, the volume was adjusted by DW to 100 ml. The solution was mixed until it became clear and stored at 4°C.

14.2 TBS (20 mM Tris, pH 7.6, 150 mM NaCl)

2 M Tris-base, pH 7.6   10   ml

5 M NaCl   30   ml

All solutions were diluted in DW to a final volume of 1,000 ml and mixed well.

14.3 1× PBS (0.01 M)

$NaH_2PO_4 \cdot H_2O$ 0.455   g

$Na_2HPO_4 \cdot 2H_2O$ 1.185   g

NaCl   8.5   g

All components were dissolved in DW, adjusted to pH 7.2 and adjusted to a final volume of 1,000 ml with DW. The solution was sterilized by autoclaving and stored at room temperature.

14.4 Washing buffer (0.01M PBS pH 7.2 and 0.1% Tween® 20)

0.01 M PBS, pH 7.2   999.9   ml

Tween® 20   0.1   ml

All components were mixed until the solution was homogeneous. The solution was freshly prepared before use.

14.5 Glycine buffer (0.1% Glycine in PBS)

Glycine   0.1   g

This component was dissolved in 0.01 M PBS pH 7.2 to a final volume of 100 ml and mixed until it became clear.

14.6 Blocking solution (4% BSA in PBS)

BSA   0.4   g

This component was dissolved in 0.01 M PBS pH 7.2 to a final volume of 10 ml and mixed until the solution became clear.

14.7 Antibody diluent (1% BSA in PBS)

BSA   0.1   g

This component was dissolved in 0.01 M PBS pH 7.2 to a final volume of 10 ml and mixed until the solution became clear.

14.8 ABComplex/HRP

One drop of reagent A to 5 ml of TBS, pH 7.6 and then add 1 drop of reagent B and 1 drop of reagent C. The solution was mixed well and used within 30 min (protected from light)

14.9 Mounting medium

Glycerol   1   ml

0.01 M PBS, pH 7.2   9   ml

All components were mixed until the solution was homogeneous.

14.10 Gelatin coating solution

Gelatin	1.5	g
Chromium potassium sulfate	0.25	g

All components were added to DW at a final volume of 500 ml and heated at 60℃ until completely dissolved. The solution was cooled down to room temperature before used.

15. Reagents for Enzyme Linked-Immunosorbent Assay (ELISA)

      15.1   Coating buffer (30 mM Na_2CO_3 and 75 mM $NaHCO_3$, pH 9.6)

          Na_2CO_3 3.18 g

          $NaHCO_3$ 6.30 g

All components were dissolved in DW, adjusted to pH 9.6 and DW was added to a final volume of 1,000 ml. The solution was sterilized by autoclaving and stored at 4°C.

      15.2   Blocking solution

          BSA   0.25 g

This component was dissolved in 0.01 M PBS, pH 7.2 to a final volume of 100 ml.

      15.3   Washing buffer (0.01 M PBS, pH 7.2, 0.5% Tween 20)

          0.01 M PBS, pH 7.2   999.5 ml

          Tween® 20   0.5 ml

All components were mixed until the solution was homogeneous. The solution was freshly prepared before use.

16. Reagents for inhibitory activity analysis

> **16.1 2× Cat L assay buffer (680 mM sodium acetate, 120 mM acetic acid, 8 mM EDTA, 16 mM DTT, pH 5.5)**
>
> | | | |
> |---|---|---|
> | 1 M Sodium acetate | 68.0 | ml |
> | Acetic acid | 686.0 | µl |
> | 0.5 M EDTA | 1.6 | ml |

All components were mixed in DW, adjusted to pH 5.5 and DW was added to a final volume of 98.4 ml. The solution was sterilized by autoclaving, added 1 M DTT to 984 µl 2× Cat L assay buffer just before use and stored at room temperature.

> **16.2 2× Cat B-cystatin assay buffer (100 mM MES, 400 mM NaCl, 2 mM EDTA, 2 mM DTT, pH 6.0)**
>
> | | | |
> |---|---|---|
> | MES | 1.95 | g |
> | NaCl | 2.34 | g |
> | 0.5 M EDTA | 0.40 | ml |

All components were dissolved in DW, adjusted to pH 6.0 and added DW up to a final volume of 99.8 ml. The solution was sterilized by autoclaving, added 2 µl 1 M DTT to 998 µl 2× Cat B-cystatin assay buffer just before use and stored at room temperature.

17. Reagent for zymography analysis

17.1 **5× Native sample loading buffer (0.313 M Tris–HCl, pH 6.8, 50% [v/v] glycerol, 0.05% bromophenol blue)**

1 M Tris-HCl, pH 6.8	3.1	ml
Glycerol	5.0	ml
1% Bromophenol blue	0.5	ml

All components were mixed in DW to a final volume of 10 ml. The solution was mixed well, separated into aliquots of 1 ml and then stored at −20°C.

17.2 **Preparation of 10% polyacrylamide gel containing 0.1% gelatin**

	10% Separating gel	5% Stacking gel	
30% Acrylamide stock	5.00	0.75	ml
1.5 M Tris-HCl, pH 8.8	3.75	-	ml
0.5 M Tris-HCl, pH 6.8	-	1.25	ml
DW	3.08	2.95	ml
10% SDS	0.15	0.05	ml
10% Ammonium persulfate	100.00	50.00	µl
TEMED	15.00	5.00	µl
0.5% Gelatin	3.02	-	ml

17.3 **Triton X-100 (2.5%)**

Triton X-100	5	ml
DW	195	ml

All components were mixed until the solution was homogeneous. The solution was freshly prepared before use.

17.4 **Developing buffer (0.1 M sodium acetate, 1 mM EDTA, 2 mM DTT, pH 5.5)**

Sodium acetate	4.1	g
EDTA	186.0	mg

DTT   154.0   mg

All components were dissolved in DW, adjusted to pH 5.5 and DW was added to a final volume of 500 ml. The solution was sterilized by filtration through a 0.22 µm filter and stored at room temperature.

18. Reagents for isolation of murine spleen cells and mitogen-induced murine spleen cell proliferation assay

    18.1 Complete RPMI medium (1% antibiotic-antimycotic, 2 mM glutamine, and 10% fetal bovine serum)

RPMI	88	ml
Fetal bovine serum	10	ml
Antibiotic-antimycotic	1	ml
Glutamine	1	ml

    18.2 RBC lysis buffer

Ammonium chloride	415	mg
0.1 M Tris-HCl	5	ml

All components were dissolved in DW, adjusted to pH 7.5 and DW was added to a final volume of 50 ml. The solution was sterilized by filtration through a 0.22 µm filter and stored at room temperature.

    18.3 MTT (5 mg/ml MTT in PBS, pH 7.2)

MTT	5	mg

This component was dissolved in 0.01 M PBS, pH 7.2 to final volume of 1 ml and mixed until the solution become clear.

    18.4 Balanced salt solution

Solution A (5.5 mM $C_6H_{12}O_6 \cdot H_2O$, 500 mM $CaCl_2 \cdot 2H_2O$, 98 mM $MgCl_2 \cdot 6H_2O$, 5.4 mM KCl and 0.145 mM Tris)

$C_6H_{12}O_6 \cdot H_2O$	1.089	g
$CaCl_2 \cdot 2H_2O$	0.0074	g
$MgCl_2 \cdot 6H_2O$	0.1992	g
KCl	0.4026	g
Tris	17.565	g

All components were dissolved in DW, adjusted to pH 7.6 by using HCl and DW was added to a final volume of 1,000 ml.

Solution B (0.14 M NaCl)

NaCl   8.19   g

The balanced salt solution was prepared by mixing 1 volume of solution A with 9 volumes of solution B and the solution was freshly prepared each week.

19. Reagent and culture media for protein expression and purification from yeast (*Pichia pastoris*)

19.1 10× YNB (13.4% Yeast Nitrogen Base)

Yeast nitrogen base   13.4   g

This component was dissolved in DW to a final volume of 100 ml and mixed until the solution became homogeneous. The solution was sterilized by filtration through a 0.22 μm filter and stored at 4℃.

19.2 500× Biotin (0.02% Biotin)

Biotin   20   mg

This component was dissolved in DW to a final volume of 100 ml and mixed until the solution became homogeneous. The solution was sterilized by filtration through a 0.22 μm filter and stored at 4℃.

19.3 100× Histidine (0.4% Histidine)

Histidine   400   mg

This component was dissolved in DW to a final volume of 100 ml and mixed until the solution became homogeneous. The solution was sterilized by filtration through a 0.22 μm filter and stored at 4℃.

19.4 10× Dextrose (20% Dextrose)

D-glucose   20   g

This component was dissolved in DW to a final volume of 100 ml and mixed until the solution became homogeneous. The solution was sterilized by filtration through a 0.22 μm filter and stored at 4℃.

19.5 10× Methanol (5% Methanol)

Methanol   25   ml

This solution was diluted in DW to a final volume of 500 ml and mixed until the solution became homogeneous. The solution was sterilized by filtration through a 0.22 μm filter and stored at 4℃.

19.6 10×glycerol (10% Glycerol)

Glycerol   50   ml

This solution was diluted in DW to a final volume of 500 ml and mixed until the solution became homogeneous. The solution was sterilized by filtration through a 0.22 µm filter and stored at room temperature.

19.7 1 M potassium phosphate buffer, pH 6.0

1 M K_2HPO_4 132   ml

1 M KH_2PO_4 868   ml

This solution was mixed and adjusted to pH 6.0 by using phosphoric acid or KOH. The solution was sterilized by autoclaving and stored at room temperature.

19.8 YPD (1% yeast extract, 2% dextrose [glucose] and 2% peptone)

Peptone   10   g

Yeast extracts   5   g

Glucose   50   ml

All components except glucose were dissolved in DW to a final volume of 450 ml, and then sterilized by autoclaving. The solution was cooled down to 50–60℃, 50 ml of glucose was added and stored at room temperature.

19.9 YPD agar plates (1% yeast extract, 2% dextrose [glucose], 2% peptone and 2% agar)

Peptone   10   g

Yeast extracts   5   g

Agar   10   g

Glucose   50   ml

All components except glucose were dissolved in DW to a final volume of 450 ml, and then sterilized by autoclaving. The solution was cooled down to 50–60℃, 50 ml of glucose was added, poured into petri dishes, allowed to harden at room temperature for 1–2 hours and stored at 4℃.

19.10 YPDS + Zeocin™ agar plates (1% yeast extract, 2% dextrose [glucose], 2% peptone, 2% agar, 1 M sorbitol and 100 µg/ml Zeocin™)

Peptone	10	g
Yeast extracts	5	g
Agar	10	g
Glucose	50	ml
Zeocin™ (100 mg/ml)	500	µl

All components except glucose were dissolved in DW to a final volume of 450 ml, and then sterilized by autoclaving. The solution was cooled down to 50–60°C, glucose and Zeocin™ were added, poured into petri dishes, allowed to harden at room temperature for 1–2 hours and stored at 4°C (protected from light).

19.11 MMH (1.34% YNB, 4x10^{-5}% biotin, 0.5% methanol, 100× Histidine and agar)

Agar	7.5	g
10× YNB	50	ml
500× biotin	1	ml
10× Methanol	50	ml
100× Histidine	5	ml

Agar was dissolved in DW to a final volume of 394 ml, and then sterilized by autoclaving. The solution was cooled down to 50–60°C, added 10× YNB, 500× biotin, 10× methanol and 100× histidine, poured into petri dishes, allowed to harden at room temperature for 1–2 hours and stored at 4°C.

19.12 MDH (1.34% YNB, 4x10^{-5}% biotin, 2% dextrose, 100× Histidine and agar)

Agar	7.5	g
10× YNB	50	ml
500× biotin	1	ml
10× Dextrose (glucose)	50	ml
100× Histidine	5	ml

Agar was dissolved in DW to a final volume of 394 ml, and then sterilized by autoclaving. The solution was cooled down to 50–60℃, added 10× YNB, 500× biotin, 10× dextrose (glucose) and 100× histidine, poured into petri dishes, allowed to harden at room temperature for 1–2 hours and stored at 4℃.

19.13 BMGY (1% yeast extract, 2% peptone, 100 mM potassium phosphate, pH 6.0, 1.34% YNB, 4×10^{-5}% biotin and 1% glycerol)

Yeast extract	5	g
Peptone	10	g
10× YNB	50	ml
500× biotin	1	ml
Potassium phosphate, pH 6.0	50	ml
10× glycerol	50	ml

Yeast extract and peptone were dissolved in DW to a final volume of 349 ml, and then sterilized by autoclaving. The solution was cooled down to 50–60℃, added 10× YNB, 500× biotin, potassium phosphate, pH 6.0 and 10×glycerol and stored at 4℃.

19.14 BMMY (1% yeast extract, 2% peptone, 100 mM potassium phosphate, pH 6.0, 1.34% YNB, 4×10^{-5}% biotin and 0.5% methanol)

Yeast extract	5	g
Peptone	10	g
10× YNB	50	ml
500× biotin	1	ml
Potassium phosphate, pH 6.0	50	ml
10× Methanol	50	ml

Yeast extract and peptone were dissolved in DW to a final volume of 349 ml, and then sterilized by autoclaving. The solution was cooled down to 50–60℃, added 10× YNB, 500× biotin, potassium phosphate, pH 6.0 and 10× methanol and stored at 4℃.

19.15 STES buffer (0.2 M Tris-HCl, pH 7.6, 0.5 M NaCl, 0.1% [w/v] SDS and 10 mM EDTA)

1 M Tris-base, pH 7.6   20   ml

2 M NaCl   25   ml

10% SDS   1   ml

0.5 M EDTA   2   ml

All solutions were diluted in DW to a final volume of 100 ml and mixed well.

19.16 TE buffer (10 mM Tris-HCl, pH 8.0 and 1 mM EDTA)

1 M Tris-base, pH 8.0   1   ml

0.5 M EDTA   200 µl

All solutions were diluted in DW to a final volume of 100 ml and mixed well.

19.17 Reagents for protein purification

All reagents are same as bacterial system.

20. Reagent for characterization of protein from yeast (*Pichia pastoris*)

20.1 Sodium acetate stock solution pH 7.0 (1 M, 100 ml)

Sodium acetate   29.4   g

This component was dissolved in DW to a final volume of 100 ml. The solution was sterilized by autoclaving and stored at room temperature.

20.2 Tris-HCl stock solution (2 M, 100 ml)

Tris-HCl   24.23   g

This component was dissolved in DW to a final volume of 100 ml. The solution was sterilized by autoclaving and stored at room temperature.

20.3 EDTA, pH 8.0 stock solution (0.5 M, 100 ml)

EDTA·Na_2·H_2O 18.6   g

This component was dissolved in DW, adjusted to pH 8.0 by using NaOH and added DW up to a final volume of 100 ml. The solution was sterilized by autoclaving and stored at room temperature.

20.4 DTT stock solution (1 M, 5 ml)

DTT   0.77   g

This component was dissolved in DW to a final volume of 5 ml. The solution was sterilized by filtration through a 0.22 µm filter and stored at −20°C.

20.5 MES stock solution (1 M, 20 ml)

MES   4.26   g

This component was dissolved in DW to a final volume of 20 ml. The solution was sterilized by filtration through a 0.22 µm filter.

20.6 Dextran sulfate stock solution (1 mg/ml, 5 ml)

Dextran sulfate   5   mg

This component was dissolved in DW to a final volume of 5 ml. The solution was sterilized by filtration through a 0.22 µm filter.

20.7 AMT buffer (100 mM sodium acetate, 100 mM MES, 200 mM Tris-HCl, 4 mM EDTA) containing 50 µg/ml dextran sulfate (DS 500K) and 10 mM DTT)

1 M Sodium acetate	5	ml
1 M MES	5	ml
2 M Tris	5	ml
0.5 M EDTA	0.4	ml
1 mg/ml Dextran sulfate	2.5	ml
1 M DTT	0.5	ml

All solutions were diluted in DW to a final volume of 50 ml, adjusted to pH 3.0-8.0 depending on the experiments and mixed well.

APPENDIX B

Vector map and its important features

1. pGEM-T Easy cloning vector
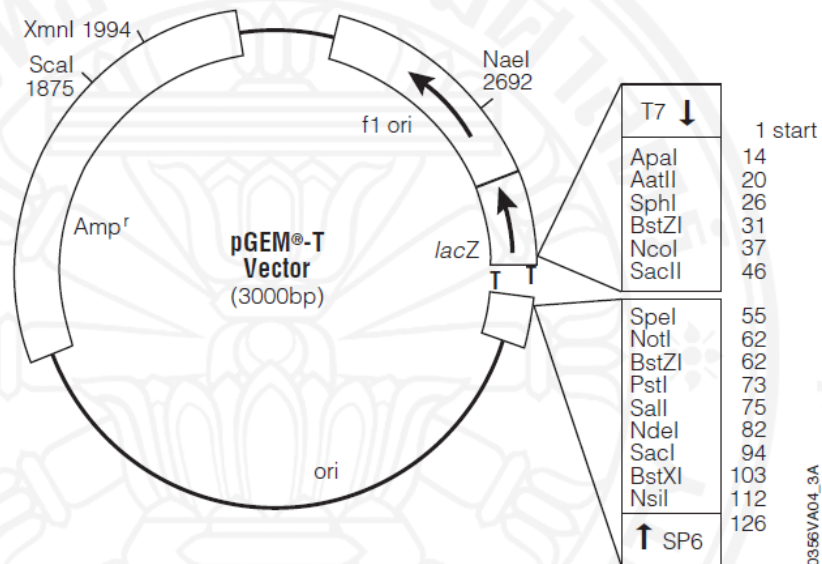
pGEM®-T Vector sequence reference points:

T7 RNA polymerase transcription initiation site	1
multiple cloning region	10–113
SP6 RNA polymerase promoter (–17 to +3)	124–143
SP6 RNA polymerase transcription initiation site	126
pUC/M13 Reverse Sequencing Primer binding site	161–177
lacZ start codon	165
lac operator	185–201
β-lactamase coding region	1322–2182
phage f1 region	2365–2820
lac operon sequences	2821–2981, 151–380
pUC/M13 Forward Sequencing Primer binding site	2941–2957
T7 RNA polymerase promoter (–17 to +3)	2984–3

2. pQE30 vector
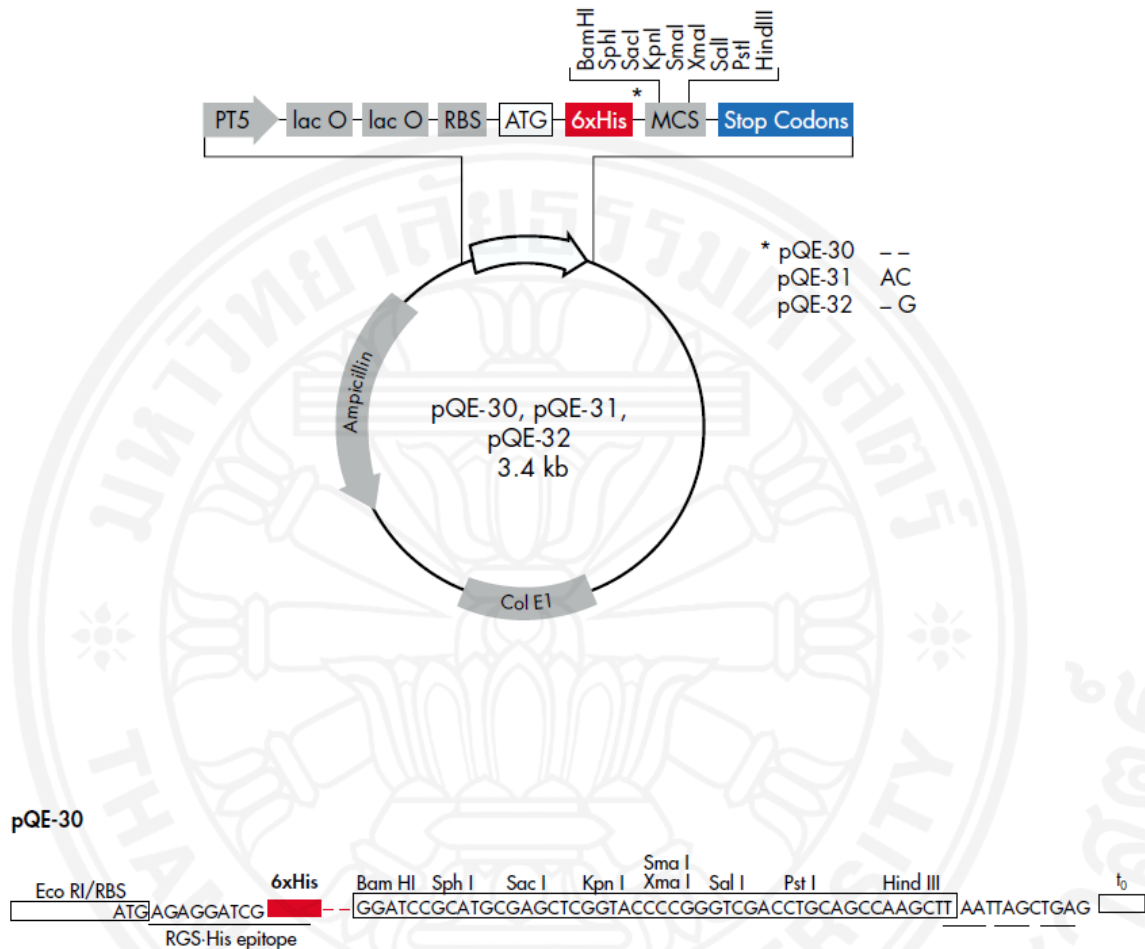
Positions of elements in bases

Vector size (bp)	3461
Start of numbering at *Xho*I (CTCGAG)	1–6
T5 promoter/lac operator element	7–87
T5 transcription start	61
6xHis-tag coding sequence	127–144
Multiple cloning site	145–192
Lambda t_0 transcriptional termination region	208–302
rrnB T1 transcriptional termination region	1064–1162
ColE1 origin of replication	1638
β-lactamase coding sequence	3256–2396

3. pPicZαB vector

Comments for pPICZα A
3593 nucleotides

5´ AOX1 promoter region: bases 1-941
5´ AOX1 priming site: bases 855-875
α-factor signal sequence: bases 941-1207
Multiple cloning site: bases 1208-1276
c-myc epitope: bases 1275-1304
Polyhistidine (6xHis) tag: bases 1320-1337
3´ AOX1 priming site: bases 1423-1443
AOX1 transcription termination region: bases 1341-1682
TEF1 promoter: bases 1683-2093
EM7 promoter: bases 2095-2162
Sh ble ORF: bases 2163-2537
CYC1 transcription termination region: bases 2538-2855
pUC origin: bases 2866-3539 (complementary strand)

* Pst I is in Version B only
Cla I is in Version C only

†The two Xho I sites in the vector allow
the user to clone their gene in frame with
the Kex2 cleavage site, resulting in
expression of their native gene without
additional amino acids at the N-terminus.

Feature	Benefit
5′ *AOX1* promoter	A 942 bp fragment containing the *AOX1* promoter that allows methanol-inducible, high-level expression of the gene of interest in *Pichia*. Targets plasmid integration to the *AOX1* locus.
α-factor secretion signal (from *Saccharomyces cerevisiae*)	Allows for efficient secretion of most proteins from *Pichia*.
Multiple cloning site	Allows insertion of your gene into the expression vector.
c-myc epitope (Glu-Gln-Lys-Leu-Ile-Ser-Glu-Glu-Asp-Leu)	Permits detection of your recombinant fusion protein with the Anti-*myc* Antibody or Anti-*myc*-HRP Antibody (Evans *et al.*, 1985). See page viii for ordering information.
C-terminal polyhistidine (6×His) tag	Permits purification of your recombinant fusion protein on metal-chelating resin such as ProBond™. In addition, the C-terminal polyhistidine tag is the epitope for the Anti-His(C-term) Antibody (Lindner *et al.*, 1997) and the Anti-His(C-term)-HRP Antibody. See page viii for ordering information.
AOX1 transcription termination (TT) region	Native transcription termination and polyadenylation signal from *AOX1* gene (~260 bp) that permits efficient 3′ mRNA processing, including polyadenylation, for increased mRNA stability.
TEF1 promoter (GenBank accession nos. D12478, D01130)	Transcription elongation factor 1 gene promoter from *Saccharomyces cerevisiae* that drives expression of the Zeocin™ resistance gene in *Pichia*.
EM7 promoter	Synthetic prokaryotic promoter that drives constitutive expression of the Zeocin™ resistance gene in *E. coli*.
Zeocin™ resistance gene (*Sh ble*)	Allows selection of transformants in *E. coli* and *Pichia*.
CYC1 transcription termination region (GenBank accession no. M34014)	3′ end of the *Saccharomyces cerevisiae CYC1* gene that allows efficient 3′ mRNA processing of the Zeocin™ resistance gene for increased stability.
pUC origin	Allows replication and maintenance of the plasmid in *E. coli*.

5´ end of *AOX1* mRNA   5´ *AOX1* priming site

```
811   AACCTTTTTT TTTATCATCA TTATTAGCTT ACTTTCATAA TTGCGACTGG TTCCAATTGA

871   CAAGCTTTTG ATTTTAACGA CTTTTAACGA CAACTTGAGA AGATCAAAAA ACAACTAATT

931   ATTCGAAACG ATG AGA TTT CCT TCA ATT TTT ACT GCT GTT TTA TTC GCA GCA
                 Met Arg Phe Pro Ser Ile Phe Thr Ala Val Leu Phe Ala Ala

983   TCC TCC GCA TTA GCT GCT CCA GTC AAC ACT ACA ACA GAA GAT GAA ACG GCA
      Ser Ser Ala Leu Ala Ala Pro Val Asn Thr Thr Thr Glu Asp Glu Thr Ala
```

α-factor signal sequence

```
1034  CAA ATT CCG GCT GAA GCT GTC ATC GGT TAC TCA GAT TTA GAA GGG GAT TTC
      Gln Ile Pro Ala Glu Ala Val Ile Gly Tyr Ser Asp Leu Glu Gly Asp Phe

1085  GAT GTT GCT GTT TTG CCA TTT TCC AAC AGC ACA AAT AAC GGG TTA TTG TTT
      Asp Val Ala Val Leu Pro Phe Ser Asn Ser Thr Asn Asn Gly Leu Leu Phe
```

Xho I*

```
1136  ATA AAT ACT ACT ATT GCC AGC ATT GCT GCT AAA GAA GAA GGG GTA TCT CTC
      Ile Asn Thr Thr Ile Ala Ser Ile Ala Ala Lys Glu Glu Gly Val Ser Leu
```

Kex2 signal cleavage   *Cla* I   *Eco*R I   *Pml* I   *Sfi* I   *Bsm*B I

```
1187  GAG AAG AGA GAG GCT GAA GC ATCGAT GAATTCAC GTGGCCCAG CCGGCCGTC TCGGA
      Glu Lys Arg Glu Ala Glu Ala
```

Ste13 signal cleavage

*Asp*718 I *Kpn* I *Xho* I   *Sac* II *Not* I   *Xba* I   *c-myc* epitope

```
1244  TCGGTACCTC GAGCCGCGGC GGCCGCCAGC TTTCTA GAA CAA AAA CTC ATC TCA GAA
                                              Glu Gln Lys Leu Ile Ser Glu
```

polyhistidine tag

```
1301  GAG GAT CTG AAT AGC GCC GTC GAC CAT CAT CAT CAT CAT CAT TGA GTTTGTA
      Glu Asp Leu Asn Ser Ala Val Asp His His His His His His ***

1353  GCCTTAGACA TGACTGTTCC TCAGTTCAAG TTGGGCACTT ACGAGAAGAC CGGTCTTGCT
```

3´ *AOX1* priming site

```
1413  AGATTCTAAT CAAGAGGATG TCAGAATGCC ATTTGCCTGA GAGATGCAGG CTTCATTTTT
```

3´ polyadenylation site

```
1473  GATACTTTTT TATTTGTAAC CTATATAGTA TAGGATTTTT TTTGTCATTT TGTTTCTTCT
```

APPENDIX C

Protein and DNA standards

1. Lambda DNA/*EcoR* I+*Hind* III Marker

Fragment sizes
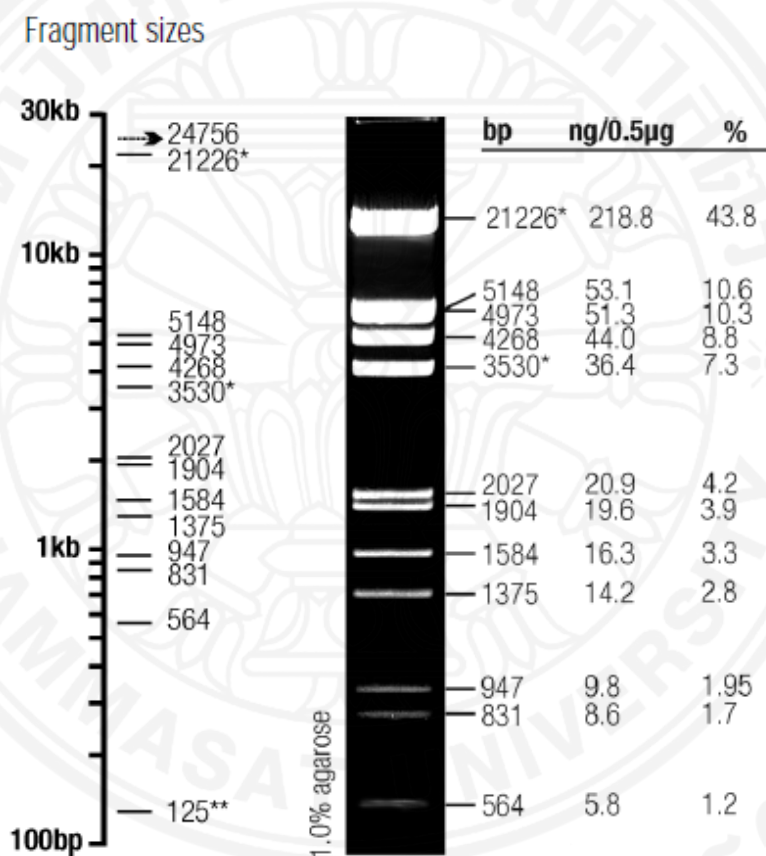
0.5µg/lane,
8cm length gel,
1X TAE, 7V/cm, 45min

2. GeneRuler™ 100 bp DNA Ladder

bp	ng/0.5µg	%
1031	66.6	13.3
900	58.1	11.6
800	51.8	10.4
700	45.4	9.1
600	38.8	7.8
500	**94.3**	**18.9**
400	35.0	7.0
300	35.0	7.0
200	35.0	7.0
100	35.0	7.0
80*	4.9	1.0

1.7% agarose

0.5µg/lane,
8cm length gel,
1X TBE, 5V/cm,1.5hrs

* The 80 and 100 bp fragments may
not be resolved on agarose gels.

bp
1031
900
800
700
600
500
400
300
200
100
80

5% polyacrylamide

1µg/lane,
20cm length gel,
1X TAE, 8V/cm, 3hrs
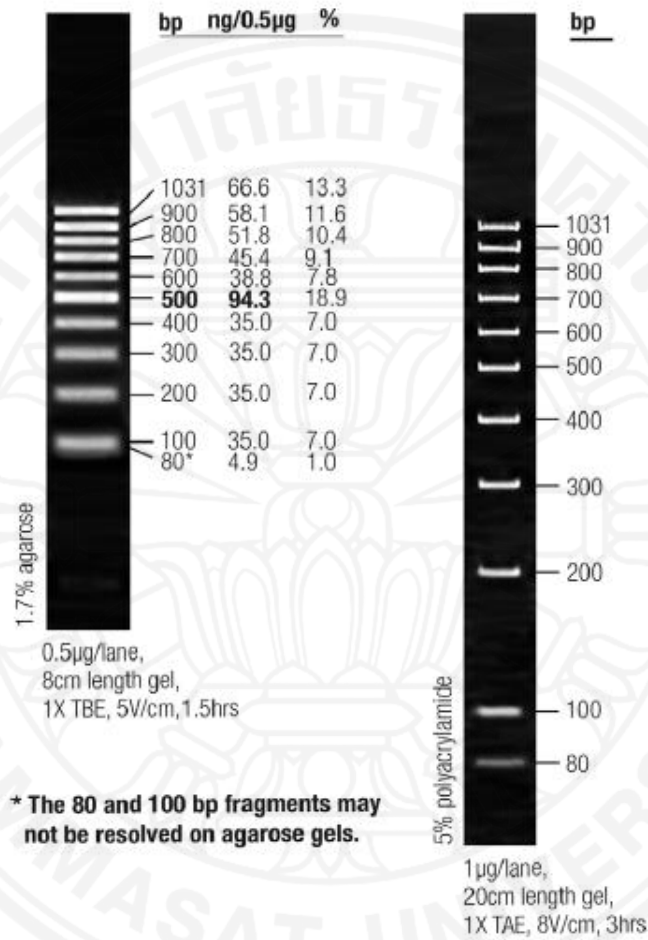
3. GeneRuler™ 1 kb DNA Ladder

bp	ng/0.5µg	%
10000	20.0	4.0
8000	24.0	4.3
6000	30.0	6.0
5000	30.0	6.0
4000	40.0	8.0
3500	51.0	10.2
3000	**88.0**	17.6
2500	33.5	6.7
2000	**92.0**	18.4
1500	24.0	4.8
1000	10.0	2.0
750	21.5	4.3
500	14.5	2.9
250	21.5	4.3

1.0% agarose

0.5µg/lane,
8cm length gel,
1X TAE, 7V/cm, 45min
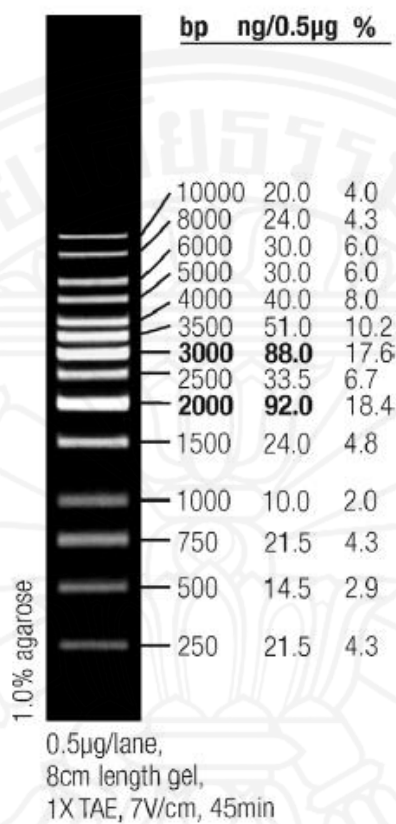
4. Protein marker (Broad range)

Myosin

ß-galactosidase
Phosphorylase b

Bovine serum albumin

Ovalbumin

Carbonic anhydrase

Soybean trypsin
inhibitor

Lysozyme
Aprotinin

200 kD
116.3
97.4
66.2
45.0
31
21.5
14.4
6.5

SDS-PAGE
Standards,
Broad Range

BIOGRAPHY

Name	Sinee Siricoon
Date of Birth	February 14, 1987
Educational Attainment	2005-2008 Bachelor of Science (Medical Technology), Faculty of Allied Health Sciences, Thammasat University, Thailand
	2009-present Ph.D. Candidate in Doctor of Philosophy Program in Biomedical Sciences Faculty of Allied Health Sciences, Thammasat University, Thailand (Temporary research student at School of Applied Sciences, RMIT University (Bundoora Campus), Melbourne, Australia)
Scholarship	2009: Thammasat University and Thailand Research Joint Fund through a Royal Golden Jubilee Ph.D. scholarship
	2014: Thammasat University Research Fund under the TU Research Scholar
Contact information	
Office address	Molecular Parasitology Unit, Graduate Program in Biomedical Sciences, Faculty of Allied Health Sciences, Thammasat University, Rangsit Campus, 99 Moo 18, Paholyothin Road, Klong-1, Klong-Luang, Pathumthani, 12120, Thailand.
Home address	179/1 Moo 4, Banbung, Chonburi, 20170, Thailand
E-mail address	vavajang6@hotmail.com

Publications

1. **Sinee Siricoon**, Suksiri Vichasri Grams, and Rudi Grams. Efficient inhibition of cathepsin B by a secreted type 1 cystatin of *Fasciola gigantica*. Molecular & Biochemical Parasitology 186(2012): 126-133

2. **Sinee Siricoon**, Suksiri Vichasri Grams, Kittisak Lertwongvisarn, Muntana Abdullohfakeeyah, Peter M. Smooker, Rudi Grams. *Fasciola gigantica* cathepsin B5 is an acidic endo- and exopeptidase of the immature and mature parasite. Biochimie 119 (2015): 6-15

3. Amornrat Geadkaew, Nanthawat Kosa, **Sinee Siricoon**, Suksiri Vichasri Grams,Rudi Grams. A 170 kDa multi-domain cystatin of *Fasciola gigantica* is active in the male reproductive system. Molecular & Biochemical Parasitology 196 (2014): 100–107

Licenses, Training and Conferences attended

1. Research trainee student at Molecular Immunology Unit, Graduate Program in Biomedical Sciences, Faculty of Allied Health Sciences, Thammasat University, Thailand (2008)

2. Trainee student (Medical Technology) in diagnostic laboratory at Thammasat Hospital, Pathumthani, Thailand (2008)

3. Trainee student (Medical Technology), Chonburi Hospital, Chonburi, Thailand (2008)

4. License on Medical Technologist from The Medical Technology Council of Thailand (2009-present)

5. International diploma course on research ethics, 5th - 8th October 2009, Faculty of Allied Health Sciences, Thammasat University (Rangsit Campus), Thailand

6. The 32th Pharmacological and Therapeutic Society of Thailand Meeting, 25th-26th March 2010, TCC LAND Auditorium Thammasat University (Rangsit Campus), Thailand

7. Current Research on Opisthorchiasis, Cholangiocarcinoma, and Fascioliasis, 28th – 29th October 2010, Udonthani Rajbhat University, Udonthani, Thailand

8. The Scientific Meeting in Allied Health Sciences, 6th January 2011, Faculty of Allied Health Sciences, Thammasat University (Rangsit Campus), Thailand

9. The 37th Congress on Science and Technology of Thailand (STT 37), 10th – 12th October 2011, Bangkok Convention Center at Central World, Bangkok, Thailand

10. Joint International Tropical Medicine Meeting 2011, 1st – 2nd December 2011, Bangkok Convention Center at Central World, Bangkok, Thailand

11. The Scientific Meeting in Allied Health Sciences, 16th May 2012, Thammasat University (Pattaya Campus), Thailand

12. The Scientific Meeting in Allied Health Sciences, 27th October 2012, Faculty of Allied Health Sciences, Thammasat University (Rangsit Campus), Thailand

13. Research training in the biology of proteases and cystatins from Fasciola gigantica. This concerns the expression of recombinant Fasciola cysteine proteases in yeast, their substrate specificity and inhibition by Fasciola cystatins, 21st May 2013 – 6th March 2014, School of Applied Sciences, RMIT University (Bundoora Campus), Melbourne, Australia

14. Human ethics, 28th March 2014, Faculty of Allied Health Sciences, Thammasat University (Rangsit Campus), Thailand

15. Special Seminar in topic: Functional analysis of Schistosoma mansoni egg-secreted proteins using lentivirus-delivered micro RNA, 10th April 2014, Faculty of Allied Health Sciences, Thammasat University (Rangsit Campus), Thailand

16. The Scientific Meeting in Allied Health Sciences, 17th – 18th May 2014, The Great Hotel and Resort, Ratchaburi, Thailand

17. Special Seminar on Laboratory Animal Anesthesia and Vivarium Management, 26th May 2014, Maruay Garden Hotel, Bangkok, Thailand

18. RGJ-Ph.D. Congress XV, 28th – 30th May 2014, Jomtien Palm Beach Resort, Pattaya, Thailand

19. Animal ethics, 9th June 2014, Faculty of Allied Health Sciences, Thammasat University (Rangsit Campus), Thailand

20. The 1st International Allied Health Sciences Conference 2014 on the Occasion of the 80th Anniversary of Thammasat University: Medical Innovation for Health, 4th – 6th November 2014, Rama Gardens Hotel, Bangkok, Thailand

21. The Scientific Meeting in Allied Health Sciences, 13th – 14th December 2014, Faculty of Allied Health Sciences, Thammasat University (Rangsit Campus), Thailand

22. Training in Ethical Principles and Guidelines for the use of Animals for Scientific Purposes, 20th January 2015, Thammasat University (Rangsit Campus), Thailand

23. 2nd Joint Symposium of Thammasat University and BK21 PLUS of CUK, 21st – 23rd January 2015, Faculty of Allied Health Sciences, Thammasat University (Rangsit Campus), Thailand

24. Special Seminar on synchrotron, 3rd March 2015, Faculty of Allied Health Sciences, Thammasat University (Rangsit Campus), Thailand

25. The Scientific Meeting in Allied Health Sciences, 20th – 21st June 2015, Kantary Hotel, Ayutthaya, Thailand

26. Training in international publication, 29th June 2015, Faculty of Allied Health Sciences, Thammasat University (Rangsit Campus), Thailand

27. Human ethics, 6th July 2015, Faculty of Allied Health Sciences, Thammasat University (Rangsit Campus), Thailand

28. Training in Biosafety Guidelines, 15th July2015, Thammasat University (Rangsit Campus), Thailand

29. Special Seminar on Real-time PCR, 12th and 14th October 2015, Faculty of Allied Health Sciences, Thammasat University (Rangsit Campus), Thailand

30. The Scientific Meeting in Allied Health Sciences, 12th December 2015, Faculty of Allied Health Sciences, Thammasat University (Rangsit Campus), Thailand

Oral presentations

1. **Siricoon S.** *Fasciola gigantica*: Cystatins of the liver fluke *Fasciola gigantica*. Academic meeting: Current Research on Opisthorchiasis, Cholangiocarcinoma,

and Fascioliasis, 28th – 29th October 2010, Udonthani Rajbhat University, Udonthani, Thailand

2. **Siricoon S.** Characterization of a novel single domain cystatin as an immunomodulator in fascioliasis. The Scientific Meeting in Allied Health Sciences, 6th January 2011, Faculty of Allied Health Sciences, Thammasat University (Rangsit Campus), Thailand

3. **Siricoon S.** Cystatins of the liver fluke *Fasciola gigantica*. The 37th Congress on Science and Technology of Thailand (STT 37), 10th – 12th October 2011, Bangkok Convention Center at Central World, Bangkok, Thailand

4. **Siricoon S.** Characterization of a novel single domain cystatin in the liver fluke *Fasciola gigantica*. The Scientific Meeting in Allied Health Sciences, 16th May 2012, Thammasat University (Pattaya Campus), Thailand

5. **Siricoon S.** Molecular and biochemical characterization of type I cystatin stefin-2 of the liver fluke *Fasciola gigantica*. The Scientific Meeting in Allied Health Sciences, 17th – 18th May 2014, The Great Hotel and Resort, Ratchaburi, Thailand

6. **Siricoon S.** Characterization of recombinant type I cystatin (stefin-2) from *Fasciola gigantica* as a tool in diagnosis of fascioliasis. The Scientific Meeting in Allied Health Sciences, 13th – 14th December 2014, Faculty of Allied Health Sciences, Thammasat University (Rangsit Campus), Thailand

Poster presentations

1. **Sinee Siricoon**, Amornrat Geadkaew, Mayuri Tharasuk, Suksiri Vichasri-Grams, Vithoon Viyanant, Rudi Grams. Molecular and biochemical characterization of a novel cystatin from the liver fluke *Fasciola gigantica*, Joint International Tropical Medicine Meeting 2011, 1st – 2nd December 2011, Bangkok Convention Center at Central World, Bangkok, Thailand

2. **Sinee Siricoon**, Amornrat Geadkaew, Mayuri Tarasuk, Suksiri Vichasri Grams, Vithoon Viyanant, Rudi Grams. Cystatins of the liver fluke *Fasciola gigantica*. RGJ-Ph.D. Congress XV, 28th – 30th May 2014, Jomtien Palm Beach Resort, Pattaya, Thailand

3. **Sinee Siricoon**, Amornrat Geadkaew, Mayuri Tarasuk, Suksiri Vichasri Grams, Vithoon Viyanant, Rudi Grams. Characterization of recombinant type I cystatin from *Fasciola gigantica* as a tool in diagnosis of fascioliasis. The Scientific Meeting in Allied Health Sciences, 13th – 14th December 2014, Faculty of Allied Health Sciences, Thammasat University (Rangsit Campus), Thailand

4. **Sinee Siricoon**, Amornrat Geadkaew, Suksiri Vichasri Grams, Rudi Grams. Molecular and biochemical characterization of Stefin-2 from the liver fluke *Fasciola gigantica.* The Scientific Meeting in Allied Health Sciences, 12th December 2015, Faculty of Allied Health Sciences, Thammasat University (Rangsit Campus), Thailand

Honors and awards

1. 2nd Class Honor, Bachelor of Science (Medical Technology) 2008, Thammasat University, Thailand

2. The Consolation Prize for oral presentation in The 1st International Allied Health Sciences Conference 2014 on the Occasion of the 80th Anniversary of Thammasat University: Medical Innovation for Health